NORTHERN TERRITORY GEOLOGICAL SURVEY

AGES2019

ANNUAL GEOSCIENCE EXPLORATION SEMINAR

19–20 March 2019, Alice Springs, Northern Territory

PROCEEDINGS

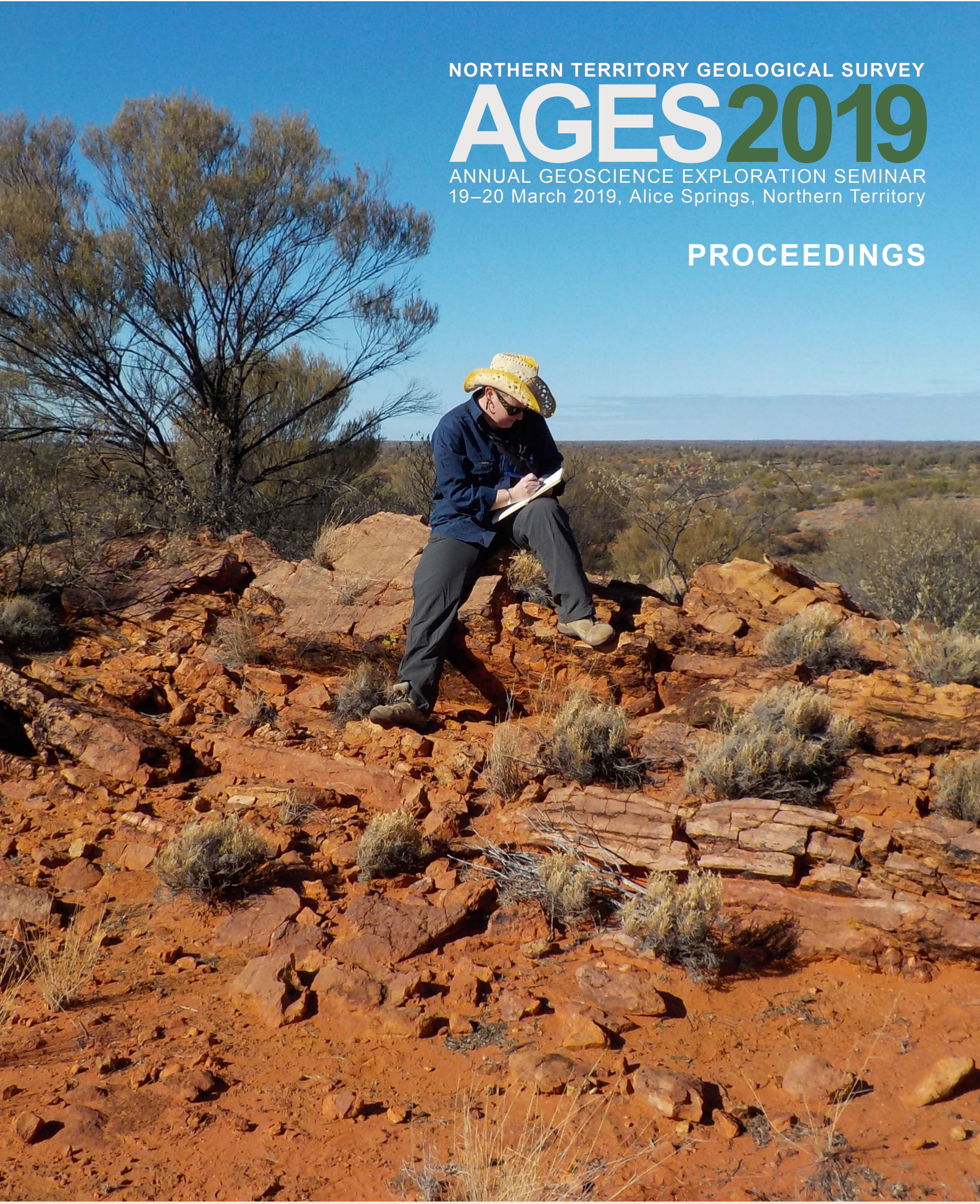

20TH ANNIVERSARY OF AGES – RESOURCING THE TERRITORY

AUSTRALIA'S NORTHERN TERRITORY

Minister's foreword

Hon. Paul Kirby, MLA
Minister for Primary Industry and Resources

On behalf of the Northern Territory Government, I welcome you to Alice Springs and to the 20th Annual Geoscience Exploration Seminar.

This year's AGES is being held at a time of renewed confidence in the resources sector with record values of mineral production in the Territory, increasing minerals exploration activity and new certainty for the future of onshore gas exploration. The exploration sector is critical to grow our resources industry, which creates jobs and economic development across the Territory. For this reason we have funded the new *Resourcing the Territory* initiative, the largest exploration initiative ever undertaken in the Territory. AGES will highlight some of the exciting programs now underway through this initiative.

AGES remains an important part of our strategy to grow the exploration sector by bringing explorers, researchers and government together to share the latest geoscience and exploration data, knowledge, and concepts that can highlight the Territory's potential and lead to the Territory's next big resource discoveries. A pre-conference workshop at AGES will also highlight the steps we are taking to streamline regulation for the minerals sector and make the Territory a more competitive place to do business.

For those of you who have travelled from interstate to attend AGES, thank you for making the effort to attend and I hope you enjoy your time in Alice Springs. I trust you will find AGES informative and useful, and that it will help you identify new opportunities for exploration and discovery in the Territory.

Hon. Paul Kirby, MLA

DEPARTMENT OF PRIMARY INDUSTRY AND RESOURCES
MINISTER: Hon. Paul Kirby, MLA
CHIEF EXECUTIVE: Alister Trier

NORTHERN TERRITORY GEOLOGICAL SURVEY
EXECUTIVE DIRECTOR: Ian Scrimgeour

BIBLIOGRAPHIC REFERENCE: *Annual Geoscience Exploration Seminar (AGES) Proceedings, Alice Springs, Northern Territory, 19–20 March 2019.* Northern Territory Geological Survey, Darwin.

BIBLIOGRAPHY: ISSN 2206-2815 (Print) ISSN 2206-2823 (Online)
ISBN 978-0-7245-7343-1 (Print) 978-0-7245-7344-8 ISBN (PDF)

Keywords: Neoproterozoic, Palaeozoic, Proterozoic, Aileron Province, Amadeus Basin, Glyde, Favenc, greater McArthur Basin, South Nicholson Basin, McArthur-Yanliao Gulf, Batten Fault Zone, Barney Creek Formation, Velkerri Formation, Beetaloo Sub-Basin, Angularli, Such Wow, Grapple, Bumblebee, Lake Mackay, Edna Beryl, McArthur River, HYC, Lantern, Wollogorang, Tanami, Mount Hardy, Alligator River, Finniss, zircon, uranium, lithium, gold, sediment-hosted Zn-Pb, petroleum systems, diagenetic mineralisation, depocentre, palaeogeography, reservoir quality, geochronology, geophysics, AusAEM, conductivity, depth imaging, legacy data, salt tectonics, ARUF, STRIKE, HyLogger™ , GEMIS.

EDITOR: GC MacDonald. Publication layout and figure preparation: KJ Johnston

Northern Territory Geological Survey
3rd floor Paspalis Centrepoint Building
Smith Street Mall, Darwin
GPO Box 4550
Darwin NT 0801, Australia

Arid Zone Research Institute
South Stuart Highway, Alice Springs
PO Box 8760
Alice Springs NT 0871, Australia

For further information contact:
Minerals and Energy InfoCentre
Phone +61 8 8999 6443
Website: **www.minerals.nt.gov.au/ntgs**
Email: geoscience.info@nt.gov.au

Cover photograph: NTGS geologist Dr Verity Normington recording observations on an isolated outcrop of newly defined Purna Kura Kura Formation, Winnall Group, south-central Amadeus Basin.

Mining Services Expo

Exhibitor floor plan

19–20 March 2019, Alice Springs Convention Centre

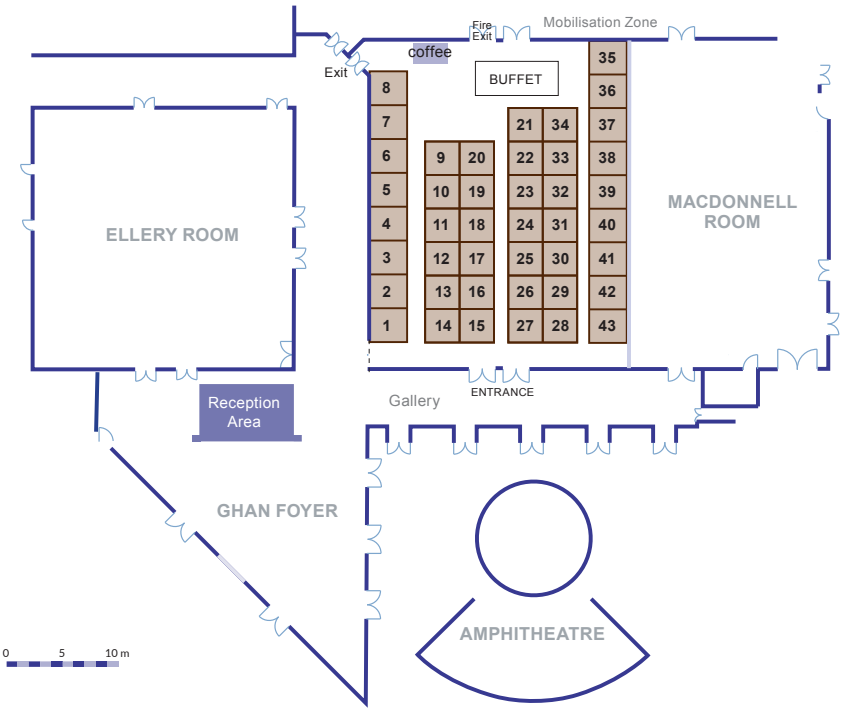

Booth and Exhibitors

1 DPIR – NT Geological Survey
2 DPIR – NT Geological Survey
3 Geoscience Australia
4 Katherine Mining Group
5 Bureau Veritas Minerals
6 Thrifty
7
8 Uber Air
9 Alice Springs Helicopters
10 DDH1 Drilling Pty Ltd
11 Bowgan Minerals Limited
12 HiSeis
13 CSIRO
14 Energy Power Systems Australia
15 Recharge Petroleum
16 Todd River Resources Ltd
17 Charles Darwin University
18 Ore Research & Exploration Pty Ltd
19 Industry Capability Network / Industry Skills Advisory Council NT
20 Arafura Resources Limited
21 Territory Hirex
22 SAE Australia Pty Ltd
23 SLR Consulting Australia Pty Ltd
24 ALS Limited
25 Fender Geophysics
26 Portable XRF Services
27 Australian Mining and Exploration Title Services Pty Ltd
28 NT Link
29 Refuel Australia
30 Titeline Drilling Pty Ltd
31 Olympus Australia
32 Intertek Genalysis
33 Civil Training
34 Brian Blakeman Surveys
35 Minerals Council of Australia NT
36 Chubb Fire & Safety
37 XM Logistics
38 Alice Springs Airport
39 Puma Energy
40 Tellus Holdings
41 Top End Importers
42 Northline Pty Ltd
43 Hastings Deering

Contents

AGES 2019 program

Day 1 Monday 18 March			
17:30–19:30	Registration and Ice Breaker	*Venue: Foyer area, Alice Springs Convention Centre*	
DAY 2 Tuesday 19 March			
08:00–08:30	Registration		
08:30–08:40	Welcome to Country		
08:40–08:50	Minister Paul Kirby	NT Government	Official opening
Session 1			
08:50–09:20	Ian Scrimgeour	NTGS	Overview of mineral and petroleum exploration and production in 2018
09:20–09:40	Anna Mayo	Todd River Resources Ltd	Where there's smoke there's fire – perseverance and reward at the Mount Hardy Zn-Cu Project
09:40–10:00	Dot Close	NTGS	Highlights from precompetitive geoscience across Northern Territory geology
10:00–10:40	*Morning tea*		
Session 2			
10:40–11:00	Tracey Rogers	NTGS	Geoscience information: What's new and what's ahead
11:00–11:20	Chantelle Lower	Kirkland Lake Gold Ltd	Lantern project update – realising opportunity through the use of numeric exploration technology
11:20–11:40	Yusen Ley-Cooper	Geoscience Australia	AusAEM_1: One step towards a national conductivity map of Australia
11:40–12:00	Alister Trier	DPIR	Preparing for exploration: Post Hydraulic Fracturing Inquiry
12:00–13:20	*Lunch*		
Session 3			
13:20–13:40	David Rawlings	Core Lithium Ltd	Update on the Finniss Lithium Project
13:40–14:00	Tim Munson	NTGS	Detrital zircon geochronology investigations of the Glyde and Favenc packages: Implications for the geological framework of the greater McArthur Basin, Northern Territory
14:00–14:20	Alan Collins	University of Adelaide	Life and times of the Proterozoic McArthur-Yanliao Gulf: Update on the ARC-Industry–NTGS Linkage Project
14:20–14:40	Sam Spinks	CSIRO	Ultra-high resolution trace element mapping provides new clues on the origin of the McArthur River (HYC) sediment-hosted Zn-Pb-Ag deposit
14:40–15:10	*Afternoon tea*		
Session 4			
15:10–15:30	Gary Ferris	Northern Cobalt Ltd	Wollogorang Project: Review of 2018 exploration program
15:30–15:50	Teagan Blaikie	CSIRO	From source to trap. Geophysical insights into base metals mineralisation in the southern McArthur Basin
15:50–16:10	Marcus Kunzmann	CSIRO	The ca 1640 Ma Barney Creek Formation in the McArthur Basin: Targeting diagenetic mineralisation and depocentre shift
16:10–16:30	Heather Sheldon	CSIRO	An integrated study of the McArthur River mineral system: From geochemistry, geophysics and sequence stratigraphy to basin-scale models of fluid flow

continued on next page

AGES 2019 program *(continued)*

DAY 2 Tuesday 19 March (continued)

16:30–17:20	Sundowner drinks	*Venue: Courtyard area, Alice Springs Convention Centre*
18:30–19:00	Pre-dinner drinks	*Venue: Foyer area, Alice Springs Convention Centre*

AGES Official Dinner

19:00–late	*Venue: Ellery Room, Alice Springs Convention Centre*

DAY 3 Wednesday 20 March

Session 1

09:00–09:20	Lidena Carr	Geoscience Australia	Exploring for the Future: South Nicholson Basin region project outcomes and sequence stratigraphy
09:20–09:40	Susannah MacFarlane	Geoscience Australia	Source rock geochemistry and petroleum systems of the greater McArthur Basin and links to other northern Australian Proterozoic basins
09:40–10:00	Claudio Delle Piane	CSIRO	A multidisciplinary evaluation of the Velkerri Formation in the Beetaloo Sub-Basin: Implications for geological history and reservoir quality
10:00–10:40	*Morning tea*		

Session 2

10:40–11:00	Tania Dhu	NTGS	New geophysical and remote sensed data in the Northern Territory
11:00–11:20	Mike Whitford	Independence Group NL	Application of electrical geophysics to exploration at the Lake Mackay Project
11:20–11:40	Barry Reno	NTGS	The greenfield Grapple and Bumblebee discoveries of the western Aileron Province: First constraints on sulfide mineralising processes
11:40–12:00	James Davis	Prodigy Gold NL	Mapping under cover with geochemistry
12:00–13:00	*Lunch*		

Session 3

13:00–13:20	Christine Edgoose	NTGS	New insights into the Neoproterozoic to early Palaeozoic stratigraphy, structure and palaeogeography of the Amadeus Basin, Northern Territory
13:20–13:40	Julie Daws	Mossman Oil and Gas Ltd	Integration of reprocessing, depth imaging and interpretation in legacy data to provide new insights into salt tectonics and sub salt imaging in the Amadeus Basin, NT
13:40–14:00	Rob Bills	Emmerson Resources Ltd	The discovery and mining of the ultra-high-grade Edna Beryl Gold Mine – the trials and tribulations
14:00–14:20	Penny Sinclair	Vimy Resources Ltd	Refreshing the Alligator River Uranium Field exploration toolkit – Angularli and Such Wow
14:20–14:30	Ian Scrimgeour	NTGS	Closing remarks

End AGES 2019

AGES 2019 major sponsors

Networking ice-breaker drinks

origin

Dinner wine

CORE LITHIUM

AGES 2019 sponsors

Coffee

ENERGY CLUB NT

Networking sundowner drinks

TELLUS

Networking pre-dinner drinks

TITELINE DRILLING PTY LTD

Overview of mineral and petroleum exploration and production in 2018

Ian R Scrimgeour [1,2]

Exploration statistics

Mineral exploration activity in the Northern Territory (NT) continued to recover during 2018 with increasing expenditure and reported on-ground activity. According to the Australian Bureau of Statistics (ABS), mineral exploration expenditure in the NT in 2017–18 was at $111.8 million, a 43% increase on a low of $78.4 million in 2016–17 (**Figure 1**). Exploration in greenfields areas (as defined by the ABS) was up 30% to $56.5 million (**Figure 2a**). The proportion of exploration expenditure in the NT that is in greenfields areas is 51%, much higher than the national average of 34% (**Figure 2b**). **Figure 1** shows a comparison of annual exploration expenditure in all states since 2000; **Figure 2** shows greenfields versus brownfields expenditure in the Northern Territory

In addition to ABS exploration statistics, which include the costs of mine site exploration, the Northern Territory Geological Survey (NTGS) collects statistics on the admissible exploration expenditure on exploration leases reported by industry to the Department of Primary Industry and Resources (DPIR). This shows that expenditure reports submitted during 2017 (which may relate to activity in 2017 and/or 2018) totalled $58.7 million, a 21% increase from the previous year. Of expenditure reported to DPIR in 2018, 28% ($16.3 million) was in the Arunta Region, 23% ($13.6 million) in the McArthur Basin, and 15% ($9.0 million) in the Pine Creek Orogen. The bulk of expenditure was for base metals (33%; $19.6 million), gold (24%; $14.1 million), rare earths (10%; $5.9 million) and lithium (9%, $5.2 million). **Figure 3** shows the breakdown of on-ground expenditure (excluding feasibility and desktop studies) by geological region and primary commodity of interest.

At the end of 2018, there were 838 granted non-extractive mineral exploration licences (compared with 812 at the end of 2017) and 588 outstanding exploration licence applications. During 2018, 179 applications were received (down from 263 in 2017), 122 granted, and 157 licences ceased (down from 340 in 2017). The area of the NT covered by granted exploration tenure sits at about 11%.

During 2018, onshore petroleum exploration activity was largely limited to the Amadeus Basin, with one seismic survey and two appraisal wells. At the end of 2018, in the onshore NT and coastal waters, there were 47 granted exploration permits, three retention licences and five production licences.

Exploration and production highlights

In the following summary of exploration and mining results for the NT during 2018, all mineral resources are assumed to have been reported in accordance with the JORC or NI43-101 codes. Where resource categories are not listed, readers are directed to the original sources for this information. Most material cited here has been sourced from company websites, news releases and stock exchange announcements by companies. As a result, details of exploration by some private and other non-listed companies that do not report publicly could not be included.

Figure 4 shows selected mineral exploration highlights for 2018. Mineral production statistics for the NT for 2017/18, collected under the NT *Mineral Titles Act*, are given in **Table 1**. This shows mineral production was a record $4.49 billion in 2017/18.

Gold and copper-gold

Pine Creek Orogen

Kirkland Lake Gold Inc's ***Cosmo Deeps*** underground mine north of Pine Creek (**Figure 5**) remained in care and maintenance in 2018 following suspension of mining in mid-2017. The company announced that this was to allow them to focus its activities on an aggressive resource definition and exploration program at the mine, including the newly

[1] Northern Territory Geological Survey, GPO Box 4550, Darwin NT 0801, Australia
[2] Email: ian.scrimgeour@nt.gov.au

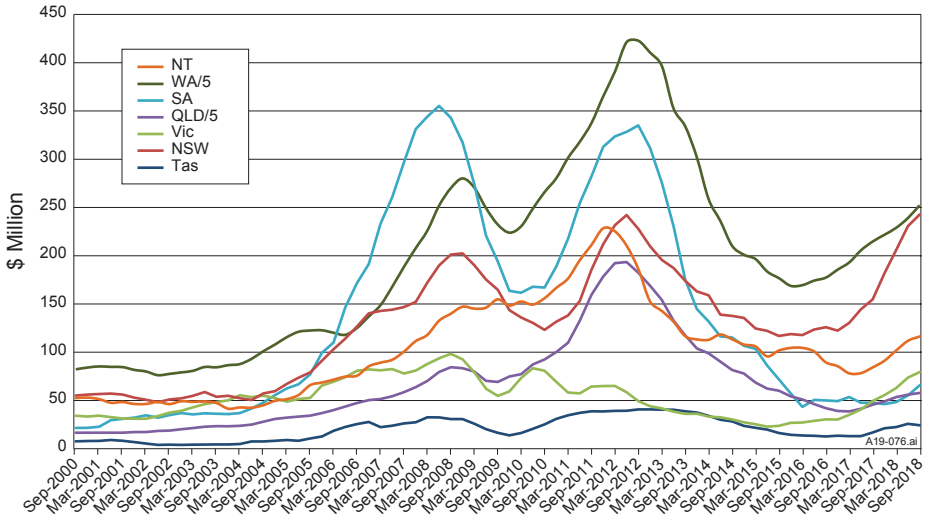

Figure 1. Annual mineral exploration expenditure for the Northern Territory and all states, calculated quarterly, for the 18 years to the September 2018 quarter.

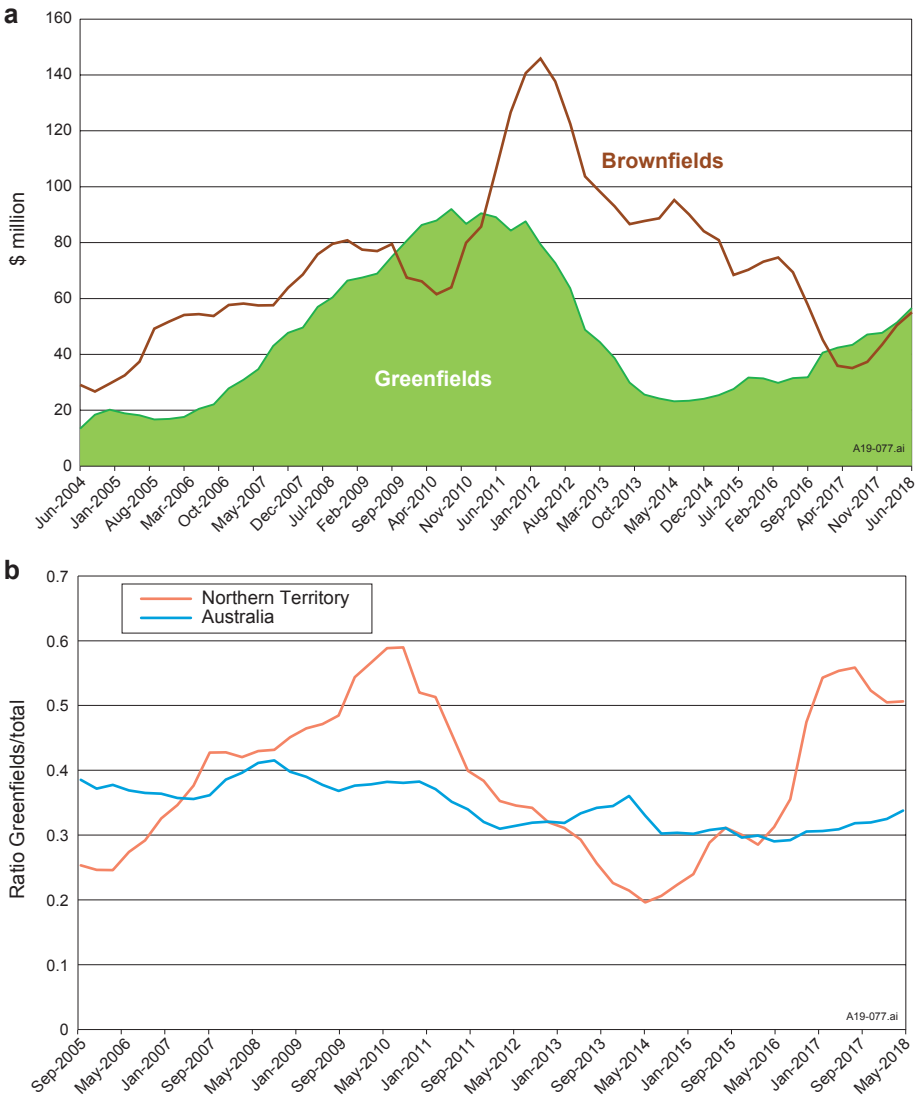

Figure 2. (**a**) Graph of mineral exploration expenditure (annual expenditure calculated quarterly) in greenfields and brownfields areas, as measured by the ABS, showing a significant rise in greenfields expenditure relative to brownfields since 2014. (**b**) Graph of the amount of greenfields mineral exploration expenditure as a proportion of total expenditure for the Northern Territory and Australia.

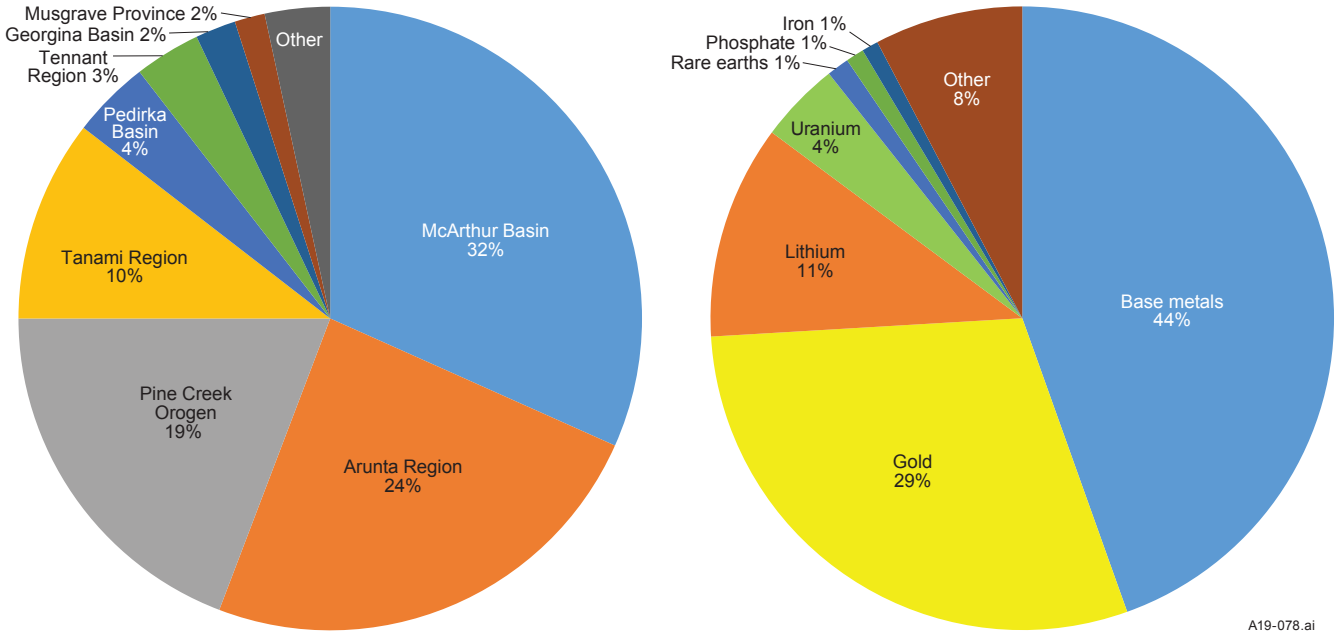

Figure 3. Summary of admissible on-ground exploration expenditure (excluding feasibility studies, desktop studies and overheads) reported to DPIR during 2018, broken down by (**a**) geological region and (**b**) primary commodity of interest. Note that exploration reported durng 2018 may have occurred during either 2017 or 2018.

discovered Lantern deposit, plus resume active regional exploration on advanced targets. The Mineral Resource at the Cosmo mine includes Measured and Indicated Resources of 4.89 Mt at 3.1 g/t Au and an Inferred Mineral Resource of 2.03 Mt at 2.9 g/t Au, for a total contained 0.57 Moz of gold. At the end of 2017, combined Mineral Resources for all of Kirkland Lake's Northern Territory assets included Measured and Indicated Resources of 26.9 Mt at 2.3 g/t Au and an Inferred Mineral Resource of 16.3 Mt at 2.5 g/t Au, for a total contained 3.22 Moz of gold.

Following the 2017 discovery of high-grade gold mineralisation at the ***Lantern*** gold deposit at Cosmo Deeps, underground development at Lantern began during April 2018. Drilling commenced from two underground platforms, with up to four underground diamond rigs in operation in the second half of 2018, and further underground development underway. No results of underground drilling were released during 2018.

In April 2018, Kirkland Lake announced drilling results from their ***Union Reefs*** project, from four deep holes (for

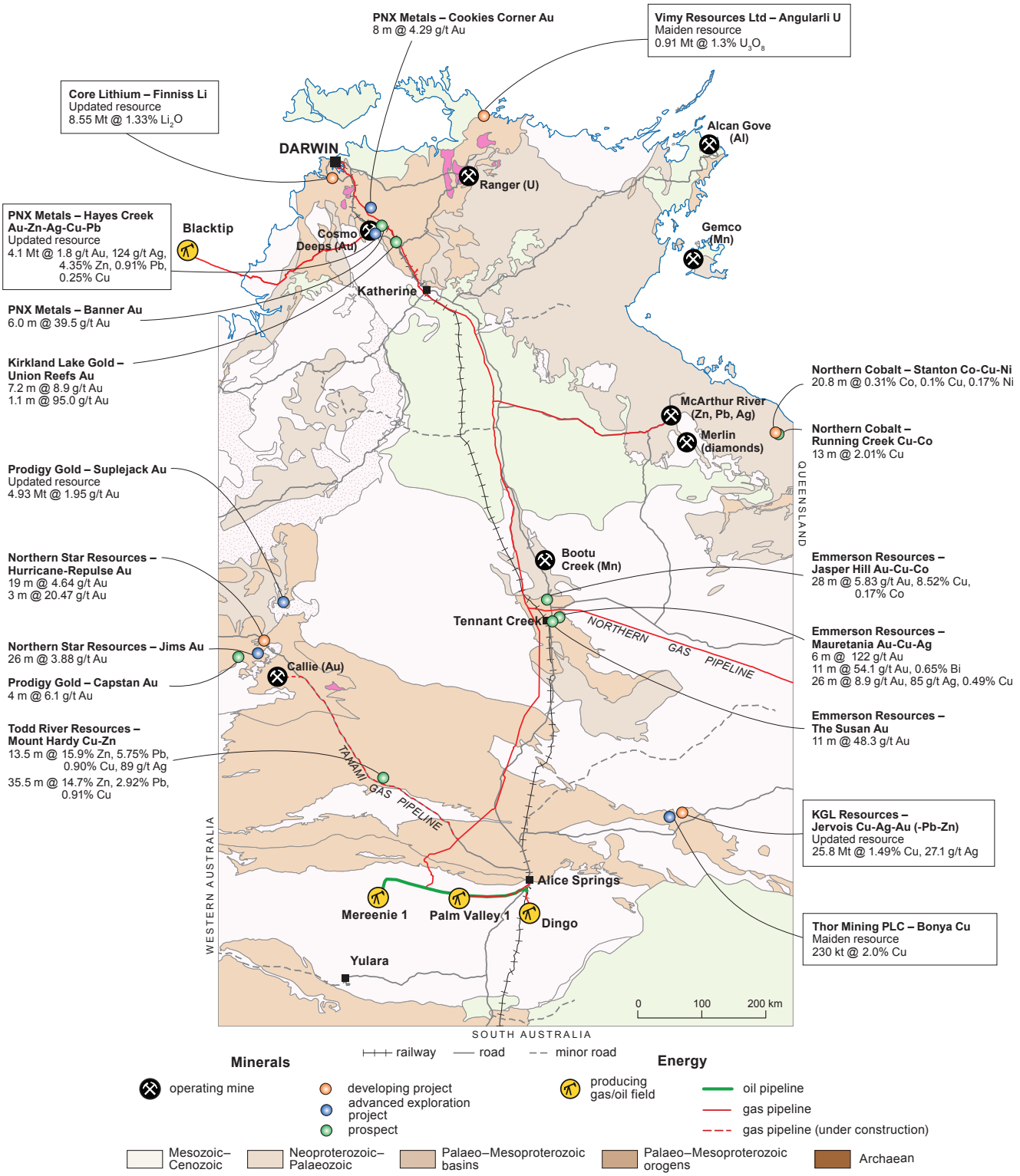

Figure 4. Map of the Northern Territory showing selected mineral exploration highlights for 2018.

Commodity	Unit of quantity	2017–18[1,5]		
		Quantity produced[2]	Quantity sold[3]	Quantity sold ($)[4]
Metallic Minerals				
Bauxite	Tonnes	12 865 457	12 475 080	$524 922 658
Gold[6]	Grams	1 275	272	$12 240
Gold Dore[7]	Grams	16 988 266	14 489 759	$780 465 196
Iron Ore	Tonnes	0	0	$0
Manganese	Tonnes	6 386 814	6 216 596	$1 974 747 145
Mineral Sands - ilmenite	Tonnes	24 070	24 070	$6 023 311
Lead Concentrate	Tonnes	6 804	14 544	$18 057 727
Zinc Concentrate	Tonnes	43 916	41 866	$68 691 817
Zinc Lead Concentrate	Tonnes	479 348	499 072	$846 148 318
Metallic Minerals Value				**$4 219 068 412**
Non-Metallic Minerals				
Crushed rock	Tonnes	1 623 882	1 360 413	$35 943 723
Diamonds	Carats	754	4 494	$656 494
Dimension Stone	Tonnes	0	0	$0
Garnet Sand	Tonnes	2 158	1 115	$293 650
Gravel[8]	Tonnes	142 607	130 707	$1 630 563
Limestone	Tonnes	8 244	2 611	$51 520
Mineral Specimens	Tonnes	0.45	0.4	$72 183
Quicklime[9]	Tonnes	26 374	24 851	$6 181 292
Sand	Tonnes	247 578	194 497	$5 275 600
Soil	Tonnes	32 831	31 204	$505 551
Vermiculite	Tonnes	0	0	$0
Non-Metallic Minerals Value	n/a			**$50 610 576**
Energy Minerals				
Uranium Oxide	Tonnes	2 090	1 811	$220 139 144
Total Minerals Value	n/a			**$4 489 818 132**

Explanatory notes
1. Fiscal year is 1st July to 30th June.
2. Data is from production returns lodged by operators under statutory obligations.
3. *Quantity Sold ($)* is in AUD and is the gross amount paid to the operator.
4. Data has been rounded and autosum applied.
5. Data is correct as at 24 September 2018 and may be subject to revision due to late lodgements and/or receipt of superior data.
6. 'Gold' does not include gold reported as gold dore; it is typically gold found as nuggets.
7. Average metallic content of reported gold dore is approximately 90% gold and 10% silver and other metals.
8. Average sales values have been applied to some non-metallic minerals if this information was not supplied.
9. Quicklime is derived from limestone. Processing input and output data is deemed operator commercial-in-confidence.

Table 1. 2017/18 mining production statistics for the Northern Territory.

4287 m) beneath the ***Prospect***, ***Crosscourse*** and ***Lady Alice*** deposits. The results included a best intersection of 1.1 m at 95.0 g/t Au from Crosscourse and 3 m at 10.8 g/t Au from Prospect, and indicated the continuation of gold mineralisation at the three deposits below known mineral resources. In November, further results were announced from a 40 hole, 15 192 m drilling program at Union Reefs. The results identified high-grade near-surface mineralisation to the south of Lady Alice pit (best intersection of 7.2 m at 8.9 g/t Au including 0.45 m at 86.0 g/t Au), and confirmed the down-plunge continuity of mineralisation at Crosscourse. Mineralisation was also identified at depth at the southern end of Union Reefs. Kirkland Lake announced that continued exploration success at Union Reefs and in underground drilling at Lantern is increasing the company's confidence that a five-year mine plan can be established that could lead to the resumption of operations in 2019.

During 2018, PNX Metals Ltd (PNX) undertook a 3470 m RC and diamond drilling program on newly acquired leases at ***Fountain Head***, aimed at identifying additional mineralisation to complement their nearby Hayes Creek gold-silver-zinc project. The program was designed

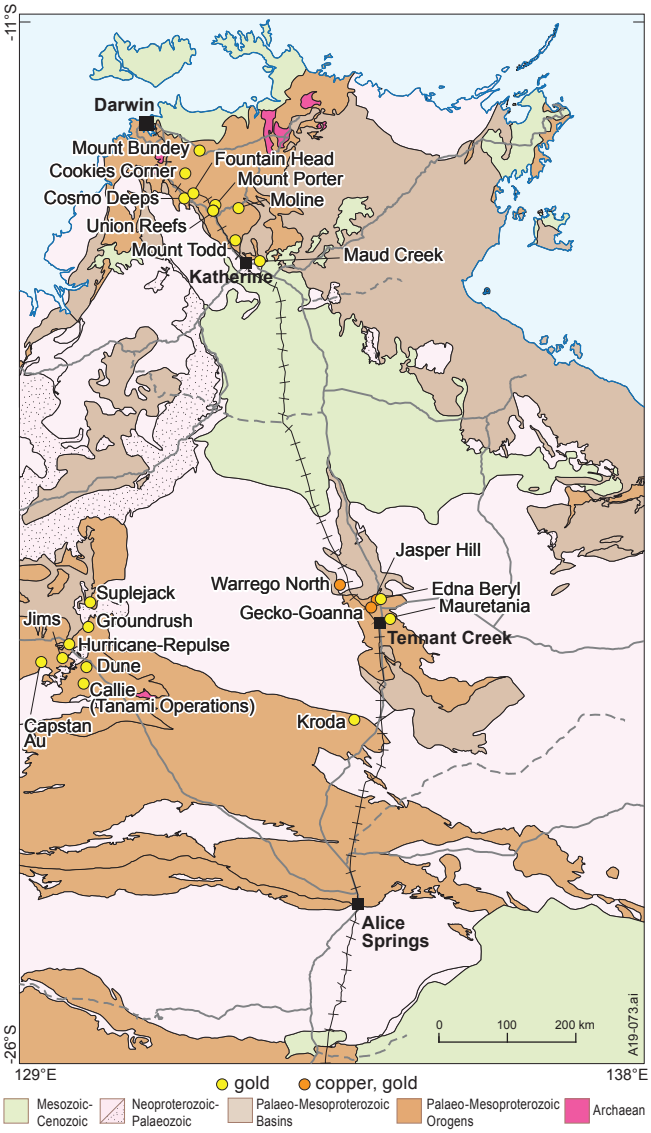

Figure 5. Location of gold and copper-gold deposits and projects mentioned in the text.

to test for gold mineralisation directly under the existing Fountain Head and ***Tally Ho*** historic mining areas and over a ~1.6 km strike extent to the northwest along the Fountain Head anticline. Highlights of drilling at Fountain Head include 3 m at 11.09 g/t Au from 93 m and 1 m at 28.0 g/t Au from 83 m. At the ***Banner*** prospect, 1.5 km northwest of Fountain Head, drilling tested a 500 m long, >1 g/t gold-in-soils anomaly and intersected high-grade gold with a best intersection of 6 m at 39.5 g/t Au from 54 m including 1 m at 215 g/t Au. In December, PNX announced drill intersections interpreted as being related to down-plunge extensions of the Tally Ho lode at Fountain Head, including 6.67 m at 11.35 g/t Au from 201 m. PNX have reported that the mineralisation intersected at Fountain Head contains coarse and 'nuggety' gold.

In October, PNX announced the results of a 16 hole, 1100 m RC drilling program at the ***Cookies Corner*** prospect, targeting the source of a consistent >0.1 g/t gold in soils anomaly. All holes intersected mineralisation associated with quartz-sulfide veins over a continuous 500 m strike, with a best intersection of 20 m at 1.93 g/t Au from 12 m, including 8 m at 4.29 g/t Au from 12 m. Cookies Corner is one of a cluster of gold targets in the northwest of PNX's ***Burnside*** exploration project located 4 km northeast to the historic ***Goodall*** mine at the convergence of the Pine Creek Shear Zone and the Howley Anticline.

PNX also commenced a diamond drilling program at the historic ***Moline*** goldfield, 38 km east-northeast of Pine Creek, to extend three previously drilled RC holes that did not reach target depth and to obtain samples for further metallurgical flotation test work. The company also announced that they plan to release Mineral Resource estimates for the Moline and ***Tumbling Dice*** prospects.

Privately-owned Bacchus Resources Pty Ltd continued gold exploration in the Pine Creek Orogen in 2018, including at their ***Woolwonga*** project, but no results have been publicly reported.

In July 2018, Ark Mines Ltd (Ark) announced that they had signed a binding term sheet with Territory Iron Pty Ltd to sell the ***Mount Porter*** gold project and associated Frances Creek project, 20 km north of Pine Creek. Mount Porter has Indicated and Inferred Resources of 355 000 t at 3.0 g/t Au for 34 200 oz of gold (1.7 g/t cut-off).

Primary Gold Ltd's ***Mount Bundey*** project includes the ***Toms Gully***, ***Rustlers Roost*** and ***Quest 29*** deposits, located 90 km southeast of Darwin. The project has total Indicated and Inferred Resources of 54.1 Mt at 1.03 g/t Au for a contained 1.795 Moz of gold. In May 2018, Hanking Australia Pty Ltd completed an off-market takeover of Primary Gold worth $37.5 million, and the company was removed from public listing.

Vista Gold Corporation (Vista) continued permitting and project optimisation work at their ***Mount Todd*** project, northwest of Katherine. Mineralisation at Mount Todd is contained in a stockwork of quartz veins and their margins, hosted within metamorphosed interbedded siltstone, shale and minor tuff of the Burrell Creek Formation. Mineral resources at Mount Todd include Measured and Indicated Mineral Resources of 279.6 Mt at 0.82 g/t Au containing 7.40 Moz of gold, and Inferred Mineral Resources of 72.5 Mt at 0.74 g/t Au containing 1.73 Moz of gold. Proven and Probable Ore Reserves are 222.8 Mt at 0.82 g/t Au containing 5.90 Moz of gold. During 2018, the company undertook high pressure grinding roll crusher and ore sorting tests with associated metallurgical test work. The company announced that the tests demonstrated the value-adding benefit of ore-sorting at Mount Todd; they plan to incorporate these results into a revised preliminary feasibility study in 2019.

Tanami–Arunta regions

Newmont Mining Corporation (Newmont)'s ***Tanami Operations***, located 550 km northwest of Alice Springs, has produced approximately 8 Moz of gold. It remains the Territory's largest gold operation, producing 408 000 oz of gold during 2017. Mineralisation consists of high-grade auriferous quartz veins in folded carbonaceous siltstone in the lower part of the Dead Bullock Formation. The operations include the flagship ***Callie*** deposit (>7.6 Moz), the 5.83 Moz ***Auron*** deposit, the >0.5 Moz ***Federation South Limb*** and the 2016 ***Liberator*** discovery. As of 31 December 2017, Proven and Probable Ore Reserves were 24.1 Mt at 5.69 g/t Au containing 4.41 Moz of gold. Additional Measured and Indicated Mineral Resources total 4.4 Mt at 5.07 g/t Au for 0.71 Moz of gold; Inferred Mineral Resources are 4.6 Mt at 5.42 g/t Au for 0.79 Moz of gold. The total pre-mining gold endowment at the mine was 14.2 Moz at the end of 2017, with resource additions of 4.21 Moz since 2012.

In August 2018, Nova Minerals Ltd announced that Newmont had earned a 70% interest in their ***Officer Hill*** project. Follow-up exploration will include diamond drilling, an airborne gravity survey and follow-up geochemistry around the ***Paris*** prospect, which was identified in 2017 using Newmont's proprietary Deep Sensing geochemistry technique.

During 2018, Northern Star Resources Ltd (Northern Star) continued to explore the Central Tanami Project (CTP) as part of a purchase and farm-in agreement with Tanami Gold NL, as well as their 100%-owned Tanami tenements. In the CTP area, regional aircore drilling programs were completed at ***Jim's Return***, ***Channel 4***, ***Terminus*** and ***Solarius*** prospects in the south and at the ***Free Fall*** area east of the ***Groundrush*** deposit. RC drilling programs were undertaken at ***Jims North***, ***Jims West***, and ***Carmen*** prospects; they returned anomalous results. Diamond drilling beneath the existing Jim's open pit returned significant gold intersections up to 170 m including 26 m at 3.88 g/t Au from 224 m and 10 m at 5.70 g/t gold from 401 m.

Northern Star also completed a program of RC and diamond drilling beneath the existing CTP treatment plant infrastructure, testing for potential shallow extensions to the main ***Hurricane–Repulse*** mineralisation. RC drilling intersected significant gold mineralisation at varying depths in all 23 drillholes completed. Significant intersections from the program included 3 m at 20.47 g/t Au from 140 m, 19 m at 4.64 g/t Au from 136 m, and 14 m at 3.19 g/t Au from 150 m. A single diamond drillhole testing the down plunge continuity of the newly discovered zones intersected mineralisation located ~130 m below the base

of the existing Hurricane pit, with 8.5 m at 6.6 g/t Au from 177.9 m. Northern Star reported that this confirms potential for significant depth extensions to the Hurricane–Repulse mineralisation.

At Northern Star's 100%-owned Tanami Regional Project, an extensive regional aircore drilling program was completed in the ***Supernova*** area, located approximately 60 km northwest of the CTP camp. Results defined isolated spot anomalies. Regional ground gravity surveys were also completed at Supernova.

During 2018, Prodigy Gold Ltd (Prodigy; formerly ABM Resources NL) focussed significant exploration at their greenfields ***Capstan project*** within their Bluebush project area, located 50 km to the northwest of the Callie deposit. Following encouraging results in 2017 that identified an 8 km long zone of gold anomalism in interpreted Dead Bullock Formation stratigraphy, a substantial aircore drilling program was undertaken in the first half of 2018 (**Figure 6**). This program defined extensive continuous trends of +50 ppb gold anomalism up to 4.5 km long and 750 m wide, with aircore drill results up to 4 g/t Au. In December 2018, Prodigy announced that follow-up RC drilling had defined a 1.2 km long zone of interest in the ***Capstan North*** prospect. Results included 4 m at 6.1 g/t Au from 128 m containing 1 m at 23.9 g/t Au. RC drilling was also undertaken at the Hat prospect at Capstan, with a best intersection of 4 m at 1.2 g/t Au from 111 m. Prodigy also drilled two stratigraphic diamond holes for 951.4 m, co-funded by NTGS under the Geophysics and Drilling Collaborations program, to better understand the stratigraphic setting of Capstan. Prodigy also undertook a 95 hole, 6550 m RAB drilling program at the ***Galaxy*** prospect, 30 km east of Capstan, where they identified an anomalous mineralised trend that extends to 6 km south of Jim's pit.

In July 2018, Prodigy announced an updated resource for their ***Suplejack*** project including the ***Hyperion–Tethys***, ***Seuss*** and ***Hyperion South*** deposits, located 17 km north-northeast of Groundrush. Indicated and Inferred Resources total 4.93 Mt at 1.95 g/t Au, containing 309 000 oz Au. The mineralisation remains open along strike and at depth. In December 2018, Prodigy announced results of a drilling program 200 m south of the existing resource area; drilling intersected thick quartz breccias in the Suplejack fault with intersections of 89 m at 0.3 g/t Au and 43 m at 0.4 g/t Au, both of which ended in mineralisation.

In July 2018, Prodigy announced the signing of a binding farm-in agreement with Newcrest Mining for Prodigy's ***Euro*** project area in the eastern Tanami whereby Newcrest will sole fund up to $12 million over seven years to ultimately earn up to a 75% interest in the project. An initial 8 hole, 1466 m RC program was completed at the ***Dune*** prospect in late 2018, targeting a structural repeat of Newmont's ***Oberon*** deposit located 1.6 km to the north. Four of the eight holes intersected zones of 3 g/t Au or more, with a best intersection of 2 m at 12 g/t Au from 105 m. The JV also completed IP surveys at Dune, and at ***Vivitar*** 20 km to the east.

Gladiator Resources Ltd (Gladiator) announced the results of their first drilling program at the North Arunta project, in which Gladiator are sole funding $6.5 million over 4.5 years to ultimately earn a 70% interest in the project from Prodigy, their joint venture partner. The project is located north and northwest of Barrow Creek, and includes the ***Kroda*** gold prospect. The program involved 12 RC and diamond holes for 2194 m at the Kroda 4 prospect, testing 350 m strike length of an IP anomaly defined in June–July 2018. The chargeability anomalies were interpreted as being in the plunge extension or duplication of gold mineralisation in historic holes at the prospect. All holes returned elevated gold over broad intervals associated with silicification, quartz veining, sulfides and elevated arsenic; the best intersection was 3 m at 1.4 g/t Au.

Warramunga Province (gold-copper-bismuth)

Emmerson Resources Ltd (Emmerson) continued to explore the Tennant Creek mineral field during 2018, with a major restructure of joint venture arrangements and alliances. In February 2018, Emmerson announced it had agreed with Evolution Mining to restructure the Tennant Creek Mineral Field Joint Venture whereby Evolution would forego its right to a 65% interest in the entire JV area and instead, take a 100% interest in the area of the JV that contains the ***Gecko***,

Figure 6. Airborne magnetic survey plane (NTGS Tanami survey) flying over Prodigy aircore rig, Tanami Desert. Photo provided by Prodigy.

Goanna and ***Orlando*** copper-gold deposits. Emmerson resumed ownership of the remaining 94% of the JV area.

In April 2018, Emmerson announced that it had sampled historic drill core from ***Jasper Hills*** in the Northern Corridor of the Tennant Creek field. Sample results returned high-grade cobalt, copper and gold intersections including 28 m at 5.83 g/t Au, 0.17% Co and 8.52% Cu from 108 m, and 14 m at 6.72 g/t Au, 0.28% Co and 2.17% Cu from 284 m. In June, Emmerson announced that RC drilling program at the ***Mauretania*** prospect intersected high-grade gold, silver, and copper with elevated bismuth and cobalt, including 26 m at 8.9 g/t Au, 85 g/t Ag, 0.49% Cu and 0.13% Bi from 53 m; 6 m at 18.9 g/t Au and 0.46% Bi; and 9 m at 2.6 g/t Au, 22.8 g/t Ag, 2.3% Cu and 0.12% Co.

In September 2018, Emmerson announced it had entered a strategic alliance with Territory Resources Limited (Territory Resources) for a mining and exploration joint venture of the Southern Project Area (SPA) at Tennant Creek that includes the historic ***Nobles Nob***, ***Juno***, ***Peko*** and ***Eldorado*** mines. As part of the alliance, Territory Resources will contribute $5 million over 5 years to earn a 75% equity in the SPA, with Emmerson being the operator and manager during the earn-in period. The alliance also involves the sale of the Warrego mill and associated lease to Territory in exchange for Territory building a 300 000 tpa carbon in pulp processing facility on the site. The alliance aims to fast-track development of Emmerson's small mining projects with processing at the new mill.

Small-scale gold mining at the high-grade ***Edna Beryl*** deposit, located 40 km north of Tennant Creek, was suspended for most of 2018. It had commenced in 2017 under a tribute mining agreement with the Edna Beryl Mining Company. In December 2018, Emmerson announced that Territory Resources has purchased the Edna Beryl Mining Company, and had immediate plans to develop and recommence mining in the tribute area at Edna Beryl.

In August 2018, Chalice Gold Mines Ltd announced that they had completed four RC drillholes for 1206 m targeting Tennant Creek-style copper-gold mineralisation at their ***Warrego North*** project, 20 km northwest of the historic Warrego mine. The drilling targeted coincident magnetic and gravity anomalies at the ***Emu*** prospect, thought to possibly represent ironstone units prospective for copper-gold mineralisation. All holes intersected highly magnetic dolerite intrusions with sporadic, low tenor copper mineralisation and no significant gold.

Copper, lead, zinc, silver

Arunta Region

During 2018, KGL Resources Ltd (KGL) continued infill and extension drilling at the ***Jervois*** copper-silver project northeast of Alice Springs (**Figure 5**), particularly focussed on the ***Rockface*** and ***Reward*** deposits. Mineralisation at Jervois occurs in a series of stratabound, subvertical sulfide-rich deposits along a 12 km strike length in the Bonya Metamorphics in the Aileron Province. Results from drilling announced in the early part of 2018 included 7.55 m at 5.43% Cu, 16.5 g/t Ag and 0.35 g/t Au from 732.72 m at Rockface, and 9.12 m at 3.55% Cu, 30.1 g/t Ag and 0.67 g/t Au from 635.9 m at Reward Deeps. In May 2018, KGL announced an updated Mineral Resource for the Jervois project with a higher copper cut-off grade of 1% Cu for resources assumed to be accessible by underground mining. This was subsequently updated in January 2019 with increased Indicated Resources. The January 2019 copper-rich resource is 21.9 Mt at 1.63% Cu and 20.2 g/t Ag, including an Indicated and Inferred Resource for the Rockface underground of 3.58 Mt at 2.58% Cu. If copper and silver contained in the existing (2015) lead-zinc resource (3.8 Mt at 3.7% Pb, 1.2% Zn, 0.72% Cu and 67.5 g/t Ag) is included, the total resource of the project is 25.8 Mt at 1.49% Cu and 27.1 g/t Ag, containing 385 200 t of copper.

Drilling at Jervois during 2018 occurred at Rockface, Reward and ***Morely***; the program intersected high-grade mineralisation including 6.16 m at 7.84% Cu, 0.07% Pb, 0.19% Zn, 37.7 g/t Ag and 0.66 g/t Au from 684.6 m at Rockface, and 9.29 m at 4.22% Cu, 0.28% Pb, 0.37% Zn, 67.5 g/t Ag and 0.82 g/t Au from 99.7 m in the oxidised zone at Reward. KGL lodged its Environmental Impact Statement for the project in October 2018.

In June 2018, Todd River Resources Ltd announced the discovery of high-grade polymetallic base metal mineralisation at the EM1 target at the ***Mount Hardy*** copper-zinc project area, 300 km northwest of Alice Springs. The first drilling program at EM1 tested an electromagnetic (EM) conductor and intersected a broad interval of massive brecciated sulfides, which assayed 25.15 m at 2.4% Cu, 4.0% Zn and 3.1% Pb from 184 m, including 9.15 m at 4.5% Cu, 7.6% Pb and 8.8% Zn from 200 m. In August, further high-grade intersections were announced, including 13.45 m at 15.9% Zn, 0.9% Cu, 5.75% Pb and 83 g/t Ag from 358.55 m, and 55.75 m at 1.0% Cu, 1.5% Pb 3.3% Zn and 43.5 g/t Ag from 131.5 m (not true width), including 7.92 m at 1.4% Cu, 5.0% Pb, 13.8% Zn and 212.3 g/t Ag from 179.38 m. In November, they announced that the deepest and northernmost hole drilled to date at EM1 had intersected a wide high-grade intersection of 35.5 m at 14.7% Zn, 2.92% Pb, 0.91% Cu and 59 g/t Ag from 431.5 m; this included 11.3 m at 22.9% Zn, 3.35% Pb, 1.00% Cu and 58 g/t Ag from 443.6 m. The company has announced that the main EM1 mineralised zone has now been extended to a vertical depth (down-dip) of ~600 m and remains open in all directions; both downhole EM and moving loop EM have generated further conductors for testing.

Independence Group NL (IGO) continued their greenfields exploration in the remote southwestern Aileron Province over a 13 000 km^2 project area north and northeast of Kintore where IGO is targeting polymetallic mineralisation as part of the Lake Mackay exploration alliance with Prodigy. This followed the discovery of polymetallic copper-silver-gold-zinc mineralisation at the ***Bumblebee*** prospect in 2015 and at the ***Grapple*** prospect in 2016 and 2017. During 2018, IGO undertook large-scale regional airborne EM (SPECTREM) surveys, with more than 8000 line km acquired by the end of September. Thirty-nine anomalies from the airborne survey were selected for ground moving loop EM (MLEM) surveys, which commenced in September. IGO also undertook further reconnaissance and selective infill soil sampling across the

project area; results identified a number of new gold-copper, nickel-cobalt and gold-only anomalies. The company have announced that they are planning 9600 m of RC drilling before the end of the 2018/19 financial year.

In November 2018, Thor Mining PLC announced a maiden Inferred Mineral Resource of 230 000 t at 2.0% Cu for the historic ***Bonya*** copper mine, 20 km west of Jervois, which they hold in joint venture with Arafura Resources.

Pine Creek Orogen

PNX Metals Ltd (PNX)'s ***Hayes Creek*** project comprises the ***Iron Blow*** and ***Mount Bonnie*** polymetallic gold-silver-zinc deposits in the basal Mount Bonnie Formation and Gerowie Tuff of the Pine Creek Orogen. Combined Indicated and Inferred Mineral Resources for the project total 4.1 Mt at 1.8 g/t Au, 124 g/t Ag, 4.35% Zn, 0.91% Pb and 0.25% Cu. In February 2018, PNX announced the results of extensional drilling at Mount Bonnie conducted in late 2017. The drilling intersected zinc, gold and silver mineralisation in 15 drillholes outside of the existing Mineral Resource envelope, extending the known mineralisation by approximately 35 m, with a best intersection of 4 m at 6.14% Zn, 1.14 g/t Au, 176 g/t Ag, 1.29% Pb, 0.11% Cu from 73 m, including 2 m at 10.28% Zn, 1.92 g/t Au, 304 g/t Ag, 2.11% Pb, 0.17% Cu. During the year, PNX submitted a Notice of Intent for development of Hayes Creek and continued to progress a definitive feasibility study.

The ***Browns*** deposit near Batchelor comprises a large sediment-hosted polymetallic oxide and sulfide resource that was briefly developed by Compass Resources Ltd in 2007–08. Doe Run Australia, a subsidiary of North American lead producer The Doe Run Company, continued exploration and appraisal activities at the project in 2018; no results have been publicly announced.

McArthur Basin

The ***McArthur River*** mine, situated about 70 km southwest of Borroloola in the McArthur Basin, is operated by McArthur River Mining Pty Ltd (MRM), a subsidiary of Glencore. At 31 December 2018, the McArthur River mine had total Reserves and Resources of 172 Mt at 9.8% Zn, 4.6% Pb and 47 g/t Ag, including Ore Reserves of 108 Mt at 9.0% Zn, 4.3% Pb and 44 g/t Ag. During 2018, MRM produced 254 300 t of zinc, 49 900 t of lead and 1.72 Moz of silver in concentrate, representing a 23% increase in zinc production from 2017. The very fine-grained, thinly bedded sulfide ore is hosted in the HYC Pyritic Shale Member of the Barney Creek Formation. In August 2018, the company received an Assessment Report from the NT Environmental Protection Agency (EPA) that provided conditions for the approval of waste rock management for the remaining 30 years of the project's mine life.

A second major shale-hosted zinc resource occurs at the ***Teena*** zinc deposit, 10 km west of the McArthur River mine. Teena was discovered in 2013 by a Teck Australia (Teck)–Rox Resources joint venture. The 2016 Inferred Mineral Resource at Teena is 58 Mt at 11.1% Zn and 1.6% Pb for 6.5 Mt of zinc and 0.9 Mt of lead metal (at a 6% Zn+Pb cut-off). No exploration results have been publicly reported from Teena during 2018.

In March 2018, Marindi Metals Ltd announced that it had entered into a binding agreement with Japan Oil Gas and Metals Corporation (JOGMEC) under which JOGMEC can earn up to 70% of their ***Carinbirini*** zinc project north of McArthur River mine by funding $4 million in exploration over 3 years. In September 2018, Marindi announced the commencement of a major diamond drilling campaign targeting three coincident gravity and versatile time-domain EM (VTEM) targets, projected to be in the Barney Creek Formation within 500–800 m of the surface. Results of this drilling are pending.

During 2018, Pacifico Minerals undertook a 37 hole, 1100 m aircore drilling program at the ***Lorella*** project, part of their Borroloola West JV with Sandfire Resources Ltd. The aircore program was designed to test for extensions of the known oxide copper mineralisation along strike from shallow flat-lying mineralisation identified by Sandfire Resources. The drilling encountered low-grade copper mineralisation, with a best intersection of 16 m at 0.32% Cu from 23 m.

In August and September 2018, Todd River Resources Ltd undertook a program of three diamond holes for 1393.1 m at their McArthur project, 75 km south-southwest of McArthur River mine. The holes were designed to test geophysical anomalies within the Mallapunyah and Wollogorang formations that were outlined from a 2017 SkyTEM airborne EM survey. The company reported that modest base metal intersections were noted.

MMG Exploration Pty Ltd (MMG) continued to actively explore in the Batten Fault Zone area in the McArthur Basin under their North Batten JV with Sandfire Resources, as well as on their own tenure. Sandfire reported that MMG undertook a significant geophysical and drilling program across the JV tenements in 2019, with no results publicly reported.

Diamonds

Merlin Diamonds Ltd's ***Merlin*** project (**Figure 7**) in the McArthur Basin comprises 14 kimberlite pipes of which nine were subject to open cut mining between 1998 and 2003, producing 507 000 ct of diamonds. The 2014 combined Probable Ore Reserve for all diamond pipes at Merlin was 2.02 Mt at 0.15 carats per tonne (ct/t) for a total of 0.61 Mct. The Indicated and Inferred Mineral Resource was 27.8 Mt at 0.16 c/t for a total of 4.35 Mct. Small-scale mining continued at Merlin during 2018 with production 3539 ct diamonds reported from the ***Ector*** deposit and from stockpiles between May and December 2018.

Bauxite and alumina

Rio Tinto Ltd operates the ***Gove*** bauxite mine in northeastern Arnhem land, which has been in production since 1971. Bauxite at Gove occurs in deeply lateritised, dissected plateau remnants overlying the Cretaceous Yirrkala Formation. At the end of 2017, the Gove operation had Proven and Probable Ore Reserves of 147 Mt at 49.4% Al_2O_3, with additional Measured, Indicated and Inferred Mineral Resources of 33 Mt at 49.3% Al_2O_3. During 2018, the Gove operation produced a record 12.54 Mt of bauxite, a 12% increase on 2017.

A new bauxite mine is in operation on the ***Dhupuma Plateau***, immediately south of the Gove mineral lease. It is run by the Aboriginal-owned Gulkula Mining Company Pty Ltd. The operation opened in August 2017 and is expected to ramp up to full annual production of 500 000 tpa bauxite within the first four years. It has a projected 15 year mine life at this rate of production. The mine is associated with a Mining Training Centre for local Aboriginal people, established with the support of Rio Tinto. The ore is sold to Rio Tinto's Gove operation.

Iron ore

During 2018, Territory Resources submitted a Notice of Intent for the ***Yarram*** iron deposit near Batchelor. The company have reported a Mineral Resource estimated at 15.1 Mt at 52.1% Fe and 0.24% P using a cut-off grade of 45% Fe. The deposit includes 4.5 Mt of higher grade ore (61.7% Fe) with lower phosphorus, suitable as either direct shipping ore or for blending with low grade ore to produce a saleable product. Territory Resources is proposing a small mining operation producing up to 1 Mt per annum.

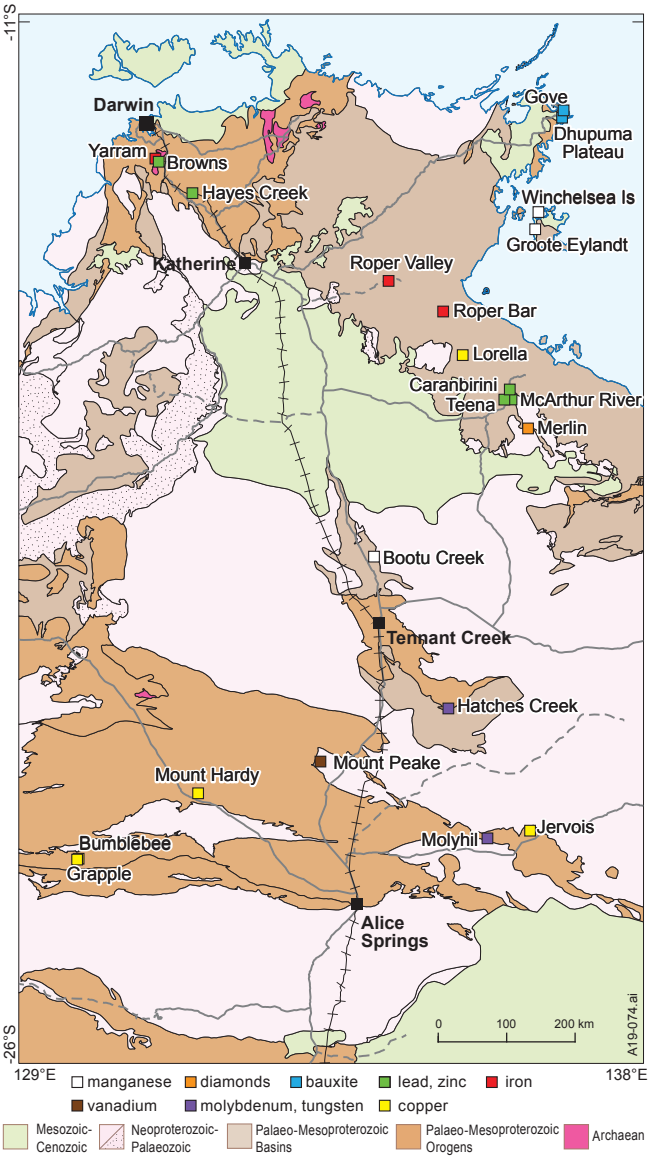

Figure 7. Location of copper, lead-zinc-silver, diamond, manganese, tungsten-molybdenum, vanadium and graphite deposits and projects mentioned in the text.

In February 2018, Britmar (Aust) Pty Ltd (Britmar) received approval for its Mining Management Plan for the ***Roper Bar*** iron ore mine, 55 km southeast of Ngukurr. No production has been reported for 2018. Northern Territory Iron Ore have a Notice of Intent in place for the development of iron ore from three deposits (Deposits C, W and X) at their ***Roper Valley*** project, 150 km east of Mataranka. Iron ore would be transported to a purpose-built barge loading facility located near the mouth of the Roper River and then transhipped by barges to ocean going vessels moored offshore in the Gulf of Carpentaria.

Manganese

Oolitic and pisolitic ore in Mesozoic sedimentary rocks on ***Groote Eylandt*** in the Gulf of Carpentaria forms one of the world's highest-grade manganese deposits. It has remaining resources of 157 Mt at 44.1% Mn. The mineralisation is a stratiform sedimentary deposit in shallow marine Cretaceous sediments, and is commonly oolitic or pisolitic. It was discovered in 1960 and has been continuously mined since 1966 by the Groote Eylandt Mining Company (GEMCO, a majority owned by South32 Ltd). Production from Groote Eylandt in 2017/18 totalled 5.66 Mt of manganese ore.

In January 2019, an exploration licence covering part of ***Winchelsea Island***, off the northwest coast of Groote Eylandt, was granted to the Winchelsea Mining Pty Ltd. This is a joint venture between the Anindilyakwa Advancement Aboriginal Corporation (AAAC) and AUS China International Mining. AAAC, the majority partner, consists of the two Traditional Owner clans of Winchelsea Island. They plan to explore for manganese of a similar style to Groote Eylandt.

A second manganese mine in the NT is hosted in Proterozoic rocks at ***Bootu Creek***, 110 km north of Tennant Creek. OM Manganese Ltd began mining operations at Bootu Creek in November 2005. At 31 December 2017, the total Reserves and Resources for Bootu Creek were 9.95 Mt at 22.4% Mn, with an Ore Reserve of 7.32 Mt at 20.7% Mn. During 2018, OM mined 1.82 Mt of manganese ore at an average grade of 21.94% Mn, producing lumps and fines totalling 814 040 t at 35.77% Mn. A tailings retreatment plant at Bootu Creek is expected to be commissioned in 2019 and will produce approximately 250 000 t per annum of manganese fines with an average grade of between 36% to 38% Mn for 8 years.

Tungsten (-molybdenum)

Thor Mining PLC continued to pursue options for development of the ***Molyhil*** tungsten-molybdenum project located near the Plenty Highway northeast of Alice Springs. Molyhil is a skarn-related scheelite–molybdenite–magnetite deposit within the Aileron Province with a Mineral Resource of 4.71 Mt at 0.28% WO_3, 0.22% MoS_2 and 18.1% Fe, most of which is in the Indicated category, and an open cut Probable Ore Reserve of 3.5 Mt at

0.29% WO_3 and 0.12% MoS_2. During 2018, the company announced an updated definitive feasibility study for a mining operation at Molyhil with a seven-year mine life with potential for subsequent underground mining. The company also finalised acquisition of a 40% interest in the nearby Bonya project area, including a number of outcropping tungsten deposits.

Following drilling programs carried out in 2016 and 2017, GWR Group Ltd announced an Exploration Target of 11.9 to 16.5 Mt at 0.2–0.5% WO_3 for the historic ***Hatches Creek*** tungsten field in the Davenport Province. The Hatches Creek field contains numerous underground mines that were mined between 1915 and 1957. Mineralisation is hosted in quartz veins containing wolframite with lesser scheelite, bismuth and copper oxides. Surface stockpiles of historically mined ore have an Inferred Resource of 225 066 t at 0.58% WO_3 for 1311 t of tungsten trioxide. In September 2018, GWR Group announced they were selling the project to Tungsten Mining NL; the company later announced that the transaction as originally structured was unable to proceed.

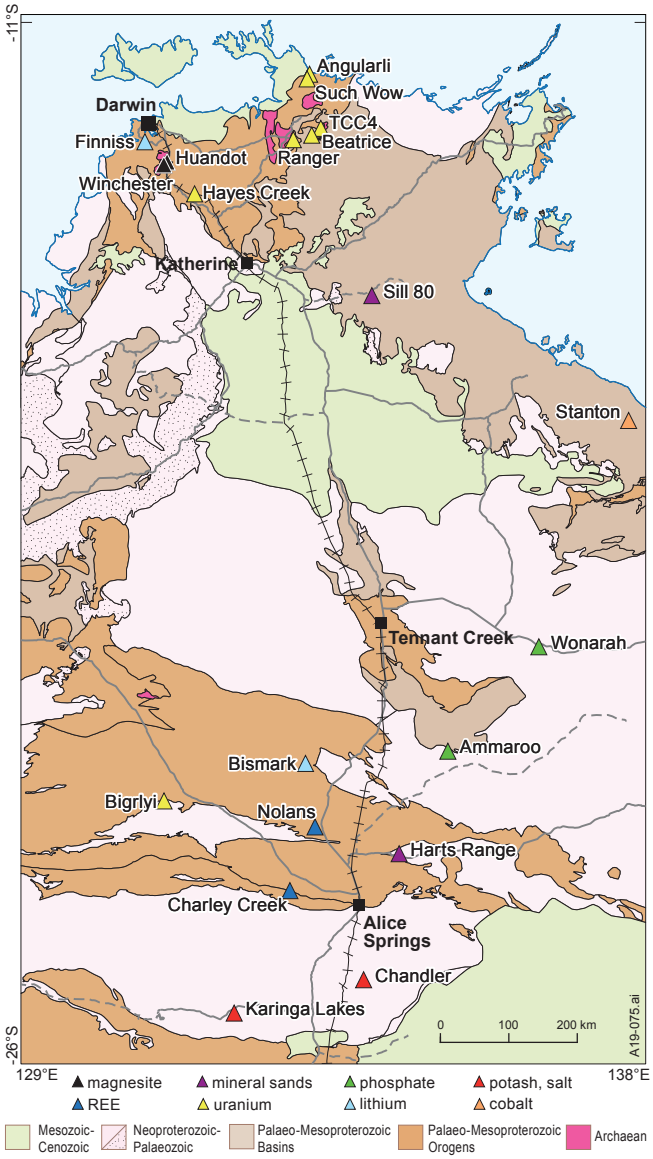

Figure 8. Location of magnesite, mineral sands, rare earths, lithium, phosphate, potash, salt and uranium deposits and projects mentioned in the text.

Vanadium-titanium-iron

TNG Limited's ***Mount Peake*** project contains a vanadium-titanium-iron deposit hosted in the Mount Peake Gabbro in the northern Aileron Province, 60 km west-southwest of Barrow Creek. It contains Measured, Indicated and Inferred Mineral Resources of 160 Mt at 0.28% V_2O_5, 5.3% TiO_2 and 23.0% Fe, and a Probable Ore Reserve of 41.1 Mt at 0.42% V_2O_5, 7.99% TiO_2 and 28.0% Fe at a cut-off grade of 15% Fe. During 2018, TNG Limited received Commonwealth and NT environmental approvals for the project, and subsequently was granted a Mining Lease. The company continued to progress financing and offtake arrangements.

Magnesite

A number of high-grade magnesite (magnesium carbonate) deposits occur near Batchelor in the Pine Creek Orogen (**Figure 8**). They consist of stratabound bodies within the Celia and Coomalie Dolostones. The deposits include ***Winchester*** (Korab Resources Ltd), with Indicated and Inferred Mineral Resources of 16.6 Mt at 43.2% MgO and ***Huandot*** (Thessaly Resources Pty Ltd), 7 km northeast of Winchester, with Indicated and Inferred Mineral Resources of 9.1 Mt at 44.3% MgO. Korab announced during 2018 that they were investigating various development options including direct shipping of magnesite rock, export of dead burned magnesia and export of caustic calcined magnesia.

Mineral sands

The ***Harts Range*** garnet sand deposit, located 170 km northeast of Alice Springs, is operated by Australian Abrasive Minerals Pty Ltd (AAM). After a year in administration, AAM announced in October 2018 that it had obtained finance and was recommissioning the processing plant for a return to production in 2019.

In 2018, Australian Ilmenite Resources Pty Ltd continued commissioning and recommenced production at the ***Sill 80*** ilmenite project in the Roper region. Ilmenite at Sill 80 occurs in surficial cover overlying sills of Derim Derim Dolerite intruding the Roper Group.

Rare earth elements

Arafura Resources Ltd (Arafura) continued to progress the ***Nolans*** rare earth-phosphate project located in the Reynolds Range, 135 km northwest of Alice Springs. Measured, Indicated and Inferred Mineral Resources at Nolans total 56 Mt at 2.6% rare earth oxides (REO), 11% P_2O_5 and 0.02% U_3O_8, containing 1.46 Mt rare earth oxides. The most abundant rare earth-bearing minerals at Nolans are apatite, monazite and allanite, with 26.4% of the mix represented by neodymium and praseodymium (NdPr). In November 2018, Arafura announced that it would build its final rare earths separation plant on site at Nolans rather than offshore. In February 2019, they further announced the results of a definitive feasibility study for the Nolans project. The planned operation will have a 23-year life and produce 4357 tpa of neodymium and praseodymium oxide and 135 808 tpa of phosphoric acid.

The plant will also produce mixed middle-heavy rare earth (SEG–HRE) carbonate and cerium hydroxide.

Lithium

Core Lithium Ltd (Core; formerly Core Exploration Ltd) continued to explore and define additional resources at their ***Finniss*** lithium project, which forms part of the Bynoe pegmatite field, 20–50 km south-southwest of Darwin. Lithium mineralisation in the Bynoe field occurs as spodumene (**Figure 8**) hosted in north-trending pegmatites up to 40 m in width, which occur along a 30 km north-trending corridor. Following the announcement of a maiden lithium Mineral Resource of 1.8 Mt at 1.5% Li_2O at the ***Grants*** prospect in May 2017, the company undertook further infill and extensional drilling, which returned high-grade intersections outside the existing resource, such as 45 m at 1.72% Li_2O from 188 m including 22 m at 2.09% Li_2O. In October 2018, the Mineral Resource at Grants was increased to 2.89 Mt at 1.5% Li_2O, with over one third in the Measured category. In May 2018, Core announced a maiden Mineral Resource for the *BP33* deposit, 6 km south of Grants; in November, they announced a subsequent upgrade to the size and confidence of the BP33 resource, reporting an Indicated and Inferred Resource of 2.15 Mt at 1.5% Li_2O. In late 2018 and January 2019, the company announced maiden Inferred Resources for the ***Sandras*** (1.3 Mt at 1.0% Li_2O), ***Carlton*** (0.79 Mt at 1.3% Li_2O) and ***Hang Gong*** (1.4 Mt at 1.2% Li_2O) deposits, bringing the total combined Mineral Resource for the Finniss project area to 8.55 Mt at 1.33% Li_2O for 115 700 t contained Li_2O. Core also announced promising exploration results from other prospects including ***Lees-Booths Link*** (13 m at 1.46% Li_2O from 193 m), and ***Turners*** and ***Talmina 3*** prospects in the southern part of the project area. Drilling results at Hang Gong and Lees-Booths Link suggest that pegmatites in these areas are shallowly-dipping and stacked, unlike the sub-vertical pegmatites at Grants and BP33.

PNX Metals Ltd announced in July 2018 that surface rock chip samples from their newly acquired ***Kilfoyle*** project, near Daly River, 130 km south-southwest of Darwin, returned high grades of lithium. This included rock chip sample assays up to 7.16% Li_2O at the ***White Rocks*** prospect, and up to 6.24% Li_2O at the northern end of the ***Goosewing*** trend. This trend also hosts evidence of historic small-scale tin-tantalum workings and indicates a strike of at least 10 km in length.

In July 2018, Kingston Resources Ltd announced the sale of its Bynoe and Arunta lithium tenements to private company Lithium Plus Pty Ltd for $1.8 million.

In the northern Aileron Province, Todd River Resources Ltd announced the results of petrography on pegmatites from the ***Bismark*** prospect near Barrow Creek that returned rock chip values of up to 4.63% Li_2O. The petrography confirmed that the pegmatites contain 33–52% spodumene.

Cobalt

In April 2018, Northern Cobalt Ltd (N27) announced an updated resources for the ***Stanton*** cobalt-copper-nickel deposit, part of their Wollogorang project in the McArthur Basin near the Queensland border. Following a major drilling program in late 2017, N27 announced an updated Indicated and Inferred Mineral Resource totalling 942 000 t at 0.13% Co, 0.06% Ni and 0.12% Cu. The mineralisation as flat lying, stratabound, occurs from surface and is non-refractory (predominantly comprising the cobalt sulfide mineral siegenite). In the first half of 2018, N27 undertook a 973 hole aircore (AC) drilling program, testing for near-surface cobalt over magnetic lows. Of the 75 magnetic features tested, 21 had significant cobalt anomalism (>100 ppm Co) in the equivalent horizon to that exposed at the surface at Stanton. These 21 targets were prioritised for a follow-up drill program that commenced in August 2018. At the first priority target at the ***GregJo*** prospect, drilling intersected broad intervals of shallow copper mineralisation of 9–20 m at 0.2%–0.5% Cu, including higher grade intervals of 1–4 m at between 1 and 5% Cu. The mineralisation is spatially associated with two structures within the GregJo fault. At the ***Running Creek*** prospect, 1.8 km east of Stanton, drilling intersected significant copper with cobalt mineralisation, with 55 m at 0.78% Cu from surface, including 13 m at 2.01% Cu and 12 m at 380 ppm Co. This followed re-interpretation of historic drilling that suggested the mineralisation is controlled by a northeast-trending structure. An IP survey over the prospect has identified a large chargeable feature at depth beneath the existing mineralisation that remains to be tested.

In the Tennant Creek mineral field, Emmerson announced that it had sampled historic drillcore from ***Jasper Hills***, within the Northern Corridor of the field. Sampling returned the following high-grade cobalt, copper and gold intersections: 28 m at 0.17% Co, 5.83 g/t Au and 8.52% Cu from 108 m including 19 m at 0.47% Co, 11.4% Cu and 0.56 g/t Au; 14 m at 0.28% Co and 6.72 g/t Au; and 2.17% Cu from 284 m including 2 m at 1.32% Co and 2% Cu. Emmerson reported that the high-grade cobalt zone transgresses the copper and consists mainly of cobaltite in association with chalcopyrite and digenite.

As part of the Lake Mackay joint venture managed by IGO, Prodigy announced assay results from rock-chip samples of up to 2.5% Co, 1.1% Ni and 46.4% Mn from pyrolusite-bearing duricrust overlying a gabbronorite intrusion at their ***Grimlock*** prospect northeast of Kintore.

Phosphate

Verdant Minerals Ltd's (Verdant) ***Ammaroo*** phosphate project is located in the southern Georgina Basin, ~80 km east of Barrow Creek. The project has Indicated Mineral Resources of 165 Mt at 15.5% P_2O_5, and total Measured, Indicated and Inferred Mineral Resources of 1.141 Bt at 14% P_2O_5 at 10% P_2O_5 cut-off. In May 2018, Verdant released a bankable feasibility study for the project for a proposed mining operation with an initial stage producing 1 Mtpa of rock phosphate concentrate (33% P_2O_5), then increasing to 2 Mtpa. The project received Federal Government environmental approval in June 2018 and NT EPA approval in October 2018.

In August 2018, Avenira Ltd announced that a demonstration plant, run by their technology partners JDC Phosphate Inc, had successfully produced high-quality super-phosphoric acid from low-quality (14%) phosphate rock tailings; they reported that this technology is potentially applicable to their large ***Wonarah*** phosphate project in the Georgina Basin.

In November 2018, Phosphate Australia Limited announced it had granted an Option to sell its wholly owned ***Highland Plains*** phosphate project to a private Canadian company, P2O5 Resources Inc.

Potash

The NT's only advanced potash project is Verdant's ***Karinga Lakes*** project, located between Erldunda and Curtin Springs, 200–300 km southwest of Alice Springs. The project area contains hundreds of salt lakes representing the eastern extension of the Lake Amadeus system. Measured, Indicated and Inferred Mineral Resources at Karinga Lakes are 8.4 Mt K_2SO_4 at an average resource thickness of 17 m and contained beneath 25 lakes with a total area of 132 km^2. The average potassium grade in the resource is 4760 mg/l (at 3000 mg/l cut-off). Consolidated Potash Corporation (formerly Aqua Guardian Group Ltd) have entered into a $3 million earn-in agreement to earn up to 40% of the project through staged evaluation of their mineral processing technology in producing sulfate of potash at Karinga Lakes. In the first half of 2018, they completed evaporation trials of an 8000 litre brine sample, which provided mixed potash salts for pilot testing. They continued to test the performance of the aMES™ technology on brine and salt samples from the project. A new evaporation trial with 11 400 litres of brine commenced in September 2018.

Salt

Tellus Holdings Ltd (Tellus) continued plans to develop an underground rock salt mine at their ***Chandler*** project near Titjikala located 120 km south of Alice Springs in the Amadeus Basin. The project consists of a proposed underground salt mine with a waste storage and isolation facility in the voids (rooms) created by underground mining. The project is focussed on a halite resource within a flat-lying, extensive evaporite unit (in excess of 200 m thick) within the Cambrian Chandler Formation. Chandler contains a Measured Mineral Resource of 309 Mt NaCl, and Indicated and Inferred Mineral Resources of 1.128 Bt NaCl and 3.103 Bt NaCl respectively, with an average halite grade of 88.6%. The total thickness of the deposit varies between 220–261 m. In 2018, Tellus continued to progress regulatory approvals for the Chandler project and have received NT and Commonwealth environmental assessment reports.

Uranium

The Territory's only operating uranium mine is at ***Ranger***, which is hosted in the lower Cahill Formation in the Pine Creek Orogen, and which has been in production since 1981. During 2017, Energy Resources of Australia Ltd (ERA) produced 1999 t of uranium oxide from the Ranger mine, a 15% decrease from 2017. All production was from stockpiles from the Ranger 3 open pit, which is now backfilled and being used as tailings facility. At the end of 2018, Ore Reserves at Ranger (entirely within stockpiles from Ranger 3 pit) are 4.90 Mt at 0.076% U_3O_8 for 3735 t of uranium oxide, (at 0.06% U_3O_8 cut-off); additional Mineral Resources (in stockpiles and in Ranger 3 Deeps) are 46.74 Mt at 0.12% U_3O_8 for 54 701 t of uranium oxide. No exploration was undertaken in 2018, and the exploration decline for the Ranger 3 Deeps deposit remains in care and maintenance.

In March 2018, Vimy Resources Ltd (Vimy) announced that it has acquired the Alligator River Project in western Arnhem Land from Cameco Australia Pty Ltd. This includes the King River–Wellington Range project JV with Rio Tinto (who own 25% of the JV). The JV includes the ***Angularli*** deposit, which was discovered by Cameco. In late March, Vimy announced a maiden Inferred Mineral Resource for the Angularli deposit of 0.91 Mt at 1.3% U_3O_8 for 25.89 Mlb (11 558 t) of uranium oxide. The resource was calculated on the basis of diamond drilling undertaken by Cameco, which included high-grade intersections of 22.9 m at 4.63% U_3O_8 from 244.6 m and 25.4 m at 1.62% U_3O_8 from 235.4 m. In late 2018, Vimy undertook a wide-spaced 10 hole, 2868 m RC drilling program at Angularli, focusing on broad alteration haloes along strike and within parallel structures to the Angularli deposit. Five of these holes located southwest of the deposit intersected significant Angularli-style hydrothermal alteration with anomalous uranium mineralisation. In December 2018, Vimy announced the results of a scoping study for a mining operation at Angularli in which underground mining would be undertaken over approximately 36 months after a pre-production mine development period of approximately 12 months. The study assumed that mining at Angularli would be undertaken using conventional long-hole open stoping methods. This would allow for the underground mine workings to be used for disposal of all the process tailings as paste fill and eliminates the need for a surface tailings storage facility.

Also during 2018, Vimy undertook a six hole, 1416 m RC drilling program at the ***Such Wow*** prospect, 15 km south of Angularli, targeting broad alteration haloes coincident with northwest to north-northwest-striking fault zones. All drillholes intersected significant hydrothermal alteration with anomalous uranium mineralisation, including a broad 30 m-wide zone in one hole.

In September–October 2018, Alligator Energy Ltd undertook a seven hole, 2138 m drilling program at the ***TCC4*** prospect, part of their Alligator Rivers uranium project in west Arnhem Land. The drilling targeted the northeastern end of a 4 km long zone of coincident SAM geophysical and radiogenic pathfinder surface anomalies. Five holes intersected key target features including graphitic schists of the Cahill Formation, and chlorite and hematite alteration in both basement and overlying sandstone cover.

Energy Metals Ltd (Energy Metals) have uranium projects in the Ngalia Basin northwest of Alice Springs, including the ***Bigrlyi*** uranium deposit, which has total

Indicated and Inferred Mineral Resources of 7.5 Mt at 0.13% U_3O_8 and 0.12% V_2O_5 at a 500 ppm U cut-off for a contained 9600 t of uranium oxide and 8900 t of vanadium oxide. During 2018, Energy Metals undertook airborne electromagnetic and deep-sensing ground penetrating radar surveys, as well as a soil geochemical survey at the Crystal Creek prospect.

Onshore petroleum

Petroleum exploration activity in the onshore basins of the Northern Territory in 2018 was largely limited to the Amadeus Basin. There was no substantial exploration in the greater McArthur Basin (including the Beetaloo Sub-basin) pending the implementation of recommendations of the Scientific Inquiry into Hydraulic Fracturing (the Inquiry). **Figure 9** shows granted petroleum tenure and basins in the NT, and the location of wells and fields mentioned in the text.

McArthur Basin

The ***Beetaloo Sub-basin*** is a significant depocentre of Mesoproterozoic Roper Group sedimentary rocks that underlies the Mesozoic Carpentaria Basin in the vicinity of Dunmarra and Daly Waters; it is NT's most advanced shale gas play. The most prospective shale units in the Roper Group occur within the Velkerri and Kyalla formations. Drilling of the middle Velkerri Formation has demonstrated the consistent presence of gas saturated, quartz-rich shale source rocks that are mature for gas over extensive areas, and which appear to meet all of the physical and chemical parameters for a successful shale gas play. Following the successful hydraulic fracturing and production testing from the Amungee NW-1H exploration well by Origin Energy Limited (Origin) in 2016, Origin announced a 2C Contingent Gas Resource Estimate for the Velkerri B-shale pool of 6.6 trillion cubic feet (Tcf) over 1968 km^2, with Original Gas In Place of 61.0 Tcf. Wells drilled to date by Santos Limited, Origin and Pangaea Resources, and as reported in associated confidential discovery reports, indicate a P50 Gas-In-Place Resource for the Velkerri B-shale alone of at least 500 Tcf, with the additional potential for liquids across the basin.

Exploration in the central part of the Beetaloo Sub-basin is operated by Origin in joint venture with Falcon Oil and Gas Ltd. Origin has announced that, subject to relevant approvals and implementation of the exploration recommendations of the Inquiry, they plan to evaluate the potential of the liquids-rich gas fairways in both the Kyalla and Velkerri plays in 2019, including the drilling and hydraulic fracture stimulation of two horizontal wells. Together with the Velkerri B-shale dry gas play discovered in 2016, this allows for the assessment of three plays and enables the most commercially prospective play to be targeted for Stage 3 drilling during 2020. Elsewhere in the Beetaloo Sub-basin, Santos have installed two water monitoring bores in late 2018 to support applications for multi-well exploration activity in 2019.

Amadeus Basin

The Territory's current onshore gas production is entirely sourced from fields in the Amadeus Basin operated by Central Petroleum Ltd (Central Petroleum). In 2018, 6.151 billion standard cubic feet (bscf) of gas was produced, comprising 4.919 bscf from ***Mereenie***, 0.429 bscf from ***Palm Valley*** and 0.803 bscf from ***Dingo***. This was a 23% increase on 2017, with gas production ramping up to meet increased demand following the completion of the Northern Gas Pipeline. Onshore oil production in the NT in 2018 was sourced entirely from the Mereenie field, with 0.194 million barrels (mmbbls) of oil produced.

In November 2018, Central Petroleum announced increased net reserves and contingent resources, with Proven and Probable (2P) gas reserves of 88.55 PJ at Mereenie, 42.00 PJ at Palm Valley and 38.18 PJ at Dingo. 2P oil reserves at Mereenie increased by 154% to 0.97 MMBbl oil.

Central Petroleum drilled two appraisal wells in 2018. The ***West Mereenie 26*** well was spudded in May 2018 and drilled to a total depth 2388 m measured depth, including a horizontal lateral length of 893 m through the Lower Stairway 2 formation. The company described the results from the well as disappointing, with mineralisation of natural fractures leading to reduction in permeability and resulting in only minor gas shows. Central Petroleum also drilled the ***Palm Valley 13*** appraisal well to a total depth 2242 m. The company reported very encouraging initial gas flows from Palm Valley 13, with further production testing to commence once connected to the Palm Valley facilities. The well intersected natural fractures as predicted within the Pacoota Sandstone.

Central Petroleum also have a farm-in agreement worth up to $150 million with Santos for a large area in the Amadeus Basin. Santos are targeting sub-salt and intra-salt plays of the Neoproterozoic lower Gillen–Heavitree Quartzite System in the southeastern part of the basin that have potential for large gas and helium accumulations. In April 2018, Santos completed acquisition of 403 km of seismic data, infilling the previous 932 km of seismic acquired in 2016 and bringing the total to 1335 km. The additional seismic lines reduce dip line spacing over the ***Dukas*** prospect to ~5 km over the central prospect area and ~10 km towards the flanks. Santos have announced they are progressing final approvals and agreements to support the drilling of the planned 2019 Dukas 1 wildcat well.

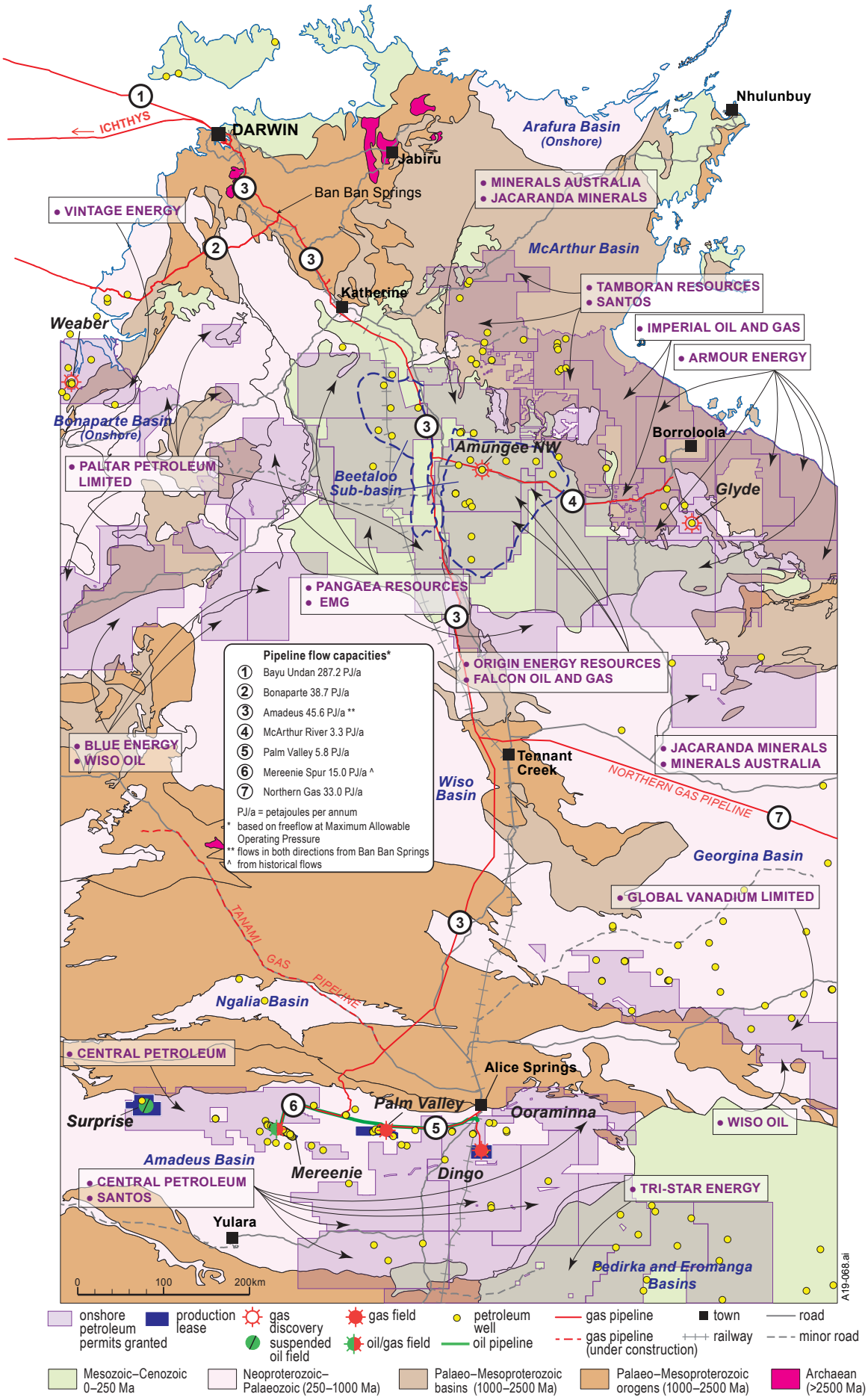

Figure 9. Map of Geological Regions of the Northern Territory showing granted exploration permits as of January 2019, along with wells and prospects mentioned in the text.

Where there's smoke there's fire – perseverance and reward at the Mount Hardy Zn-Cu Project

Anna M Mayo[1,2]

Introduction

Todd River Resources Ltd (TRT) is an Australian-based resources company that holds a large, highly prospective base metals exploration portfolio entirely within the Northern Territory (**Figure 1**). The company was created in 2017 as the base metals spin out of Australian strategic metals developer TNG Ltd (TNG). TRT is currently expanding the EM1 mineralisation at its Mount Hardy Project, a copper and zinc-rich polymetallic discovery identified in mid-2018 to the northwest of Alice Springs. In addition to Mount Hardy, TRT holds 12 other projects (**Figure 1**) including Manbarrum, a MVT-style Zn-Pb-Ag project with a JORC (2012) compliant mineral resource estimate of 22.5 Mt at 2.3% Zn+Pb; McArthur River, a Zn-Pb-Cu-Ag prospect located within the same structural corridor as the McArthur River Mine; Tomkinson, an early stage project in a known manganese province; and Rover, Petermanns Range and Stokes Yard, three early stage Cu-Au/base metals projects. TRT is also looking to advance several of its current tenement applications towards grant and is working closely with the relevant stakeholders to fast track this.

The Mount Hardy Project was initially acquired by TNG in 2012. It is located on the Tanami Highway, 300 km northwest of Alice Springs and 20 km west of the town of Yuendumu (**Figure 2**), and lies entirely on the pastoral land of Mount Doreen Station owned by M Braitling. The project comprises several high-grade structurally-controlled precious and base metal oxide and sulfide targets, including the advanced EM1 prospect, generated from geochemical and geophysical surveys.

Geological setting

The Mount Hardy Project is located in the centre of the Arunta Region's Aileron Province, wholly within the area of the Mount Doreen 1:250 000-scale mapsheet (**Figure 3**). The dominant host rock for the known mineralisation is a unit of the Palaeoproterozoic Lander Rock Formation (LRF) consisting of lower amphibolite facies biotite–muscovite–andalusite–quartz gneiss, schist, metapsammite, metapelite, and quartzite. Other local LRF units (mostly to the south of the mineralised unit) include greenschist facies muscovite–chlorite–quartz schist, gneiss, quartzite, and local conglomerate; and transitional granulite facies migmatitic cordierite–garnet–sillimanite–biotite gneiss. The LRF is interpreted to be stratigraphically equivalent to the Killi Killi Formation of the Tanami Group, which hosts the significant discoveries at The Granites, Dead Bullock Soak and Coyote. To the west and north of the target LRF unit, intrudes the Mesoproterozoic Southwark Suite, consisting of megacrystic and minor even grained biotite and biotite–muscovite granite; leucogranite, pegmatite and aplite. To the south, intrudes the Palaeoproterozoic Carrington Suite, consisting of weakly foliated to gneissic and locally migmatitic xenolithic biotite granodiorite, biotite tonalite and muscovite–biotite granite (Young *et al* 1995).

The Palaeoproterozoic Aileron Province hosts many different examples of copper-related mineralisation (eg Jervois, Home of Bullion, Mount Hardy, Perenti, and Lake McKay). The geologic processes and controls on the location and genesis of this broad spectrum of mineralisation styles are poorly understood; the temporal and genetic links between each system, as well as the larger regional tectonic processes and geologic events, are not well constrained (McGloin *et al* 2016).

Artisanal miners targeted areas containing secondary mineralisation above the water table, ie oxidised to highly visible malachite, azurite, chalcocite, chrysocolla, and cerussite (Kiek 1941). In the vicinity of the open cut at Mount Hardy, the copper carbonates persist for at least 15 m below the present floor level; they also extend up to 5 m from the veins into the host metasediments. At depth, primary mineralisation consists of predominantly chalcopyrite and pyrite with variable proportions of sphalerite, pyrrhotite, minor galena, and scarce native copper. Mineralisation forms thin stringers and blebs within quartz veins and spatially associated pegmatite, and more rarely, in the country rock. Recent drilling has identified a thick, continuous zone of brecciated massive sulfides in varying mineral ratios from surface to ~600 m down plunge, with the total extent of the mineralisation still unknown.

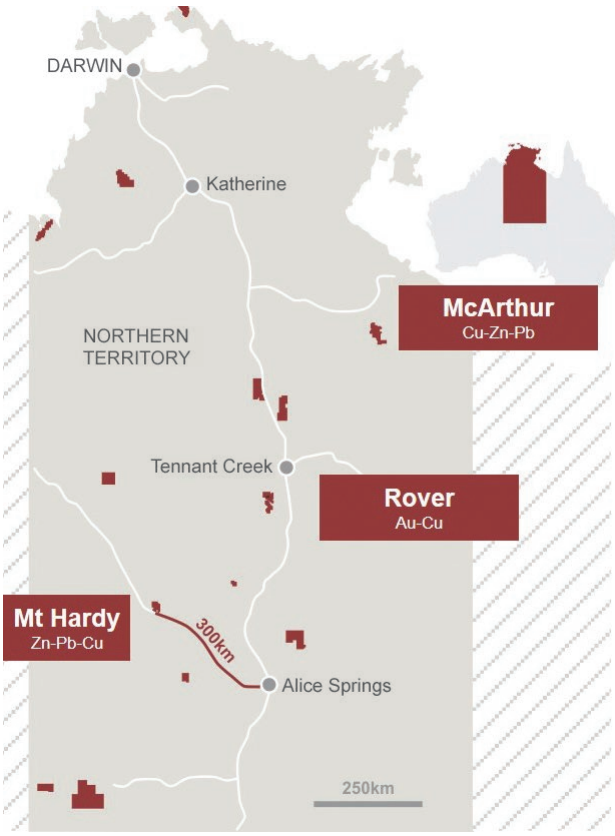

Figure 1. Todd River Resources tenement location map.

[1] Todd River Resources Ltd, North Wing, Level 2, 1 Manning St, Scarborough WA 6019, Australia
[2] Email: anna.mayo@trrltd.com.au

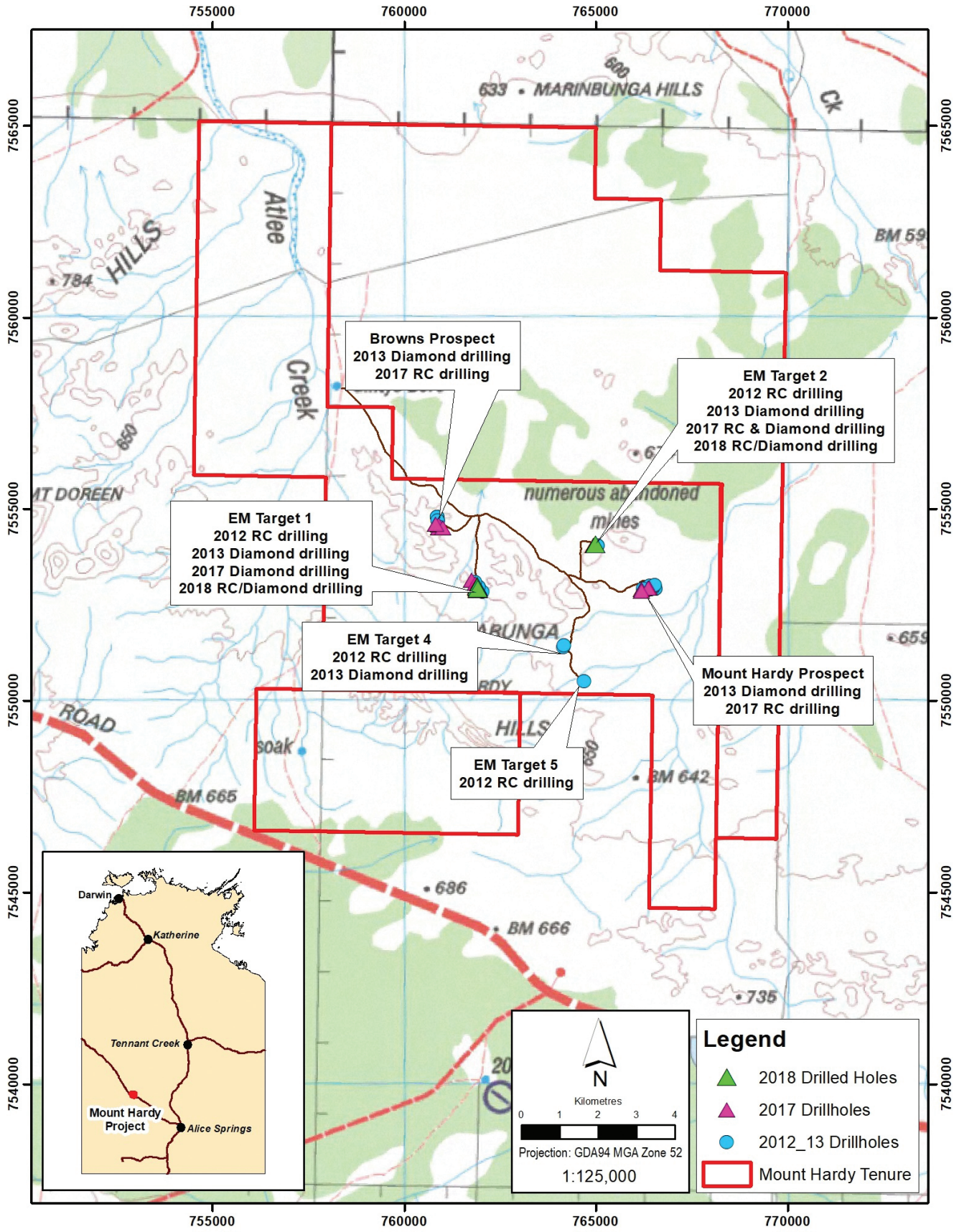

Figure 2. Mount Hardy Project location and site layout.

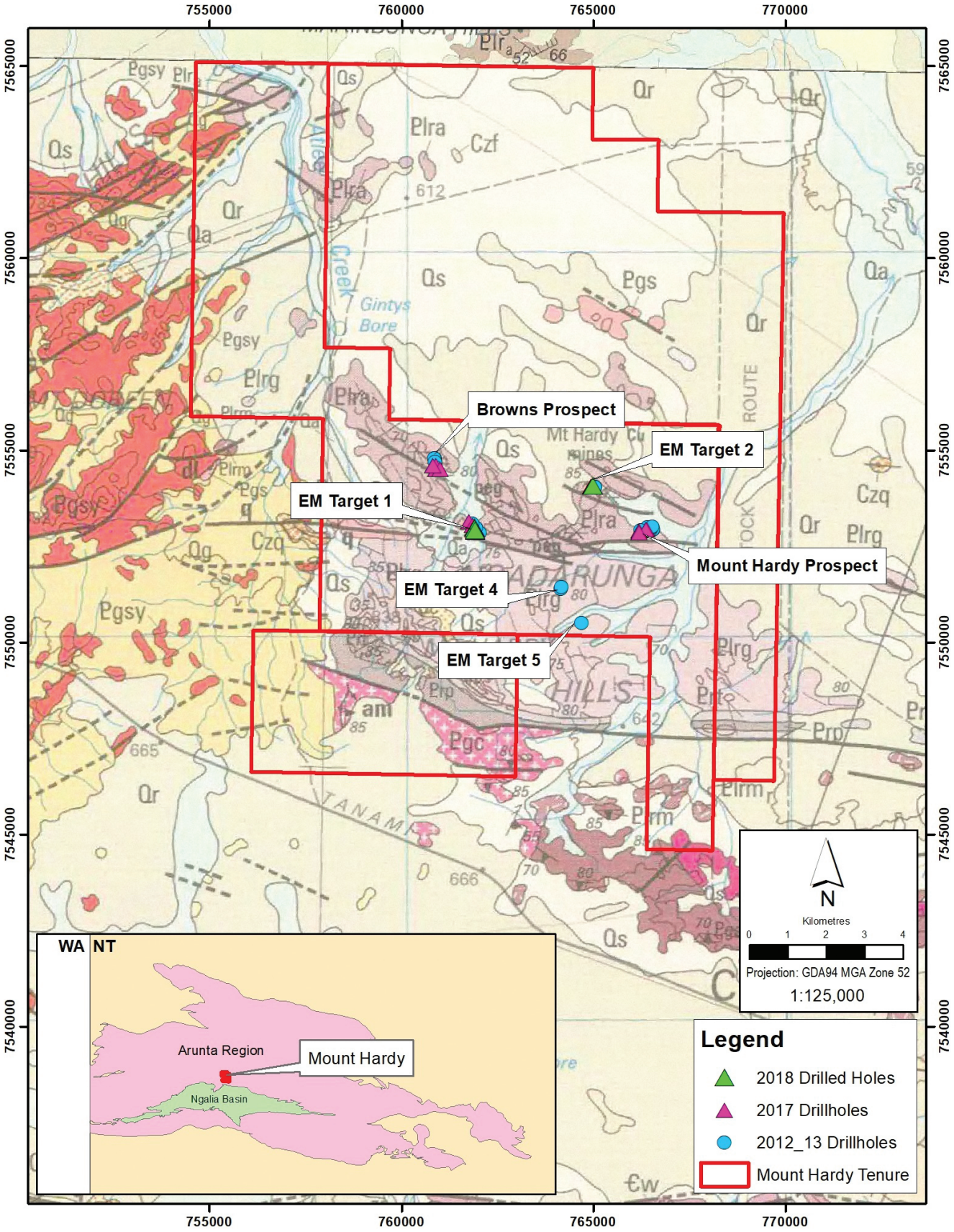

Figure 3. Regional geology of the Mount Hardy area from the Mount Doreen mapsheet (Goldberg *et al* 2008, Pl symbols indicate Lander Rock Formation, and Pg symbols indicate Proterozoic granites).

Historical mining and exploration

The Mount Hardy Copper Field was discovered in 1935, and there have been two published reports on the geology and mineralisation of the field, Kiek (1941) and Grainger (1968). The field has had small-scale prospecting work sporadically from the 1930s discovery through to the late 1960s, consisting of surface workings, small pits less than 5 m deep and limited drilling to depths of less than 50 m. There has been no large scale mining carried out. The largest historical working is the small open pit at the Mount Hardy Copper Mine, a 20 m × 6 m × 5 m cut into the low hill. There is also a 57 m long shallow costean dug by hand by aboriginal prospectors from Yuendumu in 1967 (Grainger 1968). There is no evidence of processing of any ore from the old workings on site; however, ~750 t of handpicked secondary copper ore was stockpiled and remains in place. Water access was a problem in the vicinity and hindered any onsite processing.

A timeline of historical activity carried out in the Mount Doreen 1:250 000-scale mapsheet in the Mount Hardy area is as follows:

- Mount Hardy Copper Field was discovered by WW Braitling in 1935.
- Sporadic small scale mining by aboriginal prospectors from Yuendumu took place until the 1970s.
- Uranium Development and Prospecting NL carried out diamond drilling in the area in 1956.
- Bureau of Mineral Resources (BMR) conducted aeromagnetic, radiometric and gravity surveys in 1967.
- Central Pacific Minerals held AP1722 in the Mount Hardy area from 1967–69.
- Northern Territory Geological Survey (NTGS) assessed the economic feasibility of the Mount Hardy and Clarke copper deposits from 1968 to 1972, including seven investigative drillholes totalling 505 m at the Mount Hardy Copper Mine.
- NTGS and BMR completed 2nd edition mapping of Mount Doreen 1:250 000-scale mapsheet in the 1990s.
- White Industries conducted exploration on EL 5688 from 1988–90. Rock chip and stream sediment sampling was carried out from Wolfram Hill through to Mount Hardy.
- Bruce and Mules' explored the Silver King area for gold and base metals from 1988–1991.
- MIM/Roebuck Resources Joint Venture targeted magnetic highs in the early 1990s and explored the Silver King deposit.
- Yuendumu Mining Company/Posgold explored the western parts of the Mount Doreen mapsheet from 1992 to 1996, particularly Terry's Find, 'Buger', and 'Grasshopper'.
- BMR completed airborne magnetic and radiometric surveys in 1993.
- Aberfoyle Resources were granted EL8913 and EL8608 in late 1994 and undertook ground magnetics surveys and substantial RAB drilling. Exploration failed to locate significantly anomalous gold mineralisation and the tenements were surrendered.
- BHP tested the northern Mount Doreen and southern Mount Theo 1:250 000-scale mapsheets for Cu-Au in the late 1990s but concluded that no major deposits were likely.
- Tanami Gold NL explored for Tanami-style gold mineralisation and Tennant Creek-style copper mineralisation in the Mount Doreen mapsheet from 2001 to 2005. The main target areas were the Terry's Find, Mount Hardy, and Pyramid Hill prospects. Of 42 rock chip samples collected from the Mount Hardy Project area, 14 returned copper assays between 5 and 19%.
- Deep Yellow conducted exploration for uranium in the Mount Hardy area in 2009 and 2010. No other commodities were investigated.

TNG and TRT exploration

In June 2012, TNG purchased the exploration licence from Walla Mines Ltd (who had held the ground for a period of time without work) after noting the tenement's potential for base metal mineralisation. TNG subsequently commenced exploration in July 2012 with a helicopter electromagnetic survey (HELITEM) to outline any conductors that may represent sulfide accumulations of base and precious metals. The survey was completed by Fugro Airborne Surveys and comprised 930 line km of 200 m spaced lines. Five anomalous areas within EL 27892 were field checked and mapped. Niton readings were taken from rock and soil samples; additional grab samples were collected for analysis. TNG was able to quickly define several large anomalous target zones requiring drill testing.

Initial exploration drilling occurred in October 2012 with seven RC holes testing four strong surface electromagnetic (EM) targets identified from the HELITEM survey. Results showed that the large geophysical anomalies represented mineralised systems at depths of ~100–200 m. Further work including core drilling for metallurgical test work was planned.

Induced polarisation (IP) and gravity surveys were completed in 2013, defining 17 priority EM targets. Based on the indications from the 2012 drilling and the geophysical work, a 15-hole diamond drill program totalling 2757 m was completed from March to April 2013. Drilling tested the Mount Hardy and Browns prospects, as well as the mapped mineralisation and surface IP anomalism at targets EM1, EM2 and EM4. The drilling confirmed broad zones of polymetallic mineralisation from surface to approximately 200 m depth, coinciding with the surface geophysical anomalies. Significant zones were intersected, including the following highlights:

- EM1: 21.0 m at 4.4% Zn, 1.9% Pb, 0.5% Cu and 36 g/t Ag from 211 m (MHDD0010)
- EM2: 3.8 m at 2.0% Zn, 1.8% Cu, 0.5% Pb and 18 g/t Ag from 177 m (MHDD0012)

In 2014, down-hole electromagnetic (DHEM) surveys were conducted for four core holes drilled during 2013. IP surveys were also completed at the Browns prospect, EM6,

and EM7. No on-ground exploration was undertaken at Mount Hardy during 2015 and 2016.

The Mount Hardy tenements were transferred to the new licence holder and operator Todd River Metals Pty Ltd in March 2017 as part of the spin out of TRT from TNG. A total of 14 RC and diamond holes for 2839 m were drilled across the Mount Hardy prospect areas in April to June 2017, targeting the 2014 combined surface and DHEM results. Results produced a series of new DHEM target plates. Significant polymetallic zones were again intersected, including the following highlights:

- Browns: 7 m at 1.8% Cu, 0.4% Zn, 0.2% Pb and 18 g/t Ag from 67 m (MHRC0017)
- EM1: 14.1 m at 0.34% Zn, 0.29% Cu and 0.17% Pb from 174.5 m, including 7.45 m at 0.47% Cu, 0.45% Zn and 0.11% Pb from 177.7 m (MHDD0021)
- EM2: 10.5 m at 4.15% Zn, 1.10% Cu and 0.65% Pb from 178 m (MHDD0029).

2018 exploration activities

Two main phases of drilling were completed at Mount Hardy during 2018. Five drillholes (MHDD0030–0034) and the diamond extension of a sixth drillhole (MHDDH0021A) were completed in June 2018. The breakthrough intercept came in drillhole MHDD0031A with 25.15 m at 4.0% Zn, 3.1% Pb and 2.4% Cu from 184 m, including 9.15 m at 8.8% Zn, 7.6% Pb and 4.5% Cu from 200 m (Todd River Resources 2018a). Further success came with the diamond extension of MHDD0021A returning 13.45 m at 15.9% Zn, 5.75% Pb, 0.9% Cu and 89 g/t Ag from 358.55 m (Todd River Resources 2018b).

Based on these results, an additional six drillholes (MHDD0035–0040) were approved for drilling at short notice in July 2018 over EM1, and then 12 additional drillholes (MHDD0041–0052) were completed in September 2018. The most outstanding intercept to end 2018 was intersected in MHDD0043, which returned a significant width of brecciated mineralisation with a length weighted average grade of 35.54 m at 14.7% Zn, 2.92% Pb, 0.91% Cu and 59 g/t Ag from 431.54 m, including 11.29 m at 22.9% Zn, 3.35% Pb, 1% Cu and 58 g/t Ag from 443.61 m. MHDD0043 was drilled targeting a DHEM plate modelled from MHDD0021 (Todd River Resources 2018c).

MHDD0042, the deepest drillhole at EM1 to end 2018, intersected mineralisation more than 600 m below surface and 180 m below and down-dip of the nearest drillhole, MHDD0043 (**Figure 4**). MHDD0042 returned a significant width of brecciated mineralisation with a length weighted average grade of 24.54 m at 4.86% Zn, 0.68% Cu and 0.29% Pb from 619 m, including 12.68 m at 8.21% Zn, 1.19% Cu and 0.47% Pb from 629.62 m (Todd River Resources 2019). This intersection is open in all directions; geophysical modelling of the DHEM results indicates a strong response to the north.

DHEM surveying of key drillholes was completed during the December 2018 drilling. The results have been combined with data acquired in all previous drillholes to produce 29 modelled plates, confirming the complexity of the area. Further work is underway to build a 3D geological model to be integrated with the interpreted EM plates in order to better define constraints on mineralisation and to identify new targets. Preliminary results of this work indicate that the deep mineralisation is not closed off in any direction. There are two significant deep plates modelled from the data (represented on long section in **Figure 4**) that encourage further drilling, particularly above and to the north of MHDD0042.

Future

In 2019, an initial 12-hole campaign has been planned at EM1 (**Figure 4**). Drillholes will be started with an RC collar and completed with a diamond tail to a depth of up to 800 m; a few shallower drillholes will be completed by RC alone. Drillhole locations have been planned on a grid using the DHEM to target the most likely mineralised areas, as well as extensions to known mineralisation.

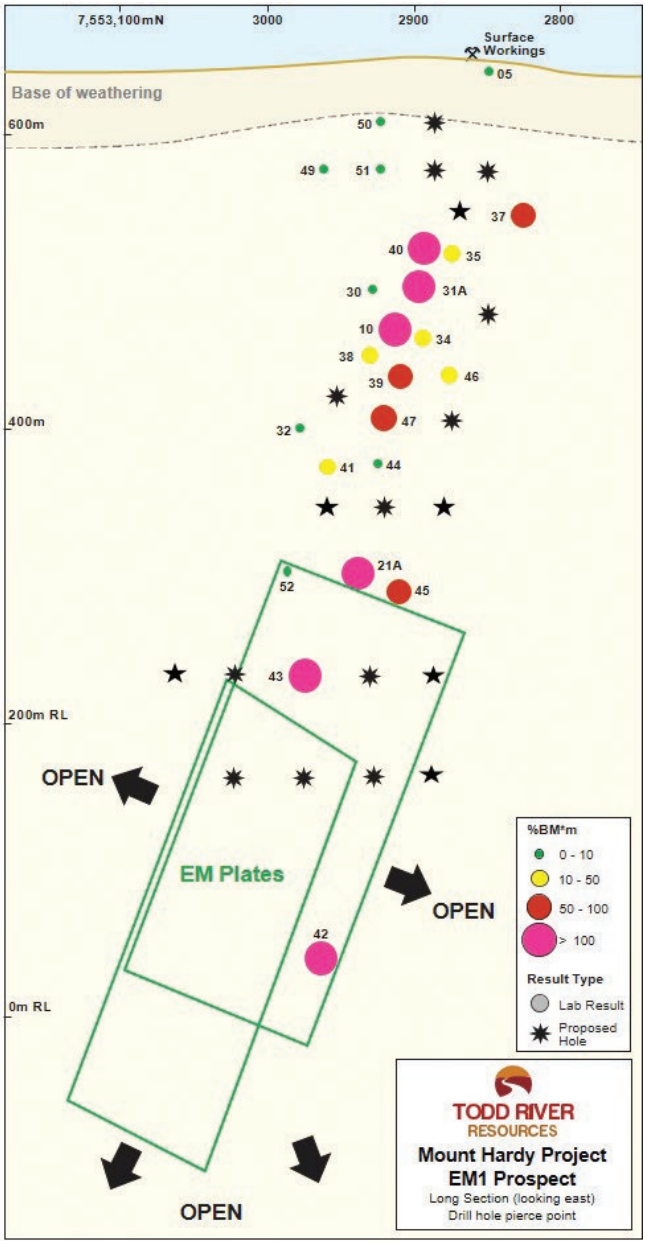

Figure 4. Mount Hardy Project, EM1 prospect area oblique long projection showing planned drillholes for the initial campaign of 2019.

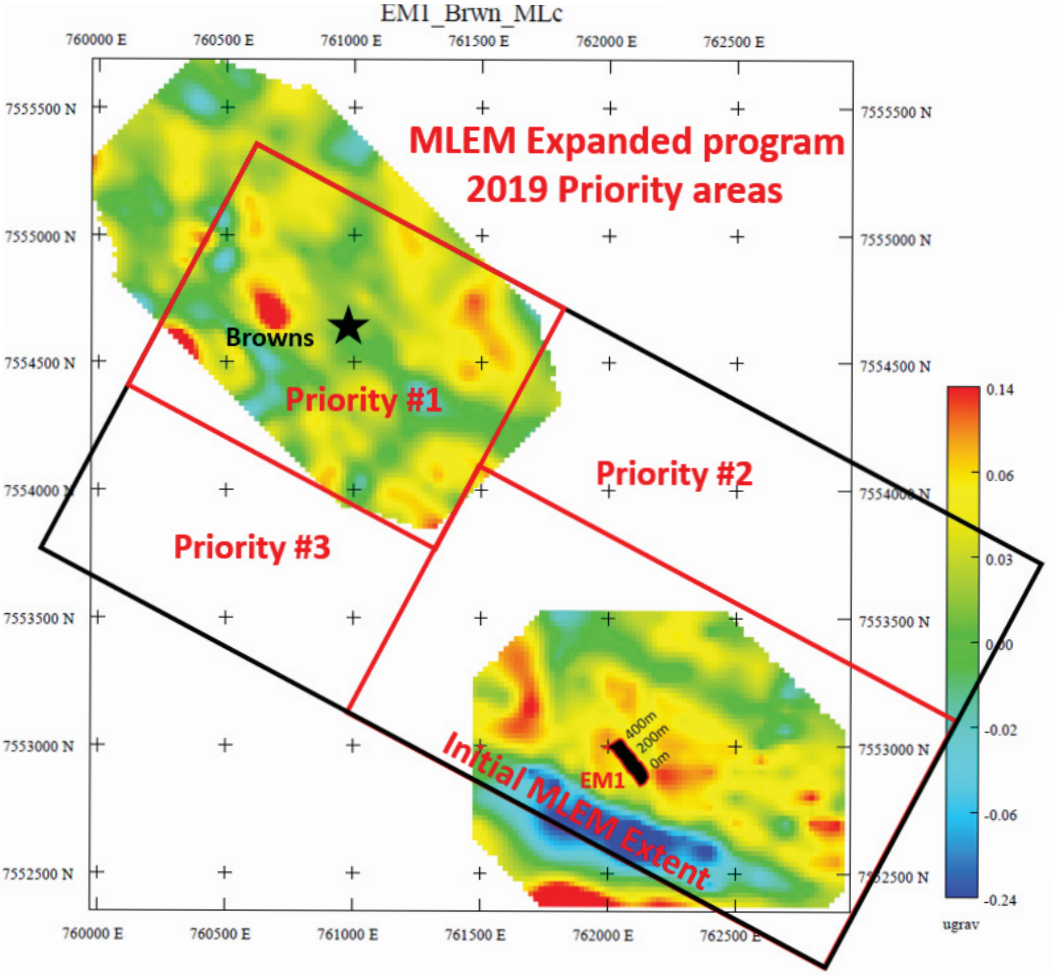

Figure 5. Mount Hardy moving loop EM survey areas. 2018 completed area – lower right. 2019 planned coverage (priority #1, 2, 3).

An initial moving loop electromagnetic (MLEM) survey was completed in mid-December 2018, focussing on a four km^2 area centred on EM1 (**Figure 5**, Todd River Resources 2019). The data generated in this survey is currently being interpreted. Following modelling and target generation, drillholes will be planned to test targets north and south of EM1 in mid-2019. The MLEM survey area will also be expanded in early 2019 (**Figure 5**) to allow better targeting for drill testing at the Browns prospect and to open up the surrounding areas, particularly those with poor surface expression. Previous drilling intersections at both Browns and EM2 are yet to be followed-up. There remains multiple untested EM anomalies along strike from the EM1 prospect signifying outstanding potential to extend the known area of mineralisation at Mount Hardy.

References

Goldberg A, Meixner AJ, Edgoose CJ, 2008. *Mount Doreen, Northern Territory (Revised first edition) 1:250 000 interpreted geological map series SF 52-12*. Northern Territory Geological Survey, Darwin.

Grainger DJ, 1968. The Mount Hardy Copper Mine, Northern Territory. *Bureau of Mineral Resources, Geology and Geophysics, Record* 1968/100.

Kiek SN, 1941. The Mount Hardy Copper Field, Central Australia. *Aerial, Geological and Geophysical Survey of Northern Australia Northern Territory Report* 55.

McGloin M, Maas R, Weisheit A, Meffre S, Thompson J, Zhukova I, Stewart J, Hutchinson G, Trumbull R, Creaser R, 2016. Palaeoproterozoic copper mineralisation in the Aileron Province: New findings on temporal, spatial and genetic features: in *'Annual Geoscience Exploration Seminar (AGES) Proceedings, Alice Springs, Northern Territory 15–16 March 2016'*. Northern Territory Geological Survey, Darwin.

Todd River Resources, 2018a. *Outstanding thick high grade copper and zinc intercept confirms significant discovery at Mount Hardy, NT.* Australian Stock Exchange media release, 20 June.

Todd River Resources, 2018b. *High-grade assays confirm base metal discovery at Mt Hardy.* Australian Stock Exchange media release, 2 August.

Todd River Resources, 2018c. *Exceptional high-grade intercept from deepest hole to date at Mt Hardy.* Australian Stock Exchange media release, 7 November.

Todd River Resources, 2019. *Todd River gears up for major exploration push at Mount Hardy Project, NT.* Australian Stock Exchange media release, 21 January.

Young DN, Edgoose CJ, Blake DH and Shaw RD, 1995. *Mount Doreen, Northern Territory (Second Edition). 1:250 000 geological map series explanatory notes, SE 52-12*. Northern Territory Geological Survey, Darwin.

Highlights from precompetitive geoscience across Northern Territory geology

Dorothy Close[1,2]

Precompetitive geoscience through funding initiatives and collaboration

Northern Territory Government funded initiatives *Creating Opportunities for Resource Exploration* 2014–2018 and *Resourcing the Territory* 2018–2020 are delivering new precompetitive geoscience data to drive progressive improvements in the understanding of the geology and resource potential of the Northern Territory. Work undertaken by the Northern Territory Geological Survey (NTGS) through these initiatives, and in collaboration with Geoscience Australia (GA), CSIRO and various universities, has enhanced the understanding of:

1. basin architecture and petroleum and mineral resource potential of the highly prospective McArthur Basin/Beetaloo Sub-basin,
2. base metal potential of the Aileron Province, currently emerging as a significant copper province for the Territory,
3. basin architecture of the Territory's only onshore petroleum-producing basin, the Amadeus Basin.

This work will be further enhanced by collaboration with GA under the federally funded *Exploring for the Future* program, which has seen significant acquisition and integration of new data in greenfields areas, such as east of Tennant Creek. Highlights of the *Exploring for the Future* and *Resourcing the Territory* initiatives include the acquisition and integration of extensive regional scale surface geochemistry and hydrogeochemistry sampling results with geophysical magnetotelluric, gravity, passive seismic, reflection seismic and airborne electromagnetics data. This is combined with systematic analysis of available drill core in the Barkley and Gulf regions. The geophysical work has included the first regional seismic acquisition over the South Nicholson Basin/Lawn Hill Platform; this has provided vital subsurface information to investigate the links between the relatively unknown South Nicholson Basin/Lawn Hill Platform and the resource rich, age equivalent McArthur Basin. Through the Territory's *Resourcing the Territory* initiative, NTGS will remap the outcropping geology of the South Nicholson Basin/Lawn Hill Platform to improve the understanding of stratigraphy and structural relationships and to provide important constraints on interpreting subsurface geology in the Barkley region.

[1] Northern Territory Geological Survey, GPO Box 4550, Darwin NT 0801, Australia
[2] Email: dorothy.close@nt.gov.au

Precompetitive geoscience through co-funded industry grants program

Under the 2018–2022 *Resourcing the Territory* initiative, the Geophysics and Drilling Collaborations (GDC) program has been revised and enhanced to encourage exploration in greenfields areas. The total funds available for each GDC Round is $1 million per annum. GDC now includes funding for reverse circulation drilling exclusively in greenfields areas with no previous drilling activity. In addition, total amount per diamond drill program has now increased to a maximum of $125 000 per project thus providing further incentive for this exploration method. There is also additional funding available under the Territory Supplier Incentive whereby a maximum of a further $10 000 per project is available for projects that engage Territory-based enterprises that employ Territorians.

The enhanced grants program offers 33% more in funding than the previous scheme and with less restrictive criteria to open the grants to more explorers. It is designed to maximise local industry participation in exploration by making service and supply by NT-based companies eligible for co-funding. This has broadened eligibility for pure greenfields exploration to allow greater participation by the junior exploration sector.

All report and data acquired through the GDC program will be publicly available six months after completion of fieldwork.

The first funding Round under the revised GDC program (2018–2019) saw the highest number of applications in the history of the program. Applications for GDC funding for 2019–2020 opened on 6 March 2019 with closing on 15 April 2019. Successful applicants will be announced in May. Further information on the Geophysics and Drilling Collaborations program can be found at www.minerals.nt.gov.au/collaborations.

Geoscience information: What's new and what's ahead

Tracey Rogers[1,2]

During 2018, in addition to the ongoing publication of reports and data generated by the Northern Territory Geological Survey (NTGS), new information and improvements in the delivery of information to industry have been focussed on capture of exploration drilling and geochemical data, and improving delivery of open file industry reports and data.

[1] Northern Territory Geological Survey, GPO Box 4550, Darwin NT 0801, Australia
[2] Email: tracey.rogers@nt.gov.au

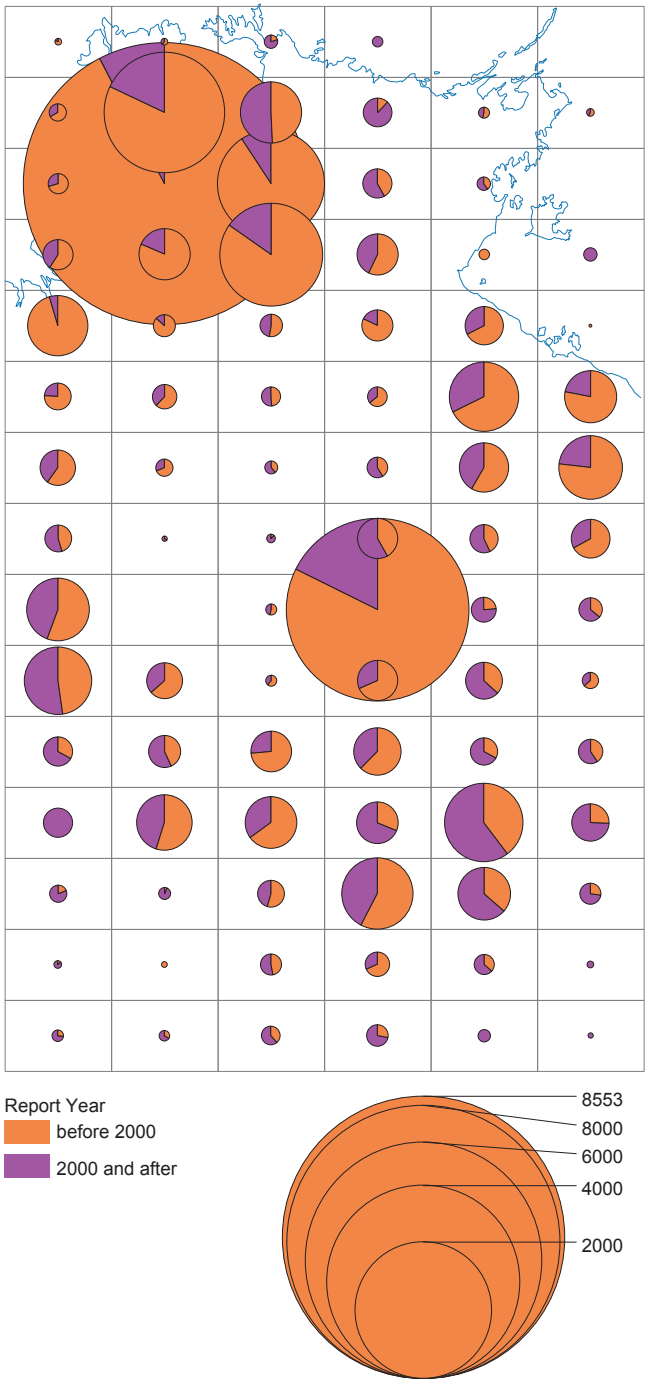

Figure 1. Number and distribution of reports with data to be captured in each 1:250 000-scale map area.

New drilling and geochemistry data

Geochemistry and drilling data submitted during the entire life cycle of all mineral titles active since October 2016 has been captured, with the exception of a very small proportion of older, hardcopy reports. This project commenced in October 2016 and is now 98.9% complete. As at February 2019, 2093 titles of 2205 have had *all* data meeting the mandatory database criteria captured. One hundred and twelve (112) titles have one or more reports outstanding; these have been delayed due to their original format and large size. Overall, 4985 reports out of 5037 have now been processed, with 52 reports remaining to be captured. The first major release of open file data was in March 2018.

Drilling and geochemistry data captured from industry reports covering historical titles over five of the 1:100 000-scale mapsheets in the Batten Fault Zone area was completed and released in October 2018. To continue building on this data compilation, under the new four year *Resourcing the Territory* initiative, a major project capturing legacy data from industry reports has commenced. Planning and preparation for progressive data capture over the area between Tennant Creek to the NT:QLD border and throughout the Barkly Region is in progress. Capture of data from another 66 reports covering the Batten Fault Zone area commenced in January 2019; the Tennant Creek 1:250 000-scale mapsheet is the next area to be targeted. **Figure 1** shows the results of a preliminary review, indicating the numbers of reports identified as containing drilling and geochemistry data that have yet to be captured in each 1:250 000-scale map area.

New and recent data is now added to the database as it is received. Now when legacy data is captured over specific areas, all data from every title that currently exists or has ever existed in the area will have been captured if sufficient metadata exists. The legacy data capture project aims to achieve 100% database coverage for exploration drilling and geochemistry data in the Northern Territory, with a caveat that some data cannot be added to the database as critical information is missing. All the data will be released in batches through STRIKE and DIP 001 – *Northern Territory Geochemical Datasets.*

STRIKE

The last twelve months has seen steady progressive improvements to STRIKE across various layers, eg display of attributes, updated and additional metadata, fixes to data and map display. Downloads are now directly accessed from a new link; the A4 portrait print layout has been updated; and searches have been improved and added for a number of layers.

Basic searches for 13 layers and advanced searches for 36 layers have been added or upgraded. Standard searches on layers accessed through the Search tab at

the top of the layer menu have been added to 13 layers including the 250 000- and 100 000-scale map indexes, mineral occurrences, mines, geochemical sampling layers and geophysical survey indexes. An advanced search functionality has been added to 21 layers, including petroleum title layers, geochronology layers, open file mineral report index and Native Title and Indigenous Land Use Agreement layers. This search function, which is accessed via the binocular icon next to the quick search text box on the upper right of the application, provides qualification using operators and the ability to query more than one attribute in the active layer. It has also increased the range of attributes that can be searched on mineral titles, historical petroleum titles, petroleum wells and drillhole layers.

In the near future, download of individual geoscience data layers and improved web map services (WMS) will be available. At present, multiple layers are included within a themed group, and the whole group has to be downloaded although only one layer may be of interest. Work is underway to permit downloading of each individual geoscience data layer so users only receive what they really want.

Improvements to the web services are nearly complete and will result in better quality services; this includes a split into two services: one for titles and one for geoscience data, making it easier for consumers to determine the layers contained within each smaller web service package.

Industry reports

The project to process the backlog of reports for open file release under the five year 'sunset clause' introduced in the *Mineral Titles Act* (MTA) continues. Over the last 12 months, reports from 2009–2010 have been open filed and added to the MEX collection on GEMIS; review of the 2011 reports for open file release is in progress. As part of the review, each report's associated MEX record is checked and updated to ensure the information is complete and correct before it is released.

PEX Geophysics now has 409 records with downloadable files. From the total of 468 records, only 59 records have no files attached. This is in contrast to the numbers at the time of launch in March 2017 when there were 456 records and 291 without files for download. Records without downloadable files are either not scanned or the datasets are greater than 1GB in digital size. Availability is indicated in the Notes field; clients can request copies using the GEMIS Request Cart.

The PEX Tenure Collection, covering industry reports on geological surveys, regional interpretation and similar reports, is under development; the current aim is to launch the collection in March 2019. This will complete the online PEX collections. It will also include the small number of geothermal exploration reports submitted under the *Geothermal Energy Act*.

Resourcing the Territory website

In mid-2018, the 'CORE' website for *Creating Opportunities for Resource Exploration* was given a basic update to reflect the new initiative, *Resourcing the Territory* and a new URL www.resourcingtheterritory.nt.gov.au. NTGS has engaged a web design and digital services company to develop a new website, incorporating a new creative look, modern design and user experience. Development of the new website is underway and it will be launched within the next couple of months. The website is aimed at attracting investors and explorers to the Territory by presenting insights and relevant information on exploration, projects and commodities to provide clients with the confidence to initiate the investment decision-making process.

New Northern Territory Geological Survey products

New or updated NTGS products released since March 2018 include 12 new Records, eight HyLogger Data Packages, two new and four updated Digital Information Packages, data and images of the NT-wide gravity stitch, and two new geological GIS datasets. Four revised geological GIS datasets have also been released.

Besides a number summarising geochronology results, Records released include the stratigraphic subdivision of the Velkerri Formation in the McArthur Basin, revised Neoproterozoic stratigraphy in the Mount Conner area in the Amadeus Basin, using tourmaline to identify base metal and tungsten mineralising processes in the Jervois mineral field and Bonya Hills area, and the AGES 2018 presentations and posters.

Together with the new geological GIS dataset for Alcoota 1:250 000-scale mapsheet released just before AGES 2018, the publication of the new GIS dataset for the Hay River 1:250 000-scale outcrop geology map in June 2018 completes NT-wide coverage of geological GIS data at this scale. However, reiterating previous statements, although the datasets conform to the same data structure, the data is not seamless and there are gaps and overlaps resulting from differences in the datum used for mapping.

Other releases include a new 1:100 000-scale geological GIS dataset for the Tawallah Range map and revised GIS datasets for the Mount Theo, Sandover River, Mount Solitaire and Tobermorey 1:250 000-scale outcrop geology maps.

An update to the metallogenic NT-wide map and new editions of three Digital Information Packages will be released for AGES 2019.

Reference

Rogers T, 2018. Geoscience Information and delivery in 2017-18: in *'Annual Geoscience Exploration Seminar (AGES) Proceedings, Alice Springs, Northern Territory, 20–21 March 2018'*. Northern Territory Geological Survey, Darwin.

Lantern project update – realising opportunity through the use of numeric exploration technology

Chantelle Lower[1,2]

Overview

Kirkland Lake Gold Limited (KL) continues to grow beyond being a mid-tier gold miner, with its record 723 477 oz of gold production during 2018 from high performing, low cost mines in Canada (Macassa) and Australia (Fosterville) (Kirkland Lake Gold Ltd 2019). The future growth of KL is supported by district-scale exploration potential in both countries. Within the Northern Territory, KL holds 56 mineral titles over 150 km^2 and 27 exploration titles (in joint venture with PNX Metals Limited) over 1420 km^2, all in the historically prolific gold producing area of the Pine Creek Orogen (**Figure 1**).

Lantern Gold Deposit update

The Lantern deposit is located within the Cosmo-Howley antiform, down sequence of the Koolpin Formation-hosted Cosmo Gold Mine, which was mined as an open pit (1989–1994) and underground operation (2010–2016). The Lantern metasedimentary rocks are hosted in more structurally complex, deformed Koolpin Formation metasedimentary rocks between the Zamu and Phantom dolerite sills. Amphibolite grade metamorphic assemblages of chlorite–biotite–amphibole–quartz–garnet–cordierite–tourmaline–carbonate +/- pyrite–pyrrhotite–arsenopyrite form intense multiphase alteration. Mineralisation occurs in sandier metagreywacke beds and in selected quartz-carbonate veins. Gold grades tend to be higher in areas of more structural complexity with a preference towards Fe-rich sedimentary rocks.

Over the last year, KL commenced exploration development comprising eight additional underground drill sites, three cross cuts and three ore drives into Lantern mineralisation. With this additional diamond drilling information and *in-situ* access to the mineralised lodes, KL geologists have further opportunity to investigate the complexities of some of the higher grade mineralisation within Lantern deposit.

Technology and Innovation

KL's investment in existing and emerging technologies has enabled the company to work with multiple suppliers to further understand and delineate the Lantern resource. The NExT project (Numeric Exploration Technologies) was founded in May 2018 as a means to drive technology-assisted exploration and project definition in the Northern Territory, enabling higher quality geological interpretations and resource models than previously possible. The project has three key components:

- quick, accurate and consistent data acquisition
- effective communication and information accessibility
- mineralisation understanding and exploration targeting.

Key projects during 2018 focussed on quick and accurate data acquisition; two major study areas were drill core logging and underground face mapping.

Drill core logging data acquisition

Existing drill core logging practices comprise recording protolith lithology, rock alteration, sulfide mineralisation and vein characteristics. A geotechnical interval log (recovery, RQD, hardness, strength, weathering, fracture count and structural sets count) is also completed on every hole. On selected drillholes, a geotechnical defect orientation log is completed where fractures are characterised by orientation, type, roughness, alteration infill and thickness. Specific gravity measurements are performed on selected holes.

KL's aim for the drill core logging project was to assess the viability of geochemical and mineralogical data collection technologies and evaluate their suitability for delineation of Lantern geological features pertinent to resource estimation. Discriminating the controls on higher grade gold mineralisation is of specific focus. Technologies applied in the project included:

- portable XRF (pXRF) niche sampling
- portable ASD (Halo) hyperspectral mineralogical niche sampling
- portable (pXRF) pulp scanning
- magnetic susceptibility niche sampling
- Orexplore tomographic X-ray attenuation
- Minalyze continuous XRF (cXRF) analysis
- NTGS HyLogger™ short wave infrared (SWIR) and thermal infrared (TIR) analysis
- Corescan continuous SWIR analysis.

A niche sampling study comprised ~1400 point samples across four drillholes. Sample measurements were taken using pXRF, Halo, and a magnetic susceptibility meter; samples were selected to characterise alteration, veining and faulting. Four representative diamond drillholes were scanned using the NTGS HyLogger and analysed by Rocksearch Australia. One drillhole was also sent to Perth for Corescan and Minalyze analysis. In a separate study, intervals from 10 Lantern drillholes were also scanned using Minalyze and Corescan in an attempt to understand local geochemical and mineralogical variability using continuous scanning technology.

All technologies showed that there was adequate mineralogical and geochemical variation within Lantern metasediments to differentiate the major lithological units. HyLogger, Corescan and Minalyze also provided high quality core photos which have potential to be used for machine learning and automated logging purposes. Continuous multi-element cXRF geochemical scans produced by Orexplore and Minalyze allow variability to be mapped at niche sample intervals not previously understood. While both suppliers are working to rectify

[1] Kirkland Lake Gold Ltd, Dorat Road, Hayes Creek NT 0822, Australia
[2] Email: CLower@klgold.com.au

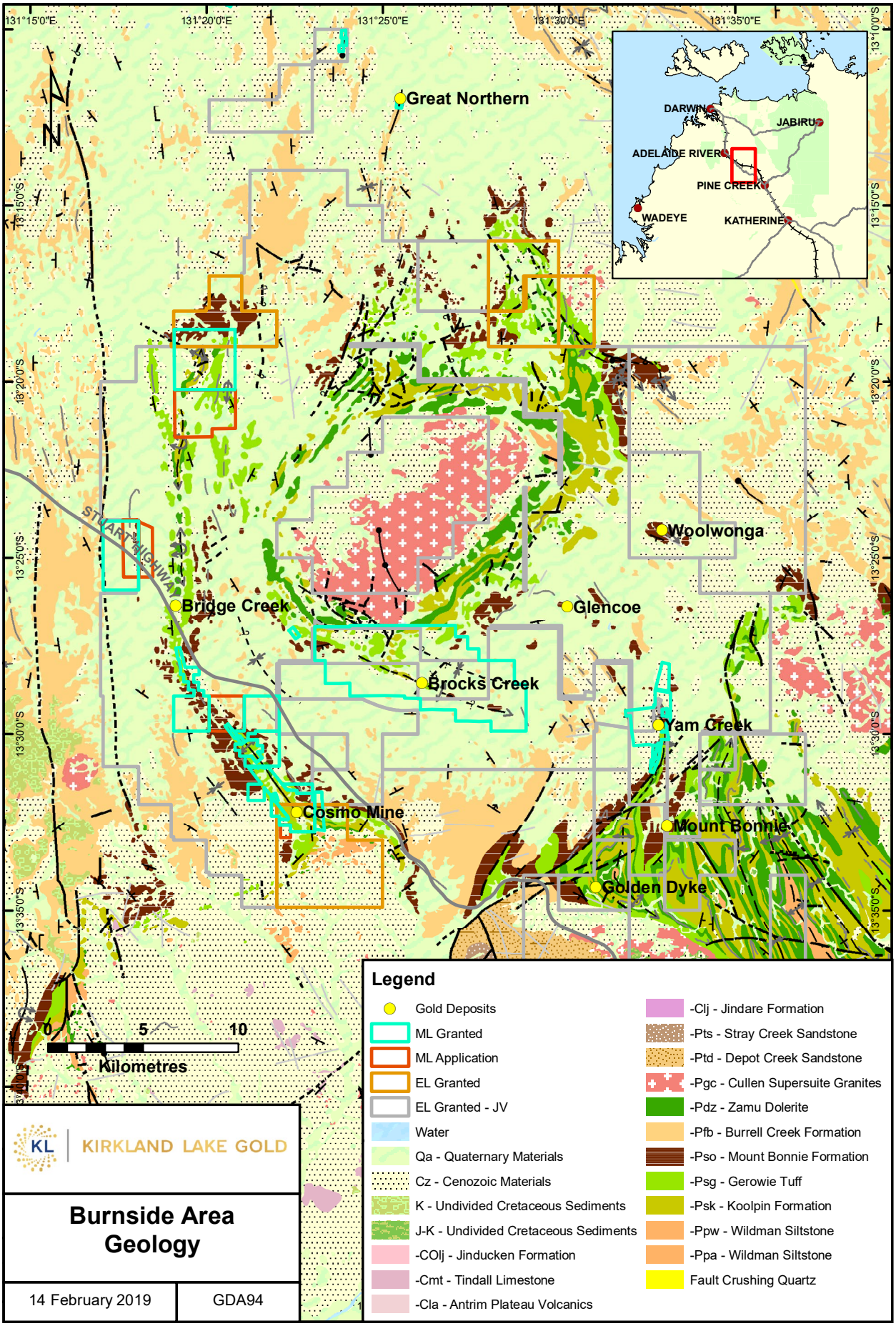

Figure 1. Burnside geology map (S Suy, KL, pers comm 2019) showing regional geology, tenement information and historical mines. The Lantern project is located at Cosmo Mine (lower left).

minor scanning artefacts, the geochemical data provided appears to be suitable for the application of calculated lithology algorithms. Corescan and HyLogger both provide hyperspectral data for mineral identification with the former able to illustrate 2D mineral relationships. The 0.5 mm precision SWIR data provided by Corescan is suitable for mineral mapping; however, it is limited in its infrared analysis range due to the abundance of anhydrous silicate minerals in Lantern's ore bearing metasediment units. While slightly lower resolution (8 mm scan intervals), the additional TIR analysis provided by HyLogger can identify the presence of many anhydrous silicate minerals observed in Lantern.

Orexplore, Minalyze, and Corescan also provide the user with the opportunity to collect geotechnical information. Orexplore allows user-defined two point defect orientation measurement using its Insight software. Minalyze has commercially-ready drill core RQD measurements and a structural defect picking interface under development. Research at the University of Tasmania has investigated the feasibility of automating geotechnical defect picking using Corescan data (Harraden *et al* 2017). At this stage, Minalyze is the only supplier that has attempted to quantify specific gravity from drill core; it has also worked on using multielement data to generate a gold-index as proxy for assaying to locate presence of gold in core without traditional core-destructive lab analyses.

Underground face mapping data acquisition

Existing underground face mapping practices comprised a hand drawn face map with an accompanying high resolution photograph. Chip sampling data was recorded on the face map and manually registered later using Surpac software. This process took 15 to 30 minutes at the face and an additional 15 minutes data entry and registration on surface.

KL's aim for the underground face mapping project was to collect more meaningful and higher resolution face mapping data with reduced time required to collect and register maps and images. The resultant data needed to be suitable for machine learning and automation. For this project, results from a previous trial at Fosterville Gold Mine were evaluated and potential suppliers selected accordingly. Within the Lantern development, two technologies were evaluated against existing practises:

- I-Site laser scanner (Maptek)
- CR Kennedy RTC360 laser scanner.

Maptek (I-Site) and CR Kennedy (RTC360) demonstrated their 3D photo-imagery laser scanners within the Lantern mine development. Both technologies were able to complete 3D registered scans in a time effective manner. The RTC360 was the fastest scanner and was able to capture an image of the development backs where I-Site was limited due to the placement of the LED light. The RTC360 was also lighter weight and easier to set up for scanning due to a purpose built tripod. Although the I-Site system did not come with its own tripod, it is built to integrate with existing site survey equipment. I-Site was able to capture a better quality image, primarily due to a stronger light source, and provided additional laser intensity data, which assisted geological interpretation. Both suppliers provided stand-alone software to manipulate the point cloud data, and both datasets could be imported into Surpac; however, the file sizes were generally too large to utilise effectively. Maptek Point Studio software was more user intuitive and efficient, with features such as automated defect mapping and additional software modules to support underground mapping/wireframing using drillhole data and existing geological interpretations.

Future Directions

Given the success of the NExT project to date, KL's goal is to work with selected semi to fully commercialised suppliers to develop products that are beneficial and effective for its Australian and Canadian operations and exploration projects. The focus of the drill core logging data acquisition project has moved to data validation of continuous scanning technologies (QXRD, petrology, wet-lab geochemistry) so that a site-based trial can be established. Given the importance but time consuming nature of geotechnical data collection, KL will work with suppliers to further develop and semi-automate geotechnical logging. Machine learning and cloud-based interfaces will be evaluated in an attempt to better categorise, validate and communicate logging and mapping information that enables offsite accessibility.

Acknowledgements

The author wishes to thank the KL Northern Territory mining operations geoscience team, and our technology suppliers: Maptek, CR Kennedy, Northern Territory Geological Survey, Rocksearch Australia, Corescan, Minalyze, Portable Analytical Systems, Olympus IMS and, Australian Laboratory Services.

References

Harraden C, Cracknell M, Lett J and Berry R, 2017. The Use of Automated Core Logging Technology to Improve Estimation of Fracture Mineralogy and Weathering for Geotechnical Index Calculations: in '*Drilling for Geology II Extended Abstracts'. Australian Institute of Geoscientists, Bulletin* 64, 73–80.

Kirkland Lake Gold Ltd, 2019. <https://www.klgold.com/home/default.aspx> [accessed February 2019].

AusAEM_1: One step towards a national conductivity map of Australia

A Yusen Ley-Cooper[1,2] and Ross C Brodie[1]

Introduction

Airborne geophysical surveys were initially conducted by Geoscience Australia (GA) and its predecessor agencies (Bureau of Mineral Resources and Australian Geological Survey Organisation) as part of regional mapping programs to build an inventory of Australia's potential resource endowment. Aerial surveys are one of the most cost effective tools for mapping and managing the Earth's resources. In conjunction with State and Territory geological surveys, for the past 50–60 years, we have systematically acquired and merged surveys to cover most of the Australian continent for the benefit of Australia's exploration investment activities.

Data collected are quality-controlled, enhanced and maintained by GA in national databases. Improvements in technology over time have led to the geophysical coverage of Australia being world-class, with over 35 million line-km of data stored. These are precompetitive datasets to be used to provide insights onto Australia's geological framework and to promote Australia's attractiveness globally to exploration companies. Knowledge gained through these surveys improves resource management and contributes to community safety.

Nowhere in Australia does exploration take place without a tremendous amount of contextual information provided by these national coverage data sets. An individual dataset might trigger some discoveries, but there would be, in all cases, several other datasets that contributed supporting information. These geophysical datasets are some of the drivers that underpin the mineral and energy industry's exploration strategies. They have been used successfully for geological mapping in remote areas that have a paucity of ground truth and outcrop.

A common problem with past national airborne geophysical coverages is that surveys were flown in a patchwork manner over many years and were registered to different datum. In the case of airborne gamma-ray spectrometric acquisition equipment, system calibration changed significantly over time. Older surveys in Australia were reported in units of counts per second, whereas modern surveys are reported in units of radioelement concentration. This meant that gamma-ray spectrometric surveys would seldom match their common borders, making it difficult to merge surveys into a continental-scale compilation thus limiting the utility of these data. Regional compilations facilitate the interpretation of large-scale features in the data, as well as the comparison of features significant distances apart. A similar problem occurred with magnetic surveys, with poor reference field removal introducing base-level shifts. In addition, the crossover tie levelling procedure commonly applied to airborne magnetic data introduced a range of spurious wavelengths into the levelled data.

The solution was to level and merge both gamma-ray spectrometric and magnetic surveys' into continental-scale compilations by acquiring new data in areas to overlap the existing surveys. This was done in a program called the Australia Wide Airborne Geophysical Survey (AWAGS; Minty *et al* 2009, Minty 2003). Data acquired have since been used to level and merge all public-domain gamma-ray spectrometric and magnetic data into seamless geophysical maps over the entire Australian continent.

Over the past three decades, airborne electromagnetic (AEM) surveying has become a routinely acquired dataset by government geoscientific agencies. Since the late 1990s, GA has been increasingly collecting AEM data over more-extensive regional areas in collaboration with State and Territory partners.

Simple levelling of AEM data from different surveys and systems yields a high degree of incoherency such that direct comparisons of the survey data are not objectively possible. Although all airborne EM systems have different characteristics, they overall should measure the same ground response. In order to allow some level of comparison, the data need to be transformed into conductivity models. GA has developed a suite of open-source algorithms that invert AEM data (Brodie 2015) to enable this transformation from data to conductivity.

Acquisition of AEM

The extent of government funded AEM survey coverage of Australia from the late 1990s to date is shown in **Figure 1**. Historically, some surveys have been particular milestones in GA's understanding, development and setting of standards of AEM data. Over this period, GA has optimised survey acquisition and contributed to the development of AEM systems to operate under Australian conditions.

In 2001, AEM was viewed as one of the emerging new mineral exploration discovery enablers for Australia. The Lower Balonne survey was a step improvement in accurate quantitative AEM surveying for land management. In 2003, GA started developing proposals to survey Australia at wide line-spacing rather than small, postage stamp areas with close line-separations. In 2007–08, GA first acquired broad line-spacing AEM surveys as part of the *Onshore Energy Security Program* (GA 2011) in the Paterson, Pine Creek and Frome regions (Roach 2012). These large-scale mapping programs have grown in size and are now an important component of projects like the *Exploring for the Future* (Ley-Cooper and Richardson 2018) AusAEM programme, a broad semi-continental scale survey aimed at enhancing exploration for new mineral, energy and groundwater resources.

The *Exploring for the Future* Australia-wide AEM (EFTF AusAEM) program is acquiring data over extents never previously attempted, some 22% of the total area of Australia. It continues a long-lasting tradition at GA of delivering precompetitive data to stimulate exploration,

[1] Geoscience Australia, Cnr Jerrabomberra Ave and Hindmarsh Drive, Symonston ACT 2609, Canberra, Australia.
[2] Email: Yusen.ley@ga.gov.au

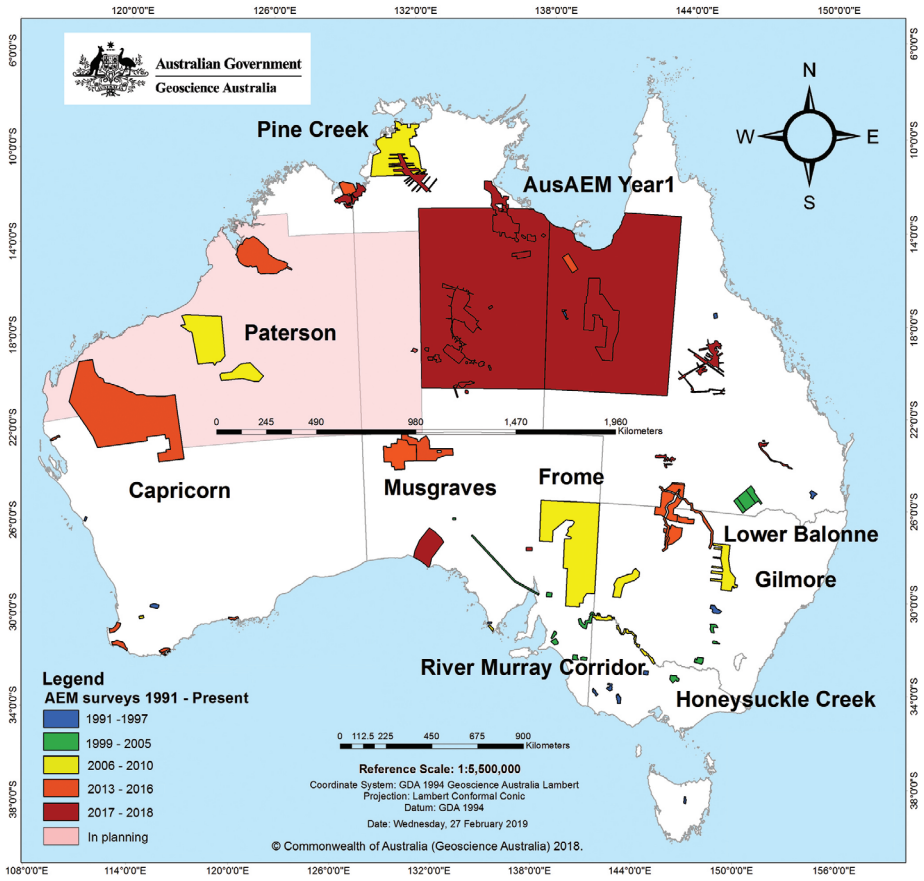

Figure 1. Historical acquisition of airborne electromagnetic data coverage. Survey funded by GA in partnership with States and Territory geological surveys and other government agencies.

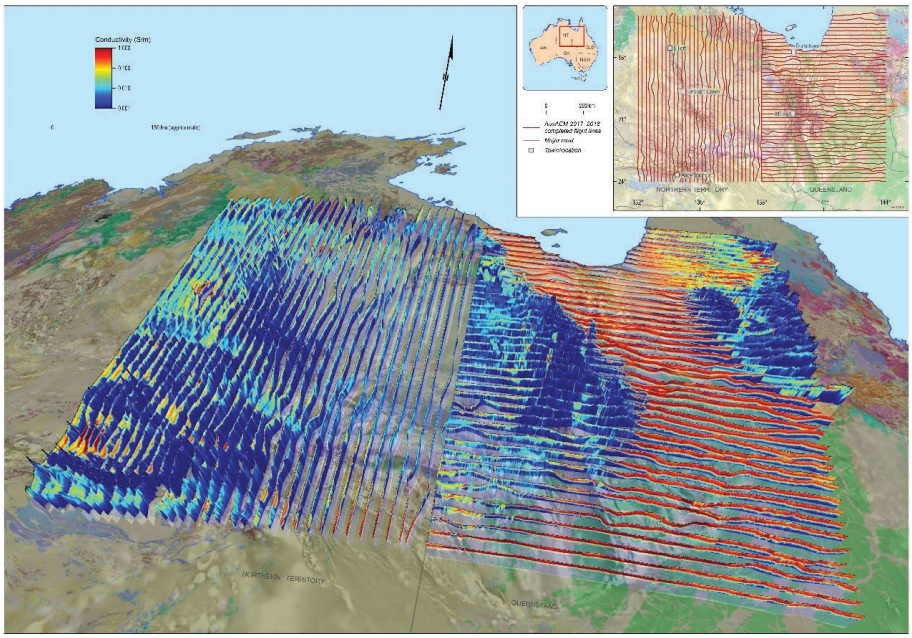

Figure 2. 3D composition of 900 km long conductivity depth-sections draped over a map of surface geology.

particularly by acquiring AEM data in areas with a paucity of data as a way of promoting exploration in new frontiers. Results from the first year of data acquisition (areas covered shown in **Figure 2)** have already proven useful in mapping the cover and basement interface. The data show new under-cover geological features that could host mineral deposits and groundwater resources. These data will provide explorers with insights in areas of thick cover with potential to generate targets for further investigation.

The image in **Figure 2** illustrates the distribution of 900 km long conductivity-depth sections from GA's 1D laterally constrained algorithm. Sections derived from the 20 km-spaced flight lines are analysed and displayed as 3D images; the sections are integrated with other datasets like gravity (**Figure 3**), magnetics, and radiometrics. The results have provided enough detail to map cover thickness and basement topography.

Inverted conductivity-depth models are enhancing our capacity to derive depth-to-target information of regional features, to map potential alteration and structural zones that delineate architecture within the regolith, and more broadly, to increase our understanding of mineral and groundwater

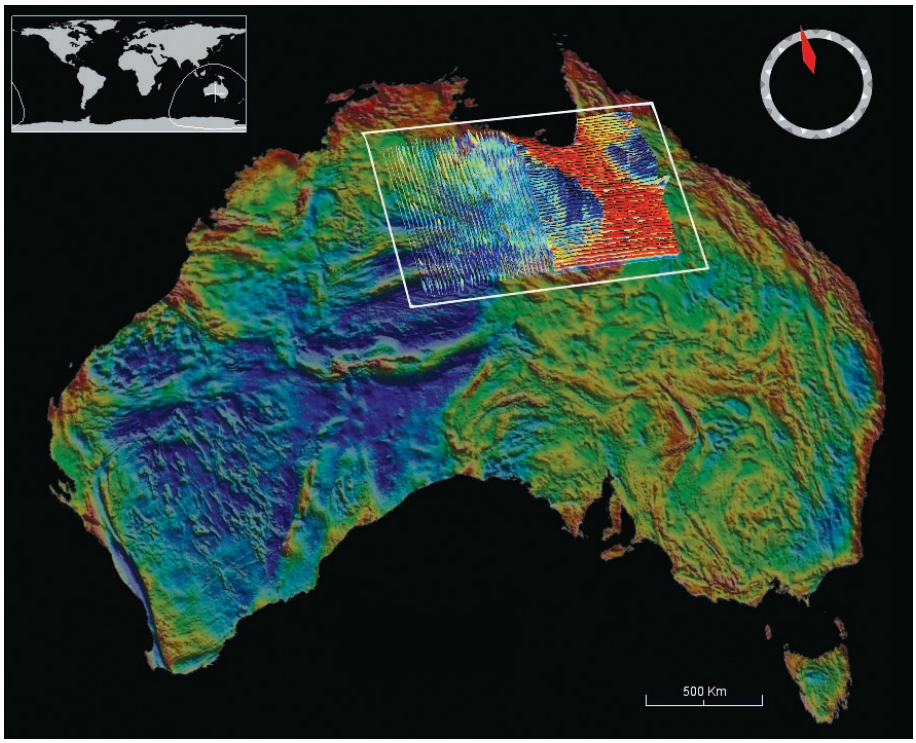

Figure 3. Extent of AusAEM's first year of acquisition draped over GA's national map of gravity. We are working towards a national AEM coverage à la radiometric and magnetics.

resource potential of the surveyed areas. Some anomalous confined conductive units in the basement and under a cover of what appears to be un-mineralized rocks, and regolith have also been unveiled by these models. In the right geological setting, these features would be of interest to mineral explorers and become the object of further examination.

AEM data also have numerous applications outside mineral exploration; in particular, the data are valuable for agricultural management and environmental monitoring. Farmers and graziers can use the data and derived products (in the form of maps and sections) to assess potential water resources to inform sustainable crop production and cattle grazing management.

Conclusion

The volume of downloads of geophysical data from the GA website is a silent testament to the usefulness of the precompetitive geophysical data for Australia. The contents of this data are conservatively valued at ~$240 million at today's cost of data acquisition per line km. However, these data have an enduring value that goes beyond a monetary figure.

Explorers can use the airborne magnetic, radiometric and electromagnetic data to reliably compare radiometric signatures observed over different parts of Australia, identify potential magnetically susceptible minerals, and identify new under-cover geological conductivity features that could host new mineral deposits and groundwater resources.

AEM is particularly useful in areas that have a significant thickness of surface cover (regolith and sedimentary basins) that can mask the underlying basement rocks. The high resolution, non-intrusive nature of the survey methods and the ability to scan the conductivity of the ground in three dimensions, have made the current AusAEM program a successful one. The program is acquiring data over extents never previously attempted. The conception of these broad-spaced large coverage surveys comes from a long-lasting tradition at GA of delivering precompetitive data to stimulate exploration, including AEM acquisition in data-poor areas as a way of promoting exploration in new frontiers.

These regional and continental data support a range of different applications, including geological mapping, mineral and petroleum exploration, geomorphological studies, and environmental and land management studies. Refinement and coverage of precompetitive geophysical data (airborne magnetics, airborne radiometric, ground gravity, and crustal reflection seismic) continues. Successful insights from less conventional methods, eg airborne EM, airborne gravity, airborne gravity gradiometry, magnetotellurics and passive seismic, have also gained traction. We are now working on the acquisition of data from these less conventional methods towards a national coverage à la gravity, radiometric and magnetics.

Aus AEM year 1 data are freely available for download from the GA website (www.ga.gov.au).

Acknowledgements

The authors acknowledge the valuable input of colleagues, mostly from the Mineral Resources Branch at Geoscience Australia. This work is published with the permission of the CEO, Geoscience Australia.

References

Geoscience Australia, 2011. *Energy security program achievements–Towards future energy discovery.* Geoscience Australia, GeoCat # 71823.

Brodie RC, 2015. *User Manual for Geoscience Australia's airborne electromagnetic, inversion*

software. Geoscience Australia. <https://github.com/GeoscienceAustralia/ga-aem.git> [accessed February 2019].

Ley-Cooper AY and Richardson M, 2018. AusAEM; acquisition of AEM at an unprecedented scale: *ASEG extended abstracts* 2018(1), 1–3.

Minty B, Franklin R, Milligan P, Richardson M and Wilford J, 2009. The radiometric map of Australia. *Exploration Geophysics* 40(4), 325–333.

Minty BRS, Milligan PR, Luyendyk APJ and Mackey T, 2003. Merging airborne magnetic surveys into continental-scale compilations. *Geophysics* 68(3), 988–995.

Roach IC, 2012. The Frome airborne electromagnetic (AEM) survey, South Australia: Implications for energy, minerals and regional geology. Geoscience Australia–Geological Survey of South Australia. *Geoscience Australia, Record* 2012/40-DMITRE Report Book 2012/00003, 296.

Update on the Finniss Lithium Project

David Rawlings[1,2]

Core Lithium has been exploring the Finniss Lithium Project, located in the Bynoe Pegmatite Field just 15 km south of Darwin (**Figure 1**), since April 2016 and has now progressed the project through various stages of feasibility and approvals for mining development. The accompanying presentation will focus on the exploration success and various facets of the lithium-rich pegmatite deposits.

The lithium prospectivity of the field was touched on by the Northern Territory Geological Survey (Ahmad 1995, Frater 2005), who recognised the favourable granite geochemistry and documented the historic tin-tantalum production. Although no economic lithium grades were encountered at that stage because all mining and drilling had been shallow, there was enough circumstantial evidence to encourage Core Lithium to drill deeper at two of the main soft-rock prospects, *Grants* and *BP33* (**Figure 1**). It quickly became clear that grades greater than 1.5% Li_2O were present. During the last two years, these prospects have been elevated from discovery status to Inferred, then Indicated, and now Measured category Mineral Resources (**Table 1**). A number of other prospects have also been explored through to Mineral Resource status: *Sandras*, *Carlton*, and *Hang Gong SW*. The global resource is expected to grow well beyond 10 Mt in the coming years as further targets are tested and drilled to mineral resource definition-spacing.

The pegmatites range from narrow 'veins' to broad lozenge-shaped bodies up to 500 m long and 60 m wide, generally trending north-northeast, parallel to regional fabric. Core Lithium has now recognised a class of pegmatite in the district that is flat-lying to shallow dipping, such as those at Hang Gong, Booths, and Lees (**Figure 1**). These are expected to represent a growing percentage of the global resource going forward as they should have better extraction economics than steeper dipping bodies. They have now been traced >1 km along strike at Lees–Booths Link.

[1] Core Lithium Ltd, Level 1, 366 King William Street, Adelaide SA 5000, Australia
[2] Email: drawlings@corelithium.com.au

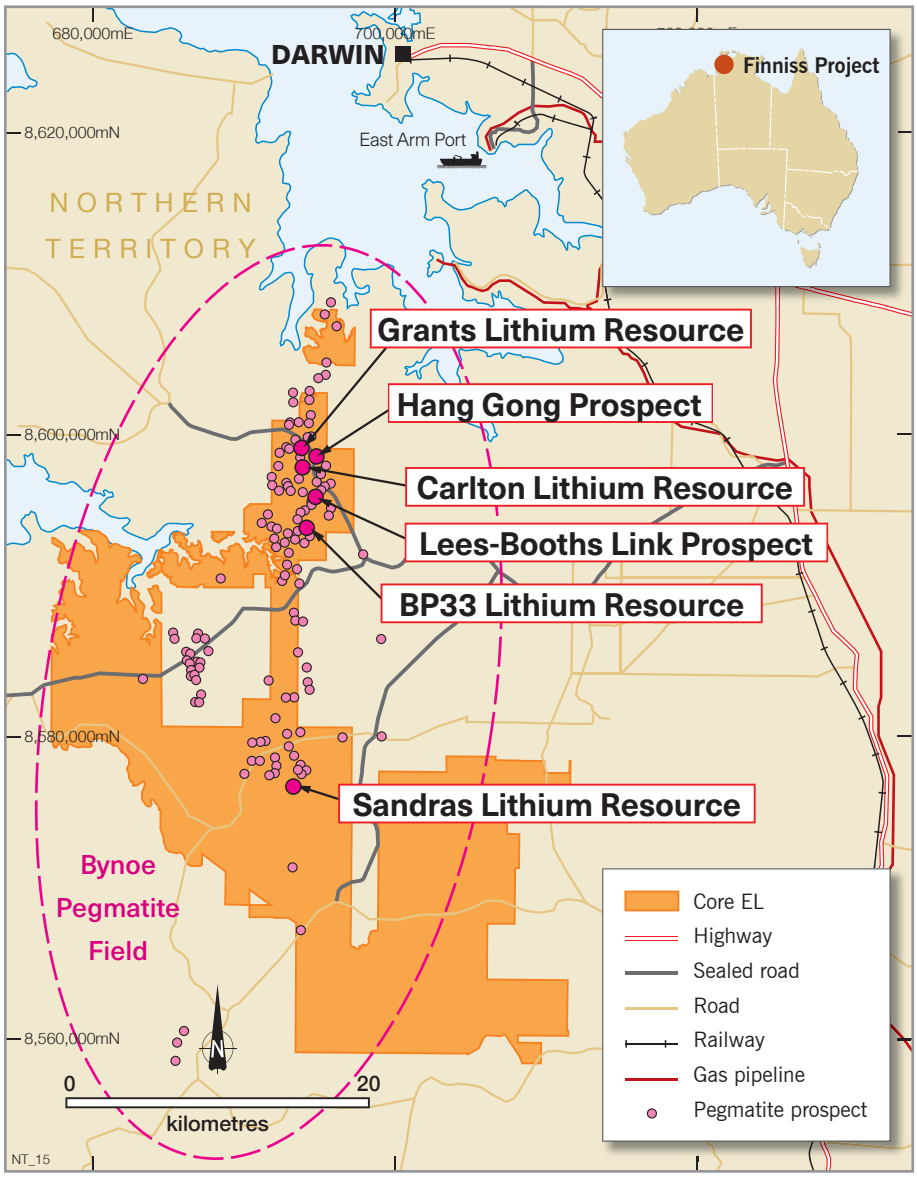

Figure 1. Core's Finniss Lithium Project – tenure, deposits and prospects.

Table 1. Finniss Project Global Resource inventory (as at 23rd January 2019).

Mineral Resource Estimate for the Finniss Lithium Project 23rd January 2019 – 0.75% Li_2O cut-off (except Sandras = 0.6%)					
Deposit	**Resource Category**	**Oxidation**	**Tonnes**	**Li_2O %**	**Contained Li_2O (t)**
Grants	Measured	Fresh	1 090 000	1.48	16 100
	Indicated	Fresh	820 000	1.54	12 600
	Inferred	Fresh	980 000	1.30	14 000
	Total		**2 890 000**	**1.48**	**42 700**
BP33	Indicated	Fresh	630 000	1.39	9 000
	Inferred	Fresh	1 520 000	1.56	24 000
	Total		**2 150 000**	**1.51**	**33 000**
Sandras	Inferred	Fresh	1 300 000	1.0	13 000
	Total		**1 300 000**	**1.0**	**13 000**
Carlton	Inferred	Fresh	790 000	1.3	10 000
	Total		**790 000**	**1.3**	**10 000**
Hang Gong SW	Inferred	Fresh	1 140 000	1.2	14 000
	Inferred	Fresh	70 000	1.2	1 000
	Inferred	Fresh	210 000	1.0	2 000
	Total		**1 420 000**	**1.2**	**17 000**
Finniss Project	**Total**		**8 550 000**	**1.33**	**115 700**

Pegmatites at the Finniss Lithium Project outcrop as highly weathered, clay-quartz saprolite, close to the Tertiary weathering surface, which is now being slowly exhumed. There is no sign of the lithium-bearing mineral spodumene at any the 100-odd historic prospects due to weathering. In drill core, the fresh pegmatite is composed of extremely coarse-grained spodumene (20–30%), quartz, albite, microcline and muscovite (in decreasing order of abundance), along with accessory ambygonite, apatite, cassiterite, ilmenite, rutile, and rare columbite, tantalite, tourmaline (elbaite), fluorite, topaz and beryl. There is no lepidolite recognised. Spodumene can either occur intergrown with the other minerals (eg poikilitic) or as solitary, large inclusion-free crystals. This textural character varies from prospect to prospect, as does the colour. The grade distribution also varies between the deposits – at BP33 and Grants, the grade is very consistent; while at Hang Gong and Sandras, it is patchy. Garnet and andalusite are common in the Burrell Creek Formation host around the periphery of the larger pegmatites.

All of the 100-odd historic mines and prospects were found by surface prospecting; however, given the limited exposure of bedrock in the district, it is unfathomable that there are not hundreds more. A mere 1 m of laterite is enough to have concealed them from the old timers and various forms of modern surface exploration like remote sensing and soil geochemistry. New discoveries will need to come on the back of innovative exploration techniques (largely geophysical) in what is largely a geophysically amorphous terrain.

Core Lithium has progressed to using auger geology to map shallow, concealed pegmatites that are identified in HyMapper and HyCam data; this exploration method has already led to the generation of five new large-scale targets to test in 2019.

Acknowledgements

Exploration over the last three years has benefitted from the contributions of many field-based geologists, including Andrew Jettner, Glen McIlwain, Ian Warland, Peter Hill, Mairi Walsh, Michael Hicks, Kim Boundy and Ian Garsed. Field support has been provided by Kim Petherick, Mike Hope, Wally Balaz, Greg McEvoy and John Francis.

References

Frater KM, 2005. Tin–tantalum pegmatite mineralisation of the Northern Territory. *Northern Territory Geological Survey, Report* 16.

Ahmad M, 1995. Genesis of tin and tantalum mineralisation in pegmatites from the Bynoe area, Pine Creek Geosyncline, Northern Territory. *Economic Geology* 42, 519–534.

Detrital zircon geochronology investigations of the Glyde and Favenc packages: Implications for the geological framework of the greater McArthur Basin, Northern Territory

Tim J Munson[1,2]

The greater McArthur Basin (Close 2014) is an informal term for a vast, predominantly sedimentary terrane stretching across the northern part of the Northern Territory from northeastern Western Australia to northwestern Queensland (**Figure 1**). It includes Palaeo- to Mesoproterozoic successions of the McArthur Basin, Birrindudu Basin and the Tomkinson Province, all of which are interpreted to be linked in the subsurface based on geophysical and drilling evidence. These successions unconformably overlie Archaean and Palaeoproterozoic metamorphosed and deformed rocks of the North Australian Craton (NAC) and are unconformably overlain by Neoproterozoic to Phanerozoic cover. The range of facies present within the successions indicates mostly shallow-marine to emergent, to lesser continental/fluvial environments of deposition in all areas. Minor felsic and mafic extrusive and intrusive rocks are present, mainly in the lower parts of the McArthur Basin; widespread thin tuff/tuffite beds are locally abundant in some intervals. Sills of the regionally extensive Derim Derim Dolerite and its equivalents intrude the upper parts of the successions in the east and south.

The sedimentary successions of the McArthur Basin were subdivided by Rawlings (1999) into five basin-wide, non-genetic depositional 'packages' bounded by regional unconformities: in ascending order, the Palaeoproterozoic Redbank, Goyder, and Glyde packages; and the Mesoproterozoic Favenc and Wilton packages; these are in part equivalent to four large stacked 'superbasins', defined by Jackson *et al* (1999, 2000) and Southgate *et al* (2000) in the Mount Isa Province and southern McArthur Basin: in ascending order, the Leichhardt, Calvert, Isa and Roper superbasins. The packages are disconformity or unconformity bounded; each is characterised by similarities in age, stratigraphic position, lithofacies composition, style and composition of volcanism, and basin-fill geometry. The definitions of these packages were subsequently informally extended by NTGS to include correlative successions within the Birrindudu Basin and Tomkinson Province.

A major goal of recent NTGS geological programs under the current four-year (2018–2022) *Resourcing the*

[1] Northern Territory Geological Survey, GPO Box 4550, Darwin NT 0801, Australia
[2] Email: tim.munson@nt.gov.au

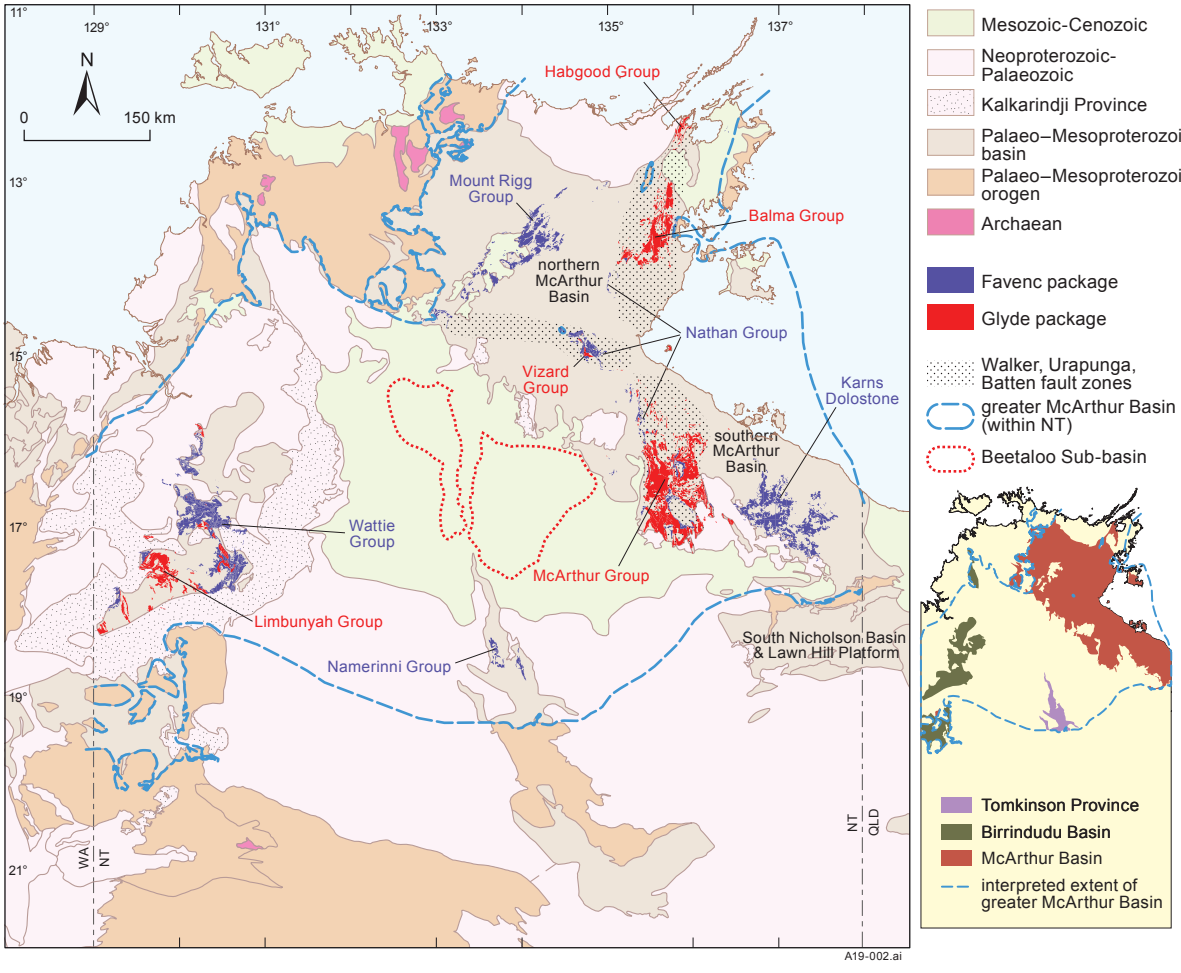

Figure 1. Location of stratigraphic groups assigned to Favenc and Glyde packages in greater McArthur Basin on map of NT geological regions derived from NTGS 1:2.5M geological regions GIS dataset.

Territory and previous (2014–2018) *Creating Opportunities for Resource Exploration* initiatives has been to establish a robust stratigraphic framework across the greater McArthur Basin to support more detailed geological studies and industry exploration programs. The first phase of this project was focused on the youngest Wilton package and results were released in Munson (2016); current work is directed at the underlying Glyde and Favenc packages.

The **Glyde package** is here defined (**Figures 1**, **2**) as including the McArthur Group (southern McArthur Basin), Vizard Group [central McArthur Basin (URAPUNGA[3] area)], Habgood and 'lower' Balma groups (northern McArthur Basin), and Limbunya Group (Birrindudu Basin). These successions are a mix of siliciclastic, carbonate and mixed carbonate/fine-grained siliciclastic rocks, deposited in the age range ca 1660–1610 Ma, in dominantly shallow-marine to emergent palaeoenvironments. Formations of the Glyde package are considered very prospective for base metals and petroleum across the greater McArthur Basin as they host significant base metals deposits in the southern McArthur Basin, including the giant McArthur River zinc-lead mine.

The **Favenc package** is here defined (**Figures 1**, **2**) as including the Karns Dolostone (southern McArthur Basin), Nathan Group (southern, central and northern McArthur Basin), Mount Rigg Group and probably 'upper' Balma Group (northern McArthur Basin), Wattie Group (Birrindudu Basin), and Namerinni Group (Tomkinson Province). It contains siliciclastic and carbonate rocks, and minor mafic volcanic rocks, deposited from ca 1610 Ma to 1580 Ma or possibly younger, in shallow-marine to fluvial palaeoenvironments.

Geochronological investigations of the Glyde and Favenc packages

All geochronological investigations of the Glyde and Favenc packages to date are summarised in **Table 1** and **Figure 2**. The majority of age determinations have been conducted on tuffs/tuffites (**Figure 3**), tuffaceous sedimentary rocks and sandstones. Tuffs and tuffites are locally abundant in some stratigraphic intervals of the greater McArthur Basin, but are rare to uncommon in other sections. They typically yield zircon populations with a relatively narrow range of ages, the weighted means of which are generally interpreted as being representative of the absolute age of the eruption and of the host stratigraphic unit, although *sensu stricto*, they are maximum deposition ages. Sandstones and tuffaceous sedimentary rocks are targeted for detrital zircons, which typically yield a much wider range of ages that reflect multiple provenances and/or sediment pathways. The youngest, statistically discrete, concordant zircon population or individuals can be used to define the maximum depositional age (MDA) of the host sedimentary unit. Detrital zircon age spectra are useful for determining sediment provenance and have been shown to be a practical tool for correlating successions across the greater McArthur Basin (Munson 2016).

[3] Names of 1:250 000 mapsheets are shown in capital letters, eg URAPUNGA.

This report summarises new geochronological results from the Glyde and Favenc packages that were sampled during NTGS field programs across the greater McArthur Basin from 2016–2018; details of these new results are reported in Kositcin *et al* (2017), Kositcin and Munson (in press), and Munson *et al* (in prep a, b). The new results are integrated with previous geochronological results and other geological data in order to test and refine intrabasinal correlations, which previously have not been very well established due to poor or non-existent intervening outcrop and inadequate temporal constraints. For this investigation, all available detrital zircon age spectra were standardised to the same age scale and compiled into comparative relative probability figures focused on stratigraphic intervals of interest, which are discussed in the following sections.

McArthur Basin: Age and correlation of Glyde package units

A number of units of the McArthur Group (southern McArthur Basin) and Vizard Group (central McArthur Basin) are relatively well dated due to the occurrence of felsic tuffs that have yielded datable zircon populations (**Figure 2**, **Table 1**). Tuffs are abundant in some Glyde package units but are rare to absent in others, with the result that some intervals are less well constrained in age.

McArthur Group

The McArthur Group is subdivided into the lower Umbolooga Subgroup and upper Batten Subgroup. Undated basal units of the Umbolooga Subgroup are poorly constrained by a ca 1713 ± 7 Ma age for the Tanumbirini Rhyolite at the top of the underlying Redbank package (Page and Sweet 1998), and by an estimated magmatic crystallisation age range of 20–40 million years for the intervening, poorly dated Goyder package (Parsons Range Group); this provides an inferred maximum age for the basal formation (Masterton Sandstone) in the range ca 1690–1670 Ma (Rawlings 1999). Maximum depositional ages of ca 1755 Ma from detrital zircon dating of the Masterton Sandstone (**Table 1**) do not better constrain the age of this unit, however an MDA of 1653 ± 17 Ma for a green tuffaceous siltstone from the overlying Mallapunyah Formation suggests that the base of the McArthur Group is probably only slightly older. The medial McArthur Group from the Tatoola Sandstone (Umbolooga Subgroup) to Lynott Formation (basal Batten Subgroup) is relatively well dated in the age range ca 1648–1636 Ma, indicating that these units must have been rapidly accumulated and that any time break between the subgroups was relatively short.

The upper McArthur Group (Batten Subgroup) is more sparsely dated: a tuff from the Stretton Sandstone has returned an age of 1625 ± 2 Ma, and the uppermost units of the subgroup were deposited in the age range ca 1614–1609 Ma. The youngest ages (1609 ± 3 Ma and 1613 ± 4 Ma) were returned from tuffs within the 'lower' Balbirini Dolostone. These are indistinguishable from an age of 1614 ± 4 Ma from a tuff within the underlying Amos Formation and are much older than an age of 1589 ± 3 Ma from a tuff within the 'upper'

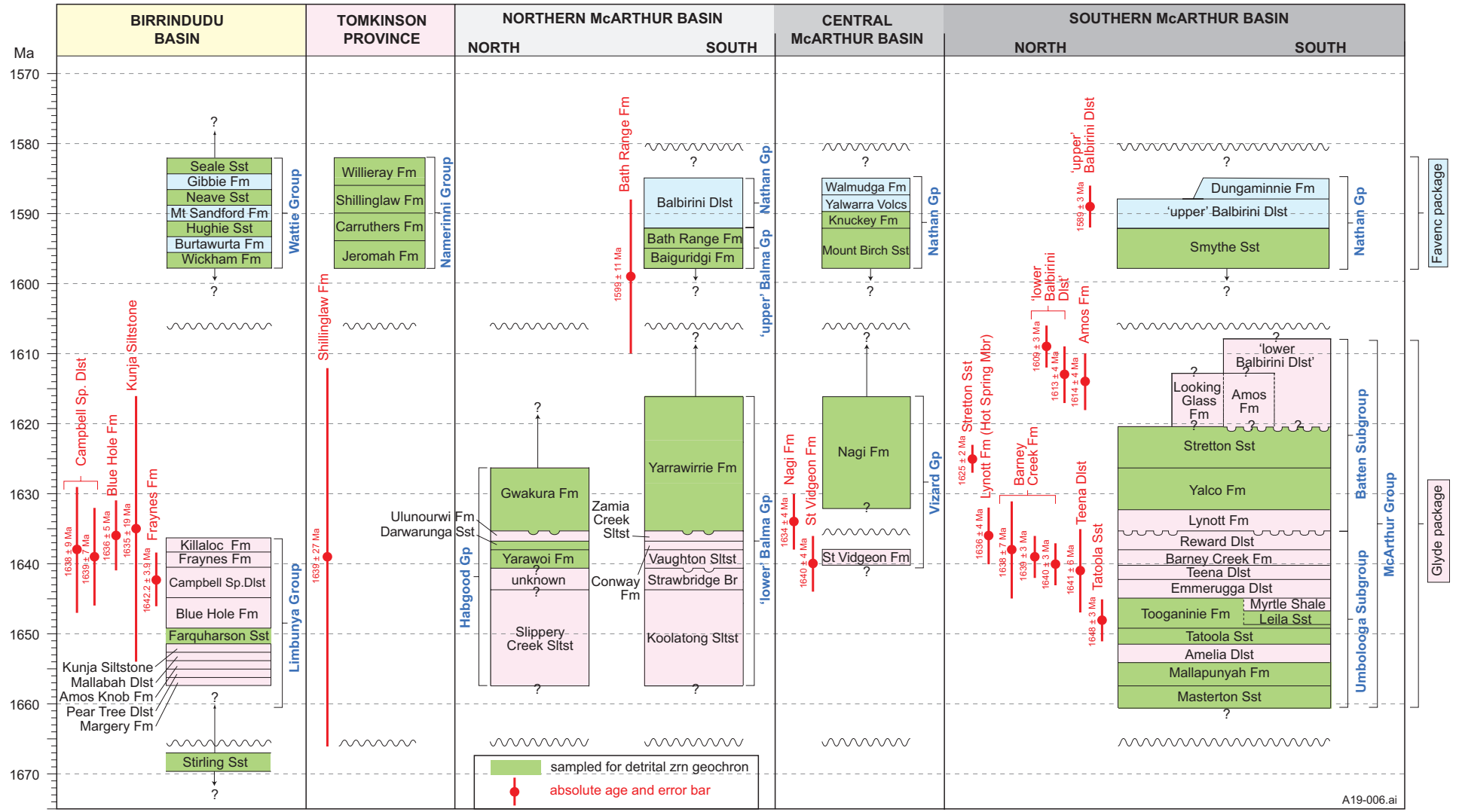

Figure 2. Stratigraphic correlation chart summarising new and previous geochronological data referred to herein (see **Table 1**). Note that age of Stirling Sandstone might be appreciably older than depicted in this chart (MDA ca 1830 Ma, see text). Unit thicknesses are diagrammatic and not to scale.

Unit	Sample	Absolute age (Ma)	MDA (youngest zrn)(Ma)	Source
Wattie Group				
Seale Sst	Sst: SHRIMP U–Pb detrital zrn		1605 ± 12	Kositcin and Carson (2017)
Neave Sst	Sst: SHRIMP U–Pb detrital zrn		1617 ± 39	Carson (2013)
Hughie Sst	Sst: SHRIMP U–Pb detrital zrn		1595 ± 22	Kositcin and Carson (2017)
Wickham Fm	Sst: SHRIMP U–Pb detrital zrn		1639 ± 16	Carson (2013)
Nathan Group				
'upper' Balbirini Dlst	Tuff: SHRIMP U–Pb zrn	1589 ± 3		Page *et al* (2000)
Smythe Sst	Sst: SHRIMP U–Pb detrital zrn		1605 ± 14	Kositcin *et al* (2017)
Knuckey Fm	Sst: SHRIMP U–Pb detrital zrn		1616 ± 7	Kositcin and Munson (in press)
Mount Birch Sst	Sst: SHRIMP U–Pb detrital zrn		1629 ± 24, 1615 ± 28	Kositcin and Munson (in press)
Namerinni Group				
Willieray Fm	Sst: LA–ICP–MS U–Pb detrital zrn		1582 ± 17 (1526 ± 26)	Munson *et al* in prep a
Shillinglaw Fm	Sst: SHRIMP U–Pb detrital zrn		1595 ± 10	Kositcin and Munson (in press)
Shillinglaw Fm	Tuffite?: SHRIMP U–Pb zrn	1639 ± 27		Nunn (1997)
Carruthers Fm	Sst: SHRIMP U–Pb detrital zrn		1688 ± 13	Kositcin and Munson (in press)
Jeromah Fm	Sst: LA–ICP–MS U–Pb detrital zrn		1592 ± 46	Munson *et al* in prep a
'upper' Balma Group				
Bath Range Fm	Sst: SHRIMP U–Pb detrital zrn		1626 ± 9	Kositcin and Munson (in press)
Bath Range Fm	Tuffaceous mdst: SHRIMP U–Pb zrn	1599 ± 11		Pietsch *et al* (1994)
Baiguridji Fm	Sst: SHRIMP U–Pb detrital zrn		1624 ± 16	Kositcin and Munson (in press)
'lower' Balma Group				
Yarrawirrie Fm	Sst: LA–ICP–MS U–Pb detrital zrn		1654 ± 11	Munson *et al* in prep a
Yarrawirrie Fm	Tuffaceous mdst: SHRIMP U–Pb zrn		1621 ± 21	Pietsch *et al* (1994)
Habgood Group				
Gwakura Fm	Sst: LA–ICP–MS U–Pb detrital zrn		1673 ± 11 (1645 ±16)	Munson *et al* in prep a
Darwarunga Sst	Sst: SHRIMP U–Pb detrital zrn		1661 ± 19	Kositcin *et al* (2017)
Yarawoi Fm	Sst: SHRIMP U–Pb detrital zrn		1705 ± 18	Kositcin *et al* (2017)
Vizard Group				
Nagi Fm	Sst: SHRIMP U–Pb detrital zrn		1631 ± 16 Ma	Kositcin and Munson (in press)
Nagi Fm	Tuff: SHRIMP U–Pb zrn	1634 ± 4		Page *et al* (2000)
Saint Vidgeon Fm	Tuff: SHRIMP U–Pb zrn	1640 ± 4		Page *et al* (2000)
Limbunya Group				
Fraynes Fm	Tuff: TIMS U–Pb zrn	1642.2 ± 3.9		Munson *et* al in prep b
Campbell Springs Dlst	Tuffite: SHRIMP U–Pb zrn	1638 ± 9		Armstrong (1998)
Campbell Springs Dlst	Tuffite: SHRIMP U–Pb zrn	1639 ± 7		Smith (2001)
Blue Hole Fm	Tuffite: SHRIMP U–Pb zrn	1636 ± 5		Smith (2001)
Farquharson Sst	Sst: SHRIMP U–Pb detrital zrn		1654 ± 12	Kositcin *et al* (2017)
Kunja Sltst	Tuff: SHRIMP U–Pb zrn	1635 ± 19		Fanning (1991)
Stirling Sst	Sst: SHRIMP U–Pb detrital zrn		1830 ± 13	Carson (2013)
McArthur Gp				
'lower' Balbirini Dlst	Tuff: SHRIMP U–Pb zrn	1613 ± 4, 1609 ± 3		Page *et al* (2000)
Amos Fm	Tuff: SHRIMP U–Pb zrn	1614 ± 4		Page *et al* (2000)
Stretton Sst	Sst: SHRIMP U–Pb detrital zrn		1634 ± 18	Kositcin and Munson (in press)
Stretton Sst	Tuff: SHRIMP U–Pb zrn	1625 ± 2		Page *et al* (2000)
Yalco Fm	Sst: SHRIMP U–Pb detrital zrn		1655 ± 17	Kositcin *et al* (2017)
Lynott Fm (Hot Spring Mbr)	Tuff: SHRIMP U–Pb zrn	1636 ± 4		Page *et al* 2000
Barney Creek Fm	Tuff: SHRIMP U–Pb zrn	1638 ± 7, 1639 ± 3, 1640 ± 3		Page *et al* (2000)
Teena Dlst (Coxco Dlst Mbr)	Tuff: SHRIMP U–Pb zrn	1639 ± 6		Page *et al* (2000)
Leila Sst	Sst: SHRIMP U–Pb detrital zrn		1756 ± 32 (1690 ± 55)	Kositcin and Munson (in press)
Tooganinie Fm	Sst: SHRIMP U–Pb detrital zrn		1758 ± 41 (1664 ± 38)	Kositcin and Munson (in press)
Tatoola Sst	Sst: SHRIMP U–Pb detrital zrn		1671 ± 13	Kositcin and Munson (in press)
Tatoola Sst	Tuff: SHRIMP U–Pb zrn	1648 ± 3		Page *et al* (2000)
Mallapunyah Fm (upper)	Tuffaceous sltst: SHRIMP U–Pb zrn		1653 ± 17	GA geochron delivery, Page *et al* (2000)
Masterton Sst	Sst: SHRIMP U–Pb detrital zrn		1755 ± 15	Hollis *et al* (2010)
Masterton Sst	Sst: SHRIMP U–Pb detrital zrn		1755 ± 6	Kositcin *et al* (2017)

Table 1. Summary of all geochronology results pertaining to the Glyde and Favenc packages. Stratigraphic units are arranged in ascending order.

Balbirini Dolostone, leading Rawlings (1999) and Haines *et al* (1999) to consider the 'lower' Balbirini Dolostone to be a separate formation at the top of the Batten Subgroup; this conclusion is followed herein.

Vizard Group

Tuffs within the Saint Vidgeon Formation and lower part of the overlying Nagi Formation are relatively well dated at 1640 ± 4 Ma and 1634 ± 4 Ma respectively. The Saint Vidgeon Formation is confidently correlated with the Barney Creek Formation (upper Umbolooga Subgroup), whereas the Nagi Formation is correlated with part or all of the Batten Subgroup (Rawlings 1999, Abbott *et al* 2001, **Figure 2**). Detrital zircon age spectra for sandstone samples from the Nagi Formation and Batten Subgroup have similar MDAs and modal distributions (**Figure 4**), which supports this interpretation. The lower part of the Saint Vidgeon Formation is not exposed, and no equivalents of the lower Umbolooga Subgroup are known from the Vizard Group.

Balma and Habgood groups

The Balma and Habgood groups in the northern McArthur Basin are not well dated, as many units are poorly exposed and neither succession has been drilled. These groups have been broadly equated with one another and with the McArthur Group (eg, Plumb and Derrick 1975, Haines 1994, Pietsch *et al* 1994, Rawlings *et al* 1997, Rawlings 1999, Haines *et al* 1999, see **Figure 5**), but intrabasinal correlations at the formation level have been largely speculative.

Pietsch *et al* (1994) dated two tuffaceous mudstones from the Balma Group. A sample from the Yarrawirrie Formation returned a detrital zircon spectrum with an MDA of 1621 ± 21 Ma (**Figure 4**), whereas a sample from the base of the Bath Range Formation at the top of the group returned a robust maximum at 1599 ± 21 Ma plus a few scattered older detrital zircons (**Figure 6**); the peak at ca 1599 Ma was considered to be 'the magmatic age of these euhedral zircons, and a good stratigraphic age for the tuff' by the analyst (R Page 1996). Haines *et al* (1999) noted that this age is within statistical error of ages determined for both the uppermost units of the McArthur Group and the upper Balbirini Dolostone of the Nathan Group (see above). The Bath Range Formation is discussed further herein under ***Age and correlation of Favenc package units***.

Figure 3. Thick (40 cm) tuff bed, commonly referred to colloquially as 'pinkite', within laminated dolostone of Saint Vidgeon Formation at type section, about 1 km south of Mount Birch in URAPUNGA (53 466246mE 8366690mN).

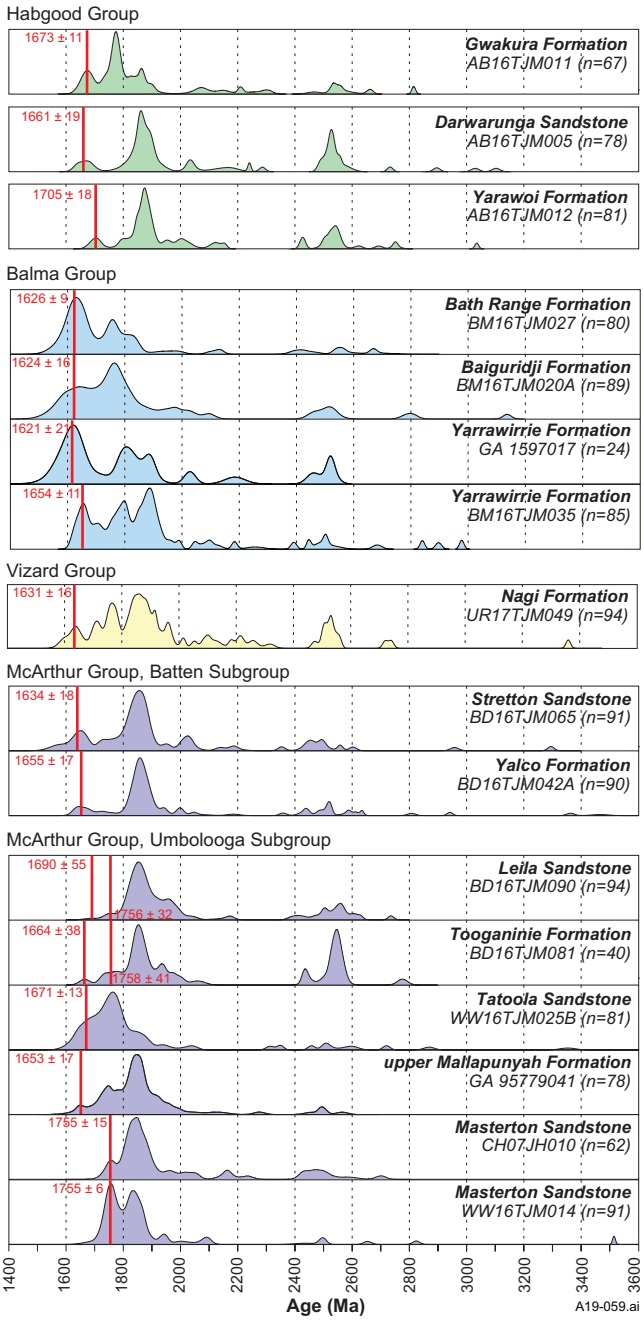

Figure 4. Comparative relative probability diagram of detrital zircon age data, with formations arranged in stratigraphic order for McArthur Group (mauve polygons), Vizard Group (yellow), Balma Group (blue), and Habgood Group (green). Detrital zircon age data for upper Mallapunyah Formation (GA 95779041) and Yarrawirrie Formation (GA 1597017) plots are from GA Geochron Delivery. References for all data provided in **Table 1**. Relative probability age spectra are not to scale vertically; associated histograms used to construct the spectra are not shown for clarity; number of concordant and near-concordant (<10%) analyses (n) is shown on right. Red lines indicate assigned maximum depositional age for each sample; if two lines present, LHS line is youngest concordant zircon(s).

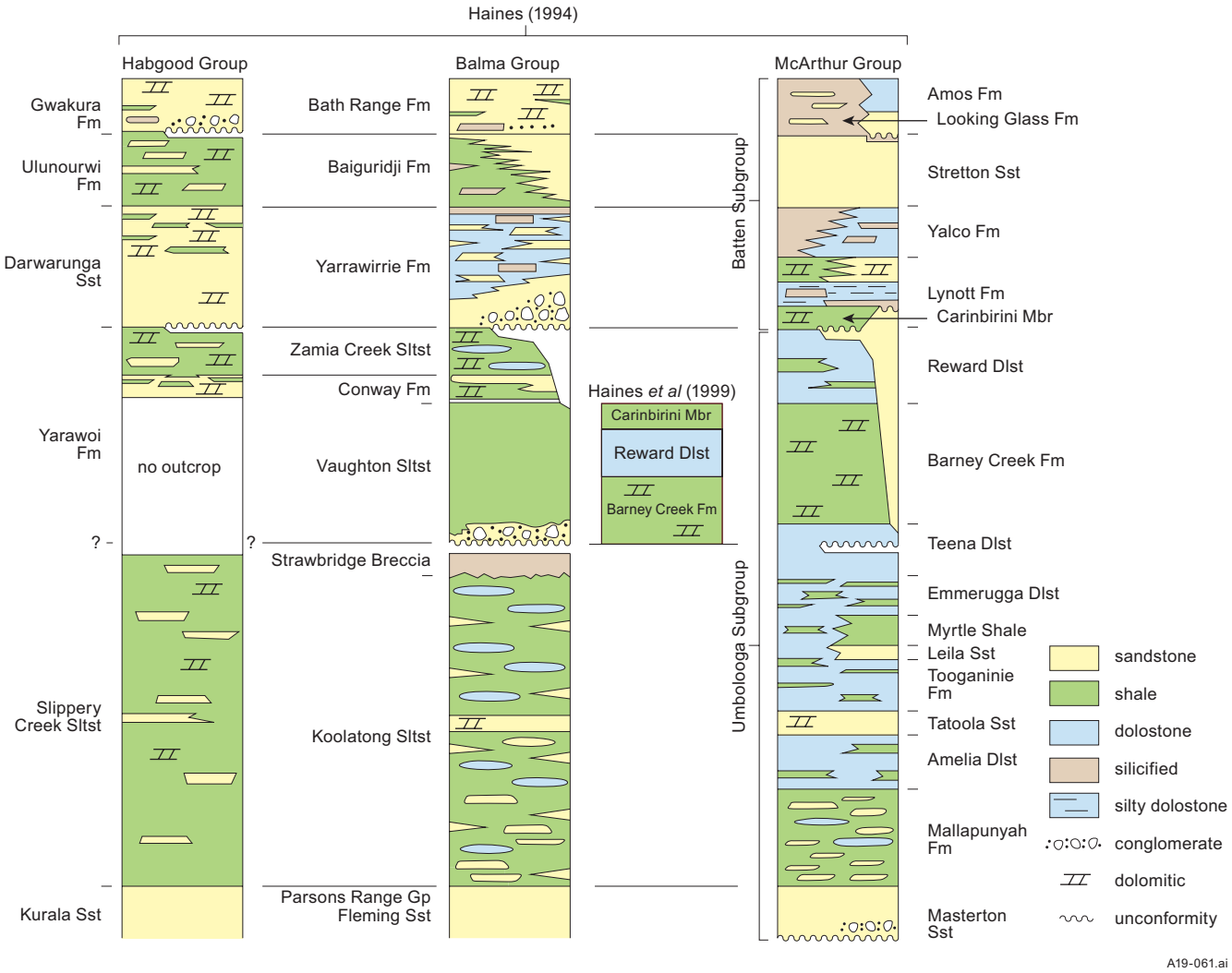

Figure 5. Schematic chart (after Frichot *et al* 2017: figure 3) showing possible correlations between McArthur, Balma and Habgood groups, as interpreted by Haines (1994: figure 2). Alternative correlation of Vaughton Siltstone with McArthur Group units, after Haines *et al* (1999), on RHS.

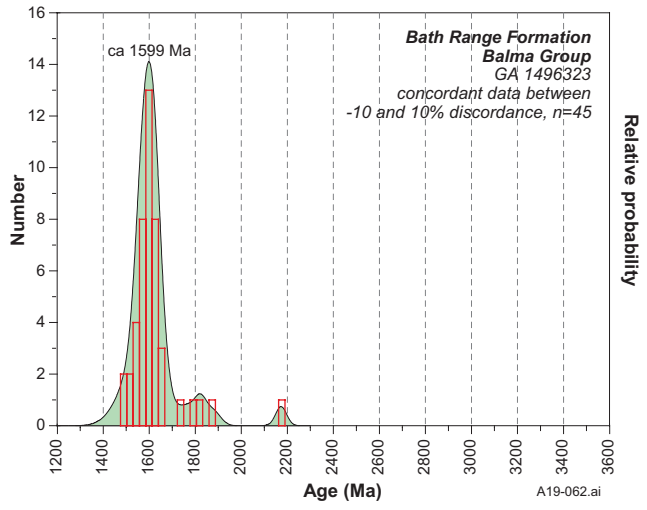

Figure 6. Probability density plot of 45 analyses on 45 euhedral zircon grains from tuffaceous mudstone near base of Bath Range Formation (sample number GA 1496323). Age maximum at ca 1599 Ma was interpreted as the main magmatic population and 'a good stratigraphic age for the tuff' by analyst (R Page, 1996). Data sourced from GA Geochron Delivery.

The detrital zircon age spectrum for a sandstone sample from the Yarrawirrie Formation (NTGS BM16TJM035) has a similar modal distribution to those of the Nagi Formation and units of the Batten Subgroup (**Figure 4**); the ca 1621 Ma MDA from the tuffaceous mudstone (GA 1597017) is consistent with a depositional age equivalent to the Batten Subgroup. A broad correlation between these units, as previously interpreted, is therefore supported by these data.

The medial to upper Habgood Group units Yarawoi Formation, Darwarunga Sandstone, Ulunourwi Formation and Gwakura Formation have previously been directly correlated with the Balma Group units Vaughton Siltstone, Yarrawirrie Formation, Baiguridji Formation and Bath Range Formation respectively, based on their apparently equivalent stratigraphic positions and from limited lithostratigraphic criteria (eg, Haines 1994, **Figure 5**). However, detrital zircon age spectra obtained from a number of sandstone samples of these formations (**Figure 4**) provide little or no support for these correlations. Spectra from three formations of the Habgood Group (Yarawoi Formation, Darwarunga Sandstone and Gwakura Formation) have appreciably older MDAs (ca 35–80 million years) than those

of upper Balma Group units, which have prominent young modes in the age range ca 1626–1621 Ma. The Habgood spectra also have significant older modes at ca 1870 Ma that are not present in the upper Balma Group. These features collectively show that there were significant dissimilarities in sediment provenances and/or sediment pathways between the two groups. Habgood Group detrital zircon age spectra have some similarities with those of both the Batten and upper Umbolooga subgroups of the McArthur Group, particularly in the amplitudes and distribution of older modes (**Figure 4**). However, MDAs that are greater than ca 1660 Ma suggest that all three Habgood Group formations might be older than previously interpreted and that they might be equivalent to units lower in the Balma and McArthur groups, as depicted in **Figure 2**.

McArthur Basin: Age and correlation of Favenc package units

Very few age determinations are available for Favenc package units in the McArthur Basin, mostly due to an abundance of carbonate lithologies and a paucity of datable igneous rocks. The age of the package is loosely constrained by a SHRIMP U–Pb zircon age of ca 1614 Ma for a tuff in the underlying Amos Formation of the upper McArthur Group (Page *et al* 2000) and by SHRIMP U-Pb zircon ages of 1492 ± 4 Ma and 1493 ± 4 Ma from rare tuffs in the Showell Member of the Mainoru Formation in the overlying lower Roper Group (Jackson *et al* 1999, see Munson 2016). A SHRIMP U–Pb zircon age of 1589 ± 3 Ma for a tuff from the 'upper' Balbirini Dolostone of the Nathan Group (Page *et al* 2000) is currently the only reliable absolute age from the package. This suggests that the package was most likely accumulated in the period 1600–1580 Ma, although it is possible that deposition extended beyond this time. As noted above, significantly older ages of ca 1609 and 1613 Ma from the 'lower' Balbirini Dolostone (Page *et al* 2000) indicate that this unit is more appropriately included in the McArthur Group.

Nathan Group

Samples were collected for geochronology from the type sections of three units of the Nathan Group: the Smythe Sandstone and Mount Birch Sandstone at the base of the group, and the Knuckey Formation, which overlies the Mount Birch Sandstone. These all returned detrital zircon age spectra with a similar broad distribution of modes and MDAs that overlap within error in the age range ca 1629–1605 Ma (**Figure 7**) and thus their MDAs are slightly younger than those of the Batten Subgroup (**Figure 4**). The distribution of modes within spectra of the Smythe and Mount Birch sandstones is similar and consistent with these units being correlatives, as indicated by Abbott *et al* (2001).

'upper' Balma Group

The detrital zircon age spectra and MDAs for the Baiguridji and Bath Range formations at the top of the Balma Group are very similar to one another and indicate that these units are related in terms of depositional age and provenance. They more closely resemble age spectra of the Nathan Group (**Figure 7**) than those of other groups of the Glyde package (**Figure 4**), particularly in having prominent relatively young modes and a similar spread of ages. This raises the possibility that these formations might be better included as the basal units of the Nathan Group in the northern McArthur Basin, (equivalents of the Smythe and Mount Birch sandstones), rather than their current placement at the top of the Balma Group. Such an arrangement would reconcile the relatively young MDA/tuff age of 1599 ± 11 Ma returned from the base of the Bath Range Formation (**Figure 6**) with the 1589 ± 3 Ma tuff age from the 'upper' Balbirini Dolostone. A regional angular unconformity is usually present between Favenc and Glyde packages, but there is no evidence of an angular unconformity either

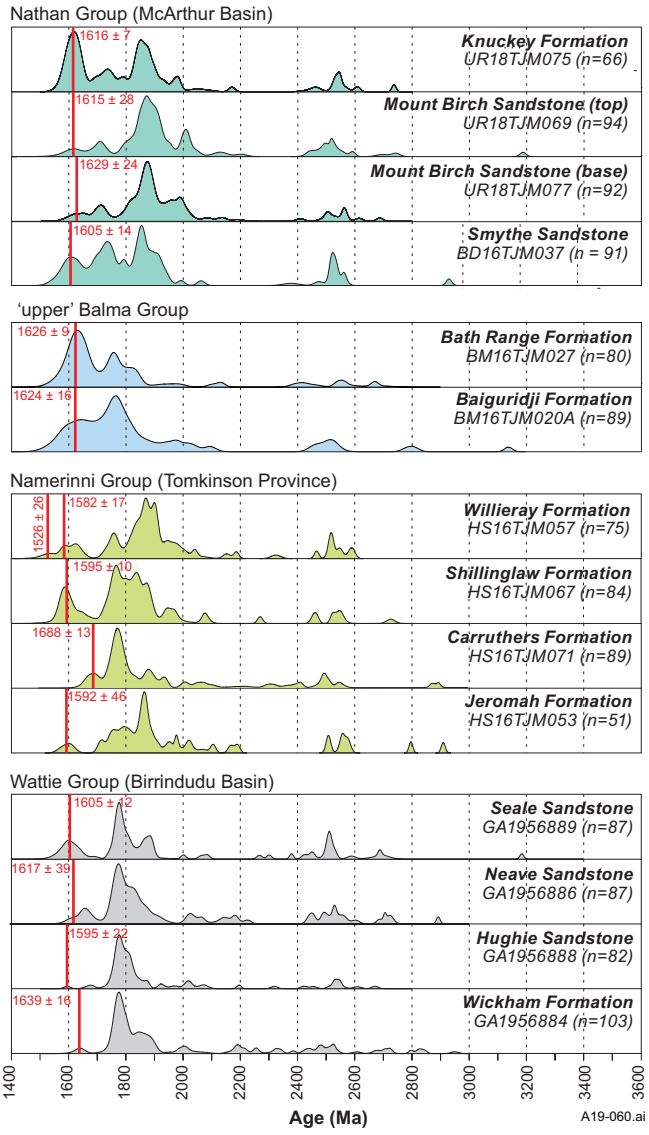

Figure 7. Comparative relative probability diagram of detrital zircon age data, with formations arranged in stratigraphic order for Wattie Group (grey polygons), Namerinni Group (green), 'upper' Balma Group (blue), and Nathan Group (green). References for all data provided in **Table 1**. Relative probability age spectra are not to scale vertically; associated histograms used to construct the spectra are not shown for clarity; number of concordant and near-concordant (<10%) analyses (n) is shown on right. Red lines indicate assigned maximum depositional age for each sample; if two lines present, LHS line is youngest concordant zircon(s).

above the Bath Range Formation or beneath the Baiguridji Formation (Haines *et al* 1999). The true affinities of these units remain unclear; however, from the available evidence, a Nathan Group age is favoured here.

Birrindudu Basin: Age and correlation of Glyde package units

Limbunya Group

In the Birrindudu Basin, the Glyde package is represented by the Limbunya Group. This group has been generally correlated with the McArthur Group, but correlations at the formation level have been more tentative due to a lack of effective age controls through much of the succession. Dunster (1998) provided a correlation chart, based on lithostratigraphic characteristics and sparse isotopic dates, that is mostly retained here (**Figure 2**): in descending stratigraphic order, the Killaloc Formation at the top of the Birrindudu Group was correlated with the Reward Dolostone at the top of the Umbolooga Subgroup of the McArthur Group; the Fraynes Formation with the Barney Creek Formation; the Campbell Springs Dolostone with the Emmerugga and Teena dolostones; the Blue Hole Formation with the Tooganinie Formation, Leila Sandstone and Myrtle Shale; the Farquharson Sandstone with the Tatoola Sandstone; the Margery Formation to Kunja Siltstone interval with the Mallapunyah Formation and Amelia Dolostone; and the Stirling Sandstone at the base of the Birrindudu Group with the Masterton Sandstone at the base of the McArthur Group. Aspects of this correlation scheme have been followed in subsequent studies, including Cutovinos *et al* (2002), Dunster and Ahmad (2013) and Hoffmann (2014, 2015).

A number of tuffs/tuffites from the upper part of the Birrindudu Group (Kunja Siltstone to Fraynes Formation) have been dated by SHRIMP U–Pb and TIMS U–Pb methods (**Table 1**, **Figure 2**). These span the age range ca 1642–1635 Ma and are indistinguishable, within error, from ages returned from the medial McArthur Group (Teena Dolostone to Lynott Formation), which range from ca 1641 Ma–1636 Ma. These data strongly support a general correlation of the Birrindudu Group with the Umbolooga Subgroup of the McArthur Group.

There are no known correlatives of the Batten Subgroup in the Birrindudu Basin. Outcrop of this subgroup is restricted to the Walker, Urapunga and Batten fault zones in the McArthur Basin (**Figure 1**). Hoffman (2015) reported that Batten Subgroup units can be mapped seismically to the west towards the Birrindudu Basin, but these strata have not been observed in outcrop in the vicinity of the Limbunya Group. Hoffman attributed this to either an erosional unconformity at the base of the overlying Wattie Group, non-deposition, or a lack of exposure at this stratigraphic level (see also **Birrindudu Basin: Age and correlation of Favenc package units** below).

Carson (2013) and Kositcin *et al* (2017) produced detrital zircon spectra for two units of the Limbunya Group: the basal Stirling Sandstone and medial Farquharson Sandstone respectively; these are compared to spectra from the McArthur Group in **Figure 8**.

The spectrum from the Stirling Sandstone is markedly dissimilar to that of the Masterton Sandstone at the base of the Umbolooga Subgroup with which it has been correlated in some past studies (see above). The MDA is appreciably older (ca 1830 Ma as compared to 1755 Ma); the spread of modes shows that these units had very different provenances and sediment pathways. These data do not exclude equivalence of these units, as younger zircons might not have been present in source areas that provided detritus to the Stirling Sandstone, but it does not support their correlation. Carson (2010) proposed that the Stirling Sandstone may represent a lateral stratigraphic equivalent of contemporaneous, although probably discontinuous, <1830 Ma basal sandstones unconformably overlying Proterozoic metamorphosed basement across the northern NAC, based on lithostratigraphic comparisons and detrital zircon suite ages. These units all have MDAs of ca 1830 Ma, similar to that of the Stirling Sandstone, and include the Depot Creek Sandstone (basal Tolmer Group, Birrindudu Basin), Mamadawerre Sandstone (basal Kombolgie Subgroup, northern McArthur Basin) and Westmoreland Conglomerate (basal Tawallah Group, southern McArthur Basin). Based on similarities in the detrital zircon spectra, Carson (2013) suggested a further possible correlation of the Stirling Sandstone with the older Palaeoproterozoic Mount Charles Formation of the Tanami Region. In either case, a sizeable hiatus of up to 200 million

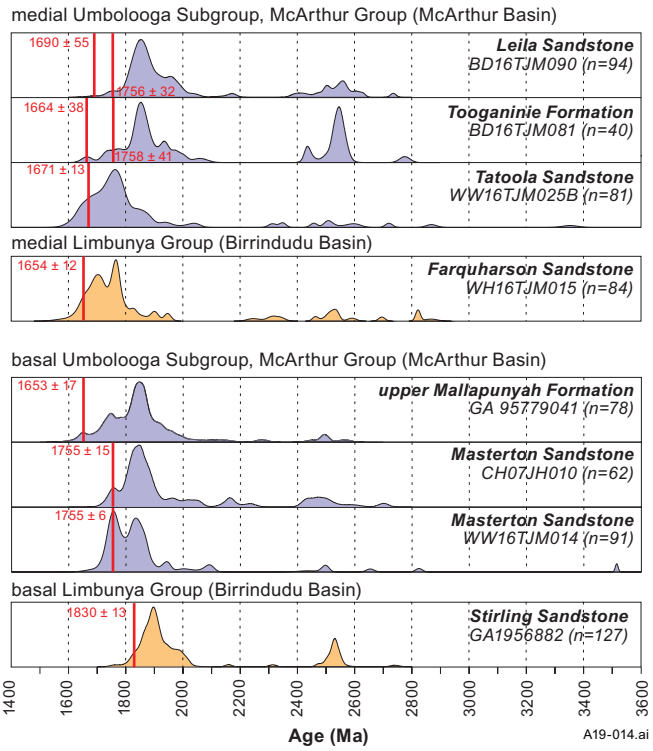

Figure 8. Comparative relative probability diagram of detrital zircon age data, with formations arranged in stratigraphic order for Limbunya Group (orange polygons) and McArthur Group (mauve polygons). References for all data provided in **Table 1**. Relative probability age spectra are not to scale vertically; associated histograms used to construct the spectra are not shown for clarity; number of concordant and near-concordant (<10%) analyses (n) is shown on right. Red lines indicate assigned maximum depositional age for each sample; if two lines present, LHS line is youngest concordant zircon(s).

years would need to be invoked between deposition of the Stirling Sandstone and the overlying Margery Formation. The relationship between these units has been previously described as conformable (Sweet *et al* 1974, Cutovinos *et al* 2002) and is clearly concordant; however, it would be expected to be discordant if the depositional age of the Stirling Sandstone is close to its MDA.

The Farquharson Sandstone has a very similar detrital zircon age spectrum to that of the Tatoola Sandstone (**Figure 8**); the MDAs for the two formations overlap within error and the major age modes are closely comparable. This supports the correlation of these units and other formations of the Birrindudu Group, both above and below the Farquharson Sandstone, with formations of the Umbolooga Subgroup above and below the Tatoola Sandstone respectively, as suggested by Dunster (1998, **Figure 2**) and summarised above.

Birrindudu Basin: Age and correlation of Favenc package units

The succession overlying the Limbunya Group in the Birrindudu Basin comprises, in ascending stratigraphic order, the Wattie, Bullita and Tijunna groups. The Tijunna Group is regarded as a correlative of the upper part of the Roper Group in the McArthur Basin (Munson 2016), but the underlying groups are poorly age-constrained and their relationships to other successions of the greater McArthur Basin have not been clearly established in previous studies, other than a general correlation of both groups with the Nathan Group of the McArthur Basin (eg Cutovinos *et al* 2002, Hoffman 2015). The Bullita Group is beyond the scope of the current study.

Wattie Group

The Wattie Group overlies the Limbunya Group with a marked angular unconformity (Cutovinos *et al* 2002). This unconformity can be correlated with the regional unconformity above the Glyde package elsewhere in the greater McArthur Basin, and indicates that the Wattie Group must be of Favenc package age or younger. There are no absolute isotopic dates from the group, but Carson (2013) and Kositcin *et al* (2017) have produced detrital zircon spectra for four sandstone units (**Table 1**, **Figure 2**), which are shown in **Figure 7**. These spectra show a spread of MDAs in the range ca 1639–1595 Ma, which is much the same as for the Nathan Group (ca 1629–1605 Ma). The spread of age modes is also similar, although there are some differences in the positioning of maxima that are interpreted to reflect sediment source variations. Overall, the age spectra for the two groups are comparable and support a general correlation with one another, although correlation at formation level remains unclear.

Tomkinson Province: Age and correlation of Favenc package units

Namerinni Group

The age of the Namerinni Group has not been well constrained previously. Ward (1983) correlated the group in general with the McArthur Group (and in particular the Umbolooga Subgroup) of the southern McArthur Basin on the basis of lithological similarities, and this has been followed in all subsequent studies. The only date from the Namerinni Group is a SHRIMP U-Pb zircon age of 1639 ± 27 Ma from the Shillinglaw Formation, obtained from an 'altered, green illitic tuff' (Nunn 1997). Nunn commented that the analyses were done on 'primary magmatic grains', inferring that this is an absolute date, and used it as evidence to correlate the Shillinglaw Formation with the Barney Creek Formation of the McArthur Group, which is reliably dated at about this age. The report for the SHRIMP analysis is no longer available, so it is not possible to query the original data to determine the nature of the ca 1639 Ma age; it should therefore be treated with caution. Hussey *et al* (2001) preferred to consider it to be a maximum depositional age and this view is strongly supported by detrital zircon age spectra for the four formations of the Namerinni Group (presented in **Figure 7**).

Robust MDAs from three of the four formations, including the Shillinglaw Formation, are in the age range ca 1595–1582 Ma; the two youngest concordant zircons in the uppermost Willieray Formation returned a weighted mean age of 1526 ± 26 Ma. The conservative MDAs are the same, within error, as those for the Wattie and Nathan groups. There is also a relatively high degree of correspondence of zircon age modes from the three groups (**Figure 7**). These results indicate that the Namerinni Group is younger than the McArthur Group and is better correlated with the Nathan and Wattie groups within the Favenc package. Consequently, the Glyde package does not appear to be represented in the Tomkinson Province unless underlying rocks of the poorly dated upper Tomkinson Creek Group are younger than previously considered. This has implications for exploration activities in the region given the significant economic potential of Glyde package rocks elsewhere in the greater McArthur Basin. The age of the unconformity that underlies the Namerinni Group might also be much younger than previously thought and could be related to the early stages of the ca 1590–1560 Ma Chewings Orogeny in the Arunta Region to the south (Scrimgeour 2013), rather than to deformation associated with the ca 1720–1710 Ma Davenport Event (Donnellan 2013) or ca 1735–1690 Ma Strangways Event (Scrimgeour 2013).

Conclusions

A significant dataset of geochronological analyses has been accumulated from samples collected across the greater McArthur Basin since the 1990s. These analyses comprise absolute age determinations of tuffs/tuffites, and detrital zircon maximum deposition isotopic age determinations of sandstones and tuffaceous sediments. Completed and ongoing NTGS projects are integrating and interpreting these data in order to date and correlate strata across the basin, and to provide widespread provenance data to assist in attaining a greatly improved understanding of the fundamental architecture and palaeogeography through time of the greater McArthur Basin.

Significant new interpretations resulting from these studies include the following:

- The Nagi Formation (Vizard Group, central McArthur Basin) and Yarrawirrie Formation (Balma Group, northern McArthur Basin) are probable correlatives and are equivalent to formations of the Batten Subgroup (southern McArthur Basin).
- The upper Habgood Group (northern McArthur Basin) is probably equivalent to units much lower in the Balma and McArthur groups than has been previously interpreted.
- The Limbunya Group (Birrindudu Basin) is strongly correlated with the Umbolooga Subgroup (lower McArthur Group, McArthur Basin). The Fraynes Formation and Farquharson Sandstone (Limbunya Group) are probable correlatives of the economically important Barney Creek Formation and the Tatoola Sandstone (Umbolooga Subgroup) respectively. Stratigraphic intervals both above and below the Farquharson and Tatoola sandstones can also be broadly correlated between these successions.
- The Batten Subgroup (upper McArthur Group) is much more restricted in geographic extent than previously determined. Outcrop of this subgroup is confined to the Walker, Urapunga and Batten fault zones in the McArthur Basin, although it has been mapped seismically in the subsurface to the west of its known areas of outcrop. There are no known equivalents of this succession in either the Birrindudu Basin or Tomkinson Province.
- The Namerinni Group (Tomkinson Province) is younger than previously determined and is equivalent to Favenc package successions, rather than the McArthur Group. The Glyde package appears to be absent in the Tomkinson Province, although it is possible that the underlying, poorly dated upper Tomkinson Creek Group might be equivalent. The unconformity underlying the Namerinni Group is less well constrained than previously determined and might be related to either the ca 1590–1560 Ma Chewings Orogeny or the ca 1720–1710 Ma Davenport Event or ca 1735–1690 Ma Strangways Event. Reassignment of the Namerinni Group to the Mesoproterozoic Favenc package has significant implications for mineral and petroleum exploration in the Tomkinson Province region.
- The Favenc package is far more extensive than previously recognised. As well as the Nathen and Mount Rigg groups and Karns Dolostone (McArthur Basin), it includes the Wattie Group (Birrindudu Basin), Namerinni Group (Tomkinson Province) and probably the Baiguridji and Bath Range formations of the 'upper' Balma Group (northern McArthur Basin).

References

Abbott ST, Sweet IP, Plumb KA, Young DN, Cutovinos A, Ferenczi PA, Brakel A and Pietsch BA, 2001. *Roper Region-Urapunga and Roper River Special, Northern Territory (Second Edition). 1:250 000 geological map series and explanatory notes, SD 53-10, 11.* Northern Territory Geological Survey and Australian Geological Survey Organisation (National Geoscience Mapping Accord).

Armstrong RA, 1998. *Ion Microprobe (SHRIMP) U-Pb dating of zircons from the Northern Territtory Part III. Precise Radiogenic Isotope Services (PRISE), Job #A98-030.* Research School of Earth Sciences, Australian National University, Canberra.

Carson CJ, 2010. The Victoria and Birrindudu basins: A U-Pb SHRIMP study and review of resource potential: in *'Annual Geoscience Exploration Seminar (AGES) 2010. Record of abstracts'. Northern Territory Geological Survey, Record* 2010-002.

Carson CJ, 2013. The Victoria and Birrindudu Basins, Victoria River region, Northern Territory, Australia: a SHRIMP U-Pb detrital zircon and Sm-Nd study. *Australian Journal of Earth Sciences* 60, 175–196.

Close DF, 2014. The McArthur Basin: NTGS's approach to a frontier petroleum basin with known base metal prospectivity: in *'Annual Geoscience Exploration Seminar (AGES) 2014. Record of abstracts'. Northern Territory Geological Survey*, *Record* 2014-001.

Cutovinos A, Beier PR, Kruse PD, Abbott ST, Dunster JN and Brescianini RF, 2002. *Limbunya, Northern Territory (Second Edition). 1:250 000 geological map series explanatory notes, SE 52-07.* Northern Territory Geological Survey, Darwin.

Donnellan N, 2013. Warramunga Province: in Ahmad M and Munson TJ (compilers). *'Geology and mineral resources of the Northern Territory'. Northern Territory Geological Survey, Special Publication* 5.

Dunster JN, 1998. Reconnaissance of the Proterozoic Rocks of the Victoria River Region. North Ltd. *Northern Territory Geological Survey, Open File Company Report* CR1998-0082.

Dunster JN and Ahmad M, 2013. Birrindudu Basin: in Ahmad M and Munson TJ (compilers). *'Geology and mineral resources of the Northern Territory'. Northern Territory Geological Survey, Special Publication* 5.

Fanning CM, 1991. *Ion microprobe U-Pb zircon dating of a tuffaceous horizon within the Kunja Siltstone, Victoria River Basin, Northern Territory. Report for Pacific Oil and Gas Pty Ltd.* Australian National University, Research School of Earth Sciences.

Frichot L, Revie D and Munson TJ, 2017. The Vaughton Siltstone of the northern McArthur Basin: Preliminary data and issues related to assessing its potential as a petroleum source rock. *Northern Territory Geological Survey, Technical Note* 2017-002.

Haines PW, 1994. The Balma and Habgood Groups, Northern McArthur Basin, Northern Territory: stratigraphy and correlations with the McArthur Group: in Hallenstein CP (editor). *'Australian mining looks north – the challenge and choices. 1994 AusIMM Annual Conference, Darwin, Australia, August 5–9, 1994.' Australasian Institute of Mining and Metallurgy, Publication Series* 5/94, 147–152.

Haines PW, Rawlings DJ, Sweet IP, Pietsch BA, Plumb KA, Madigan TLA and Krassay AA, 1999. *Blue Mud Bay, Northern Territory (Second Edition). 1:250 000 geological map series and explanatory notes, SD 53-07.* Northern

Territory Geological Survey, Darwin and Australian Geological Survey Organisation, Canberra.

Hoffman TW, 2014. New insights into the expanse of the McArthur Superbasin: in *'Annual Geoscience Exploration Seminar (AGES) 2014. Record of Abstracts.' Northern Territory Geological Survey, Record* 2014-001.

Hoffman TW, 2015. Recent drilling results provide new insights into the western Palaeoproterozoic to Mesoproterozoic McArthur Basin: in *'Annual Geoscience Exploration Seminar (AGES) 2015. Record of Abstracts.' Northern Territory Geological Survey, Record* 2015-002.

Hollis JA, Beyer EE, Whelan JA, Kemp AIS, Scherstén A and Greig A, 2010. Summary of results. NTGS laser U-Pb and Hf geochronology project: Pine Creek Orogen, Murphy Inlier, McArthur Basin and Arunta Region, July 2007–June 2008. *Northern Territory Geological Survey, Record* 2010-001.

Hussey KJ, Beier PR, Crispe AJ, Donnellan N and Kruse PD, 2001. *Helen Springs, Northern Territory (Second Edition). 1:250 000 geological map series and explanatory notes, SE 53-10*. Northern Territory Geological Survey, Darwin.

Jackson MJ, Scott DL and Rawlings DJ, 2000. Stratigraphic framework for the Leichhardt and Calvert Superbasins: review and correlation of the pre-1700 Ma successions between Mt Isa and McArthur River. *Australian Journal of Earth Sciences* 47, 381–403.

Jackson MJ, Sweet IP, Page RW and Bradshaw BE, 1999. The South Nicholson and Roper Groups: Evidence for the early Mesoproterozoic Roper Superbasin: in Bradshaw BE and Scott DL (editors). *'Integrated basin analysis of the Isa Superbasin using seismic, well-log and geopotential data: an evaluation of the economic potential of the northern Lawn Hill Platform.' Australian Geological Survey Organisation Record* 1999/19 (CD-ROM), 36–45.

Kositcin N and Carson CJ, 2017. New SHRIMP U–Pb zircon ages from the Birrindudu and Victoria Basins, Northern Territory: July 2016–June 2017. *Geoscience Australia, Record* 2017/16.

Kositcin N and Munson TJ, in press. Summary of results. Joint NTGS–GA geochronology project: greater McArthur Basin, July 2017–August 2018. *Northern Territory Geological Survey, Record*.

Kositcin N, Munson TJ and Whelan JA, 2017. Summary of results. Joint NTGS–GA geochronology project: greater McArthur Basin, July 2016–June 2017. *Northern Territory Geological Survey Record 2*017-012.

Munson TJ, 2016. Sedimentary characterisation of the Wilton package, greater McArthur Basin, Northern Territory. *Northern Territory Geological Survey, Record* 2016-003.

Munson TJ, Thompson JM, Meffre S and Orth K, in prep a. Summary of results. NTGS laser ablation ICP-MS U–Pb geochronology project: Habgood, Balma and McArthur groups (McArthur Basin), Namerinni Group (Tomkinson Province), and unnamed unit from drillhole NDW12-01. *Northern Territory Geological Survey, Record*.

Munson TJ, Denyszyn S and Kunzmann M, in prep b. A 1642 Ma age for the Fraynes Formation in the Birrindudu Basin confirms correlation with the Barney Creek Formation in the southern McArthur Basin, Northern Territory. *Australian Journal Earth Sciences*.

Nunn T, 1997. Second annual report for the period 2 June 1996 to 1 June 1997 for ELs 9022-9025, 9325-9327, 9570 Helen Springs project. *Northern Territory Department of Mines and Energy, Open File Company Report* CR1997-0444.

Page RW, Jackson MJ and Krassay AA, 2000. Constraining sequence stratigraphy in north Australian basins: SHRIMP U-Pb zircon geochronology between Mt Isa and McArthur River. *Australian Journal of Earth Sciences* 47(3), 431–459.

Page RW and Sweet IP, 1998. Geochronology of basin phases in the western Mt Isa Inlier, and correlation with the McArthur Basin. *Australian Journal of Earth Sciences* 45, 219–232.

Pietsch BA, Plumb KA, Page RW, Haines PW, Rawlings DJ and Sweet IP, 1994. A revised stratigraphic framework for the McArthur Basin, NT: in Hallenstein CP (editor). *'Australian mining looks north – the challenge and choices. 1994 AusIMM Annual Conference, Darwin, Australia, August 5–9, 1994.' Australasian Institute of Mining and Metallurgy, Publication Series* 5/94, 135–138.

Plumb KA and Derrick GM, 1975. Proterozoic of Kimberly (WA) to Mount Isa (QLD) region – regional geology: in Knight CL (editor). *'Economic Geology of Australia and Papua New Guinea. 1. Metals.' Australasian Institute of Mining and Metallurgy, Monograph* 5, 217–252.

Rawlings DJ, 1999. Stratigraphic resolution of a multiphase intracratonic basin system: the McArthur Basin, northern Australia. *Australian Journal of Earth Sciences* 46, 703–723.

Rawlings DJ, Haines PW, Madigan TLA, Pietsch BA, Sweet IP, Plumb KA and Krassay AA, 1997. *Arnhem Bay-Gove, Northern Territory (Second Edition). 1:250 000 geological map series and explanatory notes, SD 53-3, 4*. Northern Territory Geological Survey and Australian Geological Survey Organisation (National Geoscience Mapping Accord).

Scrimgeour IR, 2013. Aileron Province: in Ahmad M and Munson TJ (compilers). *'Geology and mineral resources of the Northern Territory'. Northern Territory Geological Survey, Special Publication* 5.

Smith J, 2001. Summary of results. Joint NTGS-AGSO age determination program 1999–2001. *Northern Territory Geological Survey, Record* 2001-007.

Southgate PN, Bradshaw BE, Domagala J, Jackson MJ, Idnurm M, Krassay AA, Page RW, Sami TT, Scott DL, Lindsay JF, McConachie BA and Tarlowski C, 2000. Chronostratigraphic basin framework for Palaeoproterozoic rocks (1730–1575 Ma) in northern Australia and implications for base-metal mineralisation. *Australian Journal of Earth Sciences* 47, 461–483.

Sweet IP, Mendum JR, Bultitude RJ and Morgan CM, 1974. The geology of the southern Victoria River region, Northern Territory. *Bureau of Mineral Resources, Australia, Report* 167.

Ward DF, 1983. Report on geological mapping and geochemical survey on EL2835 and 3607, and drill testing targets in EL3607, Helen Springs. Esso Australia Ltd. *Northern Territory Department of Mines and Energy, Open File Company Report* CR1983-0299A, B.

Life and times of the Proterozoic McArthur–Yanliao Gulf: Update on the ARC-Industry–NTGS Linkage Project

Alan S Collins[1,2], Juraj Farkas[1], Stijn Glorie[1], Morgan L Blades[1], Grant M Cox[1], John D Foden[1], Tony Hall[1], Justin L Payne[3], Bo Yang[1], Angus Nixon[1], Eilidh Cassidy[1], Darwinaji Subarkah[1], April Shannon[1], Dion Higgie[1], Geremiah Toledo[1], Anthony Dosseto[4], Uwe Kirscher[5], Chris Edgoose[6], Dorothy Close[6], Tim J Munson[6], Sandra Menpes[7], Saviero Spagnuolo[7], David Close[7], Elizabeth Baruch-Jurado[8], Jonathan Warburton[9] and Geoff Hokin[9]

The greater McArthur Basin covers a wide extent of northern Australia, spanning from Western Australia to Queensland and stretching from near Tennant Creek in the south to an unknown extent beneath the Arafura Sea to the north.

[1] Department of Earth Sciences, The University of Adelaide, Adelaide SA 5005, Australia
[2] Email: alan.collins@adelaide.edu.au
[3] School of Built and Natural Environments, University of South Australia
[4] School of Earth and Environmental Sciences, University of Wollongong
[5] School of Earth and Planetary Sciences, Curtin University
[6] Northern Territory Geological Survey
[7] Santos Limited
[8] Origin Energy Limited
[9] Imperial Oil and Gas Ltd

There are similarities in chemostratigraphy (eg Kunzmann *et al* 2019) and lithologies between the greater McArthur Basin and the Proterozoic sequences that crop out in North China (where they are best exposed in the so-called Yanliao Aulacogen). Recent palaeomagnetic work undertaken at Curtin University supports this link (Kirscher *et al* in press) and has led to our suggestion of the epicontinental sea forming a major McArthur–Yanliao Gulf in Nuna/Colombia (**Figure 1**). As such, a consortium of universities, industry and the Northern Territory Government obtained a three-year Australian Research Council Linkage grant to research both tectonic and palaeo-environmental importance of the basin. The grant allows the consortium to focus on unravelling the history of the basin leading to improved understanding of the tectonic evolution of Australia at

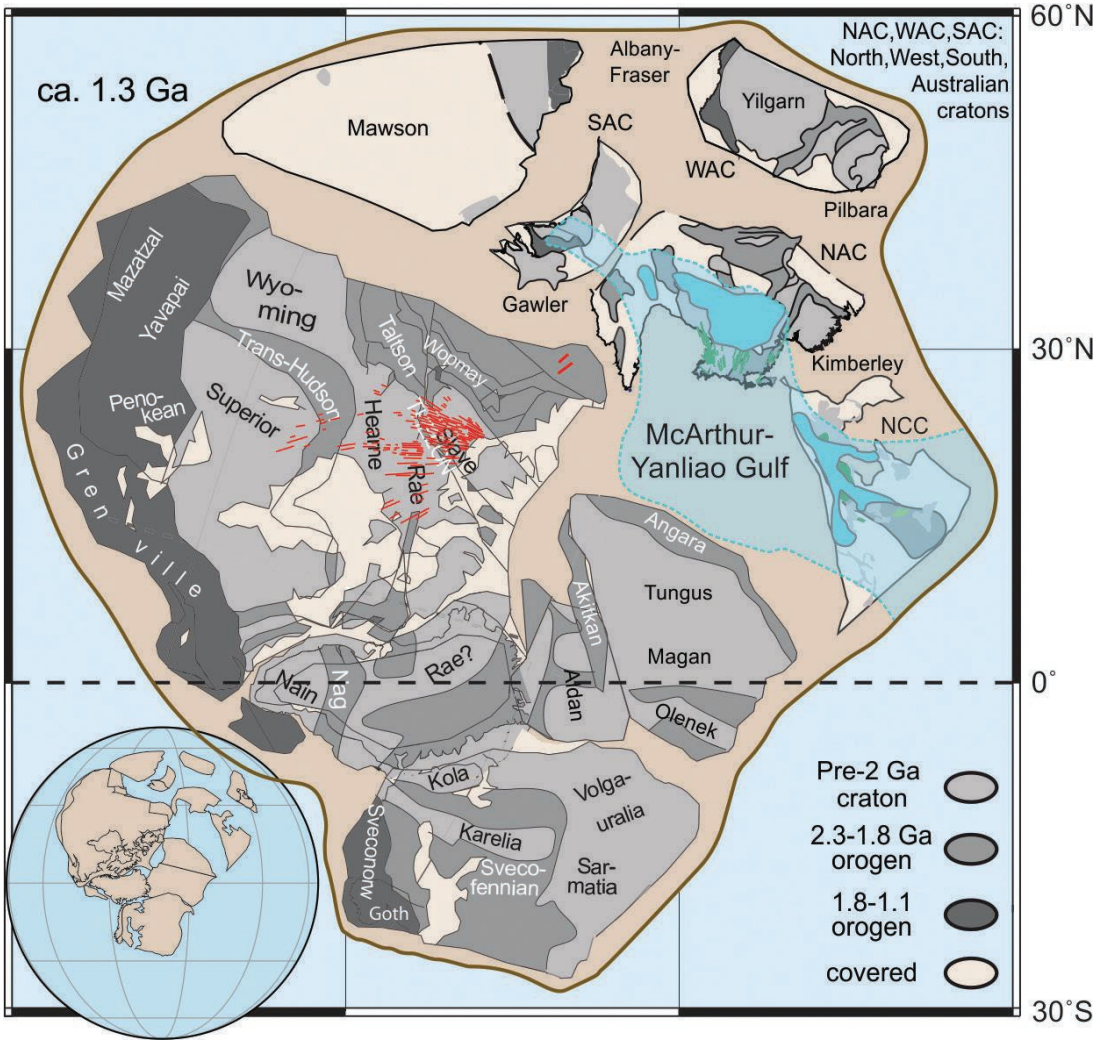

Figure 1. Tectonic assemblage map at ca 1.3 Ga. Green lines are dykes and sill associated with the ca 1.3 Ga Derim Derim–Galiwinku–Yanliao Large Igneous Province. Red lines are the ca 1.27 Ga Mackenzie dykes. Map modified from Kirscher *et al* (in review), Cox *et al* (in review).

the time, as well as that of the setting, origin and controls on the formation of the petroleum resources within the basin. In addition, the basin spans the Palaeoproterozoic–Mesoproterozoic, a fascinating time when eukaryotes gained a foothold and oxygenation of the atmosphere and ocean commenced. Consequently, the basin is an essential geological archive for global earth system development through this time period.

The partners in this project are the Australian Research Council, the Northern Territory Geological Survey (NTGS), Origin Energy Limited, Santos Limited, Imperial Oil and Gas Limited, The University of Adelaide, The University of Wollongong, The University of South Australia, and the Czech Academy of Sciences. The consortium's philosophy is to identify new data to complement existing datasets and to build a spatial and temporal framework of the chemostratigraphy, age, detrital chronology, and low-temperature thermochronology of the basin. These data will be used to: a) correlate effectively between sequences and boreholes up to 1000 km apart; b) illuminate the tectonic evolution of the basin and its margins by examining source-to-sink pathways for sediments through time; c) determine the palaeo-environmental conditions that persisted during deposition using geochemical proxies for redox, biological activity and nutrient influx; and d) study the thermal history of the basin by using low temperature thermochronometers to examine both the basin and the surrounding basement to better understand the ancient surface movements.

Over 2018, we have graduated four Honours students focussed on this project, have had several manuscripts published or placed in the publication pipeline (see references), and have undertaken three projects described below (the details of which are on the posters in the AGES 2019 foyer).

a. Detrital zircons from the Palaeoproterozoic Redbank Package to the Mesoproterozoic Favenc and Wilton packages show a distinct change in dominant age peaks from the early sandstones rich in ca 1850 Ma zircon in the former to those containing ca 1760 Ma zircon in the latter. We interpret that this reflects an increased importance of the Arunta Region as a zircon source, suggesting its uplift and erosion in the early Mesoproterozoic.
b. The ca 1820 Ma Plum Tree Volcanics mark the initiation of extension in northern Australia and herald the start of the greater McArthur Basin. The volcanics have evolved, negative εNd values (approximately -6), indicating crustal assimilation occurred during emplacement of the suite. REE trends of this suite show negative Nb and Sr anomalies, and positive Pb anomalies, which are interpreted to also indicate crustal contamination. We suggest that the volcanics formed as a result of active intraplate continental rifting due to plume impingement or lithospheric delamination after Pine Creek orogenesis.
c. We are also pioneering the measurement and interpretation of Cr isotope ($\delta^{53}Cr$) values. We report the first Cr isotope data from the McArthur Basin. Samples were collected from mid-Proterozoic organic-rich carbonates of the ca 1.64 Ga Limbunya and McArthur groups. Analysed values from -0.293‰ to +1.389‰ represent the oldest documented positively fractionated $\delta^{53}Cr$ values in marine carbonate units reported. This is suggestive of fluctuating, but increasing, pO_2 at the time of a generally reducing environment.

Herein we shall focus on two of the novel projects undertaken over the year: 1) LA–ICP MS/MS Rb−Sr dating of shales and glauconites from the Roper Group (Honours project of Ms Eilidh Cassidy and research by Farkas, Blades, Collins, Cox and Dr Sarah Gilbert); and 2) isotope constraints on the redox structure of the Mesoproterozoic basin in which the Roper Group was deposited (Honours project of Ms April Shannon and research by Cox, Farkas, Blades, Collins).

1) LA–ICP MS/MS Rb−Sr dating of shales and glauconites from the Roper Group

A total of six shale samples throughout the lower Roper group and a single glauconitic sandstone sample from the Crawford Formation were sampled for *in-situ* Rb−Sr dating, a technique currently in development (Zack and Hogmalm 2016). Age data were collected using the laser ablation-triple quadrupole-ICP-MS (LA−QQQ−ICP−MS) at Adelaide Microscopy where ^{87}Rb is separated from ^{87}Sr in the mass spectrometer using N_2O gas. The reaction cell that sits between two quadrapoles allows mass 67 to be isolated (^{87}Rb and ^{87}Sr), followed by a reaction with N_2O to produce $^{87}Sr^{16}O$, making a total mass of 103 and therefore allowing it to be identified from ^{87}Sr. Analyses consisted of ~90 × 75 µm laser spots along a single lamination (where available) for each sample. Data were processed in the software package Iolite version 3.0. Concordia diagrams were calculated using ISOPLOT 4.15 for Excel.

A nano-powder (MicaMg) and a phlogopite crystal (MDC) were used as standards. An average (or median) spline through MicaMg was used when processing in iolite to avoid introducing any false drift correction. A systematic error has also been discovered in the nano-powder. To cover for this, we have added an arbitrary 5% error correction to the results (Sarah Gilbert, pers comm 2018).

Shales analysed (**Table 1**) from Urapunga 5 drillhole yielded Rb–Sr ages of 1343 ± 54 Ma (Jalboi Formation), 1296 ± 54 Ma (Crawford Formation) and 1323.0 ± 55 Ma (Wooden Duck Member of the Mainoru Formation). These

Table 1. Shale samples from Urapunga 5 and Urapunga 6 that were used for Rb–Sr dating.

Stratigraphic Unit	Sample	Core	Depth (m)
Jalboi Formation	U5-139.9	BMR Urapunga 5	139.9
Derim Derim Dolerite	U5-229.6	BMR Urapunga 5	229.6
Crawford Formation	U5-329	BMR Urapunga 5	329
Mainorou (Wooden Duck Mbr)	U5-578.7	BMR Urapunga 5	578.7
Mainorou (Gibb Mbr)	U6-269.3	BMR Urapunga 6	269.3
Mantungula Formation	U6-422.1	BMR Urapunga 6	422.1

also yielded initial $^{87}Sr/^{86}Sr$ values of between 0.63 ± 0.13 to 0.816 ± 0.030. The single glauconite grain from the Crawford Formation yielded a similar initial $^{87}Sr/^{86}Sr$ ratio (0.76 ± 0.11) and an age of 1339 ± 68 Ma (MSWD = 0.89). The Derim Derim dolerite sample also yielded a similar initial $^{87}Sr/^{86}Sr$ value (0.7293 ± 0094) and an age of 1308 ± 16 Ma (MSWD = 0.45). All the samples from this drillhole yielded ages that post-date deposition but are consistent with both glauconite and shale yielding magmatic fluid-assisted recrystallisation (**Figure 2**).

Two shale samples were analysed from Urapunga 6 drillhole, which does not contain any intrusions within it. Both these shales yielded ages that are consistent with the interpreted age of deposition (Gibb Mbr, Mainoru Formation, 1528 ± 43 Ma, MSWD=0.21; Mantungula Formation, 1470 ± 120 Ma, MSWD = 0.27). These samples also yielded initial $^{87}Sr/^{86}Sr$ values of 0.7091 ± 0.0208 and 0.7088 ± 0.0178, which are within error of seawater during the Mesoproterozoic (Shields and Veizer 2002).

We suggest that this technique is at a stage where relatively imprecise ages can be determined for deposition of fresh shales that have not been recrystallised. In addition, sedimentary rocks that have been recrystallised in the presence of hydrothermal fluids can be identified, and the timing of their recrystallisation can be constrained.

2. Early Mesoproterozoic marine redox and the instability of oxic marine ecosystems

It has been a long-standing debate whether the emergence and diversification of eukaryotes is linked to levels of atmospheric pO_2, related to the availability of nutrients, a consequence of the timing of evolutionary advances, or is due to changes in ecosystem structures. The early Mesoproterozoic shales of the lower Roper Group are known to host putative eukaryotes. The organic and inorganic chemistry of these shales are interpreted to record a complex redox structure consisting of oxic surface waters along with active aerobic nitrogen cycling (**Figure 3**). Underlying these oxic surface waters, lower shoreface to upper shelf sediments record an oxygen minimum zone where both Fe and Mn are actively reduced and shuttled to the distal shelf where they are re-oxidised (**Figure 4**). As the oxidation of Mn requires molecular O_2, these deeper distal shelf regions were oxic. This redox structure is interpreted to be a direct result of a strong biological control on both O_2 production and O_2 demand.

The redox structure requires a shallow redoxcline well above storm weather wave base; consequently, regular vertical mixing of reduced waters into shallow oxic ecosystems is expected on short timescales. Therefore, an impediment to eukaryote diversification may not be the absolute concentration of oxygen in basin waters, but rather the long-term stability of such oxic ecosystems. Redoxcline depth is a function of the depth of O_2 demand, which is tightly coupled to organic carbon sinking rates. Proterozoic oceans were rich in dissolved organic matter that led to shallow redoxclines. The stabilisation of oxic ecosystems and the expansion of eukaryotes may have been due to ecological restructuring caused by the transition from dissolved to particulate organic matter, pushing O_2 demand, and the redoxcline, into deeper waters.

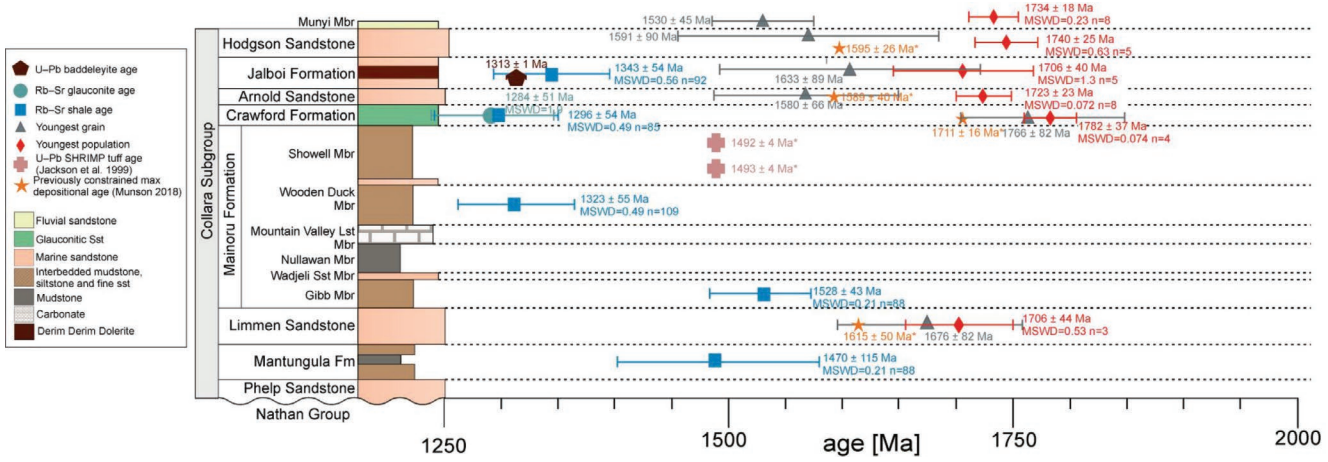

Figure 2. Compilation of U–Pb data from the lower Roper Group including baddeleyite age of the Derim Derim Dolerite (Cox *et al* 2018), Rb–Sr age of glauconite within the Crawford Formation, youngest concordant grain, youngest detrital zircon population (n=>3) along with previously published data on the Hodgson Sandstone, Arnold Sandstone, Crawford Formation and the Limmen Sandstone by Munson (2018) and U–Pb SHRIMP tuff ages from the Showell Member of the Mainorou (Jackson *et al* 1999). The maximum depositional age has been constrained by the youngest, concordant grain (red diamond) while the absolute depositional age for the Jalboi Formation, Crawford Formation, Wooden Duck Mbr (Mainorou), Gibb Mbr (Mainorou) and Mantungula Formation has been identified using Rb–Sr isotopic dating of shales within these formations and members (blue box). Fm = Formation, Mbr = Member.

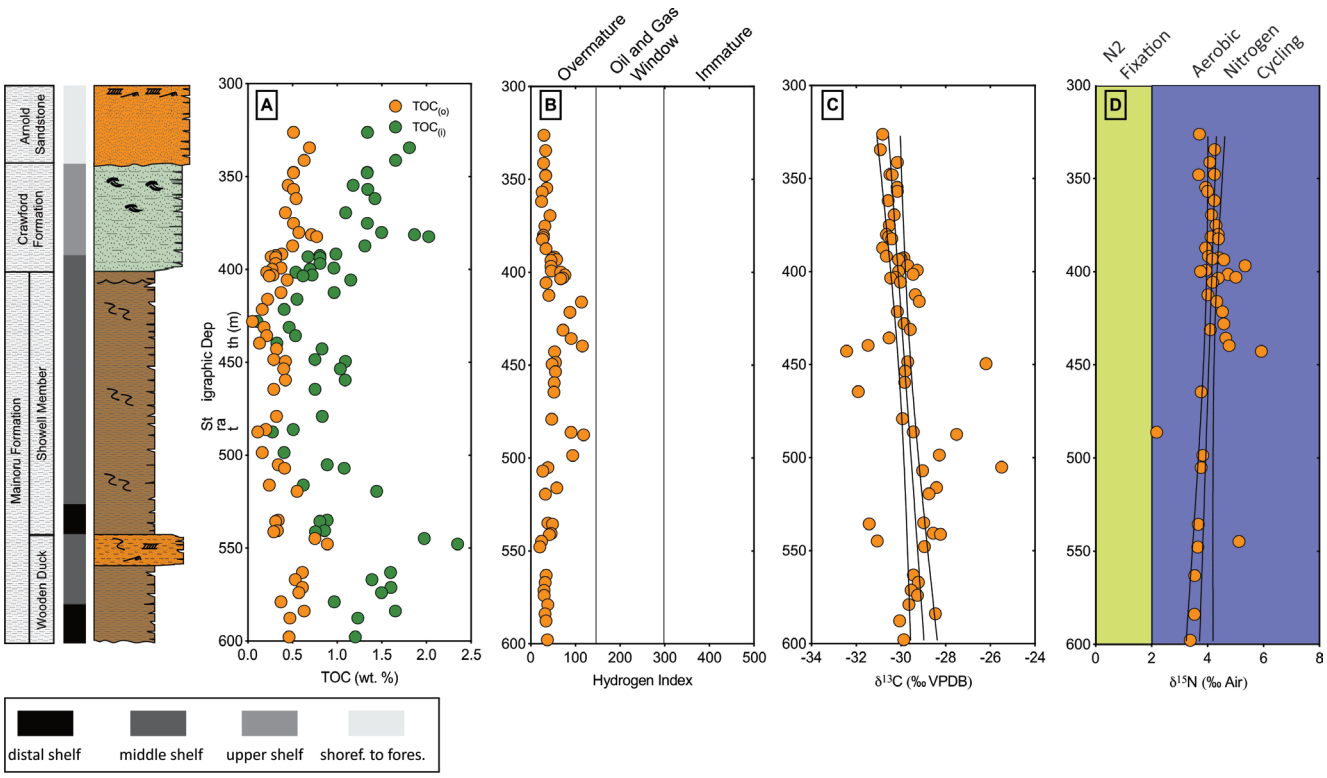

Figure 3. Organic geochemical characteristics of shale samples from Urapunga 5. (A) Measured total organic carbon (orange circles) and calculated initial organic carbon contents (green circles; following Modica and Lapierre (2012), (B) Hydrogen Index, (C) $\delta^{13}C_{org}$ and (D) $\delta^{15}N_{org}$. Black lines in (C) and (D) are linear regression (and 95% confidence interval) between the measured isotopic values and stratigraphic depth. Correlation between $\delta^{13}C_{org}$ and $\delta^{15}N_{org}$ is statistically significant at a $\alpha = 0.1$ (2-tailed p-values are 0.0019 and 0.0887 respectively). Green field in (D) is the field that can conceivably be attributed solely to N_2 fixation while the blue field in (D) are values typically associated with aerobic nitrogen cycling (Stüeken *et al* 2016).

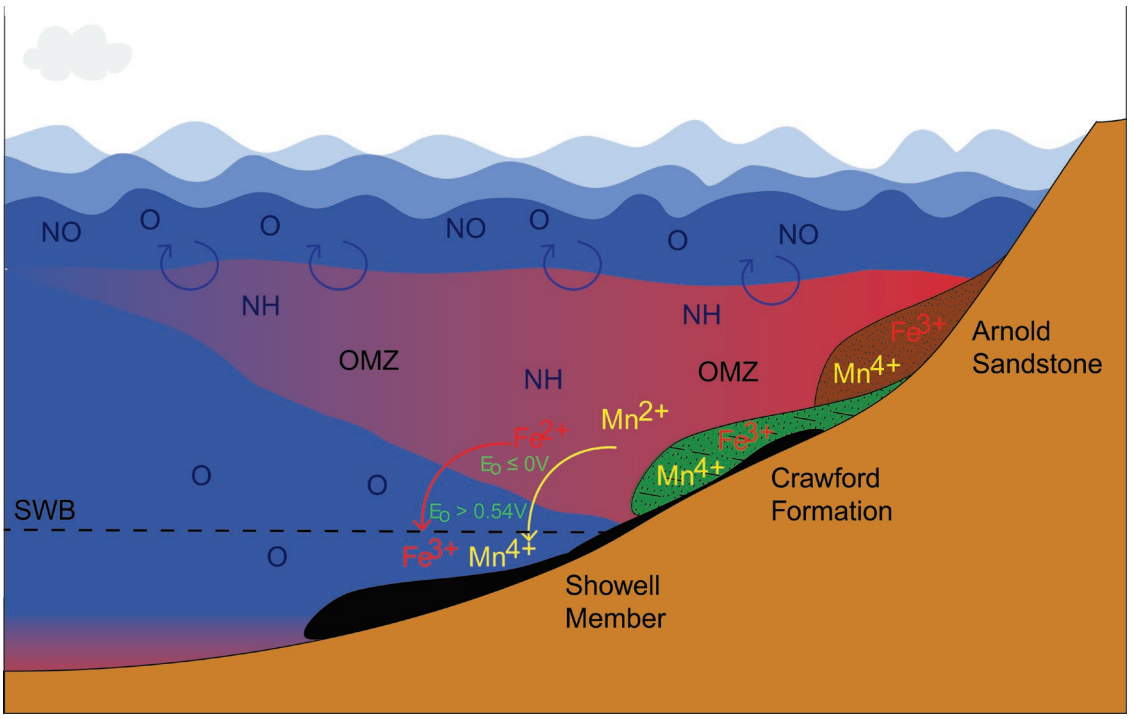

Figure 4. Schematic model of the 2D redox structure recorded by lower Roper shales. The upper layer is relatively oxic supporting aerobic nitrogen cycling. The size of the nitrate reservoir is relatively uniform from nearshore to offshore environments with no evidence for an offshore nitrate minimum. Depletions in Fe/Al and Mn/Al ratios of Arnold Sandstone and Crawford Formation shales suggests that shore face and shelf waters and sediments there were anoxic allowing both Mn and Fe to be reduced and shuttled to deeper waters. Enrichments in Fe/Al and Mn/Al ratios of Showell Member shales requires oxidation of Fe and Mn under oxidation potentials as high as the $Mn^{2+} \leftrightarrow MnO_2$ redox couplet, implying bottom water O_2 in distal shelf shales. SWB = storm weather wave base, OMZ = oxygen minimum zone.

Manuscripts published, in review or in press from these projects:

Cox GM, Jarrett A, Shannon, AV, Hall PA, Baruch ET, Hasterok D, Neilson K, Yang B, Collins AS, Blades ML and Farkas J, submitted. A very unconventional hydrocarbon play: The Roper Basin of Northern Australia. *AAPG Bulletin*.

Cox G, Sansjofre P, Blades ML, Farkas J, Collins AS, submitted. Dynamic interaction between basin redox and the biogeochemical nitrogen cycle in an unconventional Proterozoic petroleum system. *Nature Scientific Reports*.

Shannon AV, Cox GM, Kunzmann M, Blades ML, Jarrett A and Collins AS, submitted. Early Mesoproterozoic marine redox and the instability of oxic marine ecosystems. *Geobiology*.

Yang B, Smith TM, Collins AS, Munson TJ, Schoemaker B, Nicholls D, Cox G, Farkas J and Glorie S, 2017. Spatial and temporal variation in detrital zircon age provenance of the hydrocarbon-bearing upper Roper Group, Beetaloo Sub-basin, Northern Territory, Australia. *Precambrian Research* 304, 140–155.

Yang B, Collins AS, Blades ML, Capogreco N, Payne JL, Munson TJ and Cox GM, submitted. Middle–late Mesoproterozoic tectonic geography of the North Australia Craton: U–Pb and Hf isotopes of detrital zircons in the Beetaloo Sub-basin, Northern Territory, Australia. *Journal of the Geological Society*, London.

Honours theses in 2018

Cassidy E, 2018 *Tectonic Geography of the lower Roper Group, McArthur Basin, Northern Australia using detrital geochronology and shale geochemistry*. Honours Thesis, University of Adelaide.

Higgie D, 2018. *Tectonic Provenance of the Palaeoproterozoic Plum Tree Volcanics: Implications for the initiation of the McArthur Basin*. Honours Thesis, University of Adelaide.

Shannon AV, 2018. *Understanding the complexities of Proterozoic redox using carbon, nitrogen and trace metal composition of organic rich shales*. Honours Thesis, University of Adelaide.

Subarakah D, 2018. *The forgotten Mesoproterozoic of Northern Australia: a chemostratigraphy and detrital zircon study of the greater McArthur Basin*. Honours Thesis, University of Adelaide.

Toledo G, 2018. *Chromium isotope constraints on the mid-Proterozoic redox: Evidence from $\delta^{53}Cr$ of carbonates from the greater McArthur Basin, Northern Australia*. Honours Thesis, University of Adelaide.

References

Kirscher U, Liu Y, Li ZX, Mitchell RN, Pisarevsky SA, Denyszyn SW and Nordsvan A, in press. Paleomagnetism of the Hart Dolerite (Kimberley, Western Australia) – A two-stage assembly of the supercontinent Nuna? *Precambrian Research*.

Kunzmann M, Schmid S, Blaikie TN, Halverson GP, 2019. Facies analysis, sequence stratigraphy, and carbon isotope chemostratigraphy of a classic Zn-Pb host succession: The Proterozoic middle McArthur Group, McArthur Basin, Australia. *Ore Geology Reviews* 106, 150–175.

Modica CJ and Lapierre SG, 2012. Estimation of kerogen porosity in source rocks as a function of thermal transformation: Example from the Mowry Shale in the Powder River Basin of Wyoming. *AAPG Bulletin* 96, 87–108.

Shields G and Vezier J, 2002. Precambrian marine carbonate isotope database: Version 1.1. *Geochemistry, Geophysics and Geosystems* 3(6). 10.1029/2001GC000266.

Stüeken EE, Kipp MA, Koehler MC and Buick R, 2016. The evolution of Earth's biogeochemical nitrogen cycle. *Earth-Science Reviews* 160, 220–239. https://doi.org/10.1016/j.earscirev.2016.07.007

Zack T and Hogmalm J, 2016. Laser ablation Rb/Sr dating by online chemical separation of Rb and Sr in an oxygen-filled reaction cell. *Chemical Geology* 437, 120–133.

Popular science articles related to this study

Collins AS, Cox G and Yang B, 2017. What's Australia made of? Geologically, it depends on the state you're in. *The Conversation* 21st Nov 2017. https://theconversation.com/whats-australia-made-of-geologically-it-depends-on-the-state-youre-in-83575

Cox G and Collins AS, 2017. Ancient volcanic eruptions disrupted Earth's thermostat, creating a 'Snowball' planet. *The Conversation* 13th Sept 2017. https://theconversation.com/ancient-volcanic-eruptions-disrupted-earths-thermostat-creating-a-snowball-planet-82215 - >7K reads

Cox G and Collins AS, 2017 A time capsule containing 118 trillion cubic feet of gas is buried in northern Australia. *The Conversation* 11th July 2017. https://theconversation.com/a-time-capsule-containing-118-trillion-cubic-feet-of-gas-is-buried-in-northern-australia-80268 - >150K reads

Collins AS and Merdith AS, 2017. A map that fills a 500-million year gap in Earth's history. *The Conversation* 27th June 2017. https://theconversation.com/a-map-that-fills-a-500-million-year-gap-in-earths-history-79838 - >77K reads in 24 hrs; >365K reads total. Featured in The Conversation 2017 Yearbook '50 Standout Articles from Australia's Top Thinkers'.

Ultra-high resolution trace element mapping provides new clues on the origin of the McArthur River (HYC) sediment-hosted Zn-Pb-Ag deposit

Sam Spinks[1,2], Mark Pearce[1], Chris Ryan[1], Gareth Moorhead[1], Robin Kirkham[1], Heather Sheldon[1], Marcus Kunzmann[1,3], Weihua Liu[1], Teagan N Blaikie[1,3], Peter Schaubs[1] and William DA Rickard[4]

Introduction

The supergiant McArthur River (Here's Your Chance [HYC]) Zn-Pb-Ag deposit is one of the largest sediment-hosted base metal deposits in the McArthur–Isa superbasin (**Figure 1**), the world's largest Zn-Pb province. HYC is widely regarded as one of the classic examples of a sedimentary exhalative (sedex) base metal deposit (Large *et al* 1998, Ireland *et al* 2004b), which implies mineralisation occurred following exhalation of a metalliferous brine into the water column with resultant deposition of laminated base metal sulfide ore as a chemical sediment. This model of ore formation influences exploration approaches as it infers a direct control of the sedimentary environment and synsedimentary tectonic framework on base metal deposition. A review of sedimentary-hosted Zn-Pb deposits by (Leach *et al* 2005) found the term 'sedex' to be fundamentally concerning because it imparts a specific

[1] CSIRO Mineral Resources, Australian Resources Research Centre (ARRC), 26 Dick Perry Avenue, Kensington WA 6151, Australia
[2] Email: sam.spinks@CSIRO.au
[3] Northern Territory Geological Survey, GPO Box 4550, Darwin NT 0801, Australia
[4] John De Laeter Centre, Curtin University, Bentley WA 6102, Australia

Figure 1. Simplified regional geology map of the McArthur and Mount Isa basins in northern Australia showing the locations of major stratiform Zn-Pb-Ag deposits with the McArthur River (HYC) deposit in the Batten Fault Zone highlighted.

exhalative genetic component, given most deposits lack unequivocal evidence for exhalative ore. The presence of laminated ore textures, often regarded as the primary evidence for exhalative processes in these deposits, have been shown to result from carbonate replacement processes in the subsurface well after deposition of the host sediment in other similar deposits such as in the Red Dog region (Kelley *et al* 2004). Likewise, the laminated ore of the Century deposit in the Isa basin has been shown to be ca 28 My younger than the host sediment (Broadbent *et al* 1998).

The evidence for a synsedimentary-exhalative origin of HYC (and other similar deposits in the region) is predicated mainly on the observation that the ores with fine-grained laminated textures are sedimentary in origin (Large *et al* 1998), and that ore clasts that occur within intraformational breccias indicate mineralisation occurred before individual fault movements (Ireland *et al* 2004b). Trace element enrichments, eg thallium (Tl) in the ore zone and surrounding and overlying lithologies, are also reported to represent a synsedimentary origin for mineralisation (Large *et al* 2000). These features have also been interpreted by some workers to be strong evidence for subsurface diagenetic-epigenetic carbonate replacement origin for the mineral system. Despite having been well studied over the decades, controversy remains over the genetic model of the HYC mineral system.

Herein we present evidence for a carbonate replacement-style mineral system for HYC by employing state-of-the-art analytical techniques, and, critically, by quantitatively examining the mineral system through a range of scales from the sub metre to the nanometre scale.

Methods summary

Finely laminated ore occurs in the central zone, whereas the facies in the northern and southern margins are dominated by predominantly nodular carbonate and interbedded finely-laminated pyrite (eg Ireland *et al* 2004b). Samples up to ~50 cm in diameter bearing both textures were collected from the central, southern and northern margins of the HYC pit as was exposed between 2016 and 2018.

Maia Mapper ultra-high resolution XRF mapping

The Maia Mapper is a new laboratory XRF mapping system for efficient elemental imaging of drill core sections for use in minerals research and industrial applications. It targets intermediate spatial scales, with imaging of up to ~80 M pixels, each 30 µm, over a 500 long × 150 mm high sample area, as part of the analytical workflow of the CSIRO Advanced Resource Characterisation Facility, which spans spatial scales from atomic to ore deposit scales. It brings together (i) the Maia detector and imaging system, which is part of the Australian Synchrotron XFM facility (Siddons *et al* 2014), with its capabilities for high efficiency detection (1.3 sr solid-angle), event-mode operation, millisecond pixel transit times in fly-scan mode and real-time spectral deconvolution and imaging (Ryan *et al* 2014); (ii) the high brightness MetalJet D2 liquid metal micro-focus X-ray source from Excillum (http://www.excillum.com/) with indium alloy anode and 200 W power at 70 kV into an effective 20 µm source size, filtered using a 1.0 mm aluminium window; and (iii) an efficient XOS polycapillary lens with a flux gain 15 900 at 21 keV into a ~32 µm focus; all are integrated with stage raster scanning for automated imaging and analysis of drill core sections (Ryan *et al* 2018).

Imaging for Maia Mapper uses an extension of the GeoPIXE method for synchrotron XRF analysis and imaging (Ryan *et al* 2010a), which is built on a fundamental parameters approach combined with the Dynamic Analysis method for quantitative image projection (Ryan and Jamieson 1993, Ryan 2000, Ryan *et al* 2010b). Within the approximation of constant yields across the image area, these images are quantitative and can be directly interrogated for elemental concentrations. Methods have been developed for post-imaging iterative corrections in GeoPIXE to account for the effects on yields of variations in matrix composition across the image area; these are described in detail elsewhere (Ryan 2000). Synchrotron XRF uses a monochromatic X-ray beam. For Maia Mapper, which uses a filtered microfocus XRF source spectrum, the modelling of calculated X-ray yields for each chemical element is integrated over the model filtered source spectrum.

Polished slab samples 300–400 mm in length from the central, southern and northern zones of the pit were analysed on the Maia Mapper. Particular focus was paid to the distribution of Tl, which is otherwise difficult, if not impossible, to detect as a trace element within major minerals using standard laboratory XRF techniques due to X-ray peak overlaps with Pb and S. Therefore, validation of Tl distribution requires interrogation of some spatial regions to explore and extract the Tl signal. The close proximity of Tl and Pb X-ray peaks may lead to some Tl artefact when Pb is high. Hence, we use associations to select high-Tl, but low-Pb pixels to separate each element in geochemical maps (**Figure 5**).

Electron backscatter diffraction (EBSD)

Samples were polished with a 20 nm, colloidal silica suspension in dilute NaOH to remove crystal lattice damage from thin section preparation. The surface was coated with a ~5 nm carbon coat to prevent charging in the scanning electron microscope (SEM). Electron backscatter diffraction (EBSD) mapping was performed using a Zeiss UltraPlus FEGSEM fitted with an Oxford Instruments Symmetry EBSD detector and XMaxN-80 EDS detector. During mapping, both EBSD patterns and EDS spectra were collected from each point simultaneously to allow relationships between crystallographic (grain) boundaries and chemical variations to be examined. Data was acquired using an incident electron beam with a beam current of 15 nA and accelerating voltage of 20 keV. The sample normal was inclined at 70° to the incident electron beam to increase diffracted electron yield. Maps were collected with a step size between measurements of 150 nm (to ensure that sub-micron grains were captured)

and at an acquisition rate of 390 Hz. EBSD patterns were indexed against orientation databases selected by the user for the following phases: dolomite (Laue class $\bar{3}$; a = 4.807, c = 16.003), pyrite (Laue class m$\bar{3}$; a = 5.428), quartz (Laue class m$\bar{3}$; a = 4.915, c = 5.407), and sphalerite (Laue class m$\bar{3}$m; a = 5.918).

Focussed ion beam time of flight secondary ionisation mass spectrometry (FIB–TOF–SIMS)

The trace element content of pyrite was mapped at high spatial resolution using 'focussed ion beam time of flight secondary ionisation mass spectrometry' (FIB–TOF–SIMS). A focussed gallium (Ga) ion beam is used to sputter material from the surface of the sample and that material is accelerated into a time of flight mass spectrometer attached to the microscope. The resulting spectrum consists of peaks at different mass-to-charge ratios, which can be interpreted in terms of isotopes present in the sample. Plotting spatial variations in peak intensity gives a map of the relative abundance of the isotope in question. Since material is removed from the sample into the mass spectrometer, the data volume can be used to show variations in 3D. However, the maps displayed in this contribution are the signal intensity integrated over the entire depth analysed. Data were collected using a Tescan LYRA3GM FIB–SEM with a Tofwerk TOF–SIMS. Samples were coated with 10 nm of carbon to prevent charging; areas of interest were sputtered with a 69 Ga+ ion beam with an accelerating voltage 30 keV, and probe current of 300 pA using the TOF–SIMS in positive mode. Regions of interest consist of 1024 × 1024 pixels over 15 × 15 µm binned at 4 analytical pixels per display pixel to increase signal to noise ratio, which gives an effective pixel size of 58.6 nm.

Results

Paragenesis of base metal sulfides and relationship to carbonate

Large samples of laminated ore analysed on the Maia Mapper show thin laminae of base metal sulfides and pyrite as shown in the RGB element map (**Figure 2**). Discreet residual carbonate laminae are detectible in all samples analysed. For example, **Figure 2b** shows isolated calcium (Ca-blue) laminae which represent preserved carbonate (dolomite) laminae in the ore. Sphalerite (Zn-green) in these areas occurs within and around residual carbonate (**Figure 3**). In all nodular carbonate samples analysed in this study, sphalerite is spatially associated with the outer margins of carbonate (**Figure 4**). Only very minor sphalerite was detected in laminated primary (syngenetic) pyrite-organic laminae. Detailed EBSD analysis of the interfaces between sphalerite and carbonate (**Figure 5b**, **c**) shows localised Mn enrichment on the outer margins of dolomite surrounded by sphalerite, with stylolitic dissolution cavities in the carbonate hosting the majority of the sphalerite.

Thallium distribution

Interrogation of the Maia Mapper data from large HYC pit samples shows zones of high-Tl and low-Pb in some areas that seem unique spatially but not distinct in any other element image, although Fe (pyrite) is high in these zones. The sample shown in **Figure 4** hosts one such area of high-Tl within the pyritic band in the middle. By selecting this band of pixels with high-Tl, we are able to highlight the high-Tl- and low-Pb pixel associations to filter out any artefacts (overlaps) as shown in **Figure 6**. The region spectrum fit

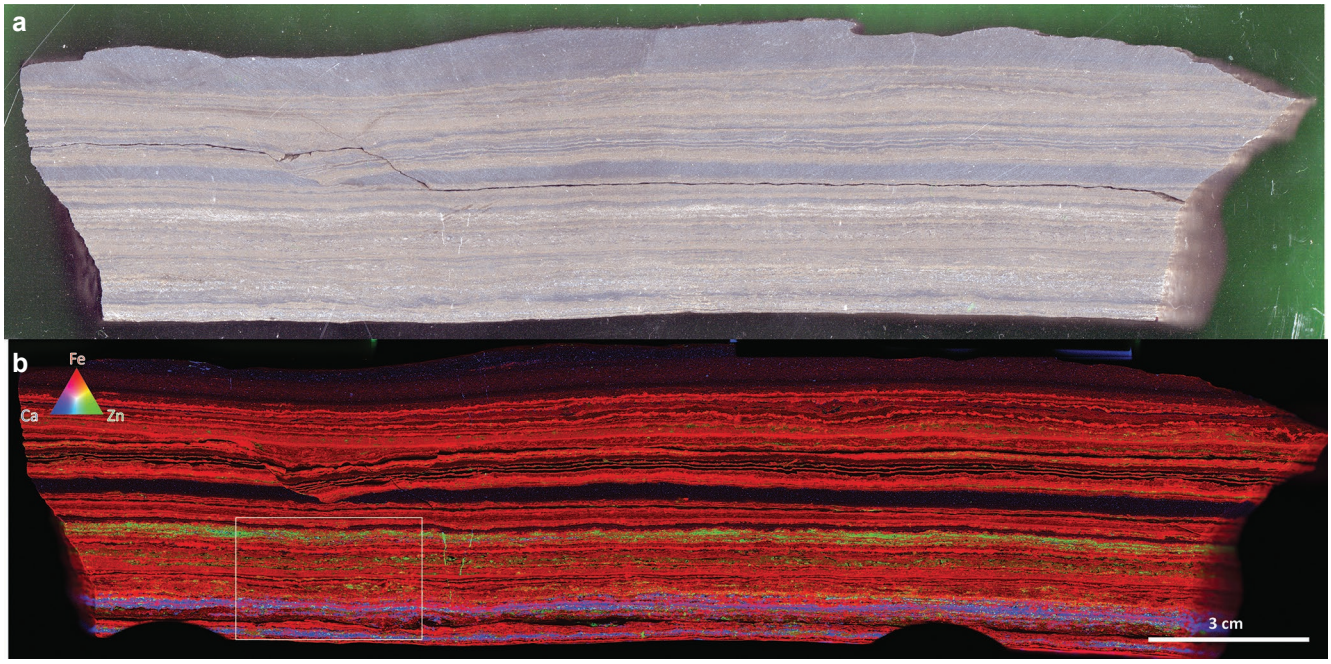

Figure 2. (**a**) Polished slab of laminated pyritic-dolomitic Zn-Pb ore (orebody 8) from central zone of HYC. (**b**) Maia Map of same sample showing distribution of iron (red), zinc (green) and calcium (blue). Zinc (sphalerite) is observed to have partially-to-fully replaced dolomitic (calcium-blue) laminae. White box indicates field of view of detailed area shown in **Figure 3**.

shows very clear Tl lines. The Tl Lα is less clear, in the side of the Pb Lα peak. But the Tl Lβ makes a good shoulder on the Pb Lβ peak, at an energy where we do not see many lines around 12.2 keV. Therefore, Tl appears genuine. This pattern is observed throughout our sample suite from HYC.

Figure 7 shows Maia Mapper data of the same slumped laminated pyrite-carbonate sample in **Figure 4**, highlighting Tl distribution. Maia Mapper analyses shows, for the first time, that high-concentration thallium is associated exclusively with pyrite. The middle

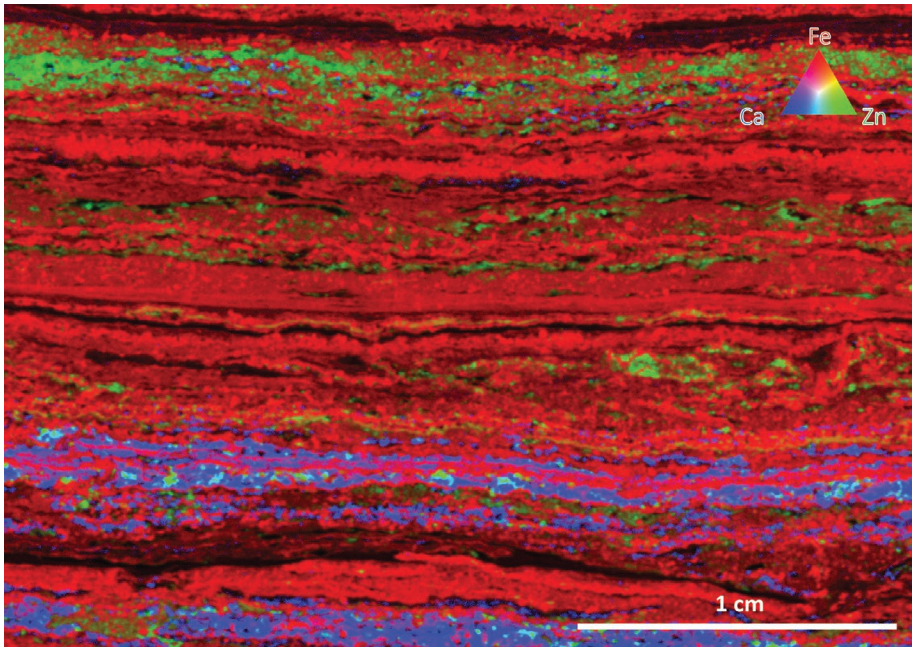

Figure 3. Maia Map of area shown by white box in **Figure 2** showing distribution of iron (red), zinc (green) and calcium (blue). Zinc (sphalerite) is observed to have partially-to-fully replaced dolomitic (calcium-blue) laminae.

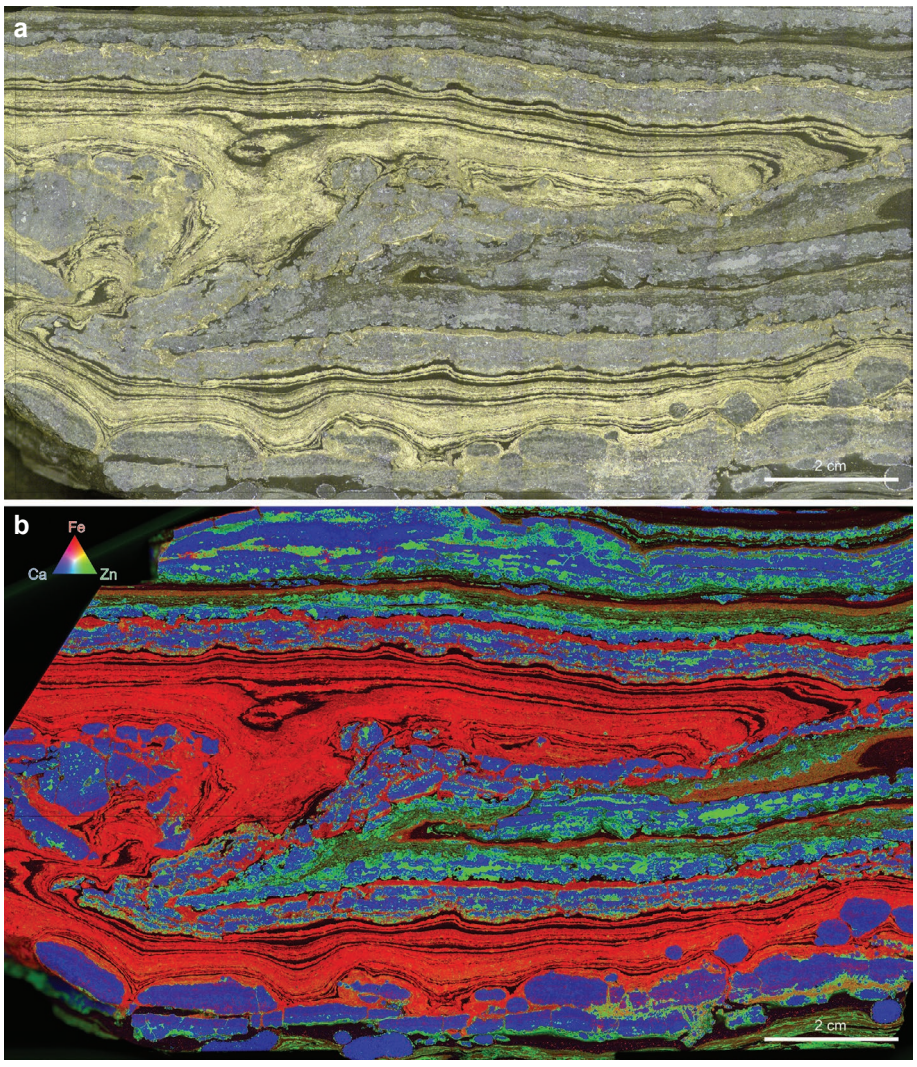

Figure 4. (**a**) Photomicrograph of polished slab of laminated and slumped pyritic and nodular carbonate Zn-Pb ore from southern margin zone of HYC. (**b**) Maia Map of same sample showing distribution of iron (red), zinc (green) and calcium (blue).

image shows Tl (red), which when compared with the photomicrograph of the sample above, demonstrates that the highest concentrations (brightest colours) correlate with paragenetically-late pyrite bands that are spatially proximal to the sphalerite (Zn - blue) occurring around the rims of nodular carbonate, also shown in **Figure 4b**. Thallium enrichment also occurs in early syngenetic laminated pyrite zones but in lower concentrations. However, galena (Pb - green), which occurs in association with certain carbonate nodule margins, is not spatially-associated with Tl enrichment in the late pyritic bands. **Figure 7c** shows the high-Tl low-Pb pixels highlighted as a distribution heat map. This image clearly shows the Tl concentration variation between the zone of syngenetic laminated pyrite and the bands of later diagenetic pyrite (up to ~811 ppm). This image also shows zones of probable X-ray artefact (overlap) with Pb in the upper and lower areas where Pb concentrations are high (**Figure 7b**).

Closer SEM analysis of the zones of Tl-enriched late pyrite (eg **Figure 7**) shows the pyrites bear rounded (possibly framboidal) cores with numerous generations of later euhedral overgrowths (**Figure 8a**). Pyrite overgrowths contain minor galena inclusions. Sphalerite that is observed replacing carbonate (dolomite) throughout, is here observed to have entirely precipitated after the latest pyrite overgrowths. Detailed analysis of these overgrown

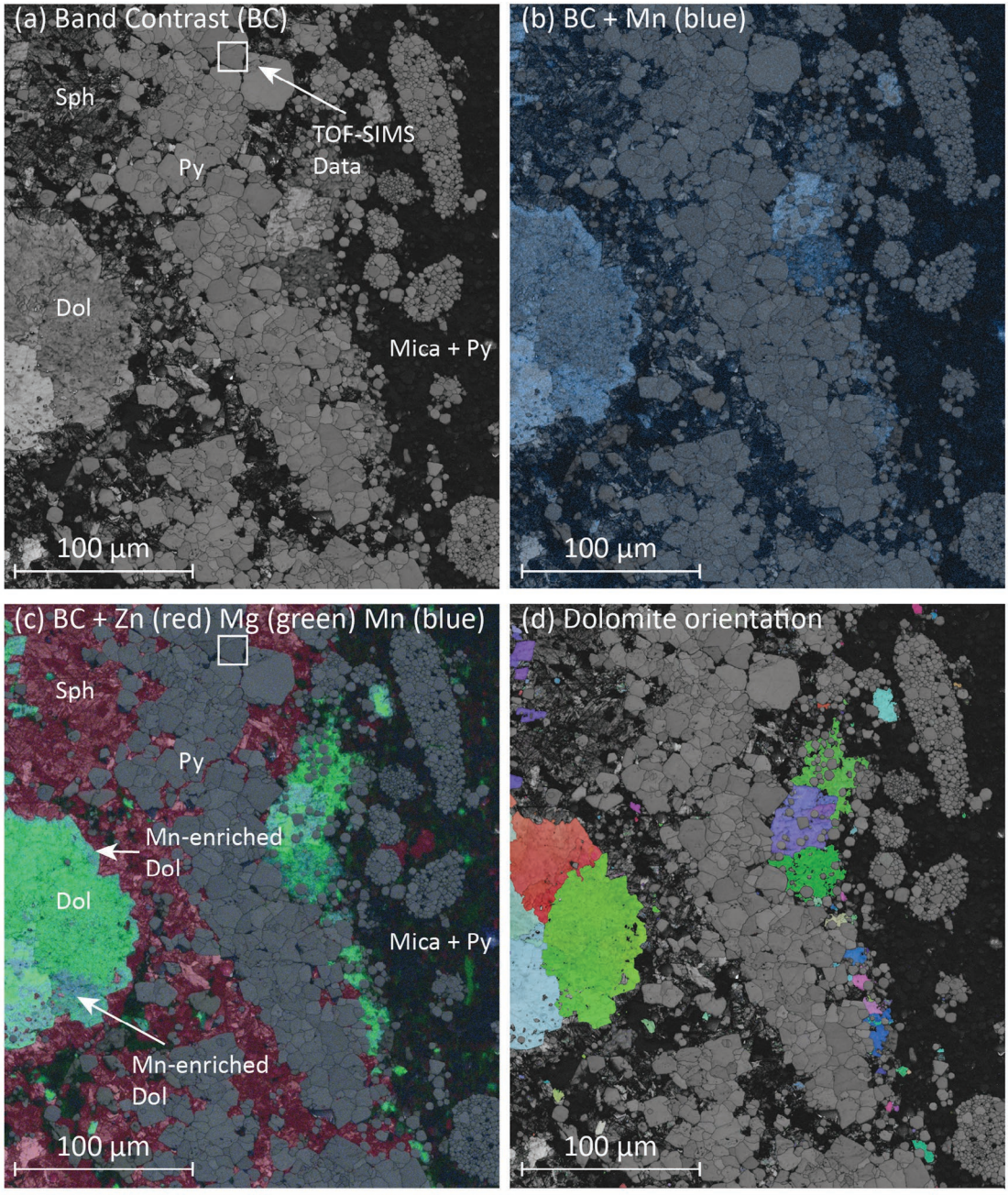

Figure 5. EBSD montage of pyritic-sphalerite-dolomite in approximate area shown in white box in **Figure 7c**. EBSD–EDS data is presented as maps combining different components of the data to show spatial relationships. (**a**) Band contrast, a measure of EBSD pattern quality, is used as a background image because it displays the microstructure complete with grain boundaries. (**b**) Overlaying Mn intensity from the EDS data shows that Mn largely resides in dolomite (cf **Figures 5b**, **d**) adjacent to phase boundaries between dolomite and sphalerite (the latter shown by the presence of Zn in **Figure 5c**. (**c**) BC+Zn (red) Mg (green) Mn (blue). (**d**) Dolomite orientation. BC=band contrast; Dol=dolomite; Sph=sphalerite; Py=pyrite.

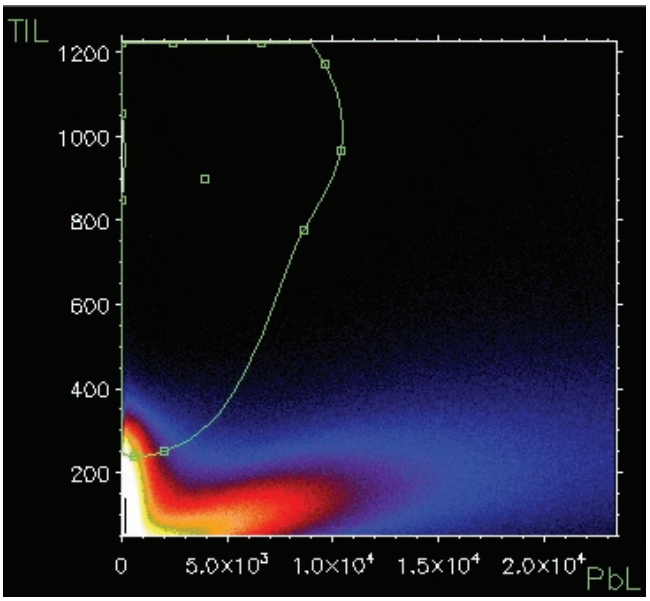

Figure 6. Comparison of thallium Lα and lead Lα regions in area outlined by white box in thallium-rich zone, shown in **Figure 7c**.

framboidal pyrites using FIB–TOF–SIMS shows that the distribution of Tl is concentrated in the diagenetic overgrowths (**Figure 8b**). The framboidal cores are mostly entirely void of detectable Tl (**Figure 9**), although in rare cases are there localised enrichments (eg **Figure 8b**).

Discussion

Carbonate replacement by Zn-Pb sulfides at HYC

The presence of laminated base metal sulfide textures is the primary observation historically presented as evidence for a syndepositional origin of the HYC and other deposits in the McArthur–Isa Zn belt (Ireland *et al* 2004b, Large *et al* 2000, Large *et al* 2005). The argument by Leach *et al* (2010) that sulfide layering, by itself, is not sufficient evidence for exhalative ore was recently disputed by Sangster (2018) who stated that sulfides mimicking synsedimentary textures is not proof of replacement processes either. Whilst this counter argument is valid, it emphasises the circular pattern of opposing arguments that arise when dealing with interpretations based on subjective, sometimes non-quantifiable observations. Sangster (2018) also noted that even though carbonate replacement is frequently mentioned in literature to be responsible for layered sulfide textures at HYC and elsewhere, the replaced mineral phase is 'seldom identified'. This highlights the difficulty in visually identifying certain residual mineral phases in altered laminated sedimentary rocks; it also reflects a problem that arises from scale. Most studies are based on thin sections that are chosen on subjective, visual observational criteria at the sampling stage. Thus, traditionally there is a significant step in scale of study, from the deposit scale to thin section scale, that can lead to subtle, but potentially key features (such as residual carbonate) being overlooked. Clearly this is dictated by a historic lack of technologies capable of quantitative petrographic analyses on large samples. New technological developments such as the Maia Mapper (Ryan *et al* 2014) can not only accommodate this gap in scale, allowing data-led decision making when choosing thin sections, but also can allow trace quantitative element mapping (eg Tl) at unprecedented ultra-high resolution.

Our data (from large pit samples up to ~300 mm long) clearly demonstrate that residual laminated carbonate is locally preserved in laminated base metal sulfide ore from the central zone of HYC (**Figure 2**, **Figure 3**). Critically, when visually inspecting these samples, residual preserved sub-1 mm laminated carbonate is extremely difficult to identify. Upon closer inspection, the textures of base metal sulfide proximal to preserved carbonate in these laminated ores are consistent with carbonate dissolution. The textures in nodular carbonate-bearing ore are more readily identifiable visually but are far clearer when Maia Mapper data is examined (eg **Figure 4**).

Whilst the presence of Mn within euhedral overgrowths at the margin of dolomite aggregates is not diagnostic of replacement processes, the patchy nature of the Mn enrichment elsewhere suggests that the initially Mn-poor dolomite has been replaced at a later stage. The spatial coincidence of Mn and sphalerite is consistent with dolomite replacement during Zn mineralisation.

Thallium hosted in late diagenetic pyrite

Thallium is a highly incompatible (and toxic) trace element that is often associated with K-bearing mineral phases due to its primary Tl^+ form, which is similar in size to the monovalent cations K^+, Rb^+ and Cs^+ (Nielsen *et al* 2013). As such Tl is readily adsorbed onto clay mineral phases and Mn oxides (Martin *et al* 2018). Unlike other alkali metals, Tl has been suggested to exhibit chalcophile behaviour in hydrothermal fluids and sulfur-bearing melts (McGoldrick *et al* 1979). However, the behaviour of Tl in mineral systems is poorly understood.

Thallium enrichments have been known at HYC (Large *et al* 2000) and among numerous other similar ore deposits worldwide for decades. Previous studies have demonstrated that Tl is present in individual pyrite crystals in the HYC ore zone. Large variations in Tl concentrations in various pyrites, ranging from 176–919 ppm, were reported from the HYC ore zone by Mukherjee and Large (2017). Whilst these analyses are useful, what is critically lacking is context at a scale greater than that of a single pyrite grain. Thus, little is hitherto known about the overall deportment of Tl in the ore zone or the metallogeny of Tl in the greater HYC mineral system. Therefore, the potential of Tl as a pathfinder element in exploration for sediment-hosted Zn deposits, and in other geochemical exploration, is currently unclear.

By using new ultra-high resolution Maia Mapper technology on large-scale ore samples, our data show that Tl is detectable in both early laminated pyrite and in late diagenetic pyrite bands, but is highly concentrated in the latter phase (**Figure 7**). However, by spatially mapping the distribution of highest concentrations of Tl in late pyrite, our detailed quantitative nm-scale mapping using FIB–TOF–SIMS makes it clear that Tl is almost entirely present within

diagenetic pyrite overgrowths (**Figure 8**). Furthermore, consistent with the observations of Broadbent *et al* (1998), Eldridge *et al* (1993), and Polito *et al* (2006), our data show that base metal sulfide mineralisation occurred after the latest diagenetic pyrite. Whilst this not only precludes syndepositional base metal mineralisation, we argue that there are implications for the timing of Tl enrichment in the HYC mineral system, which occurred prior to the deposition of base metal sulfides.

Fluid modelling

Thallium deportment in late pyrite suggests both Fe and Tl were transported in the same hydrothermal fluids, particularly given the homogeneity observed in the distribution within the overgrowths. Fluid phase modelling, assuming a temperature of ~150°C and a salinity of 15% eq NaCl (Cooke *et al* 2000), shows that TlCl is mobile across a range of pH values above a Log fO_2 (aq) of ~45, with S

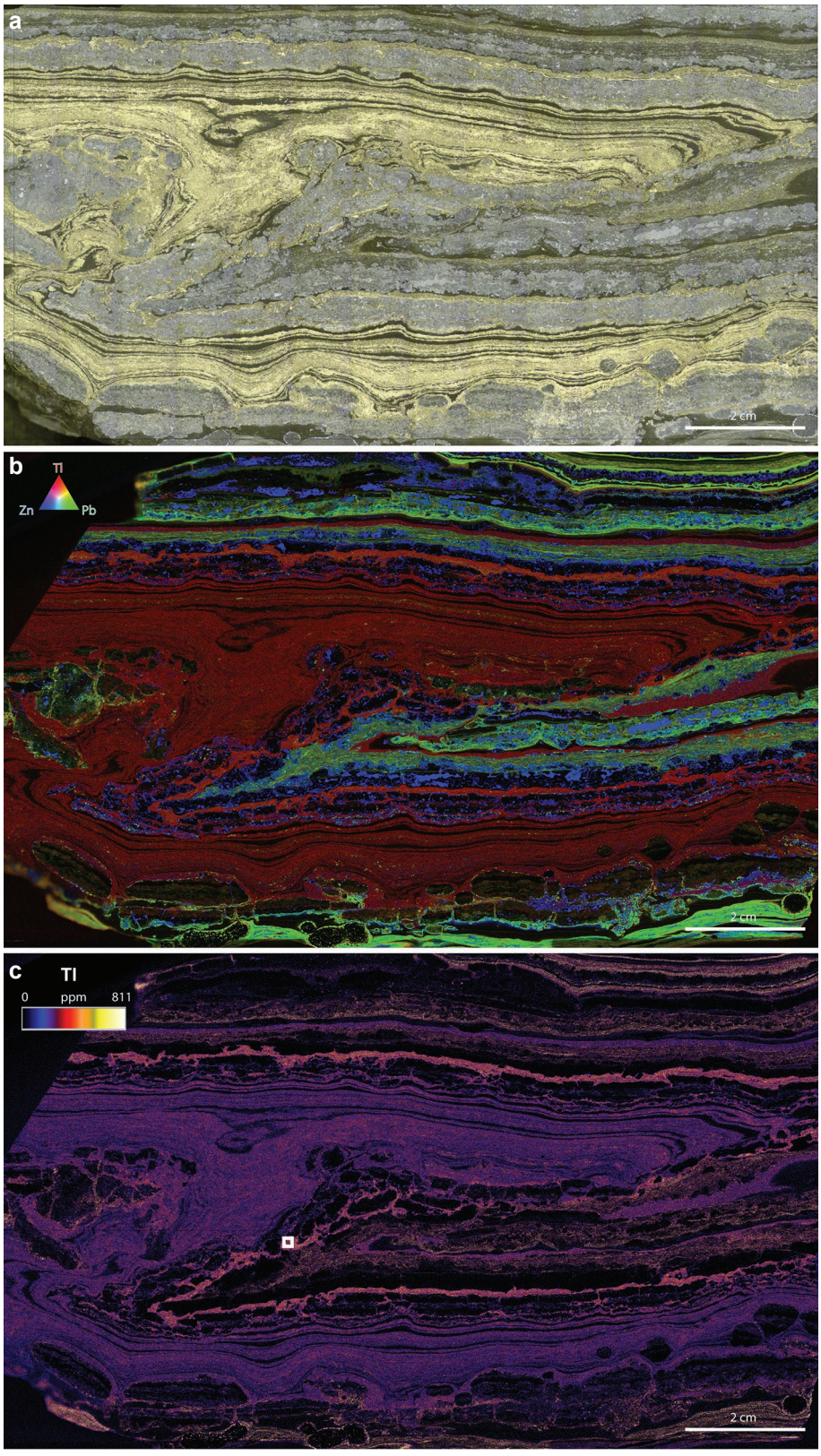

Figure 7. (**a**) Photomicrograph of polished slab of laminated pyritic-carbonate HYC Zn-Pb ore. (**b**) Maia Map of same sample showing distribution of thallium (red), zinc (green) and lead (blue). (**c**) Heat distribution map of thallium showing highest enrichments in late-stage pyrite zone. White box indicates area analysed in **Figure 5** and **Figure 6**, and approximate area of detailed TOF–SIMS analysis shown in **Figure 8**.

species buffered between pH 3–4 (**Figure 10a**). However FeCl complexes are only mobile at the same temperatures below pH 4; below Log fO_2 (aq) 45 (reducing conditions), H_2S is stable. Cooke *et al* (2000) noted the likely dominance of oxidised fluids in the Australian Proterozoic sediment-hosted Zn deposits. Our data are consistent with this; therefore, we argue that it is likely that FeCl and TlCl complexes were transported in oxidised fluids with pH below 4 (**Figure 10a**, **b**) in the presence of HSO_4^-, before being reduced thus allowing hydrothermally-derived pyrite overgrowths to precipitate.

Zinc can be transported at similar temperatures as $ZnCl_4^{2-}$ complexes across a range of pH values (0 – ~9) in oxidised fluids. Sphalerite cannot precipitate at those temperatures at pH values below ~5; therefore, pyrite and sphalerite are unlikely to have co-precipitated if the initial ore fluid was pH <4, ie transporting FeCl complexes (**Figure 10c**). Carbonate dissolution during acidic fluid influx may have created additional porosity along bedding planes. Sphalerite may have been deposited if the ore-bearing fluids were buffered to pH values >5 following acidic dissolution of carbonate, allowing reduction of the residual Zn-bearing fluid and

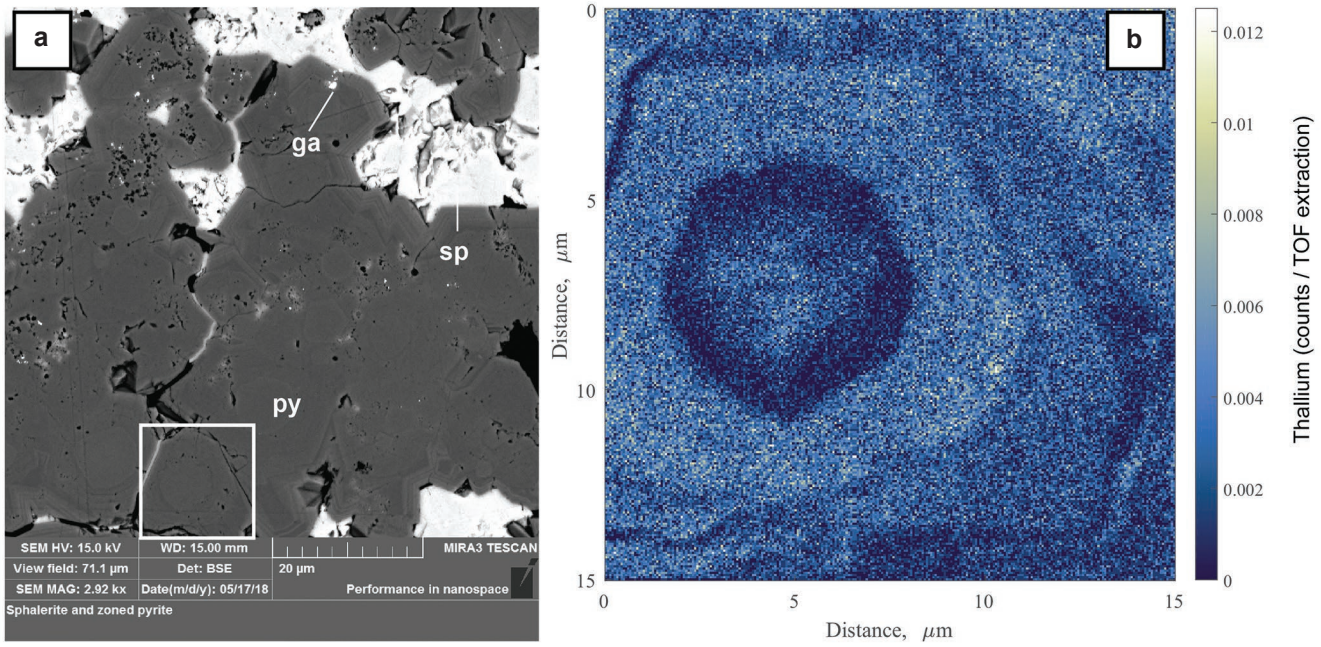

Figure 8. (**a**) SEM image of early framboidal pyrite with late zoned pyrite overgrowths in the Zn-Pb ore zone outlined in **Figure 7**. (**b**) TOF–SIMS map of Tl^{205} in zoned pyrite outlined in the white box in **8a**. The framboidal core, in this case, has rare localised enrichments in Tl, whereas the zoned overgrowths have higher Tl concentrations.

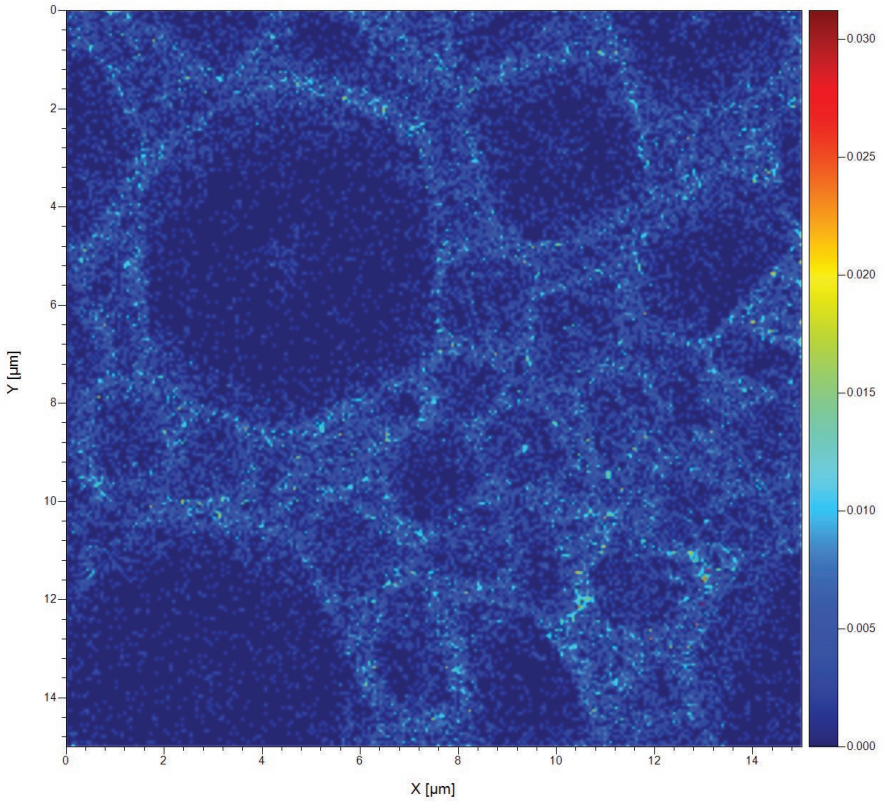

Figure 9. FIB–TOF–SIMS Tl image of framboidal pyrite cores with minimal diagenetic overgrowths, but with localised Tl enrichments on outer edge.

precipitation of sphalerite. This mechanism could explain the presence of base metal sulfides that surround latest-stage pyrite overgrowths (**Figure 8a**); this is consistent with the prior observations of Broadbent *et al* (1998), Eldridge *et al* (1993), and Polito *et al* (2006). Furthermore, as carbonates have retrograde solubilities, solubility products of Fe-Mn carbonates are lower than those of Ca-Mg-rich carbonates such that the Fe–Mn carbonates may precipitate close to the site of dissolution (Chen *et al* 2003). This is consistent with the Mn-enriched rims observed at the dissolution front observed in contact with sphalerite in **Figure 5c**.

Implications for the origin of the HYC mineral system

In the context of previous work conducted at HYC and elsewhere in the McArthur–Isa superbasin, these findings provide new quantitative insights into the genesis of sediment-hosted Zn-Pb deposits such as HYC. **Table 1** lists a summary of observations at HYC that are considered evidence for both a syndepositional-syngenetic model and a diagenetic-epigenetic model by previous studies. The summary of findings of this study in relation to each of these previous observations are also shown.

Conclusions

- Ultra-high resolution geochemical mapping of large pit samples from HYC show sphalerite is exclusively associated with carbonate dissolution. Nodular carbonate in north and south zones is partially-replaced, whereas laminated carbonate in the central zone is almost entirely replaced by base metal sulfides.
- EBSD analyses show Mn-enriched outer margins of carbonate at dissolution front in contact with sphalerite.
- Ultra-high resolution geochemical mapping shows Tl is hosted in late-stage pyrite bands, spatially associated with sphalerite. FIB–TOF–SIMS analyses shows Tl is hosted predominantly in late-stage pyrite overgrowths that precipitated (perhaps immediately) before base metal sulfides.
- Fluid modelling suggests precipitation of initial Tl-bearing pyrite overgrowths by reduction of metals transported by acidic (pH<4) oxidised fluids. Acidic dissolution of carbonate allows additional porosity and creates a pH buffering effect, raising fluid pH above 5, allowing precipitation of sphalerite at site of carbonate dissolution.
- These findings provide strong evidence for a diagenetic-epigenetic carbonate replacement origin for the HYC mineral system; they preclude a syngenetic model. This has implications for future exploration strategies for these Proterozoic sediment-hosted base metal deposits.

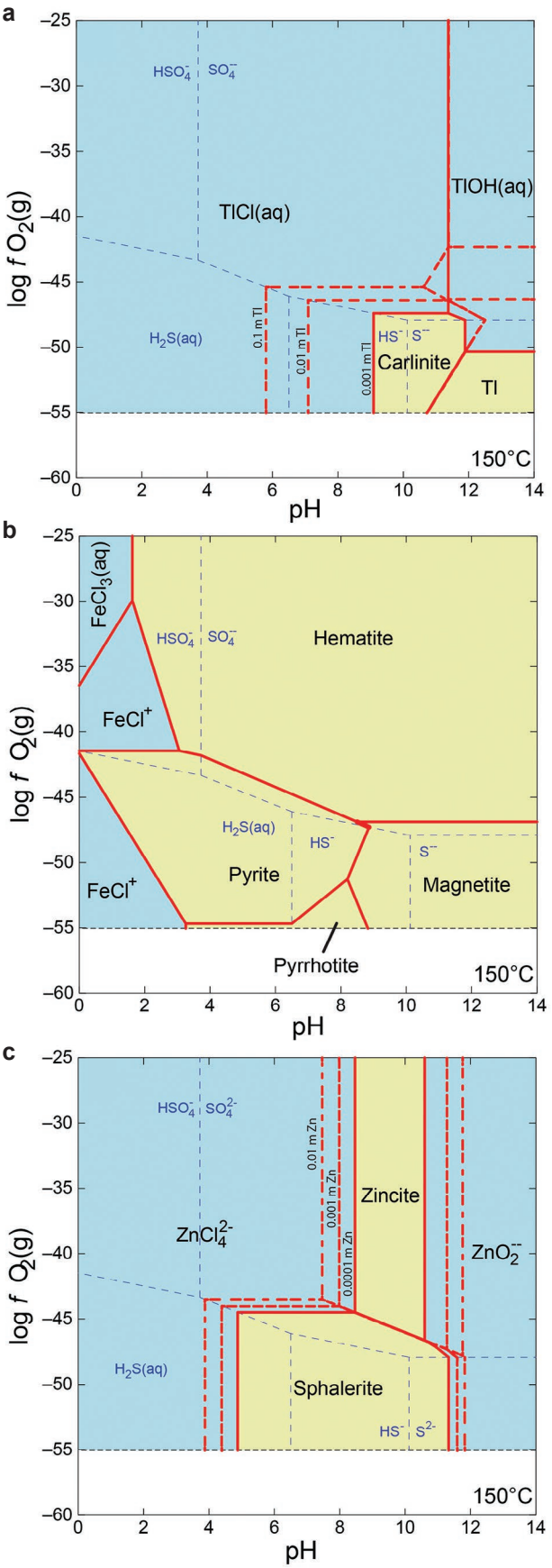

Figure 10. Stability of predominant Tl, Fe and Zn minerals and aqueous species as a function of logfO_2 and pH at 150°C: (**a**) Tl; (**b**) Fe; (**c**) Zn. Boundaries of Tl, Fe and Zn species are shown as red solid, dashed and dash-dotted lines respectively. The boundaries of sulfur species are shown with blue dashed lines in all subplots; activities of total sulfur and chloride are the same as Cooke *et al* (2000): a_∑S = 0.001 m; a_∑Cl = 5.8 m.

Table 1. Summarised constraints on the contrasting syndepositional-exhalative versus diagenetic-epigenetic genetic models based on key lines of evidence and observations. Summarised after Huston *et al* (2006).

Observation	Syndepositional-exhalative model	Diagenetic-epigenetic model	This study
Laminated ore textures (in central zone of deposit)	Consistent with deposition of sulfides as chemical sediments from water column (Ireland *et al* 2004b, Large *et al* 1998, Large *et al* 2005)	Can be produced by sulfide replacement of layered-laminated sedimentary sedimentary-diagenetic carbonate (Broadbent *et al* 1998, Eldridge *et al* 1993, Polito *et al* 2006) (**Figure 2**, **Figure 3**). Nodular carbonate also replaced by sphalerite (Ireland *et al* 2004b, Large *et al* 2005) (**Figure 4**, **Figure 5**).	Textures observed in this study show that both laminated and nodular carbonate were subject to partial to full dissolution and replacement by base metal sulfides. EBSD analyses of carbonate (dolomite) show that the outer edges are Mn-altered where in contact with replacive sphalerite.
Laminated ore clasts within intraformational breccias	Consistent with early syndepositional mineralisation prior to breccia flows (Ireland *et al* 2004a)	Can be produced by the same carbonate replacement geochemical processes as the main orebody, well after deposition.	Can be produced by the same carbonate replacement geochemical processes as the main orebody, well after deposition.
Timing of sphalerite and galena mineralisation (post-latest diagenetic pyrite overgrowths)	Not consistent.	Deposition of base metal sulfides after latest diagenetic pyrite overgrowths (**Figure 8**) indicate diagenetic-epigenetic model (Broadbent *et al* 1998, Eldridge *et al* 1993, Huston *et al* 2006, Leach *et al* 2010, Polito *et al* 2006).	Sphalerite and galena mineralisation occur after the latest pyrite overgrowths, with some minor galena occurring as micron-scale inclusions in some pyrite overgrowths. Fluid modelling demonstrates that initial acidic, oxidized ore fluids may have transported metal chloride complexes, followed by reduction, allowing precipitation of Tl-enriched pyrite overgrowths. Carbonate dissolution could have pH buffered the fluid to pH>5, allowing later precipitation of sphalerite.
Thallium (Tl) lithogeochemical anomalism (100s ppm)	Enrichment of Tl up to 200 m above ore zone could result from low-T fluid after main-stage mineralisation (Large *et al* 2000).	Enrichment of Tl up to 200 m above ore zone *indicate* fluid flow well after deposition of ore-hosting sediments low-T fluid after main-stage mineralisation (Huston *et al* 2006) (**Figure 7–9**)	Ultra-high resolution mapping of large samples show Tl enrichments are hosted in late-stage pyrite bands, proximal to sphalerite deposition associated with carbonate replacement. Nanometre-scale quantitative analyses show that Tl is hosted in late-stage pyrite overgrowths that precipitated before base metal sulfides. Fluid modelling shows sphalerite may have precipitated immediately after Tl-enriched pyrite overgrowths due to pH buffering following carbonate dissolution. Enrichment in Tl up to 200 m above ore zone (Large *et al* 2000), by this mechanism, would confirm fluid flow well after deposition of ore-hosting sediments.

Acknowledgements

The authors would like to thank McArthur River Mining, particularly Kris Masterman, for excellent support on site at HYC. This project is funded by the NTGS–CSIRO collaborative project on the McArthur Basin.

References

Broadbent GC, Meyers RE and Wright JV, 1998. Geology and origin of shale-hosted Zn-Pb-Ag mineralization at the Century deposit, Northwest Queensland, Australia. *Economic Geology* 93, 1264–1294.

Chen J, Walter MR, Logan GA, Hinman MC and Summons RE, 2003. The Paleoproterozoic McArthur River (HYC) Pb/Zn/Ag deposit of northern Australia: organic geochemistry and ore genesis. *Earth and Planetary Science Letters* 210, 467–479.

Cooke DR, Bull SW, Large EE and McGoldrick PJ, 2000. The importance of oxidized brines for the formation of Australian Proterozoic stratiform sediment-hosted Pb-Zn (sedex) deposits. *Economic Geology* 95, 1–18.

Eldridge CS, Williams N and Walshe JL, 1993. Sulfur isotope variability in sediment-hosted massive sulfide deposits as determined using the ion microprobe SHRIMP: II. A study of the H.Y.C. deposit at McArthur River, Northern Territory, Australia. *Economic Geology* 88, 1–26.

Huston DL, Stevens B, Southgate PN, Muhling P and Wyborn L, 2006. Australian Zn-Pb-Ag ore-forming systems: A review and analysis. *Economic Geology* 101, 1117–1157.

Ireland T, Bull SW and Large RR, 2004a. Mass flow sedimentology within the HYC Zn-Pb-Ag deposit, Northern Territory, Australia: Evidence for syn-sedimentary ore genesis. *Mineralium Deposita* 39, 143–158.

Ireland T, Large RR, McGoldrick PJ and Blake M, 2004b. Spatial distribution patterns of sulfur isotopes, nodular carbonate, and ore textures in the McArthur River (HYC) Zn-Pb-Ag deposit, Northern Territory, Australia. *Economic Geology* 99, 1687–1709.

Kelly KD, Dumoulin JA and Jennings S 2004. The Anarraaq Zn-Pb-Ag and barite deposit, northern Alaska: Evidence for replacement of carbonate by barite and sulfides. *Economic Geology* 99, 1577–1591.

Large RR, Bull SW, Cooke DR and McGoldrick PJ, 1998. A genetic model for the HYC deposit, Australia: Based on regional sedimentology, geochemistry, and sulfide-sediment relationships. *Economic Geology* 93, 1345–1368.

Large RR, Bull SW and McGoldrick PJ, 2000. Lithogeochemical halos and geochemical vectors to stratiform sediment hosted Zn-Pb-Ag deposits Part 2. HYC deposit, McArthur river, North Territory. *Journal of Geochemical Exploration* 68, 105–126.

Large RR, Bull SW, McGoldrick PJ and Walters S, 2005. Stratiform and strata-bound Zn-Pb-Ag deposits in Proterozoic sedimentary basins, northern Australia. *Economic Geology* 100, 931–963.

Leach DL, Bradley DC, Huston D, Pisarevsky SA, Taylor RD and Gardoll SJ, 2010. Sediment-hosted lead-zinc deposits in earth history. *Economic Geology* 105, 593–625.

Leach DL, Sangster DF, Kelly KD, Large RR, Garven G and Allen CR, 2005. Sediment-hosted Pb-Zn deposits: A global perspective. *Economic Geology* 100, 561–608.

Martin LA, Wissocq A, Benedetti MF and Latrille C, 2018. Thallium (Tl) sorption onto illite and smectite: Implications for Tl mobility in the environment. *Geochimica et Cosmochimica Acta* 230, 1–16.

McGoldrick PJ, Keays RR and Scott BB, 1979. Thallium: a sensitive indicator of rock/seawater interaction and of sulfur saturation of silicate melts. *Geochimica et Cosmochimica Acta* 43, 1303–1311.

Mukherjee I and Large R, 2017. Application of pyrite trace element chemistry to exploration for SEDEX style Zn-Pb deposits: McArthur Basin, Northern Territory. *Australia. Ore Geology Reviews* 81, 1249–1270.

Nielsen SG, Wasylenki LE, Rehkamper M, Peacock CL, Xus Z and Moon EM, 2013. Towards an understanding of thallium isotope fractionation during adsorption to manganese oxides. *Geochimica et Cosmochimica Acta* 117, 252–265.

Polito PA, Kyser TK, Golding SD and Southgate PN, 2006. Zinc deposits and related mineralization of the Burketown mineral field, including the world-class century deposit, northern Australia: Fluid inclusion and stable isotope evidence for basin fluid sources. *Economic Geology* 101, 1251–1273.

Ryan CG, 2000. Quantitative trace element imaging using PIXE and the nuclear microprobe. *International Journal of Imaging Systems and Technology* 11, 219–230.

Ryan CG and Jamieson DN, 1993. Dynamic analysis: on-line quantitative PIXE microanalysis and its use in overlap-resolved elemental mapping. *Nuclear Instruments and Methods in Physics Research* B77, 203–214.

Ryan CG, Kirkham R, Hough RM, Moorhead G, Siddons DP, De Jonge MD, Paterson DJ, De Geronimo G, Howarde DL and Cleverley JS, 2010a. Elemental X-ray imaging using the Maia detector array: The benefits and challenges of large solid-angle. *Nuclear Instruments and Methods in Physics Research, Section A: Accelerators, Spectrometers, Detectors and Associated Equipment* 619, 37–43.

Ryan CG, Kirkham R, Moorhead GF, Parry D, Jensen M, Faulks A, Hogan S, Dunn PA, Dodanwela R, Fisher LA, Pearce M, Siddons DP, Kuczewski A, Lundstrom U, Trolliet A and Gao N, 2018. Maia Mapper: High definition XRF imaging in the lab. *Journal of Instrumentation* 13.

Ryan CG, Siddons DP, Kirkham R, Dunn PA, Kuczewski A, Moorhead G, De Geronimo G, Paterson DJ, De Jonge MD, Hough RM, Lintern MJ, Howard DL, Kappen P and Cleverley J, 2010b. The new Maia detector system: Methods for high definition trace element imaging of natural material. *AIP Conference Proceedings* 1221, 9–17.

Ryan CG, Siddons DP, Kirkham R, Li ZY, De Jonge MD, Paterson DJ, Kuczewski A, Howard DL, Dunn PA, Falkenberg G, Boesenberg U, De Geronimo G, Fisher LA, Halfpenny A, Lintern MJ, Lombi E, Dyl KA, Jensen M, Moorhead GF, Cleverley JS, Hough RM, Godel B, Barnes SJ, James SA, Spiers KM, Alfeld M, Wellenreuther G, Vukmanovic A and Borg S, 2014. Maia X-ray fluorescence imaging: Capturing detail in complex natural samples. *Journal of Physics: Conference Series* 499, 012002.

Sangster DF 2018. Toward an integrated genetic model for vent-distal SEDEX deposits. *Mineralium Deposita* 53, 509–527.

Siddons DP, Kirkham R, Ryan CG, De Geronimo G, Dragone A, Kuczewski AJ, Li ZY, Carini GA, Pinelli D, Beuttenmuller R, Elliot D, Pfeffer M, Tyson TA, Moorhead GF and Dunn PA, 2014. Maia X-ray microprobe detector array system. *Journal of Physics: Conference Series* 499, 012001.

Wollogorang Project: Review of 2018 exploration program

Gary Ferris[1,2] and Michael Schwarz[1]

Background

In April 2018, Northern Cobalt ('N27' or 'the Company') announced a resource upgrade for the Stanton Cobalt Deposit from the results of drilling in late 2017. The new total Mineral Resource Estimate, prepared in accordance with the JORC Code, is 942 000 t at 0.13% Co, 0.06% Ni and 0.12% Cu (the previous Mineral Resource Estimate of 500 000 t at 0.17% Co, 0.09% Ni and 0.17% Cu was reported by N27 in its prospectus in September 2017). Importantly, the contained cobalt within the resource increased and has been largely moved from inferred to indicated status indicating a greater degree of confidence.

Introduction

The Wollogorang Project is located close to the NT–QLD border in the Gulf of Carpentaria (**Figure 1**). N27 listed on the Australian Stock Exchange (ASX) in October 2017 and immediately commenced drilling at the Stanton Cobalt Deposit, completing 70 reverse circulation (RC) and 10 diamond core holes. The aim was to upgrade the existing inferred Mineral Resource, as well as obtain material for metallurgical and scoping studies. A further 57 RC holes were drilled on existing regional prospects previously defined by CRA, for a combined total of 11 856 m drilled between October and early December 2017.

[1] Northern Cobalt Ltd, 67 Goodwood Road, Wayville SA 5034, Australia
[2] Email: gferris@northerncobalt.com.au

During this period, the Company also completed a new aeromagnetic and radiometric survey totalling 3685 line-km of high-resolution magnetic and radiometric data at 25 m flight line spacing covering the Stanton Cobalt Deposit and surrounding cobalt prospects. This new magnetic data, together with historical soils and lag geochemical data, formed the basis for the 2018 exploration program. This paper provides a review of the Company's 2018 exploration program on the Wollogorang project.

Geology

The project area is located within the Wearyan Shelf tectonic element of the southeastern Palaeo– to Mesoproterozoic McArthur Basin, a 5–12 km thick platform cover sequence of mostly unmetamorphosed sedimentary and lesser volcanic rocks deposited on the North Australian Craton, containing dolostone, sandstone and shale units with minor felsic and mafic volcanics (Rawlings 1999, Goulevitch 2002).

The main geological units of interest in the project area are the Gold Creek Volcanics (interlayered basalt lavas and sedimentary rocks) and the Wollogorang Formation (carbonaceous shales and dolomite). To the west of Stanton, these formations are overlain by the flat-lying 250 m thick Pungalina Member (Echo Sandstone) and the Karns Dolostone (**Figure 2**). The Stanton Cobalt Deposit and copper mineralisation at the *Gregjo* and *Running Creek* prospects are all hosted within the Gold Creek Volcanics.

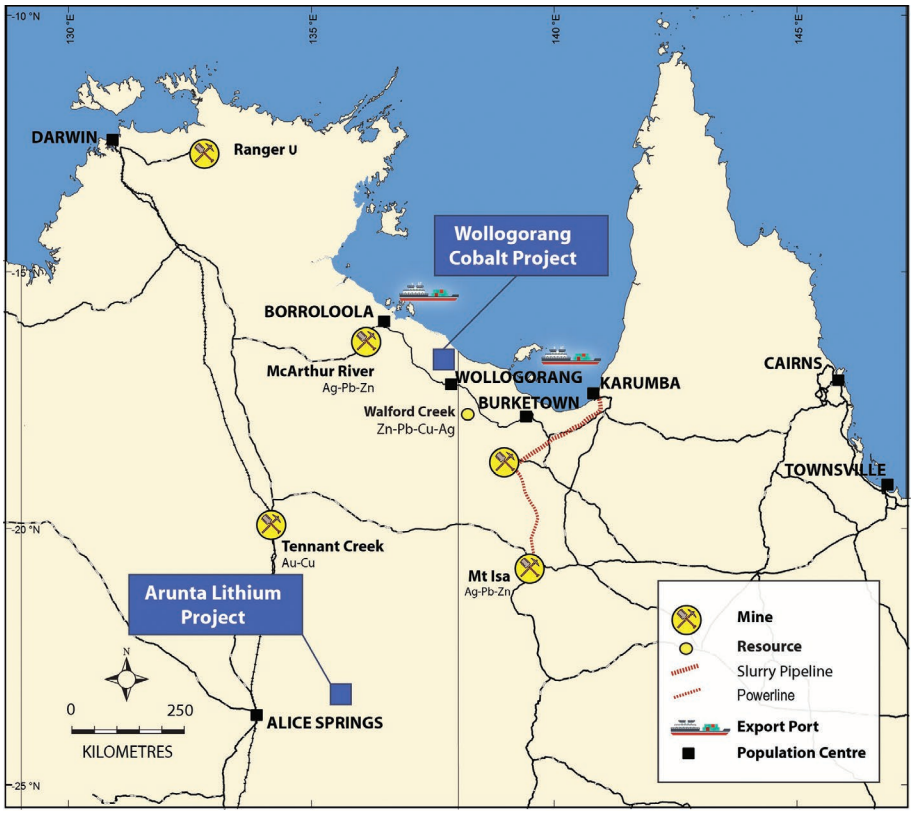

Figure 1. Regional location and projects.

2018 Exploration Highlights

- Completed 1203 aircore (AC) and rotary air blast (RAB) drillholes across the project area.
- Significant drillhole intersections at Running Creek Prospect include:
  - 55 m at 0.78% Cu from 0 m (18RAB102), including 33 m at 1.08% Cu from 11 m, and 13 m at 2.01% Cu from 11 m
  - 27 m at 0.67% Cu from 3 m (18RAB095)
  - 19 m at 0.78% Cu from 10 m (18RAB096)
  - 4 m at 1.5% Cu from 8 m (18RAB094).
- Significant intersections for the Gregjo Prospect include:
  - 7 m at 1.26% Cu from 5–12 m (18RAB013)
  - 20 m at 0.72% Cu from 1 m (18RAB020), including 1 m at 1.4% Cu and 3 m at 1.67% Cu
  - 11 m at 0.65% Cu from 16 m (18RAB031), including 1 m at 1.97% Cu
  - 3 m at 1.57% Cu from 13 m (18RAB051).
- Completed additional heli-borne aeromagnetic and radiometric survey covering eastern half of project area.
- Completed induced polarisation surveys at Gregjo and Running Creek prospects.

Drilling

The objective of the 2018 drilling program was to continue the exploration program undertaken since listing on the ASX to outline areas with cobalt and copper potential, with a focus on the region surrounding the Stanton Cobalt Deposit. The Company completed 14 395.4 m of drilling during 2018, comprising 977 AC holes for 6431.9 m and 225 RAB holes for 7964.5 m (see **Table 1** for a summary of N27's 2018 drilling).

Table 1. Summary of 2018 drilling.

Location	AC drilling		RAB drilling	
	holes	metres	holes	metres
Regional	944	6074.9	95	3279.5
Gregjo	33	357	86	2737.5
Running Creek			44	1947.5
Total	**977**	**6431.9**	**225**	**7964.5**

The 2018 drilling program was completed using an AC/RAB system mounted on a 6WD Toyota to gain access to sites without the need to clear tracks (**Figure 3**). Initial drilling was shallow AC with 944 regional holes completed

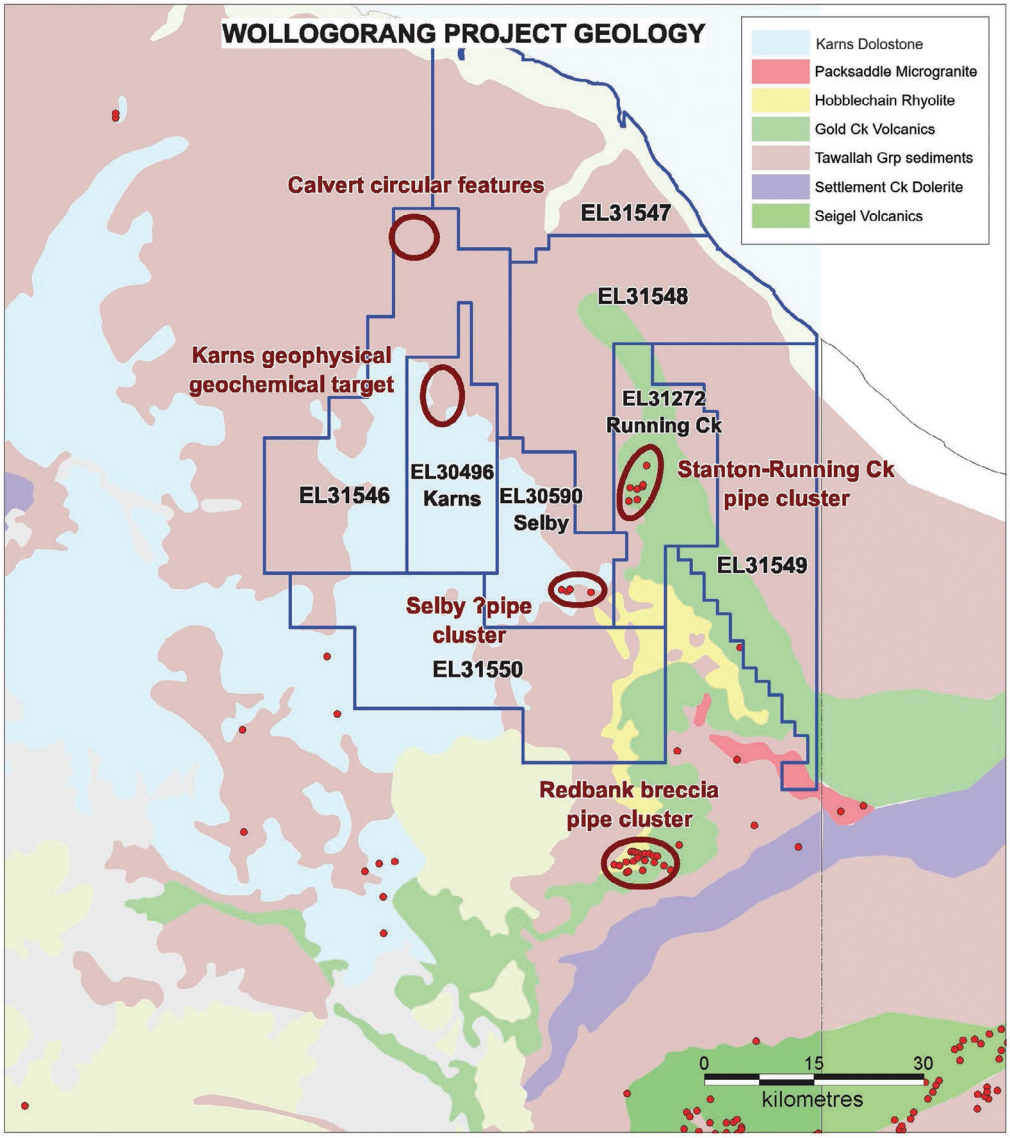

Figure 2. Regional geology of the Wollogorang Project area showing current and historical prospects, and known pipe clusters.

Figure 3. AC/RAB rig at Wollogorang Project.

over magnetic lows. A total of 75 magnetic targets were tested of which 21 returned cobalt assays >100 ppm (**Figure 4**). A review of historical surface sampling at the Stanton Cobalt Deposit showed that lag sampling reported an average cobalt content of 147 ppm Co at surface, hence holes reporting >100 ppm Co were targeted by follow-up deeper RAB drilling.

In late 2018, a further 95 regional RAB holes were completed over these 21 target areas for 3279.5 m (average depth 34.5 m). Samples are currently awaiting assaying by pXRF.

Gregjo Prospect

The Gregjo Prospect is located ~3.4 km south of the Stanton Cobalt Deposit. Initially, CRA discovered surficial copper mineralisation within a flat-lying siltstone (**Figure 5**).

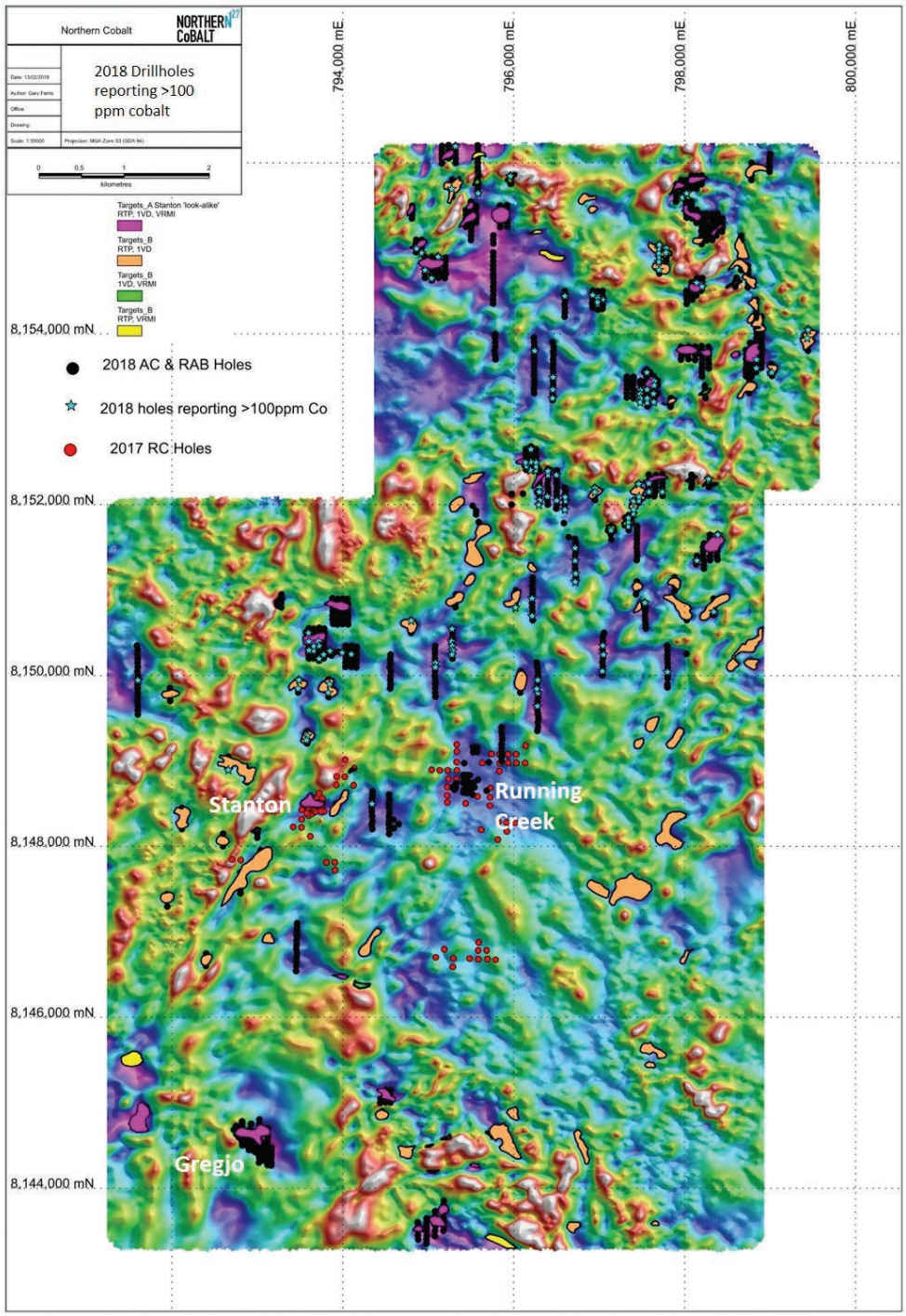

Figure 4. 2018 program drillholes reporting >100 ppm Co (background TMI–RTP image with N27 target areas).

CRA completed 6 RC holes totalling 146 m, with the best intersection reported being 12 m at 0.32% Cu from surface in hole PD92RC28 (Palmer 1993).

N27 completed 33 shallow AC holes, totalling 357 m (average depth 10.8 m). Best pXRF results include 12 m at 0.2% Cu from 0–12 m (18AC943), 7 m at 0.24% Cu from 1–8 m (18AC939), and 6 m at 0.28% Cu from 7–13 m (18AC944).

The Company drilled a further 86 RAB holes for 2737.5 m (average depth 31.8 m) to test for deeper mineralisation at Gregjo. Best laboratory results were:

- 7 m at 1.23% Cu from 1 m (18RAB103), including 1 m at 4.24% Cu
- 15 m at 0.53% Cu from 5 m (18RAB009), including 4 m at 1.08% Cu
- 20 m at 0.72% Cu from 1 m (18RAB020), including 1 m at 1.4% Cu and 3 m at 1.67% Cu
- 11 m at 0.65% Cu from 16 m (18RAB031), including 1 m at 1.97% Cu
- 3 m at 1.57% Cu from 13 m (18RAB051), including 1 m at 0.78% Cu.

Copper mineralisation appears to be spatially associated with at least two structures within the Gregjo Fault. Higher grade copper occurs adjacent to and within the interpreted fault structures that are steeply dipping. Vertical RAB drilling has difficulty intersecting these zones but once the lateral extent of mineralisation is defined, deeper angled RC drillholes will be used to target high-grade mineralisation in conjunction with results from the recently completed IP survey.

Lower grade mineralisation extends laterally from the fault structures within shallow dipping, pyritic sandstone and siltstones (**Figure 6**). This style of mineralisation has many similarities with Aeon Metals' Walford Creek Cu-Co deposit, ~90 km to the southeast.

Figure 5. Surface copper mineralisation at Gregjo Prospect.

Running Creek Prospect

The Running Creek Prospect is located ~1.8 km east–northeast of the Stanton Deposit. Copper mineralisation was discovered at Running Creek in the 1950s with reports of malachite and azurite ore (~30–40 tonnes) mined by hand from a 10 m deep shaft and a small 3 m-deep pit (Randell 2012).

Exploration by CRA in the 1990s as part of the Running Creek joint venture included various airborne and ground geophysical surveys, detailed lag sampling and geological mapping and drilling. The best drillhole intersections reported from Running Creek were:

- 13.4 m at 1.2% Cu from 32.1 m in hole DD94RC63 (Palmer *et al* 1995)
- 29 m at 0.74% Cu from 0 m in hole PD95RC236, including 7 m at 1.77% Cu from 22–29 m
- 23 m at 1.66% Cu from 10 m in hole PD95RC247, including 6 m at 3.92% Cu from 14–20 m; and 3 m at 2.22% Cu from 26–29 m (Menzies *et al* 1996).

Minor cobalt was reported from 2 drillholes including 1 m at 0.12% Co from 18–19 m (PD94RC41) and 5 m at 0.11% Co from 70–75 m (PD94RC83, Palmer *et al* 1995).

N27 completed 44 RAB holes at Running Creek (**Figure 7**) for 1947.5 m (average depth 44.2 m) with the best copper intersections reported including:

- 55 m at 0.78% Cu from 0 m (18RAB102), including 33 m at 1.08% Cu from 11 m, and 13 m at 2.01% Cu from 11 m
- 27 m at 0.67% Cu from 3 m (18RAB095)
- 19 m at 0.78% Cu from 10 m (18RAB096)
- 4 m at 1.5% Cu from 8 m (18RAB094)

The Running Creek prospect also contains anomalous cobalt with the best intersections reported including 6 m at 0.11% Co from 29–35 m (18RAB100) and 5 m at 0.16% Co from 20–25 m (18RAB123). Drillhole 18RAB102, with 55 m of copper mineralisation from surface, also showed anomalous cobalt with 22 m at 380 ppm Co from 22 m; this hole ended in mineralisation with the last metre assaying 450 ppm Co and 0.37% Cu.

Mineralisation at the Running Creek Prospect appears to be associated with northeast-trending structures. The prospect area was originally identified by CRA in the 1990s as a group of small, individual copper and cobalt mineralised systems with limited extent. Reinterpretation by Northern Cobalt of the main controls of mineralisation along northeast-trending structures has linked the individual mineral systems and led to the significant copper intersection in drillhole 18RAB102 as well as cobalt intersections throughout the project area (**Figure 8**).

Magnetic Survey

Based on the success of the 2017 helicopter airborne magnetic and radiometric survey over the Stanton Cobalt Deposit and surrounding prospects, N27 completed a high resolution aeromagnetic and radiometric survey over the

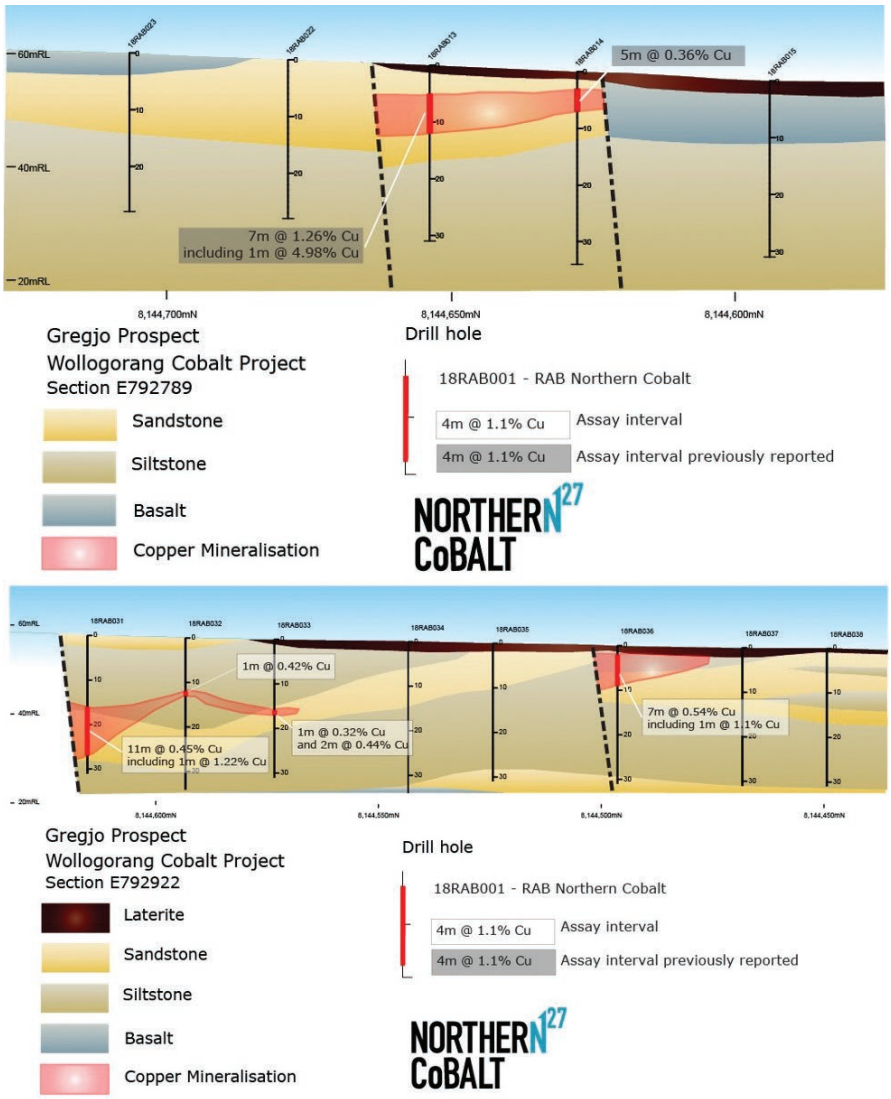

Figure 6. Cross sections at Gregjo Prospect. Profile lines are shown on **Figure 10**.

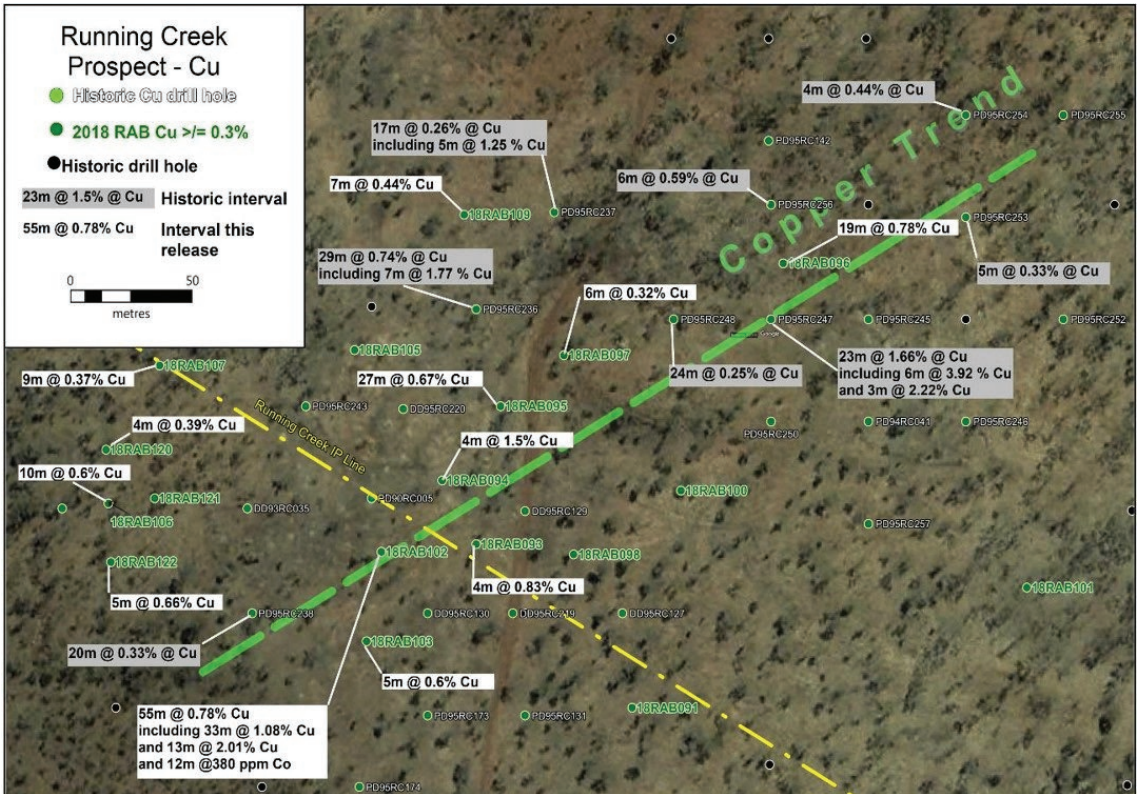

Figure 7. Google Earth image showing drillhole results from Running Creek Prospect, highlighting interpreted copper trend.

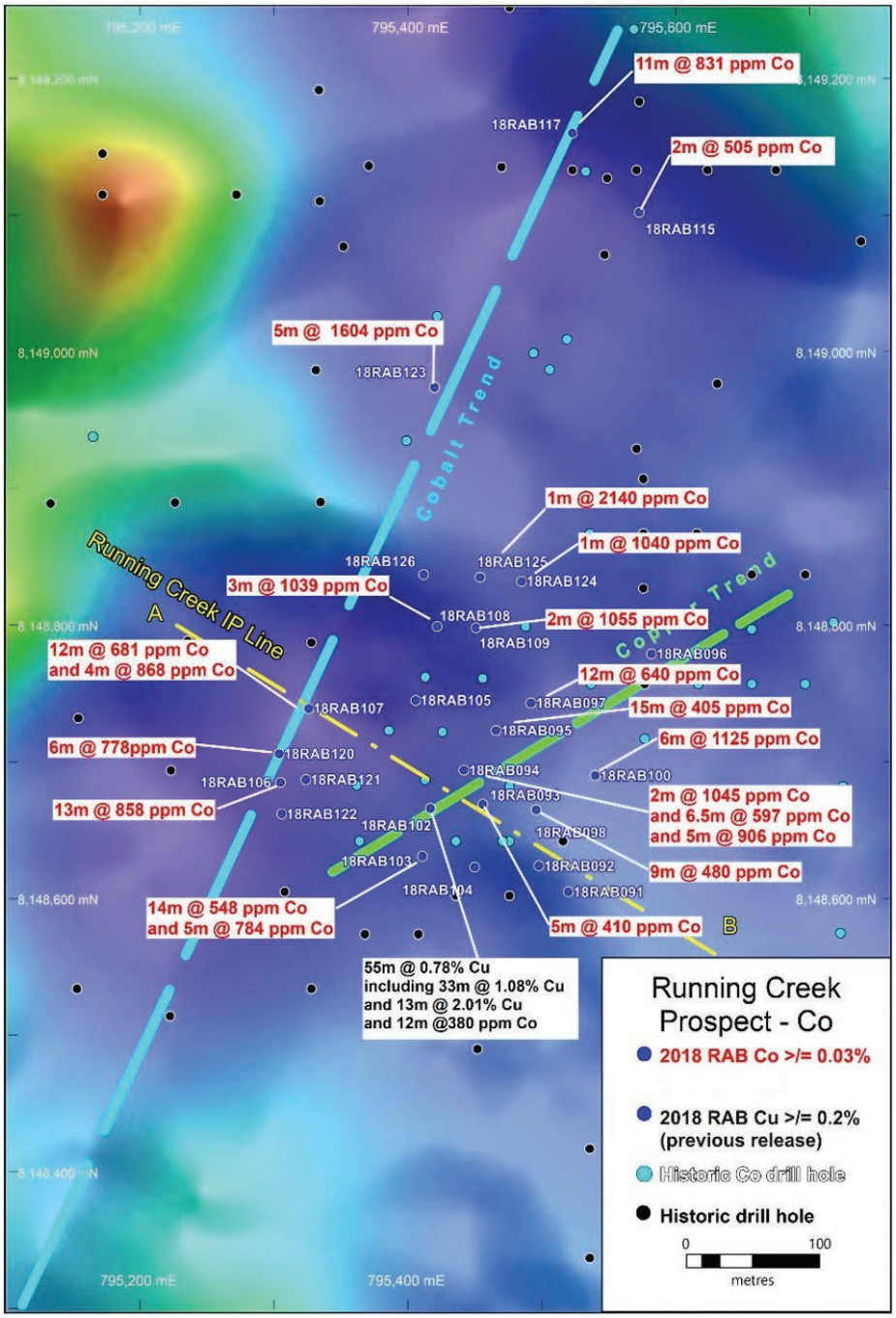

Figure 8. TMI–RTP image showing significant cobalt results from Running Creek Prospect.

Wollogorang Project at a flight line spacing of 75 m. The new 2018 survey (Area 2) covers ~1720 km^2 and expands the 2017 heli-borne survey by almost twenty-fold (**Figure 9**). This newly acquired data was partly co-funded by a grant of $100 000 awarded by the NT government and will be used to assist in further exploration in 2019.

Induced Polarisation (IP) Survey

N27 completed Dipole-Dipole IP surveys at the Gregjo and Running Creek prospects, which returned highly encouraging results in both areas. Mineralisation at the Gregjo Prospect is associated with a northwest-trending structure (**Figure 10**). The Gregjo Prospect was originally identified by CRA in the 1990s as a surface geochemical anomaly of limited extent with minor copper mineralisation. Reinterpretation of the main controls of mineralisation along northwest-trending structures and subsequent drill testing by N27 in 2018 has identified the copper source of the surface geochemical anomaly.

The results of the IP survey at Gregjo identified a large chargeable feature beneath the currently identified mineralisation (**Figure 11**). The Company interprets this feature to represent an extension of high-grade oxide copper mineralisation identified at surface to primary mineralisation at depth. **Figure 11** shows the anomaly in sections 1, 2 and 4, it but appears to be missing from section 3, possibly due to unfavourable host rocks at this location or being offset by a cross cutting fault. The distance between sections 1 and 4 exceeds 800 m of strike.

Results from the IP survey at Running Creek Prospect has also identified a large chargeable feature beneath the currently identified mineralisation (**Figure 12**). N27 interprets this feature similarly to that at Gregjo as

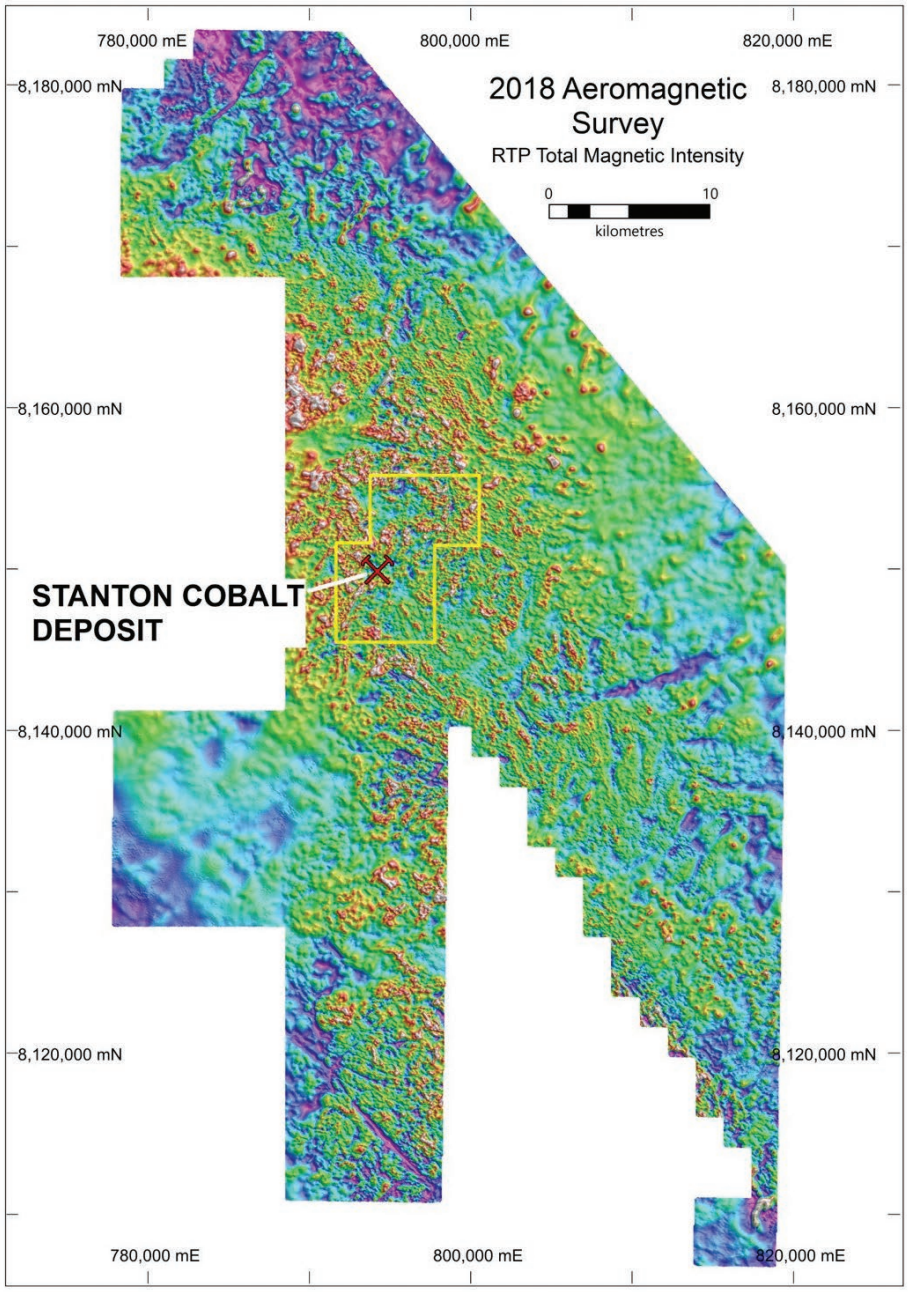

Figure 9. Newly acquired heli-mag data over Wollogorang Project area. Yellow box shows area of 2017 heli-mag survey.

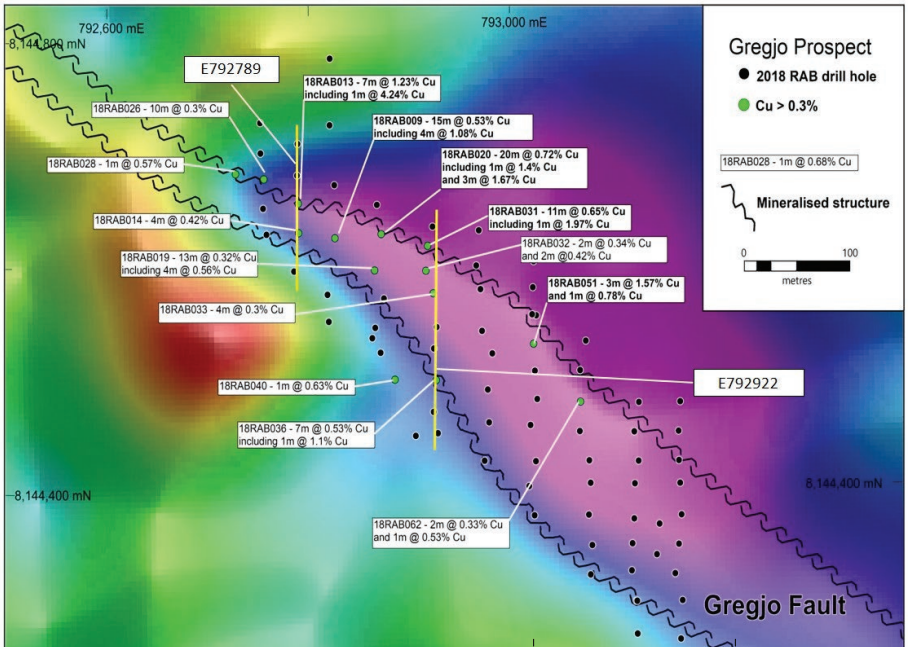

Figure 10. TMI–RTP image of Gregjo Prospect highlighting significant structure. Cross-sections related to northwest-trending section lines (yellow) are shown in **Figure 6**.

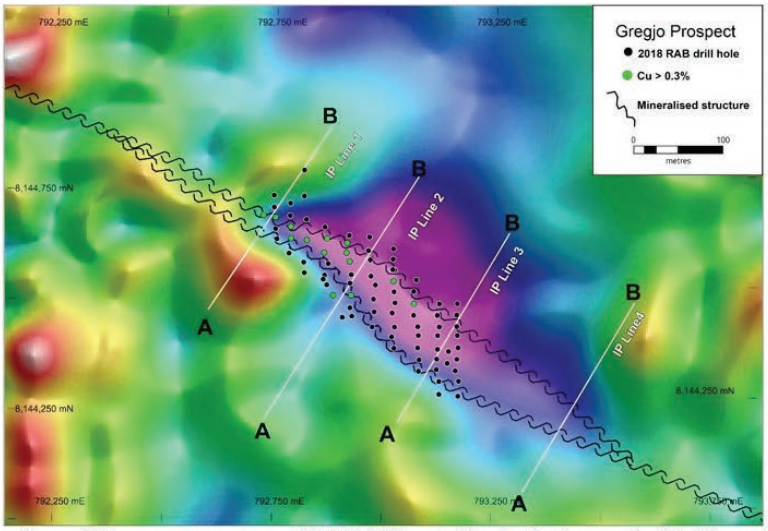

Plan of IP survey traverses and RAB drilling at Gregjo (background – TMI image)

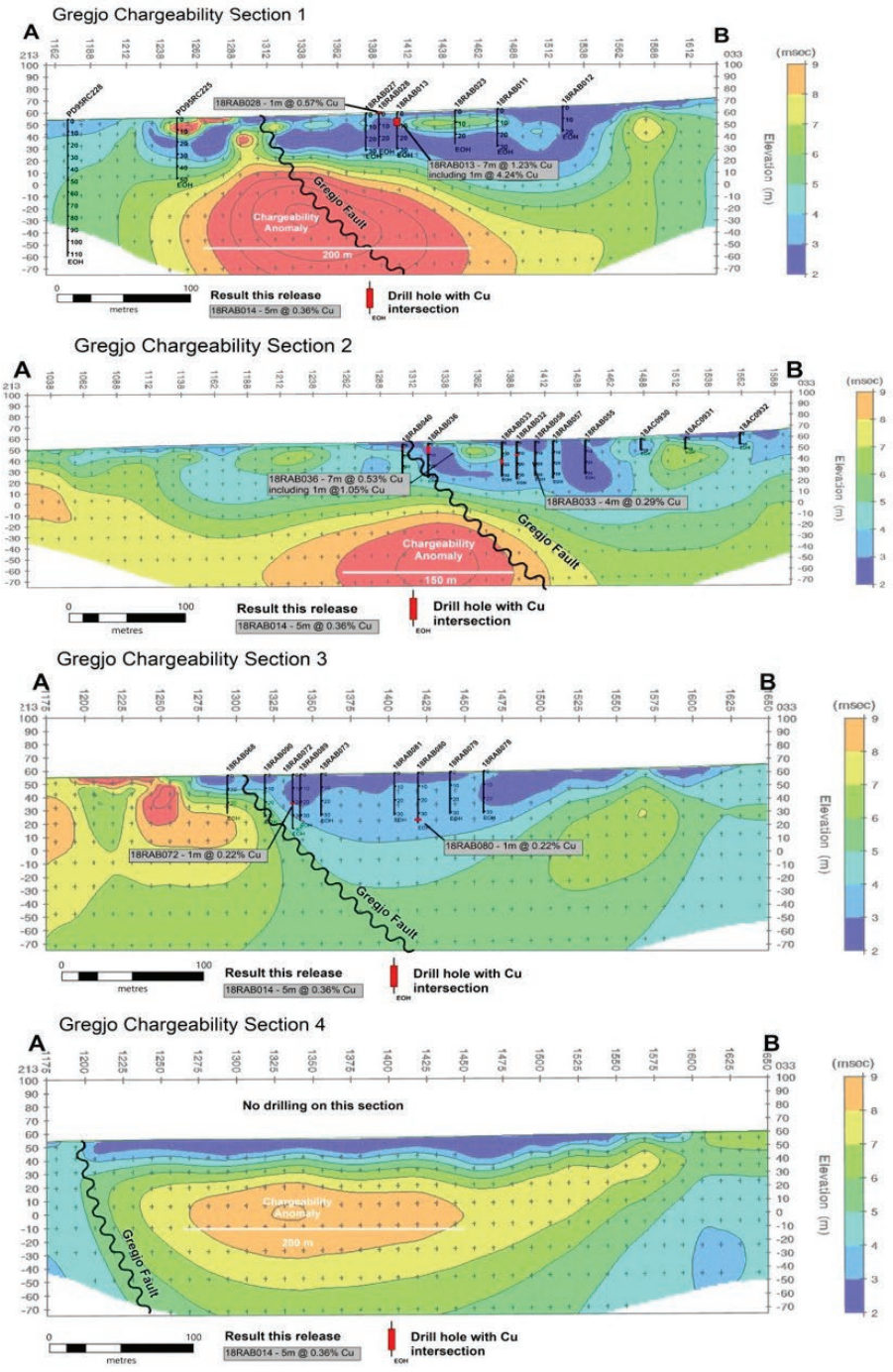

Figure 11. Induced polarisation chargeability plan view and sections 1–4 at Gregjo Prospect.

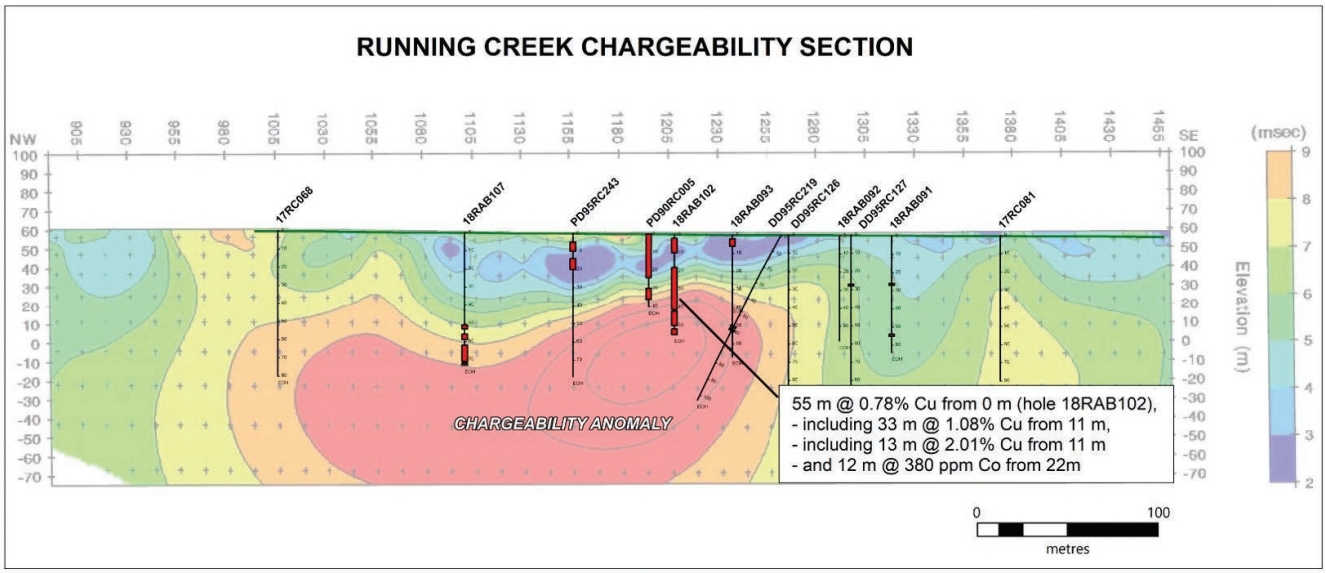

Figure 12. Induced polarisation chargeability section at Running Creek Prospect (see **Figure 8** for line location).

representing an extension of high-grade copper-cobalt mineralisation at depth; this feature will be tested by further drilling in 2019.

Exploration Program for 2019

Following the successful exploration results for 2018, the Company is planning drilling programs at the Running Creek and Gregjo prospects to follow-up on drilling results and targets outlined by the IP surveys. The Company is awaiting pXRF results for samples from the RAB drilling to the northeast of Stanton and Running Creek; this data will be integrated with available geochemical and geophysical data to assist in future exploration in this region. The Company will continue to assess the newly acquired magnetic and radiometric data by incorporating data from the 2018 drilling programs.

References

Goulevitch J, 2002. *Final Report EL8413 'Running Creek', Darwin*. Exploremin Pty Ltd. Geological Consultants.

Menzies DC, McCoy AD and Louwrens DJ, 1996. Running Creek farm-in and joint venture, EL 8413 Running Creek No.3, NT. Second annual report for year ending 28 December 1995. CRA Exploration Pty Ltd and WJ and EE Fisher Pty Ltd. *Northern Territory Geological Survey, Open File Company Report* CR1996-0066.

Palmer DC, 1993. Running Creek farm-in and joint venture, EL 5468 Running Creek, NT. Fifth annual report for year ending 12 August 1992. CRA Exploration Pty Ltd and WJ and EE Fisher Pty Ltd. *Northern Territory Geological Survey, Open File Company Report* CR1993-0136.

Palmer DC, Louwrens DJ and Menzies DC, 1995. Running Creek farm-in and joint venture, Mineral Claims 2688–91, 4561–67, 4604–06 and 4608–14 (NT). Final report for period ending 14th December 1994. CRA Exploration Pty Ltd and WJ and EE Fisher Pty Ltd. *Northern Territory Geological Survey, Open File Company Report* CR1995-0281.

Randell J, 2012. *Independent Geological Report. Stanton Nickel-Cobalt Deposit, for Auminco Coal Pty Ltd. Job No. 2463-03.* Geos Mining Mineral Consultants.

Rawlings DJ, 2006. *Robinson River, Northern Territory. 1:250 000 geological map series explanatory notes, SE 53-04*. Northern Territory Geological Survey, Darwin.

ASX Announcements used in this abstract

- 9 April 2018: Stanton resource upgrade increases contained cobalt
- 30 May 2018: Regional cobalt targets identified on Wollogorang Project
- 28 August 2018: Copper discovered at first drill target
- 19 September 2018: Copper discovery grows at Gregjo Prospect
- 9 October 2018: Copper intersection confirms new model at Running Creek
- 19 October 2018: Cobalt system developing at Running Creek
- 14 December 2018: Cobalt and copper system confirmed at Running Creek
- 22 January 2019: Geophysics highlight potential at Gregjo
- 25 January 2019: Quarterly Activities and Cashflow Report 31 December 2018

From source to trap. Geophysical insights into base metals mineralisation in the southern McArthur Basin

Teagan N Blaikie[1,2,3] *and Marcus Kunzmann*[1,3]

Introduction

The ca 1815–1450 Ma southern McArthur Basin contains sedimentary sequences from four vertically stacked and unconformity-bound superbasins (**Figure 1**; Rawlings 1999, Jackson *et al* 2000, Ahmad *et al* 2013). These superbasins evolved in response to far-field plate boundary processes, which influenced periods of extension and crustal shortening across the basin. Extension and shortening events varied in their orientation and intensity, and resulted in the development of a complex fault and depositional architecture.

This abstract discusses results from the interpretation and modelling of new and historical geophysical data from across the southern McArthur Basin. We summarise the tectonic evolution of the basin, which was derived from integration of our geophysical and structural interpretation into the geodynamic framework of the North Australian Craton. We also discuss implications of new geophysical modelling results for understanding Zn-Pb-Ag mineralisation within the basin, with a focus on metals source regions, fault and sub-basin architecture, and tectonic triggers for fluid migration.

[1] CSIRO Mineral Resources, Australian Resources Research Centre, Kensington WA 6151, Australia
[2] Email: Teagan.Blaikie@csiro.au
[3] Northern Territory Geological Survey, GPO Box 4550, Darwin NT 0801, Australia

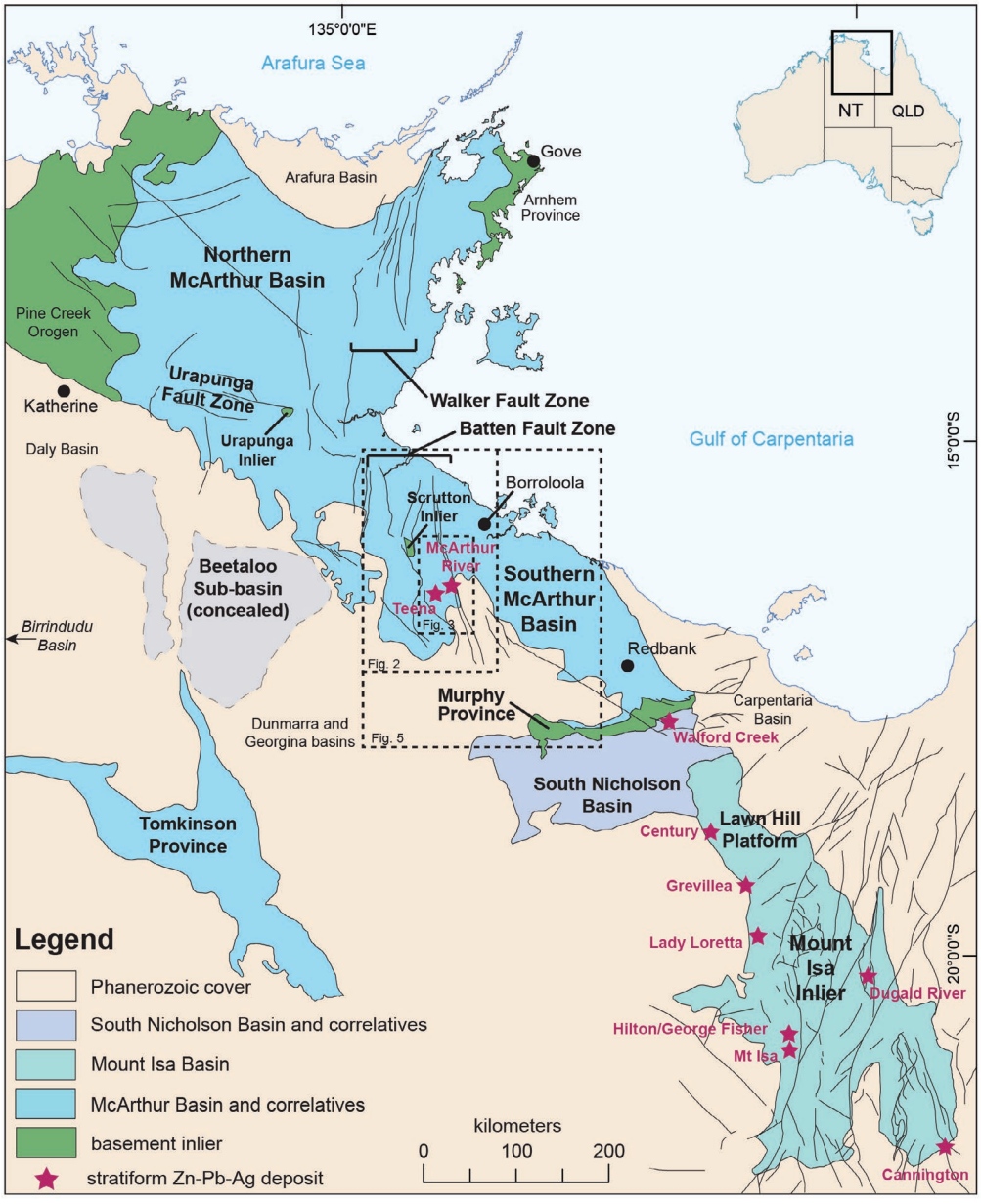

Figure 1. Regional geological map of McArthur and Mount Isa Basins showing location of major stratiform Zn-Pb-Ag deposits (after Ahmad *et al* 2013).

Regional scale geophysical modelling

Recent acquisition and modelling of gravity data across the Batten Fault Zone and southern McArthur Basin has provided new insight into the 3D architecture of the region. Both solid geology and structural interpretations of Proterozoic stratigraphy were completed, with most regions mapped down to formation scale (eg Blaikie and Kunzmann 2018). This allowed the lateral extent of major lithological units to be defined, as well as constrained 2D forward models of the Batten Fault Zone. Interpretations were also integrated with the detailed sedimentological evaluation and sequence stratigraphic framework developed by Kunzmann *et al* (2019) for the middle McArthur Group. This allowed observations of different depositional cycles, and shifting of depocentres to be placed in context of the structural framework.

Seven cross-sections were forward modelled and define the current 3D architecture of the region, including the nature of major basin controlling structures. The cross-sections were located along 500 m spaced gravity profiles, which were acquired along six east–west and one north–south traverse during the Batten Fault Zone gravity survey conducted in late 2017 (CSIRO 2018). **Figure 2** shows a 3D rendering of all cross-sections. The sections highlight the architecture of the fault zone, including regional scale folding, nature of major faults, and variations in the preserved thickness of stratigraphy.

Of significance for Zn-Pb-Ag mineralisation, forward modelling suggests that an anomalously thick sequence of mafic volcanics are preserved within the Tawallah Group in several regions of the Batten Fault Zone. The largest of these volcanic units has a strong spatial association to known mineralisation, including the McArthur River and Teena deposits. The volcanic unit is interpreted to be a thick accumulation of either or both of the Settlement Creek Dolerite and Gold Creek Volcanics. These units have experienced extensive potassic metasomatism and base metals depletion (eg Pietsch *et al* 1991, Haines *et al* 1993, Rawlings *et al* 1993); they have previously been interpreted as the source of base metals in the region (Cooke *et al* 1998, Huston *et al* 2006). Geophysical modelling has also identified regions of granitic basement within the Batten Fault Zone. Granitic clasts are recognised within several siliciclastic units of the Tawallah Group. These granites may represent a secondary source of metals, which were leached directly from the basement, or from clasts preserved within the Tawallah Group.

Recognition of anomalously-thick mafic volcanics within the Tawallah Group and felsic volcanics within the basement provides significant evidence of crustal pre-conditioning for base metals mineralisation; this implies that the source of base metals was located relatively close to major deposits discovered in the region. Modelling also recognises a number of aquifer and basement tapping faults, which would have provided a pathway for metal rich fluids to ascend.

Modelling sub-basin architecture

The McArthur Group was deposited during intermittent periods of extension and minor crustal shortening, which formed a complex array of sub-basins and palaeohighs. Forward models of the Batten Fault Zone were constructed at a regional scale, and although they model major sub-basin bounding faults, they do not focus on sub-basin architecture (less than 5 km scale). Integration of high-resolution geophysical data with the sequence stratigraphic framework developed by Kunzmann *et al* (2019) allowed more detailed geophysical models of sub-basin architecture to be constructed (eg Blaikie *et al* 2018, Blaikie and Kunzmann 2018).

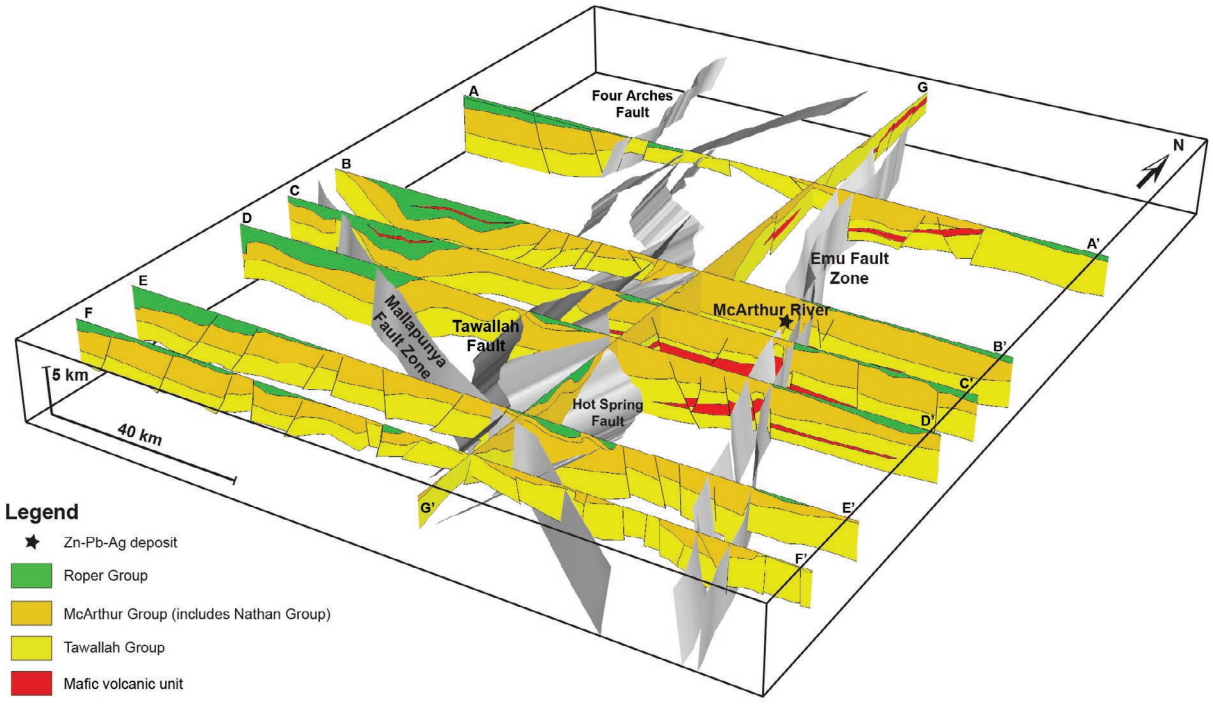

Figure 2. 3D rendering of forward modelled geological sections with surfaces for major faults overlain.

Two styles of sub-basins in the Batten Fault Zone are recognised from the interpretation of geophysical data (**Figure 3**; note: Barney Creek Formation may not be preserved in all sub-basins). North–south trending transtensional sub-basins developed between segments of the north–northwest-trending Emu Fault Zone (eg Glyde sub-basin. **Figure 3**; Type 1); and approximately east–west-trending sub-basins developed adjacent to east–west-trending normal and north–northwest-trending transfer faults located between the Hot Spring Fault and Emu Fault Zone (eg Teena sub-basin. **Figure 3**; Type 2).

These sub-basins are too small for detailed modelling on the regional scale cross-sections; however, many have high-resolution geophysical data acquired over them plus a number of drillholes to constrain interpretations. **Figure 4** shows the 3D architecture of the Glyde sub-basin, determined from forward modelling of gravity and magnetics, and interpretation of AEM data. Interpretation and modelling show thickening of the Barney Creek Formation between the Emu Fault Zone and Cowdreys Fault, with the greatest thickening of the formation occurring adjacent the Emu Fault Zone (**Figure 4**).

Tectonic evolution of the southern McArthur Basin

The structural and solid geological interpretation, and forward modelling of the potential field data, highlight the nature and overprinting relationships of major fault systems, regional scale folding and variations in the preserved thickness of stratigraphy within the Batten Fault Zone. This has allowed a synthesis of the basins depositional and structural evolution to be developed.

The Tawallah Group (ca 1710–1790 Ma) was deposited during at least two extensional events, separated by a mild period of inversion (**Figure 5a–c**). These events were driven by subduction roll-back and collisions along the southern and eastern margins of the North Australian Craton (Betts and Giles 2006). North–south-directed extension at

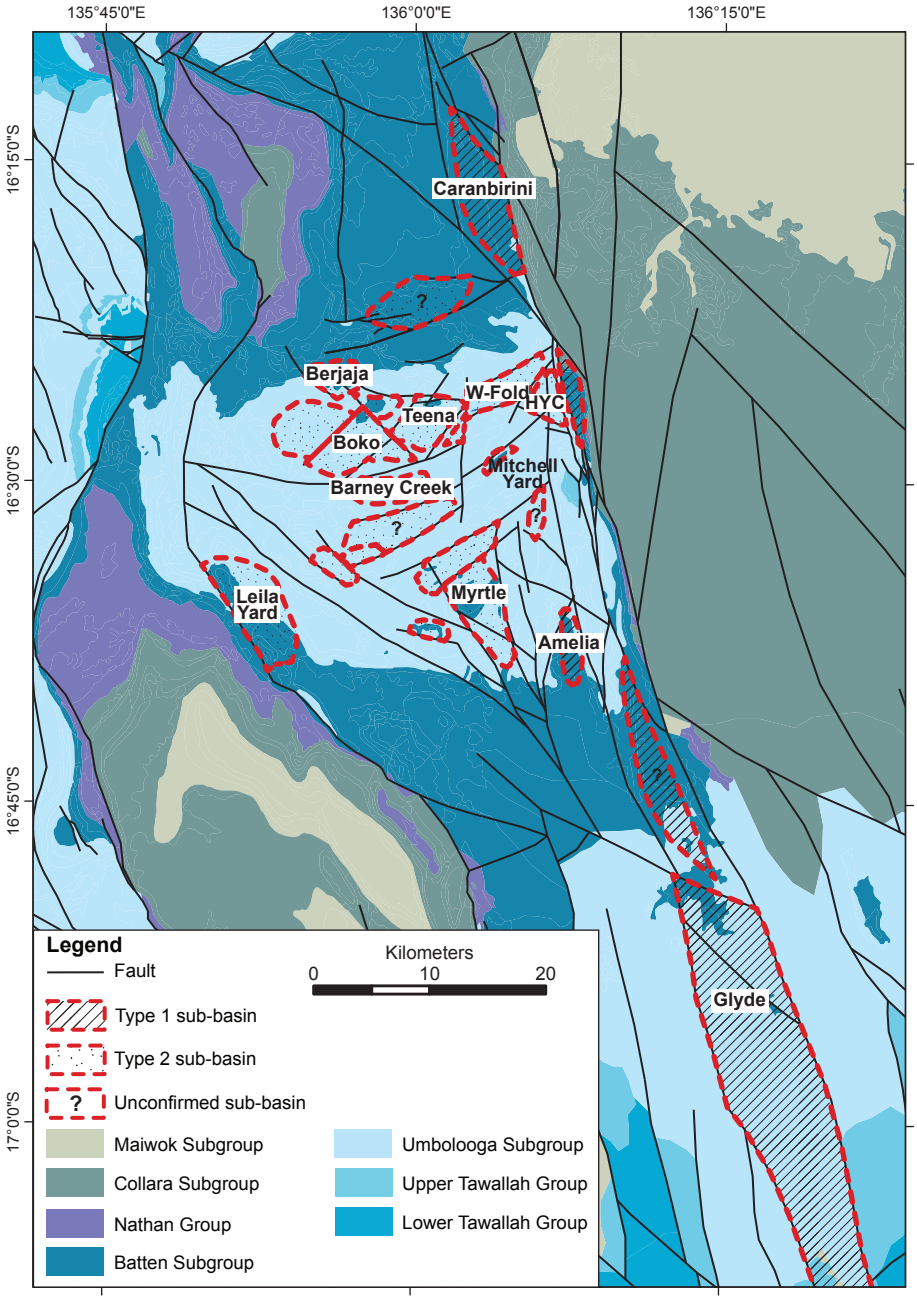

Figure 3. Map of geophysically defined, and previously interpreted (eg McGoldrick *et al* 2010) sub-basins in the central Batten Fault Zone.

ca 1760–1740 Ma caused the reactivation and development of northwest normal and northeast to north–northeast strike-slip faults (**Figure 5a**). A minor, east–west-directed inversion event is recognised at ca 1740 Ma (**Figure 5b**; Bull and Rogers 1996), which caused reverse movement along north–northeast faults. Northwest–southeast extension between ca 1730–1690 Ma caused development of north–northeast to northeast normal faults and strike-slip movement along northwest faults (**Figure 5c**).

Deposition of the ca 1670–1600 Ma McArthur Group and the ca 1600–1575 Ma Nathan Group occurred predominantly within a sag basin, which experienced short-lived periods of extension and inversion in response to deformation occurring at the margin of the North Australian Craton. A broadly north–south-directed period of extension occurred during deposition of the middle McArthur Group (ie during Barney Creek Formation; **Figure 5d**). This event compartmentalised the basin, causing significant deepening of sub-basins in some areas, and uplift and erosion in others (McGoldrick *et al* 2010 ,Kunzmann *et al* 2019). We speculate that a minor compressional event at ca 1640 Ma caused syn-depositional uplift along extensional faults resulting in an influx of breccias into previously developed sub-basins. The timing of this event is coincident with the Riversleigh Event on the Lawn Hill Platform (eg Bradshaw *et al* 2000), which has been correlated to the accretion of the Warumpi province (eg Hollis *et al* 2013; Scrimgeour *et al* 2005) on the southern margin of the craton at ca 1640 Ma (Betts and Armit 2011; Gibson *et al* 2017). Alternatively, if collision of the Warumpi province occurred at ca 1130 Ma as proposed by Wong *et al* 2015, then the ca 1640 Ma deformation recognised in the north Australian basins may be related to intraplate instability associated with broader scale plate reorganisation, which triggered a reversal in plate motion (eg Idnurm 2000).

The Isan Orogeny, driven by orogenesis at the margins of the North Australian Craton, caused significant uplift and erosion across the southern McArthur Basin. Initially, sedimentation of the upper McArthur and Nathan groups continued during the onset of the earliest phase of the orogeny. Sedimentation had ceased by ca 1570 Ma, with minor east–west folding and reverse faulting along extensional basin faults occurring during the late first stage of the orogeny (**Figure 5e**). The late Isan Orogeny caused reverse movement along north–northwest to north–northeast faults, which resulted in significant uplift and erosion, particularly in the north of the Batten Fault Zone (**Figure 5f**).

During the Mesoproterozoic, renewed basin development caused the widespread deposition of the Roper Group across the region (**Figure 5g**). Following this period of deposition, northeast–southwest-directed crustal shortening caused thrust faulting and folding in the Batten Fault Zone (**Figure 5h**; Rogers 1996, Keele and Wright 1998, Rawlings *et al* 2004). Timing of this event is not well constrained but is thought to be after the ca 1313 Ma (Collins *et al* 2018) emplacement of the Derim Derim Dolerite dykes and sills.

Tectonic triggers of fluid migration

Zn-Pb-Ag mineralisation within the McArthur Basin occurred when fluids from aquifers at depth (ie Tawallah Group; Polito *et al* 2006) flowed upward into a suitable trap at or near the surface. Although extensional conditions are favourable for formation of suitable metal traps, such as restricted sub-basins in the case of the McArthur Basin, they are not conducive to mineralisation because fluids will largely tend to migrate downward (Sheldon and Schaubs 2018). However, compressional stresses associated with a short-lived, ca 1640 Ma compressional event provide a

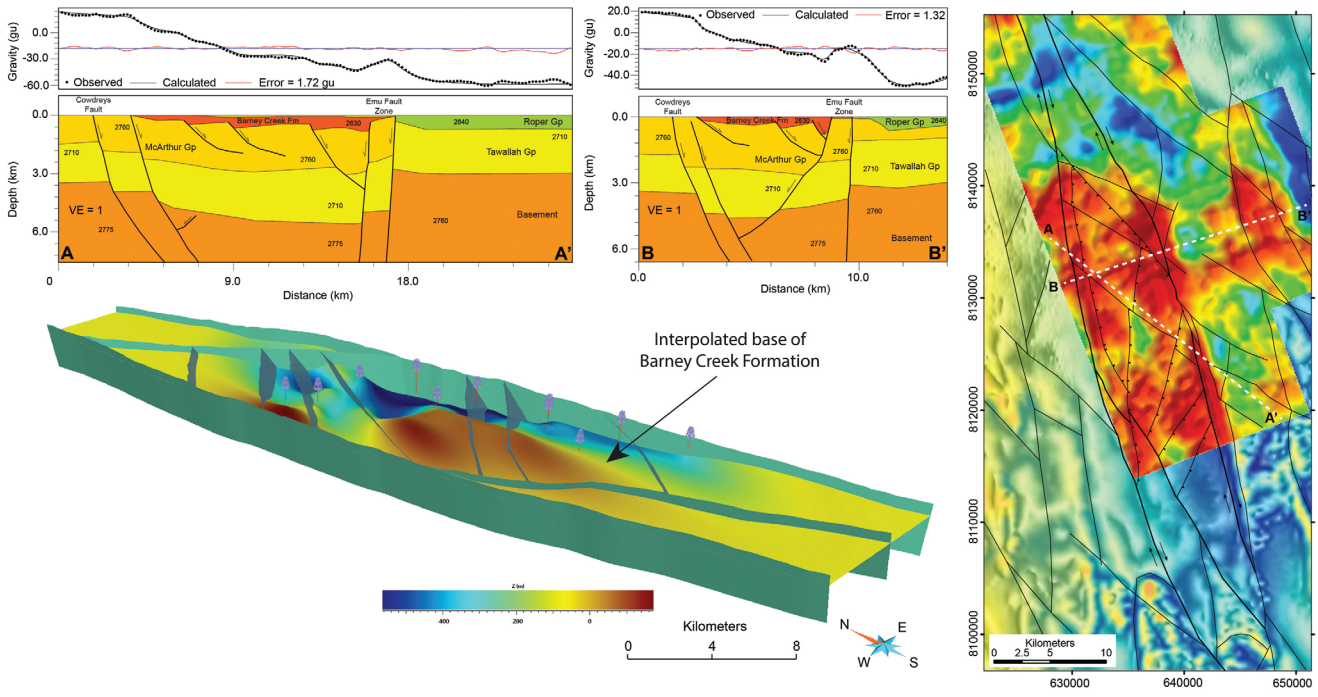

Figure 4. Architecture of the Glyde sub-basin determined from geophysical interpretation and modelling. (**a-b**) Forward modelled cross-sections of the Glyde sub-basin. **c**) Falcon gravity data (acquired by Armour Energy 2013) overlain with interpreted faults. (**d**) 3D model of the Glyde sub-basin showing location of wells, major faults and an interpolated surface for the base of the Barney Creek Formation.

mechanism to drive metal rich fluids upward and into the host stratigraphy.

Syn-depositional deformation associated with crustal shortening was first documented by Hinman (1995) at McArthur River where inversion of extensional structures and an influx of mass-flow breccias into the HYC sub-basin was interpreted. Folding and reverse faulting was recognised largely in close proximity to the Emu Fault Zone, but is also observed in other regions of the Batten Fault Zone (Hinman 1995, Rogers 1996). The onlap of strata of the upper Barney Creek Formation onto stratigraphy that was reversely faulted and incised during inversion indicates that sedimentation of the Barney Creek Formation continued during the onset of deformation (Hinman 1995). Recent evidence for a diagenetic

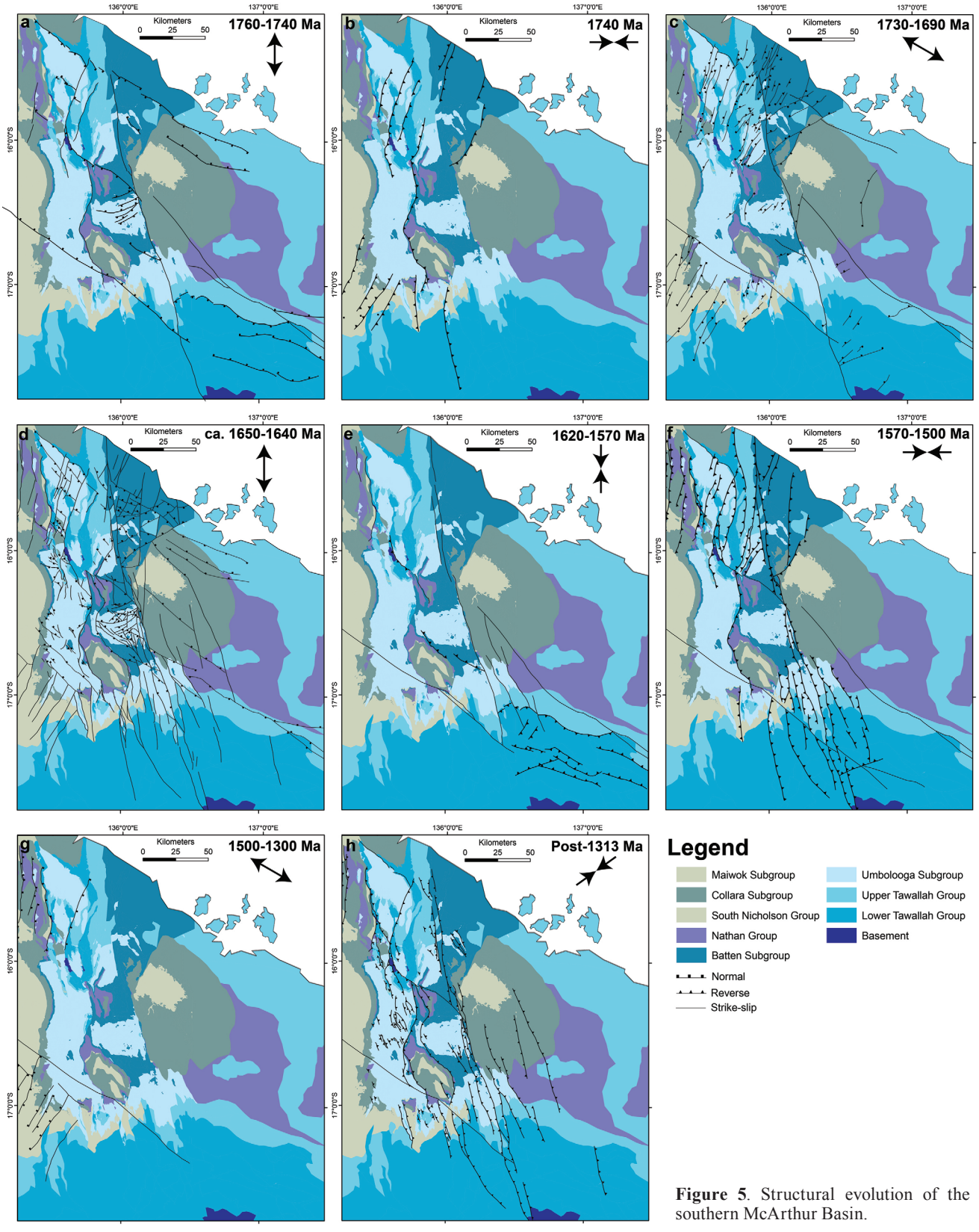

Figure 5. Structural evolution of the southern McArthur Basin.

origin of Zn-Pb-Ag mineralisation at McArthur River (Spinks *et al* 2018), which stratigraphically occurs in the lowermost Barney Creek Formation, suggests that mineralisation may have occurred tens to hundreds of meters below the sea floor. This means that fluid flow and mineralisation may have occurred at about the time the upper Barney Creek Formation was deposited (Kunzmann *et al* 2019), ie the proposed time of the onset of deformation at ca 1640 Ma.

Conclusions

Geophysical interpretation and modelling results from this study have important implications for understanding Zn-Pb-Ag mineralisation within the region. Modelling has recognised potential source rocks for metals in the form of anomalously thick sequences of mafic volcanics within the Tawallah Group. Modelling also identified potential fluid pathways in the form of sub-basin bounding faults that tap the basement and aquifers within the Tawallah Group.

A new synthesis for the structural and tectonic evolution of the southern McArthur Basin was developed from the integration of modelling results into the geodynamic framework of northern Australia. Results of this work led to a correlation between a short-lived compressional event occurring towards the end of deposition of the Barney Creek Formation and inversion on the Lawn Hill Platform. This event is thought to be driven either by deformation related to the accretion of the Warumpi province at ca 1640 Ma, or by broader scale tectonic instability due to a reversal in plate motion. This event may have provided the mechanism for pumping metal-bearing fluids up faults and leading to mineralisation within the basin.

References

Ahmad M, Dunster JN and Munson TJ, 2013. Chapter 15: McArthur Basin: in Ahmad M and Munson TJ (compilers). '*Geology and mineral resources of the Northern Territory'. Northern Territory Geological Survey, Special Publication* 5.

Armour Energy, 2013. 2012 Glyde Sub-Basin Airborne Gravity Gradiometer and Magnetometer Survey - Acquisition and Processing Report. *Northern Territory Geological Survey, Open File Petroleum Report* PR2013-0005.

Betts PG and Armit RJ, 2011. *Proterozoic Mount Isa Synthesis Section II: Eastern Australian Proterozoic Correlations, Appendix 2: NWQMEP Report*. Queensland Geological Survey.

Betts PG and Giles D, 2006. The 1800–1100 Ma tectonic evolution of Australia. *Precambrian Research* 144, 92–125.

Blaikie T, Soerensen C, Munday T, Schaubs P, Spinks S, Schmid S and Kunzmann M, 2018. Characterising the subsurface architecture and stratigraphy of the McArthur Group through integrated airborne EM and gravity inversion. *ASEG Extended Abstracts* 2018(1), 1–6.

Blaikie TN and Kunzmann M, 2018. Understanding the architecture of the Batten Fault Zone from the regional to sub-basin scale. Insights from geophysical interpretation and modelling: in *'Annual Geoscience Exploration Seminar (AGES) Proceedings, Alice Springs, Northern Territory, 20–21 March 2018'*. Northern Territory Geological Survey, Darwin.

Bradshaw BE, Lindsay JF, Krassay AA and Wells AT, 2000. Attenuated basin-margin sequence stratigraphy of the Palaeoproterozoic Calvert and Isa Superbasins: The Fickling Group, southern Murphy Inlier, Queensland. *Australian Journal of Earth Sciences* 47, 599–623.

Bull SW and Rogers JR, 1996. Recognition and significance of an early compressional deformation event in the Tawallah Group, McArthur Basin, NT. *Contributions of the Economic Geology Research Unit 55*, 28–32.

Collins A, Farkas J, Glorie S, Cox G, Blades ML, Yang B, Nixon A, Bullen M, Foden JD, Dosseto A, Payne JL, Denyszyn S, Edgoose CJ, Close D, Munson TJ, Menpes S, Spagnuolo S, Gusterhuber J, Sheridan M, Baruch-Jurado E and Close DF, 2018. Orogens to oil: government–industry–academia collaboration to better understand the greater McArthur Basin: in *'Annual Geoscience Exploration Seminar (AGES) Proceedings, Alice Springs, Northern Territory, 20–21 March 2018'*. Northern Territory Geological Survey, Darwin.

Cooke DR, Bull SW, Donovan S and Rogers JR, 1998. K-metasomatism and base metal depletion in volcanic rocks from the McArthur basin, northern territory-implications for base metal mineralization. *Economic Geology* 93, 1237–1263.

CSIRO, 2018. *Batten Fault Zone: gravity survey*. Northern Territory Geological Survey, Darwin. https://geoscience.nt.gov.au/gemis/ntgsjspui/handle/1/86883.

Gibson GM, Hutton LJ and Holzschuh J, 2017. Basin inversion and supercontinent assembly as drivers of sediment-hosted Pb–Zn mineralization in the Mount Isa region, northern Australia. *Journal of the Geological Society* 174(4):773. https://doi.org/10.1144/jgs2016-105.

Haines PW, Pietsch BA, Rawlings DJ and Madigan TL, 1993. *Mount Young, Northern Territory. 1:250 000 geological map series explanatory notes, SD 53-15*. Northern Territory Geological Survey, Darwin.

Hinman M, 1995. *Structure and kinematics of the HYC-Cooley zone at McArthur River*. Australian Geological Survey Organisation, Canberra.

Hollis JA, Kirkland CL, Spaggiari CV, Tyler IM, Haines, PW, Wingate MTD, Belousova EA and Murphy R, 2013. Zircon U–Pb–Hf isotope evidence for links between the Warumpi and Aileron Provinces, west Arunta region. *Geological Survey of Western Australia*. *Record* 2013/9.

Huston DL, Stevens B, Southgate PN, Muhling P and Wyborn L, 2006. Australian Zn-Pb-Ag Ore-Forming Systems: A Review and Analysis. *Economic Geology* 101, 1117–1157.

Idnurm M, 2000. Towards a high resolution Late Palaeoproterozoic - earliest Mesoproterozoic apparent polar wander path for northern Australia. *Australian Journal of Earth Sciences* 47, 405–429.

Jackson MJ, Scott DL and Rawlings DJ, 2000. Stratigraphic framework for the Leichhardt and Calvert Superbasins:

Review and correlations of the pre-1700 Ma successions between Mt Isa and McArthur River. *Australian Journal of Earth Sciences* 47, 381–403.

Keele RA and Wright JV, 1998. Analysis of some fault striations in the Proterozoic southern McArthur Basin, Northern Territory, with reference to pre-and post-Roper Group stress fields. *Australian Journal of Earth Sciences* 45, 51–61.

Kunzmann M, Schmid S, Blaikie TN and Halverson GP, 2019. Facies analysis, sequence stratigraphy, and carbon isotope chemostratigraphy of a classic Zn-Pb host succession: The Proterozoic middle McArthur Group, McArthur Basin, Australia. *Ore Geology Reviews* 106, 150–175.

McGoldrick P, Winefield P, Bull S, Selley D and Scott R, 2010. Sequences, synsedimentary structures, and sub-basins: the where and when of SEDEX zinc systems in the southern McArthur Basin, Australia. *Society of Economic Geologists, Special Publication* 15, 1–23.

Pietsch BA, Rawlings DJ and Creaser PM, 1991. *Bauhinia Downs, Northern Territory, 1:250 000 geological map series explanatory notes, SE 53-3*. Northern Territory Geological Survey, Darwin.

Polito PA, Kyser TK and Jackson MJ, 2006. The role of sandstone diagenesis and aquifer evolution in the formation of uranium and zinc-lead deposits, Southern McArthur Basin, Northern Territory, Australia. *Economic Geology* 101, 1189–1209.

Rawlings DJ, 1999. Stratigraphic resolution of a multiphase intracratonic basin system; the McArthur Basin, northern Australia. *Australian Journal of Earth Sciences* 46, 703–723.

Rawlings DJ, Korsch RJ, Goleby BR, Gibson GM, Johnstone DW and Barlow M, 2004. The 2002 southern McArthur Basin seismic reflection survey. *Geoscience Australia, Record* 2004/17.

Rawlings DJ, Pietsch BA, Madigan TL and Haines PW, 1993. *Tawallah Range, Northern Territory : 1:100 000 geological map series explanatory notes, 6066*. Northern Territory Geological Survey, Darwin.

Rogers J, 1996. *Geology and tectonic setting of the Tawallah Group, southern McArthur Basin, Northern Territory*. CODES. University of Tasmania.

Scrimgeour IR, Kinny PD, Close DF and Edgoose CJ, 2005. High-T granulites and polymetamorphism in the southern Arunta Region, central Australia: Evidence for a 1.64 Ga accretional event. *Precambrian Research* 142, 1–27.

Sheldon HA and Schaubs PM, 2018. Investigating controls on mineralisation in the Batten Fault Zone using numerical models: in *'Annual Geoscience Exploration Seminar (AGES) Proceedings, Alice Springs, Northern Territory, 20–21 March 2018'*. Northern Territory Geological Survey, Darwin.

Spinks S, Pearce M, Ryan C, Kunzmann M and Fisher L, 2018. Finally mapping thallium: Evidence of a diagenetic origin for a classic sedimentary 'exhalative' Zn-Pb Deposit? Abstract 2345. *Resources for Future Generations 2018 (RFG 2018), 16–21 June 2018*. Vancouver, Canada.

Wong BL, Morrissey LJ, Hand M, Fields CE and Kelsey DE, 2015. Grenvillian-aged reworking of late Paleoproterozoic crust of the southern North Australian Craton, central Australia; implications for the assembly of Mesoproterozoic Australia. *Precambrian Research* 270, 100–123.

The ca 1640 Ma Barney Creek Formation in the McArthur Basin: Targeting diagenetic mineralisation and depocentre shift

Marcus Kunzmann[1,2,3] and Teagan N Blaikie[1,3]

Introduction

The ca 1640 Ma Barney Creek Formation is a dominantly fine-grained siliciclastic unit of the McArthur Group in the southern McArthur Basin (**Figures 1, 2**). It is of significant economic importance because it hosts the world-class McArthur River Zn-Pb-Ag deposit (eg Croxford 1975, Eldridge *et al* 1993, Large *et al* 1998, Ireland *et al* 2004a, b) and the Teena Zn-Pb prospect (Taylor *et al* 2017). In addition, it is one of the oldest active petroleum systems in the world and may be an important hydrocarbon source rock or unconventional reservoir (eg Jackson *et al* 1986, Summons *et al* 1988, Baruch *et al* 2015). The Barney Creek Formation is also an important archive of early life on Earth. Due to its generally low thermal maturity, it hosts the oldest unambiguous indigenous biomarkers in the world and represents a unique archive of mid-Proterozoic surface environments (eg Brocks *et al* 2005, Lee and Brocks 2011).

The Zn-Pb mineralisation in the Barney Creek Formation is typically stratiform and hosted by pyritic, organic matter-rich and dolomitic siltstones deposited in sub-basin depocentres. The timing of mineralisation is debated but generally considered to be syngenetic or diagenetic (eg Eldridge *et al* 1993, Large *et al* 1998). These characteristics highlight the need for detailed sedimentological, stratigraphic, and structural basin reconstructions for mineral exploration. Specific questions focus on the distribution and formation of sub-basins, on individual sub-basin reconstructions, and on understanding lateral and stratigraphic heterogeneity of the Barney Creek Formation. It is also important to develop sedimentological and stratigraphic models for targeting mineralisation that take into account the implications of syngenetic versus diagenetic mineralisation.

In this contribution, we extend our earlier work on the sedimentology and stratigraphy of the Barney Creek Formation from the southernmost Batten Fault Zone (**Figure 1**; Kunzmann *et al* 2018, 2019) to the entire Batten Fault Zone. We show that a significant shift in the depocentre occurred across the Batten Fault Zone from south to north at the Barney Creek–Reward transition (**Figure 2**). Considering new evidence for the timing of mineralisation (Taylor *et al* 2017, Spinks *et al* 2019), we propose to target mineralised strata by using a combination of sequence stratigraphy and facies maps.

[1] CSIRO Mineral Resources, 26 Dick Perry Avenue, Kensington WA 6151, Australia
[2] Email: marcus.kunzmann@csiro.au
[3] Northern Territory Geological Survey, GPO Box 4550, Darwin NT 0801, Australia

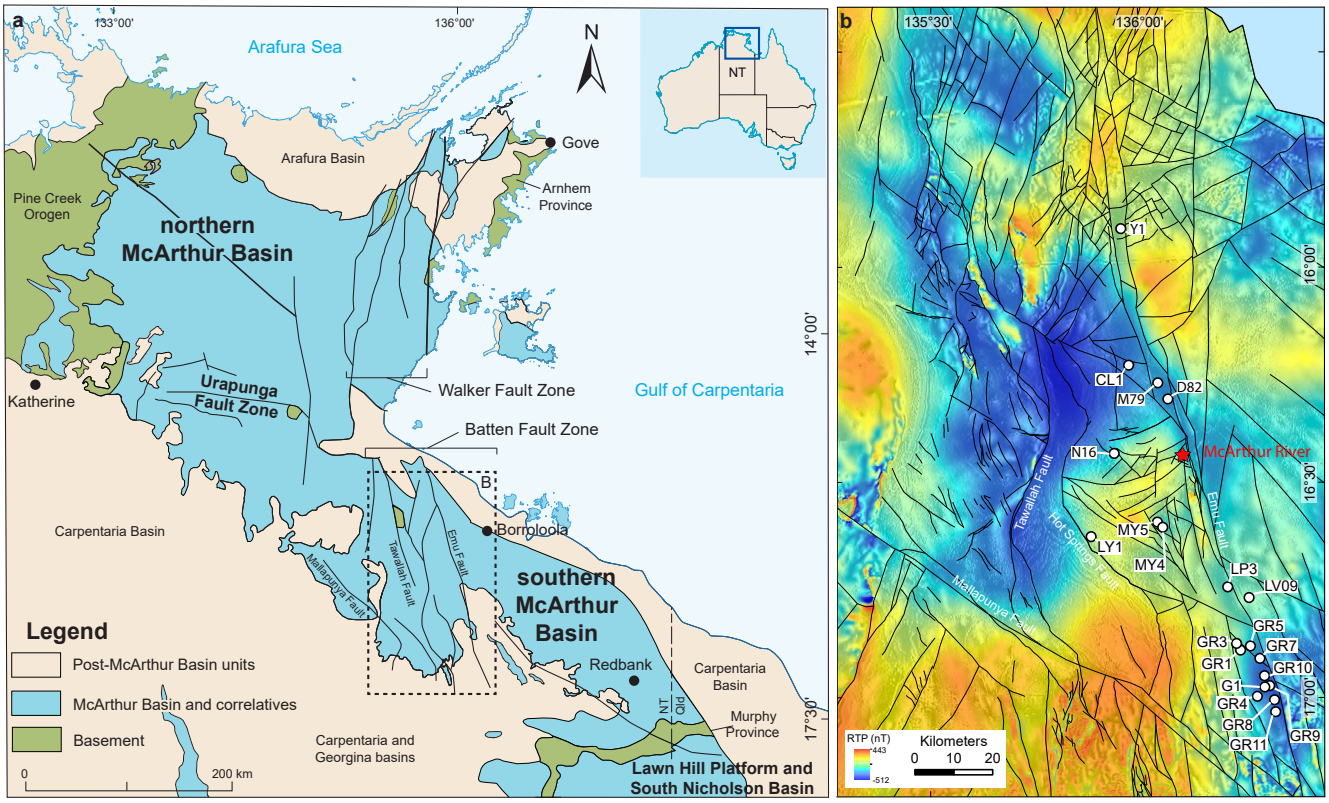

Figure 1. Simplified geological map of the McArthur Basin and magnetic image of the Batten Fault Zone. (**a**) Geographical distribution of McArthur Basin and equivalent stratigraphy, as well as basement inliers and younger sedimentary cover. (**b**) Reduced to pole magnetic image overlaid on the tilt-derivative of the Batten Fault Zone (location shown in **a**) highlighting the current structural complexity of the basin (modified from Kunzmann *et al* 2019). Also shown are the location of the McArthur River deposit and studied drill cores.

Geological setting

The greater McArthur Basin is part of a Proterozoic basin system on the North Australian Craton (eg Giles *et al* 2002, Betts *et al* 2003, Gibson *et al* 2017). It can be subdivided into the northern and southern McArthur Basin, separated by the east–west striking Urapunga Fault Zone (**Figure 1**). The most important structural features are the Walker and Batten Fault zones in the northern and southern McArthur Basin respectively (**Figure 1**). These fault zones are north-south-striking corridors, each about 80 km wide and 200 km long.

The ca 1670–1600 Ma McArthur Group is a mixed siliciclastic–carbonate succession (**Figure 2**) exposed in the southern McArthur Basin. The group is between 1 and 3.5 km thick. The Barney Creek Formation sits stratigraphically in the middle part of the McArthur Group and was deposited in a highly compartmentalised basin, characterised by km-scale sub-basins and paleohighs (eg McGoldrick *et al* 2010, Kunzmann *et al* 2019). Two types of sub-basins were recently recognised from the interpretation of geophysical data (Blaikie and Kunzmann 2019). Type 1 sub-basins are north–south striking transtensional sub-basins that developed along the north–northwest trending Emu Fault (**Figure 1**). In contrast, Type 2 sub-basins trend east–west and developed adjacent to east–west striking normal and north–northwest striking transfer faults located between the Hot Spring and Emu faults (Blaikie and Kunzmann 2019).

The Barney Creek Formation is 10–900 m thick and is subdivided into three members: the W-Fold Shale, the HYC Pyritic Shale, and the Cooley Dolostone (Jackson *et al* 1987). These members are overlain by the undifferentiated upper part of the formation (**Figure 2**). The W-Fold Shale represents the basal part of the formation and is composed of green or red siltstone, pink dololutite, or dolarenite with green or red siltstone laminae (Jackson *et al* 1987, Davidson and Dashlooty 1993, Kunzmann *et al* 2019). The HYC Pyritic Shale Member, which hosts the McArthur River deposit and Teena prospect, consists of dolomitic siltstones and minor silty black shale. Tuff beds in the HYC Pyritic Shale Member yielded SHRIMP U–Pb zircon ages of 1638 ± 7 Ma, 1640 ± 3 Ma, and 1639 ± 3 Ma (Page and Sweet 1998). The Cooley Dolostone is a locally developed carbonate breccia related to faults that interfingers with other members of the Barney Creek Formation (Jackson *et al* 1987). The undifferentiated upper part of the formation is dominated by dolomitic siltstones, carbonate mass-flow deposits, and dolarenite (Jackson *et al* 1987, Kunzmann *et al* 2019).

The Barney Creek Formation comprises two 3rd-order transgressive–regressive sequences, referred to as sequences B1 and B2 (Kunzmann *et al* 2019). Sequence B1 comprises the W-Fold Shale, the HYC Pyritic Shale Member, and the lower half of the undifferentiated Barney Creek Formation. The transgressive systems tract (TST) records deepening of shallow subtidal and intertidal environments of the Coxco Dolostone Member of the underlying Teena Dolostone (**Figure 2**) to deep subtidal environments in the Barney Creek Formation. It culminates in a maximum flooding surface (MFS) in the HYC Pyritic Shale Member. This MFS is typically developed as bituminous dolomitic siltstone on palaeohighs and in shallow parts of sub-basins, but can be developed as highly pyritic black shale and silty shale in sub-basin depocentres (**Figure 3**; Kunzmann *et al* 2019). A thick regressive systems tract (RST) follows the TST and can record shoaling to subtidal environments on paleohighs. It is capped by a maximum regressive surface (MRS) as sequence boundary that sits within silty dolarenite turbidite deposits in sub-basins (Kunzmann *et al* 2019). Sequence B2 comprises the upper part of the undifferentiated Barney Creek Formation and most of the overlying Reward Dolostone (**Figure 2**). A thin TST records renewed deepening of the depositional environment and culminates in a highly pyritic black shale or silty shale in sub-basins or muddy dolostone facies on paleohighs (Kunzmann *et al* 2019). The overlying RST records shoaling to shallow subtidal and intertidal environments in the upper Reward Dolostone.

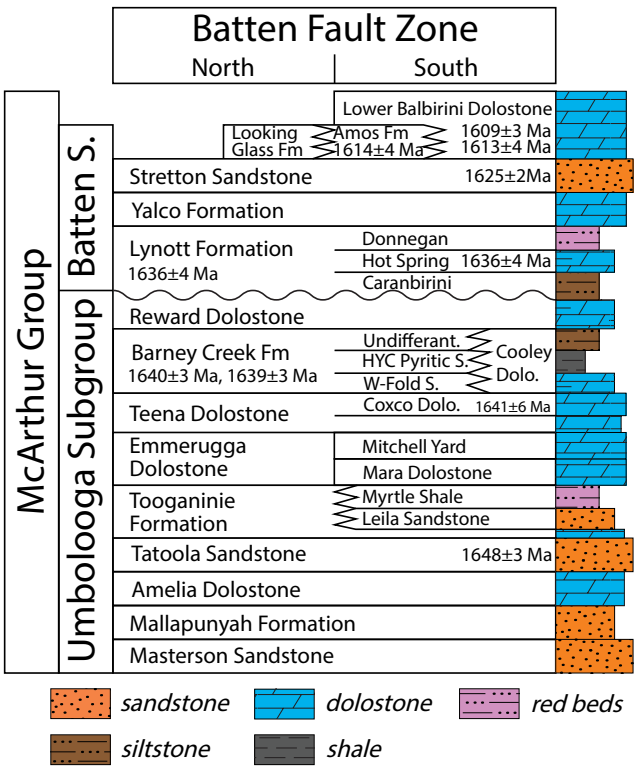

Figure 2. Stratigraphy, dominant lithology, and geochronological constraints of the McArthur Group. Stratigraphy modified from Ahmad *et al* (2013), radiometric ages from Page and Sweet (1998) and Page *et al* (2000).

Methods

This work is based on detailed lithostratigraphic logging of 18 drill cores, supported by the interpretation of wireline data from two additional wells (**Figure 1**). A facies analysis of the middle McArthur Group, as well as a carbon isotopic and sequence stratigraphic framework of this succession, is discussed in detail in Kunzmann *et al* (2019). However, the stratigraphic interpretation in Kunzmann *et al* (2019) focuses only on the southern Batten Fault Zone. In this contribution, we extend it to the entire Batten Fault Zone to better understand the spatial variability of the Barney Creek Formation.

Results and Discussion

Targeting diagenetic mineralisation and fluid pumping

The HYC Pyritic Shale Member and the undifferentiated upper part of the Barney Creek Formation are generally pyrite- and organic matter-rich. However, the maximum flooding surfaces of sequences B1 and B2 have even higher pyrite and organic matter contents, in particular in sub-basin depocentres where they can be developed as silty and black shales (Kunzmann *et al* 2019). This suggests that they represent the most suitable chemical traps for oxidised base metal brines. Therefore, we had previously proposed to target these intervals in sub-basin depocentres for Zn-Pb mineralisation (Kunzmann *et al* 2018). This targeting concept focused on syngenetic models for mineralisation. However, recent microanalytical results from the McArthur River deposit suggest that the mineralisation postdates earliest diagenesis and highlights the importance of carbonate replacement (Spinks *et al* 2019). This implies that the host rocks were already buried at the time of mineralisation. Constraining the depth below the seafloor at which the mineralisation occurred is challenging though. Based on the paragenetic relationships observed at McArthur River (Spinks *et al* 2019), it seems likely that the burial depth was on the order of ten to a few hundred meters. We suggest that the maximum flooding surfaces, where developed as silty and black shales, would have already been compacted and lithified at such depths, thus significantly reducing their porosity and permeability. For this reason, we suggest that the shale facies of the maximum flooding surfaces would have acted as physical traps (seals) to ascending base metal brines.

The new model for the mineralisation at McArthur River is consistent with observations from Teena (Taylor *et al* 2017) and has implications for exploration. Of particular importance is the maximum flooding surface of sequence B1 because the mineralisation at McArthur River and Teena occur in the HYC Pyritic Shale Member (eg Eldridge *et al* 1993, Taylor *et al* 2017). Instead of targeting the maximum flooding surface for mineralisation, the transgressive deposits below should be the target. Their stratigraphic occurrence, and that of the capping maximum flooding surface as physical trap (seal), can be predicted with sequence stratigraphy. Ideally, this should be coupled to facies maps that show where in the basin the maximum flooding surface in the HYC Pyritic Shale Member is developed as shale (and not as siltstone) to provide ideal seal properties. This model should be testable with detailed stratigraphic studies of mineralised sub-basins. At Teena, the most carbonaceous and pyritic interval (ie maximum flooding surface?) occurs above the mineralised zone of the HYC Pyritic Shale Member (Taylor *et al* 2017), which is generally consistent with our model.

A syngenetic model for the mineralisation implies that fluid pumping occurred at the time the host rocks of the HYC Pyritic Shale Member were deposited. This means the pumping of fluids would have happened during extension and deepening of sub-basins (McGoldrick *et al* 2010, Blaikie and Kunzmann 2019). However, numerical fluid flow modelling

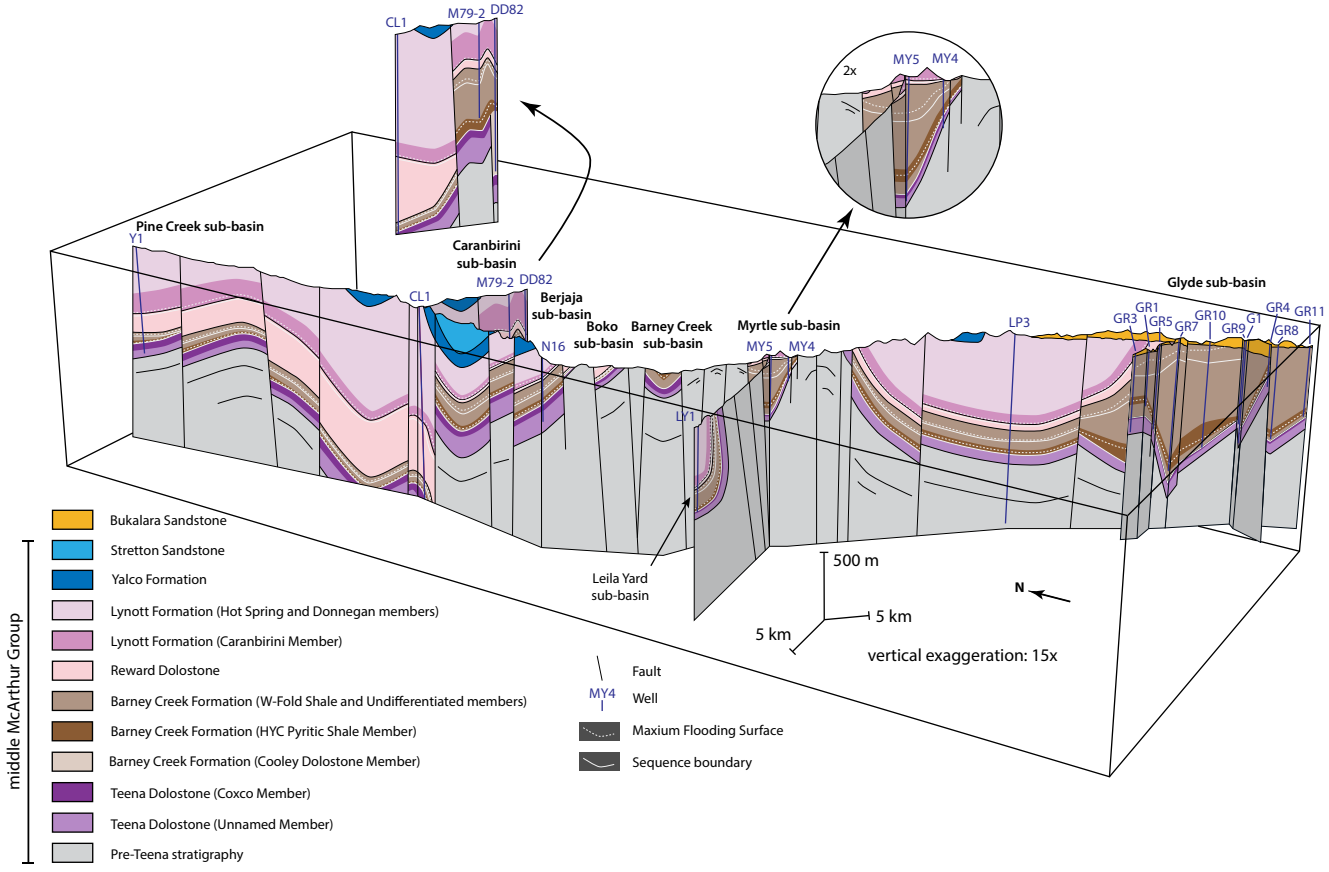

Figure 3. Three-dimensional geological cross-section across the Batten Fault Zone. In the southern and central part (south of well CL1), the Barney Creek Formation is thick but the overlying Reward Dolostone is thin. The opposite relationship is observable in the northern part of the Batten Fault Zone.

demonstrates that extensional deformation is generally not conducive to support upward flow of fluids (Sheldon *et al* 2019). In contrast to models of syngenetic mineralisation, diagenetic models suggest fluid pumping after the host rocks were deposited. One hypothesis is that fluid pumping occurred during deposition of the upper Barney Creek Formation. Our detailed logging shows that carbonate mass flow breccias are common in this stratigraphic interval, indicating instability of shallow depositional environments potentially linked to a short-lived compressional event. This event may be related to accretion of the Warumpi Province at the southern margin of the North Australian Craton or intraplate instability associated with broader scale plate reorganisation (Blaikie and Kunzmann 2019).

Depocentre shift

Core logging on a regional scale across the Batten Fault Zone shows a shift in the depocentre at Barney Creek–Reward time (**Figure 3**). In the central and southern part of the Batten Fault Zone, the Barney Creek Formation is relatively thick, whereas the overlying Reward Dolostone is thin. Furthermore, the Reward Dolostone comprises shallow marine facies. In contrast, in the northern part of the Batten Fault Zone, the Barney Creek Formation is much thinner, whereas the Reward Dolostone is very thick and represents hundreds of meters of deep marine strata. In this area, the overlying Caranbirini Member of the Lynott Formation also seems to be thicker than further to the south.

The observed depocentre shift indicates that major extension in the northern part of the Batten Fault Zone occurred later in the basin's history when compared to the southern and central region. The Caranbirini Member is lithologically similar to the Barney Creek Formation and shows excellent metal host compositions (Kunzmann *et al* 2019). Therefore, the Caranbirini Member may be a potential exploration target, depending on the timing of fluid pumping, availability of a metal source, and the structural framework and evolution.

Conclusions

Based on a diagenetic model for the mineralisation at Teena and McArthur River (Taylor *et al* 2017*,* Spinks *et al* 2019), and on our sedimentological and stratigraphic insights, we propose to target Zn-Pb mineralisation in the Barney Creek Formation by integrating sequence stratigraphy and facies maps. Furthermore, our regional scale study of the middle McArthur Group demonstrates that a depocentre shift occurred across the Batten Fault Zone at Barney Creek–Reward time. A thicker Caranbirini Member in the northern part of the fault zone may be an exploration target.

Acknowledgements

We thank colleagues from CSIRO and NTGS for discussions and support, namely Peter Schaubs, Heather Sheldon, Sam Spinks, Susanne Schmid, Tim Munday, Tim Munson, Dot Close, and Matt McGloin. This project is financially supported by CSIRO Mineral Resources and NTGS.

References

Ahmad M, Dunster JN and Munson TJ, 2013. McArthur Basin: in Ahmad M and Munson TJ (compilers). *'Geology and mineral resources of the Northern Territory.*' *Northern Territory Geological Survey*, *Special Publication* 5.

Baruch ET, Kennedy MJ, Löhr SC and Dewhurst DN, 2015. Feldspar dissolution-enhanced porosity in Paleoproterozoic shale reservoir facies from the Barney Creek Formation (McArthur Basin, Australia). *American Association of Petroleum Geologists Bulletin* 99(9), 1745–1770.

Betts PG, Giles D and Lister GS, 2003. Tectonic environment of shale-hosted massive sulphide Pb-Zn-Ag deposits of Proterozoic northeastern Australia. *Economic Geology* 98, 557–576.

Blaikie TN and Kunzmann M, 2019. From source to trap. Geophysical insights into base metals mineralisation in the southern McArthur Basin: in *'Annual Geoscience Exploration Seminar (AGES) Proceedings, Alice Springs, Northern Territory, 19–20 March 2019'*. Northern Territory Geological Survey, Darwin (this volume).

Brocks JJ, Love GD, Summons RE, Knoll AH, Logan GA and Bowden SA, 2005, Biomarker evidence for green and purple sulphur bacteria in a stratified Palaeoproterozoic sea. *Nature* 437, 866–870.

Croxford NJW, 1975. The McArthur deposit: A review of the current situation. *Mineralium Deposita* 10, 302–304.

Davidson GJ and Dashlooty SA, 1993. The Glyde sub-basin: A volcaniclastic-bearing pull-apart basin coeval with the McArthur River base-metal deposit, Northern Territory. *Australian Journal of Earth Sciences* 40, 527–543.

Eldridge CS, Williams N and Walshe JL, 1993. Sulfur isotope variability in sediment-hosted massive sulfide deposits as determined using ion microprobe SHRIMP: II. A study of the H.Y.C. deposit at McArthur River, Northern Territory, Australia. *Economic Geology* 88, 1–26.

Gibson GM, Hutton LJ and Holzschuh J, 2017. Basin inversion and supercontinent assembly as drivers of sediment-hosted Pb-Zn mineralization in the Mount Isa region, northern Australia. *Journal of the Geological Society* 174, 773–786.

Giles D, Betts PG and Lister GS, 2002. Far-field continental backarc setting for the 1.80–1.67 Ga basins of northeastern Australia. *Geology* 30 (9), 823–826.

Ireland T, Bull SW and Large RR, 2004a. Mass-flow sedimentology within the HYC Zn-Pb-Ag deposit, Northern Territory, Australia: Evidence for syn-sedimentary ore genesis. *Mineralium Deposita* 39, 143–158.

Ireland T, Large RR, McGoldrick P and Blake M, 2004b. Spatial distribution patterns of sulfur isotopes, nodular carbonate, and ore textures in the McArthur River (HYC) Zn-Pb-Ag Deposit, Northern Territory, Australia. *Economic Geology* 99, 1687–1709.

Jackson MJ, Powell TG, Summons RE and Sweet IP, 1986. Hydrocarbon shows and petroleum source rocks in sediments as old as 1.7×10^9 years. *Nature* 322, 727–729.

Jackson MJ, Muir MD and Plumb KA, 1987. Geology of the southern McArthur basin, Northern Territory. *Bureau of Mineral Resources Bulletin* 220.

Kunzmann M, Blaikie TN, Halverson GP and Schmid S, 2018. Sedimentology and carbon isotope chemostratigraphy of the Glyde sub-basin, McArthur basin: Implications for base metals exploration: in *'Annual Geoscience Exploration Seminar (AGES) Proceedings, Alice Springs, Northern Territory, 20–21 March 2018'*. Northern Territory Geological Survey, Darwin.

Kunzmann M, Schmid S, Blaikie TN and Halverson GP, 2019. Facies analysis, sequence stratigraphy, and carbon isotope chemostratigraphy of a classic Zn-Pb host succession. The Proterozoic middle McArthur Group, McArthur Basin, Australia. *Ore Geology Reviews* 106, 150–175.

Large RR, Bull SW, Cooke DR and McGoldrick PJ, 1998. A genetic model for the HYC deposit, Australia: Based on regional sedimentology, geochemistry, and sulphide-sediment relationships. *Economic Geology* 93, 1345–1368.

Lee C and Brocks JJ, 2011. Identification of carotane breakdown products in the 1.64 billion year old Barney Creek Formation, McArthur Basin, Australia. *Organic Geochemistry* 42, 425–430.

McGoldrick P, Winefield P, Bull S, Selley D and Scott R, 2010. Sequences, synsedimentary structures, and sub-Basins: The where and when of SEDEX zinc systems in the southern McArthur Basin, Australia. *Society of Economic Geology Special Publication* 15, 1–23.

Page RW and Sweet LP, 1998. Geochronology of basin phases in the western Mt Isa Inlier, and correlation with the McArthur Basin. *Australian Journal of Earth Sciences* 45, 219–232.

Rage RW, Jackson MJ and Krassay AA, 2000. Constraining sequence stratigraphy in North Australian basins: SHRIMP U–Pb zircon geochronology between Mount Isa and McArthur River. *Australian Journal of Earth Sciences* 47, 431–459.

Sheldon HA, Schaubs PM, Blaikie TN, Kunzmann M, Schmid S and Spinks S, 2019. An integrated study of the McArthur River mineral system: From geochemistry, geophysics and sequence stratigraphy to basin-scale models of fluid flow: in *'Annual Geoscience Exploration Seminar (AGES) Proceedings, Alice Springs, Northern Territory, 19–20 March 2019'*. Northern Territory Geological Survey, Darwin (this volume).

Summons RE, Powell TG and Boreham CJ, 1988. Petroleum geology and geochemistry of the Middle Proterozoic McArthur Basin, Northern Australia: III. Composition of extractable hydrocarbons. *Geochimica et Cosmochimica Acta* 52, 1747–1763.

Spinks S, Pearce M, Ryan C, Moorhead G, Kirkham R, Sheldon H, Kunzmann M, Blaikie T, Schaubs P and Rickard W, 2019. Ultra-high resolution trace element mapping provides new clues on the origin of the McArthur River (HYC) sediment-hosted Zn-Pb-Ag deposit: in *'Annual Geoscience Exploration Seminar (AGES) Proceedings, Alice Springs, Northern Territory, 19–20 March 2019'*. Northern Territory Geological Survey, Darwin (this volume).

Taylor MI, McMillan NE, Dalrympe IJ and Hayward N, 2017. Teena zinc-lead deposit: in Phillips N (compiler). *'Australian Ore Deposits'*. *Australasian Institute of Mining and Metallurgy Monograph* 32, 483–484.

An integrated study of the McArthur River mineral system: From geochemistry, geophysics and sequence stratigraphy to basin-scale models of fluid flow

Heather A Sheldon[1,2], Peter M Schaubs[1], Teagan N Blaikie[1,3], Marcus Kunzmann[1,3], Susanne Schmid[1] and Sam Spinks[1]

Introduction

In 2016, CSIRO embarked on a project with the Northern Territory Geological Survey to improve understanding of sediment-hosted base metal mineralisation in the southern McArthur Basin. The project has taken an integrated approach that includes acquisition and interpretation of new gravity data, re-interpretation of existing geophysical datasets, detailed sedimentological and stratigraphic analysis, petrography, geochemistry, and basin-scale numerical modelling of fluid flow. This abstract reports on the insights gained from numerical modelling, focusing on the integration of information from other areas of the project that have helped to refine and improve the numerical models.

Geological background and conceptual model for mineralisation

The southern McArthur Basin contains a Palaeo- to Mesoproterozoic succession of carbonate, siliciclastic, and volcanic units deposited in an intracratonic basin to the north of the southern margin of the North Australian Craton (Ahmad *et al* 2013). Far-field plate boundary processes resulted in a long history of extension and shortening events, creating a complex depositional architecture and fault network (Betts and Giles 2006, Blaikie and Kunzmann 2019). Significant base metal mineralisation in the basin includes the ca 1640 Ma McArthur River and Teena Zn-Pb-Ag deposits, located on the eastern side of the Batten Fault Zone (**Figure 1**). These deposits occur in the Barney Creek Formation, a succession dominated by dolomitic siltstones deposited in fault-bounded sub-basins that formed during north–south extension (McGoldrick *et al* 2010, Kunzmann *et al* in press). Mineralisation occurred by reaction of an oxidised basinal brine with anoxic sediments of the Barney Creek Formation at or below the sea floor (Rye and Williams 1981, Eldridge *et al* 1993, Hinman 1995, Large *et al* 1998). The brine likely originated from evaporitic deposits and leached metals from deeply buried volcanic units before returning to the surface via the Emu Fault, a long-lived structure that forms the eastern boundary of the Batten Fault Zone (**Figure 1**; Cooke *et al* 1998, Large *et al* 1998, Williford *et al* 2011).

Previous numerical modelling studies

Previous numerical modelling of the McArthur River mineral system suggested that the required fluid circulation could be driven by thermal or thermohaline convection. In this case, fluids descend down the Tawallah Fault on the western side of the Batten Fault Zone and migrate through a siliciclastic aquifer unit where they leach metals from the underlying volcanics, before returning to the surface via the Emu Fault and depositing metals on the seafloor (Garven *et al* 2001, Yang *et al* 2004, Yang 2006).

[1] CSIRO Mineral Resources, CSIRO Mineral Resources, 26 Dick Perry Avenue, Kensington WA 6151, Australia
[2] Email: heather.sheldon@csiro.au
[3] Northern Territory Geological Survey, GPO Box 4550, Darwin NT 0801, Australia

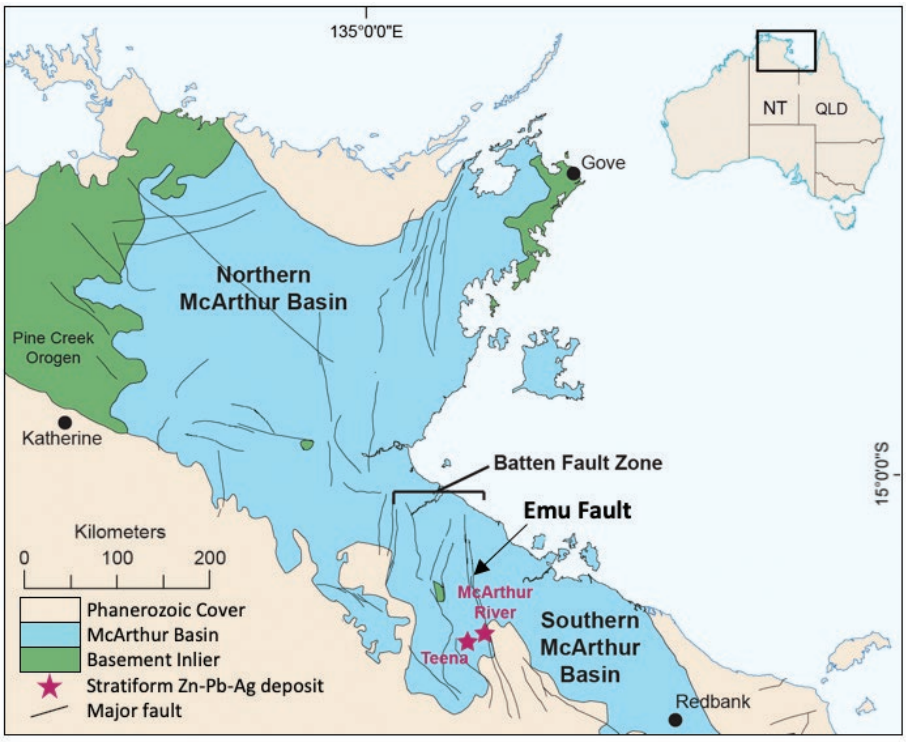

Figure 1. Location map of the McArthur River and Teena deposits.

None of these modelling studies considered the effect of deformation on fluid flow. Given the tectonically active setting of the mineralisation, a primary focus of the present numerical modelling effort has been to explore the interaction and competition between thermal convection and deformation-driven flow in this mineral system.

Numerical modelling approach

We use the open-source finite element code MOOSE (Multiphysics Object Oriented Simulation Environment; https://mooseframework.inl.gov) to solve the equations describing elasto-plastic deformation, fluid flow and conductive-advective heat transport in a fluid-saturated porous rock (CSIRO and INL 2018). Fluid flow is driven by changes in fluid pressure caused by deformation, and by density variations associated with the temperature gradient (ie thermal convection). Variations in permeability between the geological units in the model further control the direction and magnitude of fluid flow. Heat is transported by conduction and advection with the moving pore fluid.

The geometry of the model is a simplified representation of the key hydrostratigraphic units on the eastern side of the Batten Fault Zone (**Figure 2**). The Tawallah Fault, which forms the western boundary of the Batten Fault Zone and was included in previous modelling studies, is not represented in this model; instead, we explore a scenario where an east-dipping aquifer intersects the seafloor to the west of the Emu Fault. We have included a cross fault terminating at the Emu Fault, representing one of the approximately east–west oriented normal faults that are associated with known mineralisation. This simplified geometry is not intended to reflect the complex fault and depositional architecture of the area (cf Blaikie and Kunzmann 2019); rather it represents the key features relevant to this study of fluid flow in the Batten Fault Zone, with geological units corresponding to those used in previous modelling studies. The geological units were assigned appropriate mechanical, thermal and fluid flow properties consistent with their lithologies, with the fault and aquifer having relatively high permeabilities and the fault being mechanically weaker than the other units. The pore fluid was treated as pure water with properties determined by the IAPWS-95 equation of state (Wagner and Pruß 2002).

The top boundary represents the seafloor at 200 m water depth, consistent with the inferred depositional environment of most parts of the Barney Creek Formation being below storm wave base (Bull 1998, Schmid 2015, Kunzmann *et al* in press). The initial fluid pressure gradient is hydrostatic. The base of the model is subject to a fixed heat flux of 100 mW/m^2. The model is initialised in a conductive steady state to establish the initial conductive geothermal gradient, prior to simulation of convection and deformation.

New insights into the McArthur River mineral system

The current multi-disciplinary project has resulted in some important new insights into the McArthur River mineral system, which we have explored through numerical modelling.

The timing of mineralisation at McArthur River has been the subject of much debate, with some authors arguing for syn-depositional mineralisation (eg Large *et al* 1998, Ireland *et al* 2004), while others argue for a diagenetic or epigenetic origin (Eldridge *et al* 1993, Rye and Williams 1981, Logan *et al* 2001, Symons 2007). Previous numerical modelling studies treated the Emu Fault as a high-permeability pathway from the basement to the seafloor, resulting in discharge of hot fluids onto the seafloor, consistent with the syn-depositional mineralisation

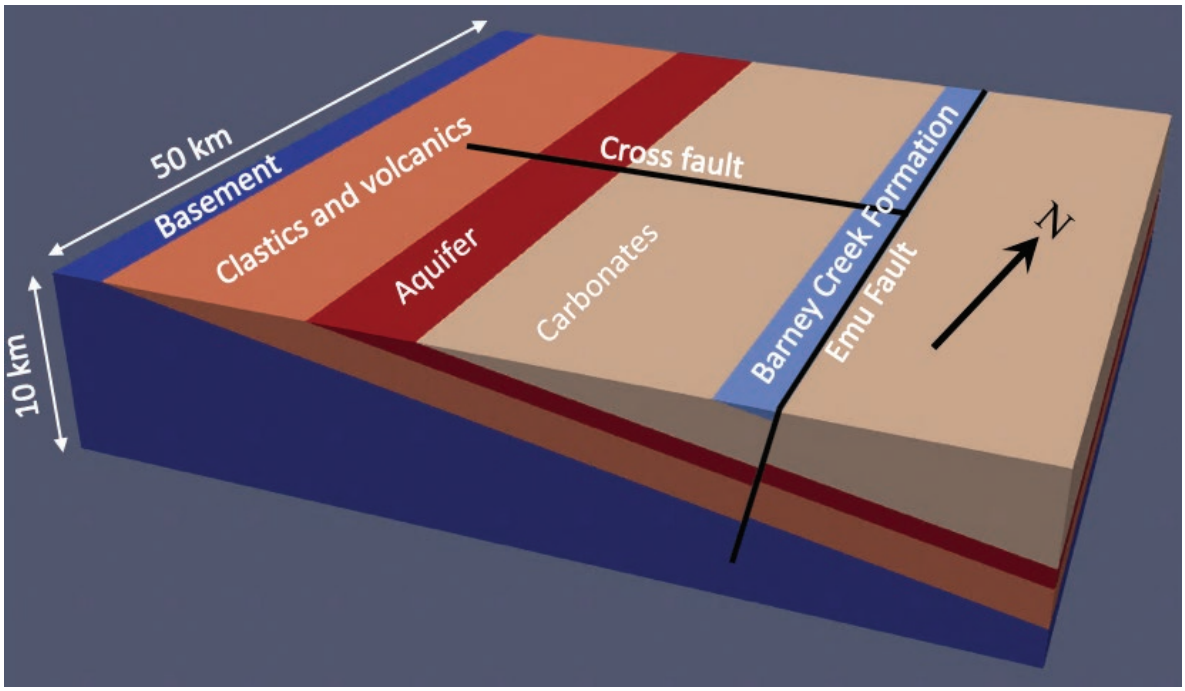

Figure 2. Geometry of the numerical models.

model. However, geochemical and petrographic studies conducted in this project support a diagenetic origin (Spinks *et al* 2019) whereby mineralisation occurred tens to hundreds of metres below the seafloor. This implies that the mineralising fluid moved laterally out of the Emu Fault into the adjacent Barney Creek Formation, instead of continuing its ascent up the Emu Fault to the seafloor. Consequently, we infer that the Emu Fault did not act as a high-permeability fluid pathway all the way to the seafloor. This assumption is reasonable because faults in porous sediments often act as low permeability barriers rather than pathways for fluid flow (eg Barnicoat *et al* 2009).

Detailed stratigraphic analysis of the Barney Creek Formation provides an explanation for diversion of fluids out of the Emu Fault before reaching the seafloor. The known mineralisation is hosted by dolomitic and organic-rich siltstones of the HYC Pyritic Shale Member in the lower Barney Creek Formation. Within this member, a third-order maximum flooding surface is developed as organic-rich black shale and silty shale (Kunzmann *et al* in press). Consistent with our model for diagenetic mineralisation, this interval is likely to have acted as an impermeable barrier to ascending brines because the black shale would have undergone more rapid porosity reduction in the first few hundred metres of burial than the underlying siltstone. Furthermore, shearing of such a clay-rich rock in the Emu Fault zone would have resulted in further permeability reduction. Thus, we postulate that the Emu Fault ceased to act as a fluid pathway where it encountered the black shale, causing fluid to be diverted laterally into the more permeable underlying siltstones where it deposited metals.

The effect of different permeability scenarios in the Emu Fault is illustrated in **Figure 3**. The left column in **Figure 3** shows the case where the Emu Fault has high permeability all the way to the seafloor. Note the pattern of thermal convection in the Emu Fault, with hot fluid exiting through the top of the model (**Figure 3a**, **3g** and **3i**). The convection is three-dimensional (**Figure 3d**), with exchange of fluids between the aquifer and faults facilitating transfer of metals from the source to the site of deposition. There is minimal movement of fluid from the Emu Fault into the Barney Creek Formation (**Figure 3e**). The right side of **Figure 3** shows the case where the Emu Fault has lower permeability than the Barney Creek Formation in the top 300 m of the model. The black shale is not represented explicitly in this model, but the Barney Creek Formation is assigned a highly anisotropic permeability, implicitly representing the effect of horizontal layers of very low permeability. Convection still occurs in the faults and aquifer, but the upwelling fluid is diverted laterally out of the Emu Fault into the Barney Creek Formation (**Figure 3d** and **3f**), which is consistent with the diagenetic mineralisation hypothesis.

On a larger scale, geophysical modelling and stratigraphic analysis have provided insights into the tectonic regime at the time of mineralisation. The HYC Pyritic Shale Member was deposited in rapidly subsiding sub-basins adjacent to the Emu Fault, bounded by east–west normal faults, in a predominantly extensional tectonic setting (Blaikie and Kunzmann 2019). However, our analysis has identified a short-lived inversion event during deposition of the upper Barney Creek Formation, consistent with previous structural analysis of the McArthur River deposit (Hinman 1995). This event would have occurred when the mineralised part of the HYC Pyritic Shale Member was undergoing late-stage diagenesis, tens to a few hundred metres below the seafloor. Thus, the inversion event could correspond to the time of mineralisation.

Extensional deformation tends to result in downward fluid flow (McLellan *et al* 2004, Oliver *et al* 2006) that could override convective upwelling. Conversely, inversion would be expected to drive upward flow, enhancing the convective upwelling. To investigate the effect of extensional deformation and inversion on convective fluid flow, the model was allowed to establish convection without deformation; then north–south extension or shortening was applied at a range of strain rates. **Figure 4** shows the effect of this deformation on the maximum vertical fluid flux in the Emu Fault, with positive values indicating upward flow. This figure illustrates that extensional deformation tends to reduce the rate of convective upwelling but does not completely override it for the range of strain rates shown in **Figure 4**. Further simulation results (not shown here) have shown that overriding the upward convective flow requires unrealistically high strain rates. Conversely, the results shown in **Figure 4** indicate that crustal shortening (inversion) enhances the rate of upward flow. We conclude that convection would have continued during extensional deformation while the inversion event would have temporarily enhanced the upward flow.

Summary and conclusions

A multi-disciplinary study of the southern McArthur Basin has provided new insights into the McArthur River mineral system. New 3D numerical models demonstrate the complex 3D nature of convective fluid flow in this mineral system. Geochemistry and petrography support a diagenetic origin for the mineralisation, implying low permeability at the top of the Emu Fault, which is consistent with stratigraphic and sedimentological analysis of the Barney Creek Formation. Numerical modelling confirms that such a permeability scenario would result in upwelling fluids being diverted out of the Emu Fault into the Barney Creek Formation. Structural and stratigraphic interpretations of the basin suggest a dominantly extensional setting for the Barney Creek Formation, while a short-lived inversion event may have occurred around the time of mineralisation. Numerical models suggest that the convective flow (and therefore mineralisation) would have continued during extensional deformation, unless the deformation occurred at an extremely high strain rate, while inversion would have enhanced the upward convective flow. These results indicate that although it is not necessary to invoke inversion to explain upward flow of mineralizing fluids in this system, the inversion event may have enhanced mineralisation in areas of convective upwelling.

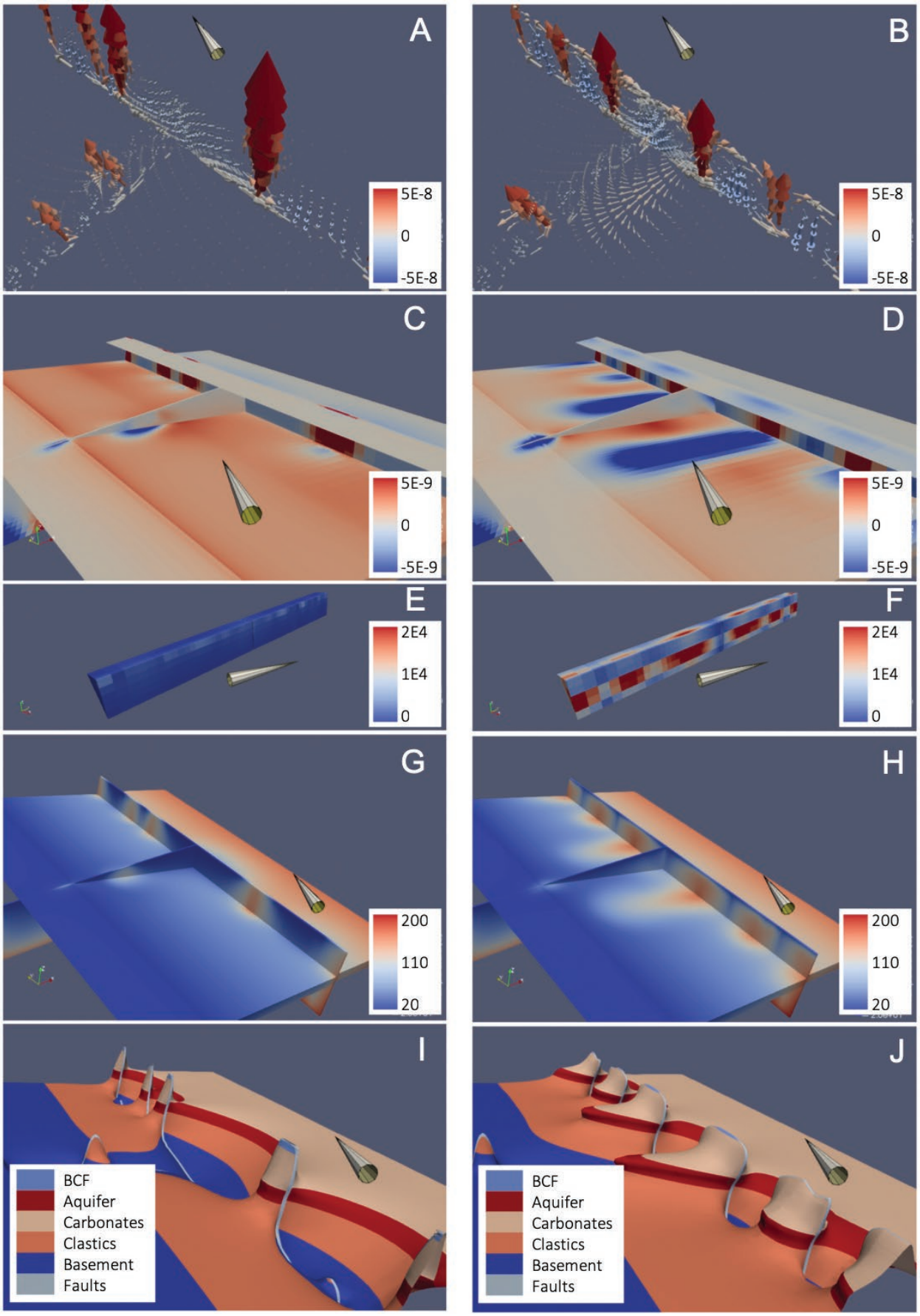

Figure 3. Convection without deformation. **Left side**: Emu Fault has high permeability throughout. **Right side**: Emu Fault has low permeability in top 300 m. Cone indicates North. (**a–b**) Fluid flow vectors. Arrows scaled with magnitude of fluid flux. Colours represent vertical component of fluid flux (m s^{-1}). (**c–d**) Horizontal component of fluid flux in aquifer, faults and Barney Creek Formation (m s^{-1}). Blue = west northwest, red = east southeast. (**e–f**): Time-integrated fluid flux in Barney Creek Formation (m^3/m^2). Vertical exaggeration x10. (**g–h**) Temperature in aquifer and faults (°C). (**i–j**) 120°C isosurface coloured by geological units.

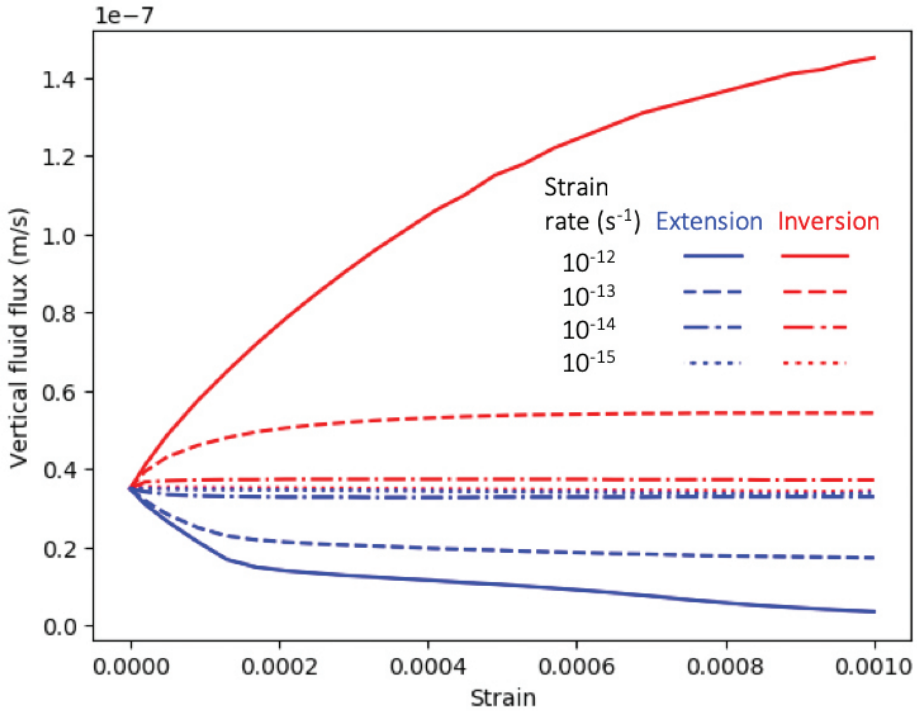

Figure 4. Effect of deformation on convection: Maximum vertical fluid flux in the faults as a function of strain rate.

Acknowledgements

Simulations were run on facilities provided by the Pawsey Supercomputing Centre. Andy Wilkins (CSIRO) is acknowledged for his support in developing the necessary modules for MOOSE.

References

Ahmad M, Dunster JN and Munson TJ, 2013. Chapter 15: McArthur Basin: in Ahmad M and Munson TJ (compilers). '*Geology and Mineral Resources of the Northern Territory*'. *Northern Territory Geological Survey, Special Publication* 5.

Barnicoat AC, Sheldon HA and Ord A, 2009. Faulting and fluid flow in porous rocks and sediments: Implications for mineralisation and other processes. *Mineralium Deposita* 44, 705–718.

Betts PG and Giles D, 2006. The 1800–1100 Ma Tectonic evolution of Australia. *Precambrian Research* 144, 92–125.

Blaikie TN and Kunzmann M, 2019. From source to trap. Geophysical insights into base metals mineralisation in the southern mcarthur basin: in '*Annual Geoscience Exploration Seminar (AGES) Proceedings, Alice Springs, Northern Territory, 19–20 March 2019*'. Northern Territory Geological Survey, Darwin (this volume).

Bull SW, 1998. Sedimentology of the palaeoproterozoic Barney Creek Formation in DDH BMR McArthur 2, Southern McArthur Basin, Northern Territory. *Australian Journal of Earth Sciences* 45, 21–31.

Cooke DR, Bull SW, Donovann S and Rogers JR, 1998. K-metasomatism and base metal depletion in volcanic rocks from the McArthur Basin, Northern Territory: Implications for base metal mineralization. *Economic Geology* 93, 1237–63.

CSIRO and INL, 2018. MOOSE's PorousFlow Module. https://github.com/idaholab/moose/raw/devel/modules/porous_flow/doc/theory/theory.pdf.

Eldridge CS, Williams N and Walshe JL, 1993. Sulfur isotope variability in sediment-hosted massive sulfide deposits as determined using the ion microprobe SHRIMP; II, a study of the HYC deposit at McArthur River, Northern Territory, Australia. *Economic Geology* 88, 1–26.

Garven G, Bull SW and Large RR, 2001. Hydrothermal fluid flow models of stratiform ore genesis in the McArthur Basin, Northern Territory, Australia. *Geofluids* 1, 289–311.

Hinman MC, 1995. Structure and kinematics of the HYC-Cooley Zone at McArthur River. *Australian Geological Survey Organisation Record* 1995/5.

Ireland T, Bull W and Large RR, 2004. Mass flow sedimentology within the HYC Zn-Pb-Ag deposit, Northern Territory, Australia: Evidence for syn-sedimentary ore genesis. *Mineralium Deposita* 39, 143–58.

Kunzmann M, Schmid S, Blaikie TN and Halverson GP, in press. Facies analysis, sequence stratigraphy, and carbon isotope chemostratigraphy of a classic Zn-Pb host succession: the proterozoic Middle McArthur Group, McArthur Basin, Australia. *Ore Geology Reviews*.

Large RR, Bull SW, Cooke DR and McGoldrick PJ, 1998. A genetic model for the HYC deposit, Australia; Based on regional sedimentology, geochemistry, and sulfide-sediment relationships. *Economic Geology* 93, 1345–68.

Logan GA, Hinman MC, Walter MR and Summons RE, 2001. Biogeochemistry of the 1640 Ma McArthur River (HYC) lead-zinc ore and host sediments, Northern

Territory, Australia. *Geochimica et Cosmochimica Acta* 65, 2317–36.

McGoldrick P, Winefield P, Bull SW, Selley D and Scott R, 2010. Sequences, synsedimentary structures, and sub-basins: The where and when of SEDEX zinc systems in the southern McArthur Basin, Australia: in Goldfarb RJ, Marsh EE and Monecke T (editors). *'The Challenge of Finding New Mineral Resources: Global Metallogeny, Innovative Exploration, and New Discoveries'*. Society of Economic Geologists, 1–23.

McLellan JG, Oliver NHS and Schaubs PM, 2004. Fluid flow in extensional environments; numerical modelling with an application to Hamersley iron ores. *Journal of Structural Geology* 26, 1157–71.

Oliver NHS, McLellan JG, Hobbs BE, Cleverley JS, Ord A and Feltrin L, 2006. Numerical models of extensional deformation, heat transfer, and fluid flow across basement-cover interfaces during basin-related mineralization. *Economic Geology* 101, 1–31.

Rye DM and Williams N, 1981. Studies of the base metal sulfide deposits at McArthur River, Northern Territory, Australia: III. the Stable Isotope Geochemistry of the HYC, Ridge, and Cooley Deposits. *Economic Geology* 76, 1–26.

Schmid S, 2015. Sedimentological review of the Barney Creek Formation in drillholes LV09001, BJ2, McA5, McArthur Basin. *Northern Territory Geological Survey, Record* 2015-006.

Spinks S, Pearce M, Ryan C, Moorhead G, Sheldon HA, Kunzmann M, Blaikie TN, Schaubs PM and Rickard WDA, 2019. Ultra-high resolution trace element mapping provides new clues on the origin of the McArthur river (HYC) sediment-hosted Zn-Pb-Ag deposit: in '*Annual Geoscience Exploration Seminar (AGES) Proceedings, Alice Springs, Northern Territory, 19–20 March 2019*'. Northern Territory Geological Survey, Darwin (this volume).

Symons DTA, 2007. Paleomagnetism of the HYC Zn-Pb SEDEX deposit, Australia: Evidence of an epigenetic origin. *Economic Geology* 102, 1295–1310.

Wagner W and Pruß A, 2002. The IAPWS Formulation 1995 for the thermodynamic properties of ordinary water substance for general and scientific use. *Journal of Physical and Chemical Reference Data* 31, 387–535.

Williford KH, Grice K, Logan GA, Chen J and Huston D, 2011. The molecular and isotopic effects of hydrothermal alteration of organic matter in the paleoproterozoic McArthur River Pb/Zn/Ag ore deposit. *Earth And Planetary Science Letters* 301, 382–92.

Yang J, 2006. Full 3-D numerical simulation of hydrothermal fluid flow in faulted sedimentary basins: example of the Mcarthur Basin, Northern Australia. *Journal of Geochemical Exploration* 89, 440–44.

Yang J, Bull SW, and Large RR, 2004. Numerical investigation of salinity in controlling ore-forming fluid transport in sedimentary basins: Example of the HYC Deposit, Northern Australia. *Mineralium Deposita* 39, 622–31.

Exploring for the Future: South Nicholson Basin region project outcomes and sequence stratigraphy

Lidena Carr[1,2], Chris Southby[1], Paul Henson[1], Chris Carson[1], Jade Anderson[1], Susannah MacFarlane[1], Amber Jarrett[1], Tanya Fomin[1] and Ross Costelloe[1]

Introduction

Exploring for the Future (EFTF) is a four year $100.5 million initiative by the Australian Government conducted in partnership with state and territory government agencies, Geoscience Australia, CSIRO, and universities. The EFTF initiative aims to boost northern Australia's attractiveness as a destination for resource exploration investment. As part of this program, Geoscience Australia's researchers have gathered, on an unprecedented scale, new pre-competitive data and information about the energy, mineral, and groundwater resource potential concealed beneath the surface in northern Australia.

A major EFTF deliverable, the acquisition of crustal seismic reflection data in the region between the southern McArthur Basin and the Mount Isa western succession, crossing the South Nicholson Basin and Murphy Province, was completed in August 2017 (**Figure 1**). Prior to this survey, the region contained no seismic data, minimal well data and minor subsurface geological data (Carr *et al* 2016). Five seismic lines were acquired in an orientation to best image geological features as identified in outcrop, and subsurface geophysical anomalies as identified in gravity and magnetics data (**Figure 1**). The acquisition was designed to explore both exposed and undercover sedimentary basins to better understand the location and scale of the region's potential resources and crustal architecture. The seismic program was undertaken in tandem with regional groundwater (Wallace *et al* 2018), surface geochemistry (Bastrakov *et al* 2018), and petroleum and mineral systems geochemistry (Jarrett *et al* 2018a; 2018a,b) studies.

The primary aim of the survey was to investigate prominent areas with a low measured gravity response ('gravity lows') in the region to determine if they represent thick basin sequences similar to the nearby Beetaloo Sub-basin, a highly prospective petroleum province (Cote *et al* 2018, Close *et al* 2016) . The gravity low that straddles the Northern Territory–Queensland border to the north of Camooweal (**Figure 1**), which is entirely overlain by the Georgina Basin, was a primary target of the survey. This new dataset has greatly improved our understanding of the geology and resources of the region. It was initially released in Alice Springs at the 2018 Annual Geoscience Exploration Seminar (Henson *et al* 2018). This paper provides an update

[1] Energy Systems Branch, Geoscience Australia, GPO Box 378, Canberra ACT 2601, Australia
[2] Email: Lidena.Carr@ga.gov.au

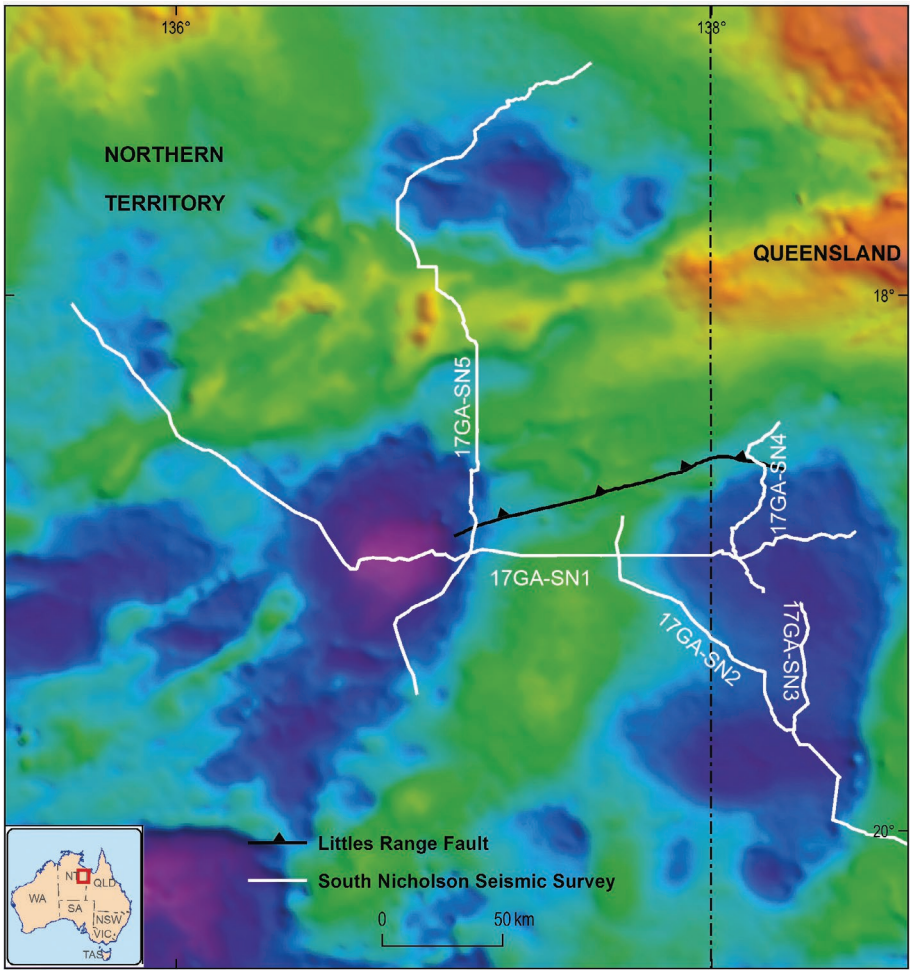

Figure 1. Bouguer gravity image of the South Nicholson region showing seismic lines collected for the study the South Nicholson Seismic Survey (after Carr *et al* in press). Dark blue indicates low gravity response.

of project results and presents an initial interpretation of the sequence stratigraphy.

Seismic interpretation

Acquisition of new 2D seismic data over the South Nicholson Basin region as part of the EFTF program has delivered new scientific insights that will progress understanding of regional energy and mineral resource potential. The South Nicholson seismic survey has revealed a previously unknown new sedimentary basin that straddles the Northern Territory–Queensland border and coincides with a large gravity low northwest of Mount Isa (**Figure 1**). This basin is ~120 km wide as imaged by the seismic data, ~190 km long as defined from regional gravity data (**Figure 1**) and up to ~8 km deep. Our interpretation suggests that the new basin contains a thick McNamara Group or Isa Superbasin age sedimentary succession overlain by a relatively thin succession of the South Nicholson Group; these are for the most part unconstrained (Carr *et al* in press). As outlined by Henson *et al* (2018), the sequences imaged on the seismic data are mostly unknown due to the lack of well data; however, existing seismic data interpretations in the Century Mine area (ie lines 06GA-M1 and 06GA-M2) and correlations with surface mapping suggest that the McNamara Group units and overlying Mesoproterozoic units (which have proven gas discoveries and host major Cu, Pb, and Zn resources elsewhere) may extend undercover to the west of their current outcropping locations in Queensland and into the new basin (Henson *et al* 2018).

The seismic data on lines 17GA-SN1 and 17GA-SN2 images basin-bounding faults and hence, also the basin architecture. This includes the Isa Superbasin horizon and overlying sequences, which have a sag-type geometry. Below the Isa Superbasin horizon, the geometry of the lower sequence suggests an extensional phase followed by contraction, which occurred before deposition of the overlying units. These units are flat-lying with some contractional features suggesting reactivation of early structures. While we have interpreted this lower horizon as base Calvert/Leichhardt Superbasin, the authors would like to emphasise that this is based on its stratigraphic position, rather than any direct control on the stratigraphy. **Figure 2** shows the base Isa Superbasin horizon's interpolated surface intersecting the four seismic lines 17GA-SN1, 17GA-SN2, 17GA-SN3 and 17GA-SN4 in the new basin. More work is required to further constrain the southern and southwestern extent of this basin.

A second gravity low observed further west in the Northern Territory, imaged on both 17GA-SN1 and 17GA-SN5 (**Figure 1**), is not interpreted as a basin. The cause of the gravity low is not clear, but we interpret this feature as a felsic igneous complex. Further, there are examples of felsic volcanic units in the CALVERT HILLS map area and further north (Roberts *et al* 1962). This igneous complex occurs adjacent to the Littles Range Fault (**Figure 1**), suggesting that this major structural trend has acted as a conduit for this intrusion and may have also provided pathways to focus mineral bearing fluids (Carr *et al* in press).

The generally north–south-trending 17GA-SN5 seismic line (**Figure 3**) is oriented largely orthogonal to the southern outcropping boundary of the South Nicholson Basin, broadly defined by the Littles Range Fault. A series of parallel east–west striking structures are clearly defined in geological

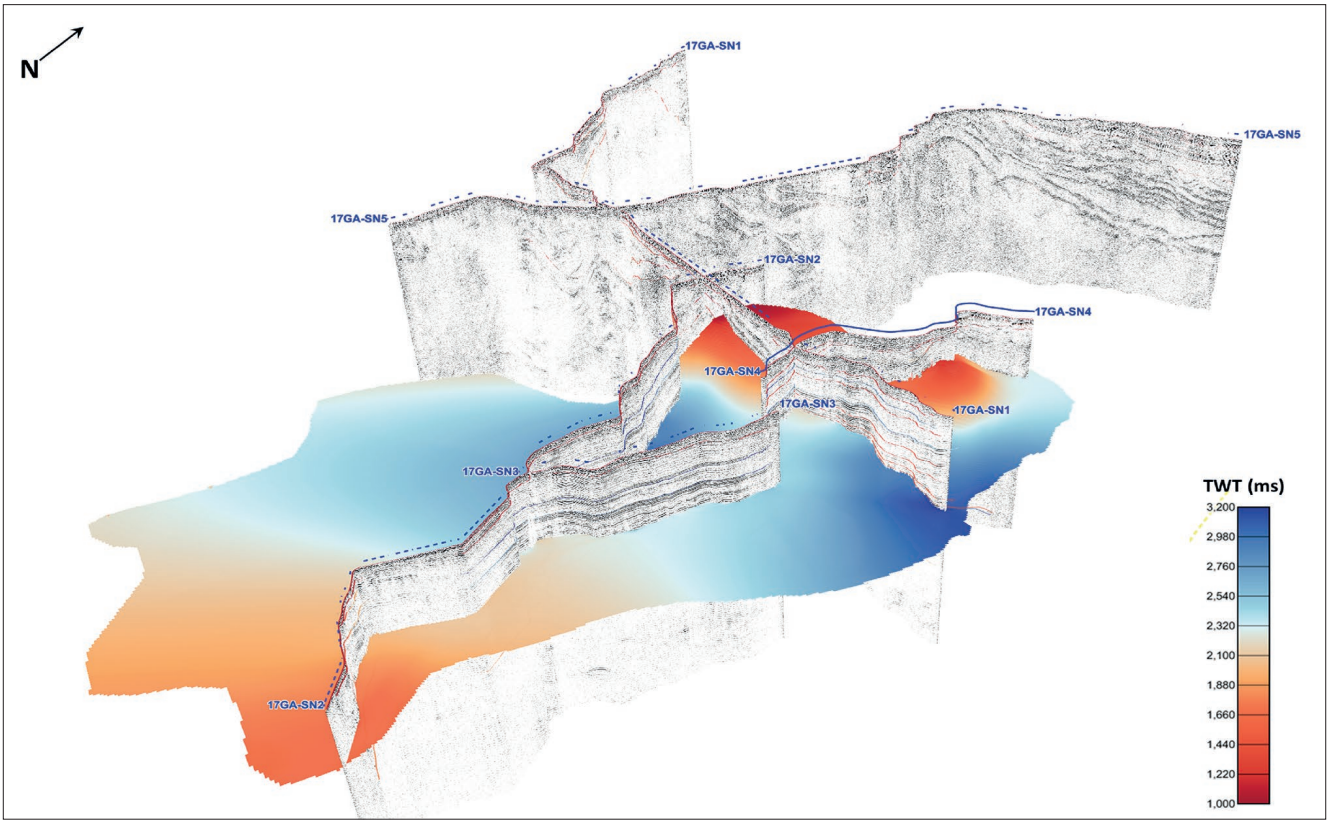

Figure 2. Geological model used as basis for seismic modelling. The vertical extent is 150 m. The velocity (v) and density (d) are shown for each layer (see **Figure 1** for location).

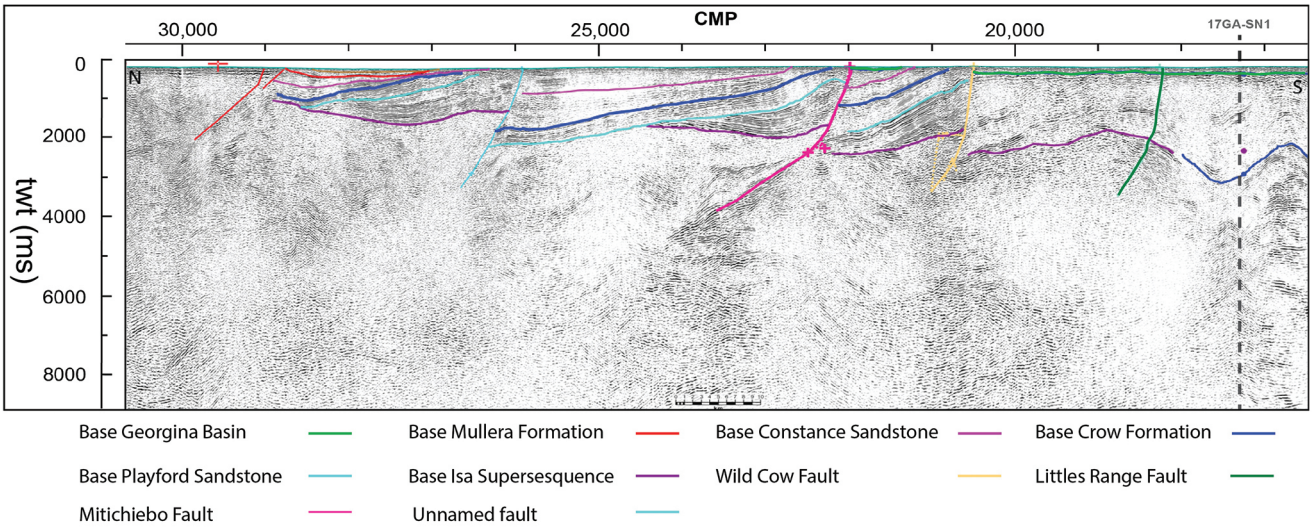

Figure 3. Seismic line 17GASN5 showing north (left) over south (right) thin skinned deformation.

maps in this area; significant displacement is interpreted across faults. The new seismic data has imaged structures in the area consistent with a structural architecture of thin-skinned, north over south, low angle thrusting (**Figure 3**); the timing of this deformation is yet to be determined. These structures are in contrast to the relatively undeformed basin to the south, indicating that there is a sharp transition in structural character south of the Littles Range Fault.

The northern extent of the 17GA-SN5 seismic line traverses a large gravity low to the north of the Murphy Province, over an area of outcropping McArthur Basin units. From the northern boundary of the Murphy Province where lower Tawallah Group units outcrop, to the northern extent of the seismic line where the McArthur Group units outcrop, the new seismic data images an unexpectedly deep basin sequence of semi-continuous, northward dipping reflectors that reach a total depth of 5500 ms twt or ~15 km. This basin sequence hosts the Redbank copper mine; hence, these new findings are likely to have implications for understanding the genesis of this mineral system. The newly identified deep section of stratigraphy is also encouraging for energy prospectivity as it remains relatively undeformed and may be thick enough for hydrocarbon generation (Carr *et al* in press).

Seismic sequence stratigraphy

The eastern end of seismic line 17GA-SN1 from Common Mid Point (CMP) 11 000 to 2000 appears to be orientated close to the dip direction of the new basin. This allows the geometries of the depositional sequences to be determined; however, the vertical resolution of the seismic data, being ~50 ms (~130 m) at 1000 ms TWT deep and 70 ms (~200 m) at 2800 ms TWT depth, limits the detail to which the sequences can be interpreted.

The seismic data in the South Nicholson Group succession occurs between 600 ms and 1600 ms depth; it appears washed out and difficult to interpret, possibly due to the presence of carbonate rocks in the overlying Georgina Basin. The Isa Superbasin succession is better imaged and interpretation of a basic sequence stratigraphic framework has been attempted (**Figure 4**). Due to the low vertical resolution of the seismic data, the sequences interpreted within the Isa Superbasin succession have been divided into two para sequences: 1) lowstand, and 2) combined transgression and highstand parasequences. Three sequences have been interpreted (**Figure 4**) and are described below.

The initial phase (Sequence 1) of deposition at the base of the Isa Superbasin succession shows discontinuous and chaotic seismic reflectors with medium to low amplitudes typical of sediments accumulating in the footwall of normal fault blocks. These are interpreted to be proximal debris and talus slopes or alluvial fans. Overlying these basal sediments is a package of discontinuous to semi-continuous medium amplitude reflectors. These onlap onto the talus/debris sediments below and are interpreted to be a combined transgressive and highstand sequence.

The overlying Sequence 2 begins with a lowstand regressive parasequence. The seismic character of this parasequence shows discontinuous to continuous medium amplitude reflectors with down lapping and prograde geometries. There also appear to be channels (**Figure 4**: blue line) present within this lowstand package. The overlying combined transgression/highstand parasequence extends to the basin bounding fault at the western extent of the new basin; the seismic character of this package is interpreted as continuous medium to high amplitude reflectors. These onlap onto the underlying Calvert/Leichardt sequence in the proximal (western) part of the basin and also onto the lowstand in the distal part of the basin. The proximal part of the parasequence appears aggradational with vertical stacking of reflectors; however, the distal part thickens towards the basin deep indicating deposition during an active extensional phase.

Sequence 3 comprises an initial lowstand parasequence with high amplitude, continuous reflectors in the proximal part. These reflectors then become discontinuous and low to medium amplitude in the central basin, with some possible progrades in the central part; they are chaotic in the distal part of the basin. The overlying transgression/highstand parasequence has low amplitude, semi-continuous to discontinuous reflectors in the lower two thirds and high

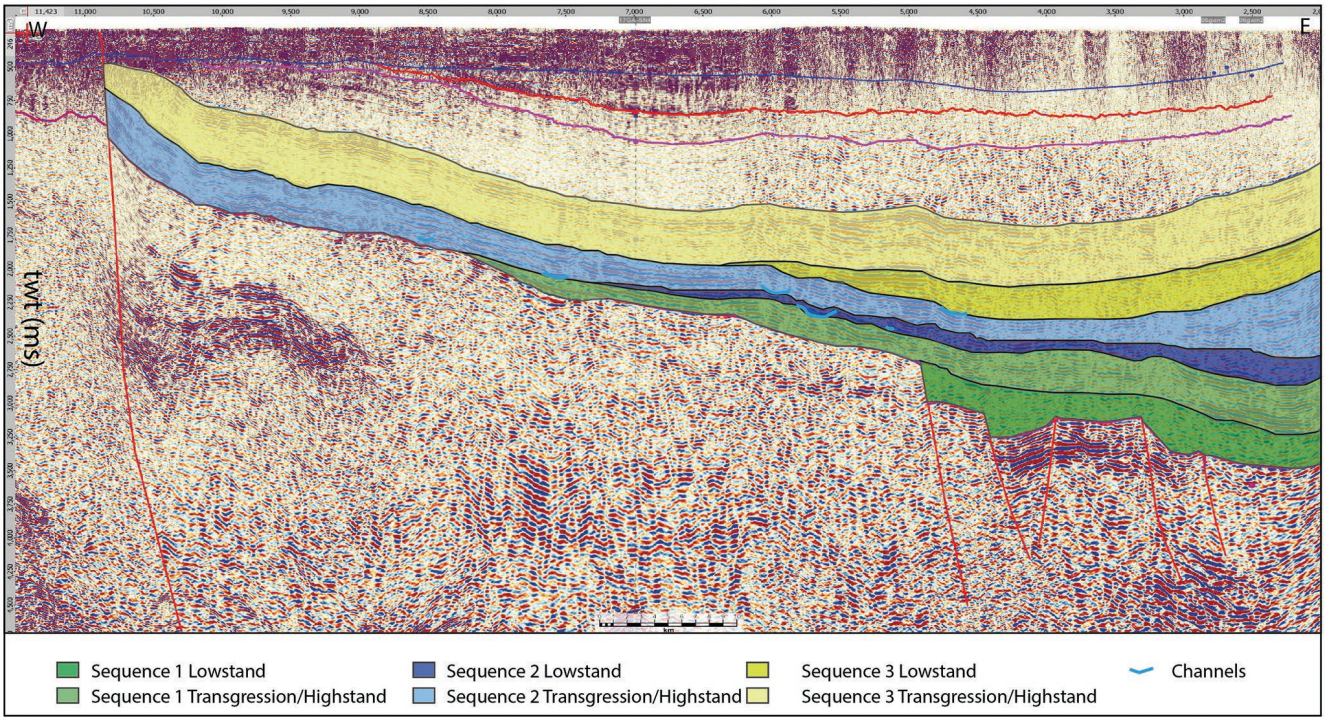

Figure 4. Sequence stratigraphic interpretation of the Isa Superbasin succession of seismic line 17GA-SN1 (see **Figure 1**) showing three interpreted sequences and para sequences. Horizontal scale is Common Mid Point **(**CMP); vertical scale is two way time (ms).

amplitude, continuous reflectors in the upper third. This change in seismic character may represent a change in depositional environment from shallow water, high energy chaotic deposition in the lower portion to deeper water, low energy deposition of more continuous sheet sandstones or mudstones in a shelf environment (Kirk 2013, 2014). This transgressive highstand package has a relatively constant thickness across the basin, indicating that it was deposited during a thermal sag phase.

A sequence stratigraphic interpretation on the overlying South Nicholson Group has not been attempted due to the low data resolution as described above; however, the overall seismic character is described as comprising low amplitude, discontinuous to chaotic reflectors. The overall geometry is subparallel to parallel and conformable within the package. This indicates that it was deposited during a thermal sag phase and may represent deepening basin conditions.

Conclusion

The new South Nicholson Basin seismic survey is a foundational dataset acquired as part of the EFTF program. This survey links the highly prospective resource rich areas of the McArthur Basin and Mount Isa Province via a continuous seismic traverse. Decades of scientific research undertaken in both regions provides a framework to interpret the new data in the South Nicholson Basin region and will act as a catalyst for scientific knowledge transfer across the border. The seismic data will be combined with additional EFTF data collected over the region (ie magnetotelluric surveys, airborne electromagnetic surveys and passive seismic surveys) to greatly improve resource evaluations in northern Australia. The *Exploring for the Future* program aims to further de-risk exploration within greenfield regions and position northern Australia for future exploration investment.

Acknowledgements

This paper is published with the permission of the CEO of Geoscience Australia. The authors would like to acknowledge the considerable contributions from our colleagues at the Northern Territory Geological Survey and the Queensland Geological Survey.

References

Bastrakov E N, Main P, Wygralak A, Wilford J, Czarnota K and Khan M. 2018. Northern Australia geochemical survey data release 1 – Total (fine fraction) and MMI™ element contents. *Geoscience Australia, Record* 2018/06.

Carr LK, Southby C, Henson P, Carson C, Costello R, Anderson J, Gorton J, Hutton L, Troup A, Williams B, Khider K, Bailey A, Jarrett AJM and Fomin T, in press. Exploring for the Future: South Nicholson Basin: Seismic interpretation and data release 2018. *Geoscience Australia*.

Carr LK, Korsch RJ, Palu TJ and Reese B. 2016. Onshore Basin Inventory: the McArthur, South Nicholson, Georgina, Wiso, Amadeus, Warburton, Cooper and Galilee basins, central Australia. *Geoscience Australia, Record* 2016/04. http://dx.doi.org/10.11636/Record.2016.004

Close DI, Baruch ET, Altmann CM, Cote AJ, Faiz M, Mohinudeen FM, Richards B and Stonier S, 2016. Unconventional gas potential in Proterozoic source rocks: Exploring the Beetaloo Sub-basin: in '*Annual Geoscience Exploration Seminar (AGES) Proceedings,*

Alice Springs, Northern Territory 15–16 March 2016'. Northern Territory Geological Survey, Darwin.

Côté A, Richards B, Altmann C, Baruch E and Close D, 2018. Australia's premier shale basin: five plays, 1 000 000 000 years in the making. *The APPEA Journal* 58, 799–804. https://doi.org/10.1071/AJ17040.

Henson P, Carr LK, Fomin T, Gerner E, Costelloe R, Southby C, Anderson J, Bailey A, Lewis C, Champion D, Huston D, the Northern Territory Geological Survey and the Queensland Geological Survey, 2018. Exploring for the Future - Discovering the South Nicholson Basin region with new seismic data: in '*Annual Geoscience Exploration Seminar (AGES) Proceedings, Alice Springs, Northern Territory, 20–21 March 2018'*. Northern Territory Geological Survey, Darwin.

Jarrett AJM, Hall L, Carr L, Anderson J, Orr ML, Bradshaw BE and Henson P, 2018a. Source rock geochemistry of the Isa Superbasin and South Nicholson Basin, northern Australia: Baseline regional hydrocarbon prospectivity. *Geoscience Australia, Record* 2018/038.

Jarrett AJM, Chen J, Hong Z, Palatty P, Anderson J, McLennan S, Lewis C and Henson P, 2018b. Exploring for the Future- Source rock geochemistry data of the Isa Superbasin and South Nicholson Basin, TOC and Rock-Eval data release 1 Northern Australia: Baseline regional hydrocarbon prospectivity. *Geoscience Australia, Record* 2018/45.

Kirk R, 2013. *Operational sequence stratigraphy training course notes, held at Geoscience Australia, Canberra, Australia, 2–4 April 2013*. Geoscience Australia, Canberra.

Kirk R, 2014 *Seismic Facies Mapping, Newsletter 5*. Rob Kirk Consultants, South Australia.

Roberts HG, Rhodes JM and Yates K R, 1962. *Explanatory notes on the Calvert Hills 1:250 000 geological sheet*. Department Of National Development. Bureau of Mineral Resources Geology and Geophysics.

Wallace L, Schroder I, de Caritat P, English P, Boreham C, Sohn J, Palatty P and Czarnota K, 2018. Northern Australia Hydrogeochemical Survey: Data release, preliminary interpretation and atlas – Tennant Creek, McArthur River and Lake Woods regions. *Geoscience Australia, Record* 2018/48.

Source rock geochemistry and petroleum systems of the greater McArthur Basin and links to other northern Australian Proterozoic basins

Amber Jarrett[1,2], Susannah MacFarlane[1], Tehani Palu[1], Chris Boreham[1], Lisa Hall[1], Dianne Edwards[1], Grant Cox[3], Tim J Munson[4], Jochen Brocks[5], Lidena Carr[1] and Paul Henson[1]

Northern Australia contains extensive Proterozoic sedimentary basins that contain organic-rich rocks with the potential to host both major petroleum accumulations and basin-hosted mineral systems (**Figures 1–5**). These intracratonic basins comprise the greater McArthur Basin (McArthur and Birrindudu basins, and Tomkinson Province; Close 2014), the Isa Superbasin, and the South Nicholson Basin. The sedimentary successions within these basins are assumed to be of equivalent age and to have been deposited under similar climatic controls, resulting in correlative lithology, source facies and stratigraphic intervals.

The greater McArthur Basin contains Paleoproterozoic to Mesoproterozoic organic-rich mudrocks with the potential to generate conventional oil and gas deposits, and self-sourced continuous shale oil and shale gas targets (Munson 2014, Revie 2017a, b, Weatherford Laboratories 2017). Exploration has focused on the Beetaloo Sub-basin where organic-rich mudrocks of the Velkerri Formation contain up to 10 wt% total organic carbon (TOC) and have been assessed to contain 118 trillion cubic feet (Tcf) of gas-in-place (Munson 2014, Revie 2017a, Weatherford Laboratories 2017, Revie and Normington 2018). Other significant source rocks include the Kyalla Formation of the Roper Group, the Barney Creek, Yalco and Lynott formations of the McArthur Group, the Wollogorang, and perhaps the McDermott formations of the Tawallah Group, and the Vaughton Siltstone of the Balma

[1] Geoscience Australia, GPO Box 378, Canberra ACT 2601, Australia
[2] Email: Amber.Jarrett@ga.gov.au
[3] The University of Adelaide, Adelaide SA 5005, Australia
[4] Northern Territory Geological Survey, GPO Box 4550, Darwin NT 0801, Australia
[5] Research School of Earth Sciences, Australian National University, Acton ACT 0200, Australia

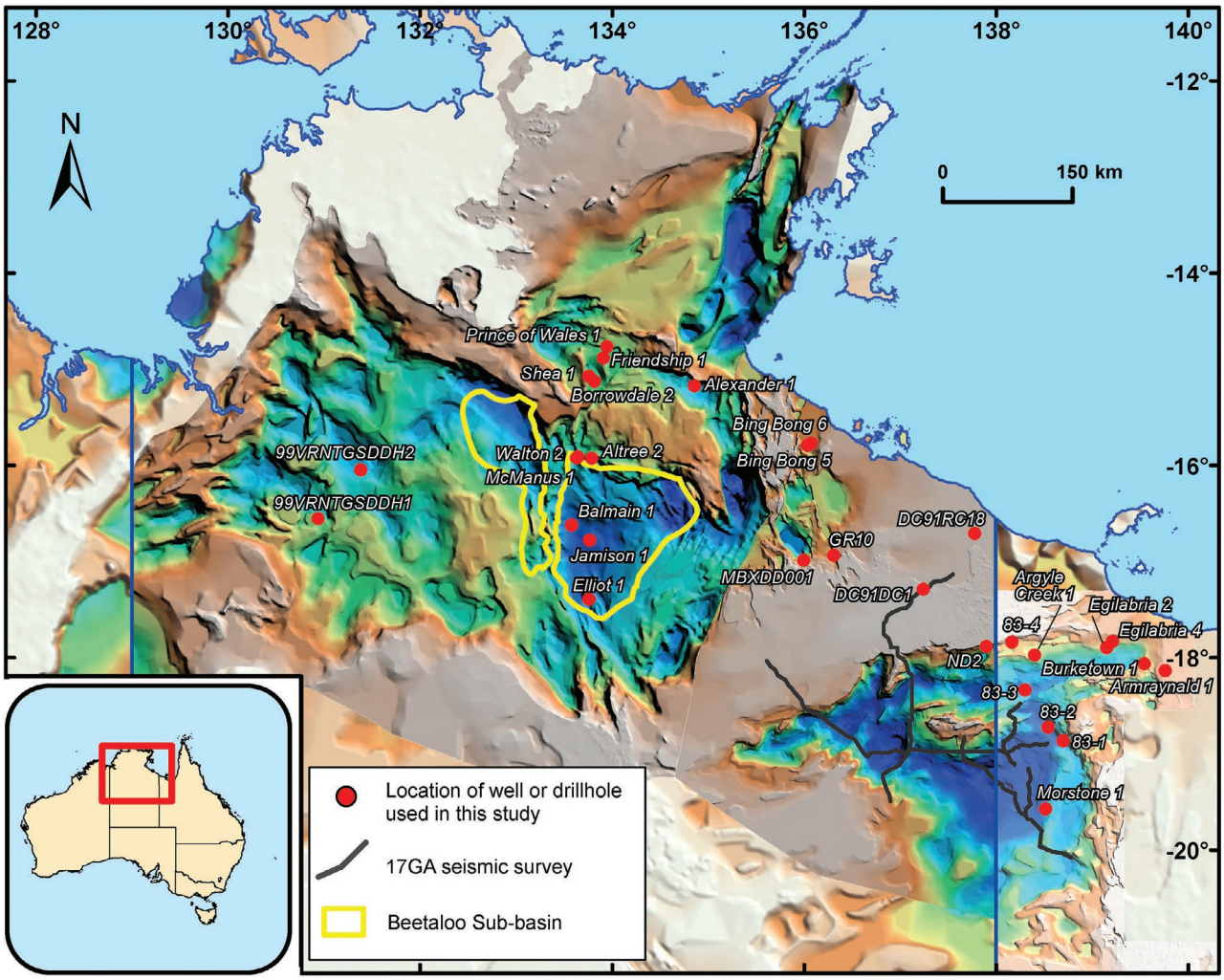

Figure 1. Location map of wells and drillholes used during this study and the location of the Geoscience Australia 2017 South Nicholson Basin seismic survey. Merged background combining the Proterozoic (v2), greater McArthur and northwest Queensland SEEBASE® images showing the basin containers of the greater McArthur Basin including the Beetaloo Sub-basin, and the South Nicholson Basin (Frogtech Geoscience 2018a, b; Frogtech 2006). Beetaloo Sub-basin outline (Department of Primary Industry and Resources, 2017) and South Nicholson Basin outline (Raymond 2018).

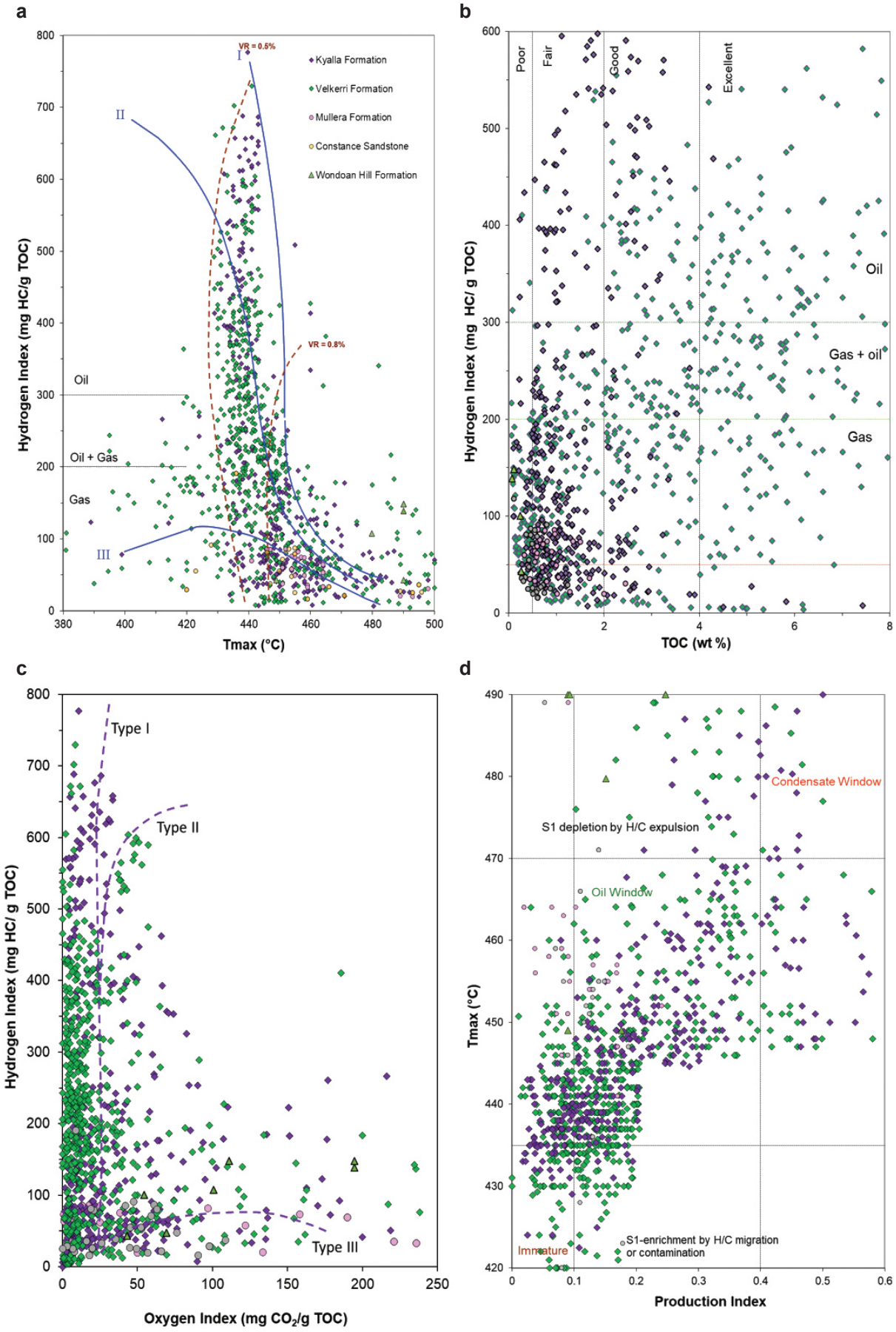

Figure 2. Rock-Eval pyrolysis data for the Mesoproterozoic Urapungan Petroleum Supersystem in northern Australia. **(a)** T_{max} (°C) versus HI (mg HC/g TOC). **(b)** TOC (wt%) versus HI (mg HC/g TOC). **(c)** OI (mg CO_2/g TOC) vs HI (mg HC/g TOC. **(d)** Production index versus T_{max} **(°C)**. Data points for the greater McArthur Basin sourced from Revie and Normington (2018); those for Isa Superbasin and South Nicholson Basin both collated from the literature in Jarrett *et al* (2018a) and 678 newly generated data points from Jarrett *et al* (2018b).

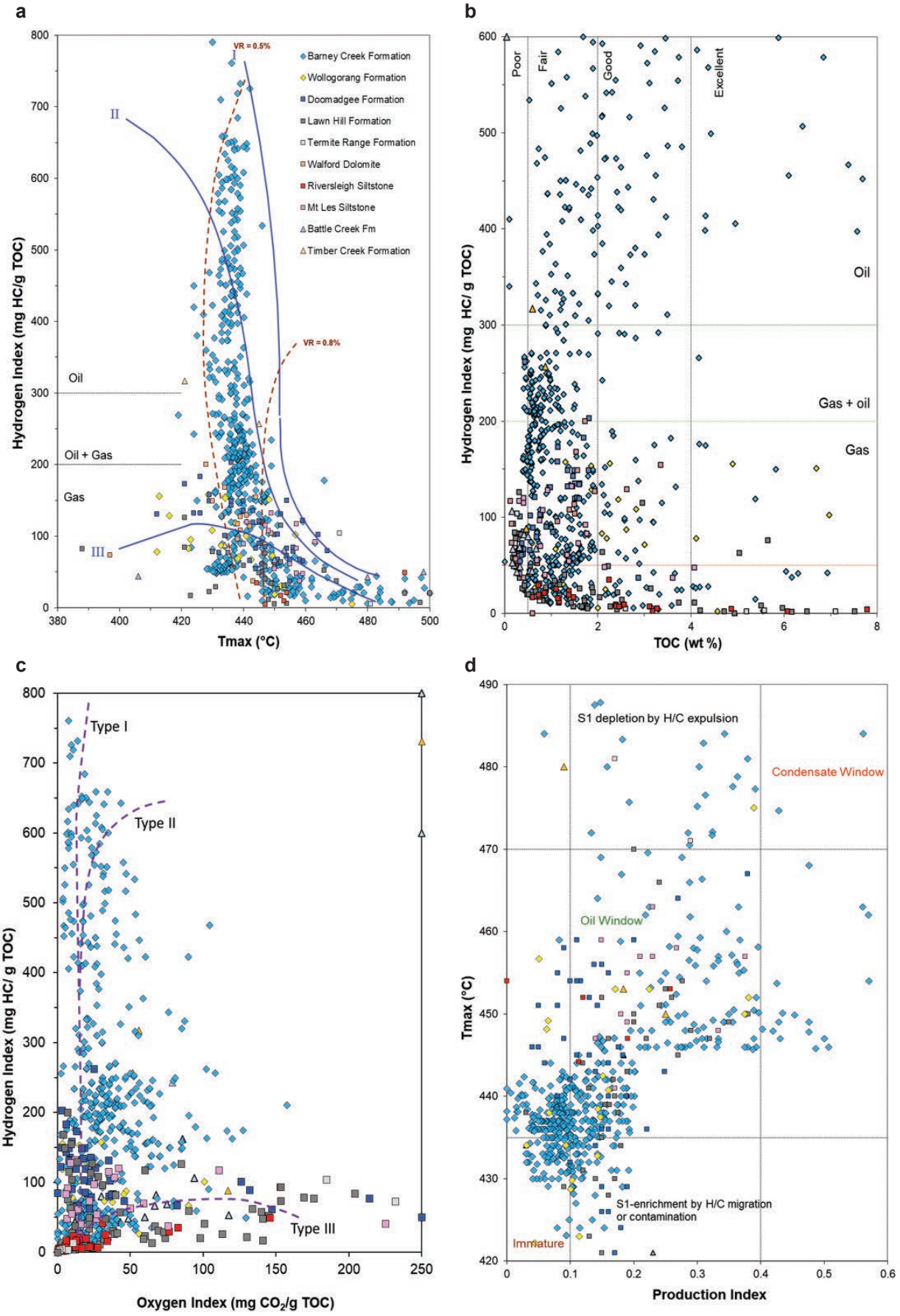

Figure 3. Rock-Eval pyrolysis data for the Paleoproterozoic McArthur Petroleum Supersystem and the Wollogorang Formation in northern Australia. **(a)** T_{max} (°C) versus HI (mg HC/g TOC). **(b)** TOC (wt%) versus HI (mg HC/g TOC). **(c)** OI (mg CO_2/g TOC) vs HI (mg HC/g TOC. **(d)** Production index versus T_{max} **(°C)**. Data points for the greater McArthur Basin sourced from Revie and Normington (2018); those for Isa Superbasin and South Nicholson Basin both collated from the literature in Jarrett *et al* (2018a) and 678 newly generated data points from Jarrett *et al* (2018b).

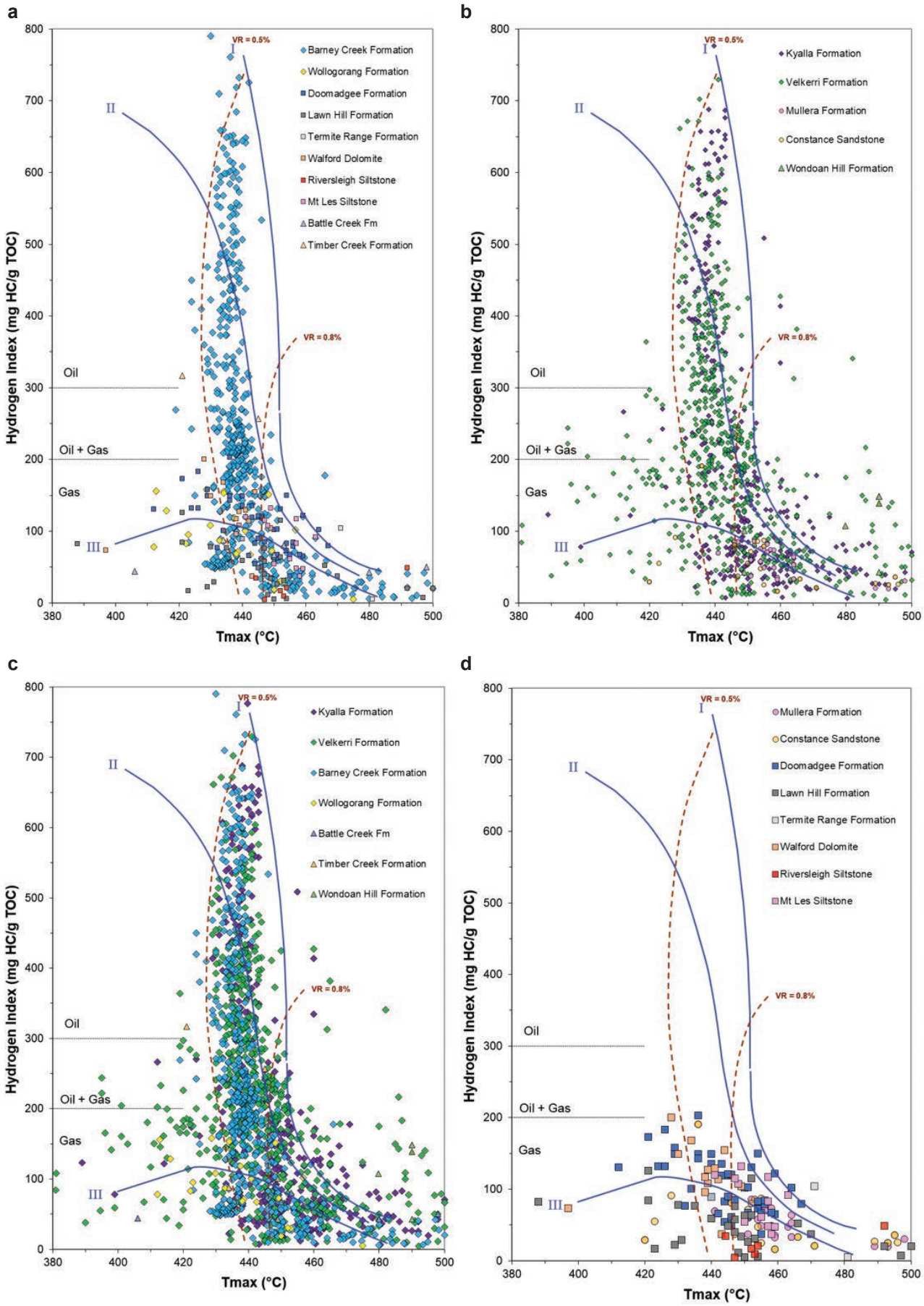

Figure 4. Rock-Eval pyrolysis data (T_{max} **(°C) versus HI (mg HC/g TOC)**) for Proterozoic units in northern Australia demonstrating the variability between **(a)** the Proterozoic McArthur Petroleum Supersystem, **(b)** the Urapungan Petroleum Supersystem, **(c)** data from the greater McArthur Basin sourced from Revie and Normington (2018), and **(d)** data from the South Nicholson Basin and Isa Superbasin both collated from the literature in Jarrett *et al* (2018a) and 678 newly generated data points from Jarrett *et al* (2018b).

Group in the northern McArthur Basin (Munson 2014, Frichot *et al* 2017). These source rocks are hosts to diverse play types; for example Coté *et al* (2018) described five petroleum plays in the Beetaloo Sub-basin: the Velkerri shale dry gas play, the Velkerri liquids-rich gas play, the Kyalla shale gas play, the Kyalla hybrid liquid-rich gas play, and the Hayfield sandstone oil/condensate play. This highlights the large shale and tight gas resource potential of the McArthur Basin for which the full extent is poorly understood and insufficiently quantified. More work is needed to characterise the source rocks, the petroleum generative potential, the fluid types and migration pathways, and the thermal and burial history in order to fully understand and quantify the hydrocarbon prospectivity of the basin.

The *Exploring for the Future* (*EFTF*) program is a four-year (2016–2020) $100.5 million initiative by the Australian Government conducted in partnership with state and Northern Territory government agencies, other key government, research and industry partners and universities. *EFTF* aims to boost northern Australia's attractiveness as a destination for investment in resource exploration. The Energy Systems Branch at Geoscience Australia has undertaken a regional study on the prospectivity of several northern Australian basins by expanding our knowledge of petroleum and mineral system geochemistry. Herein we highlight some of the results of this ongoing program with a primary focus on the greater McArthur Basin.

Petroleum supersystems

A petroleum supersystem is a continental-scale framework linking basins of similar age, structural history, depositional environment and hydrocarbon potential. It may include a family of similar source rocks rather than one single source-reservoir-seal pair (Bradshaw *et al* 1994). Seven petroleum supersystems are recognised across Australia (Bradshaw *et al* 1994) of which two are identified in the *EFTF* project area: the McArthur and Urapungan supersystems. A regional

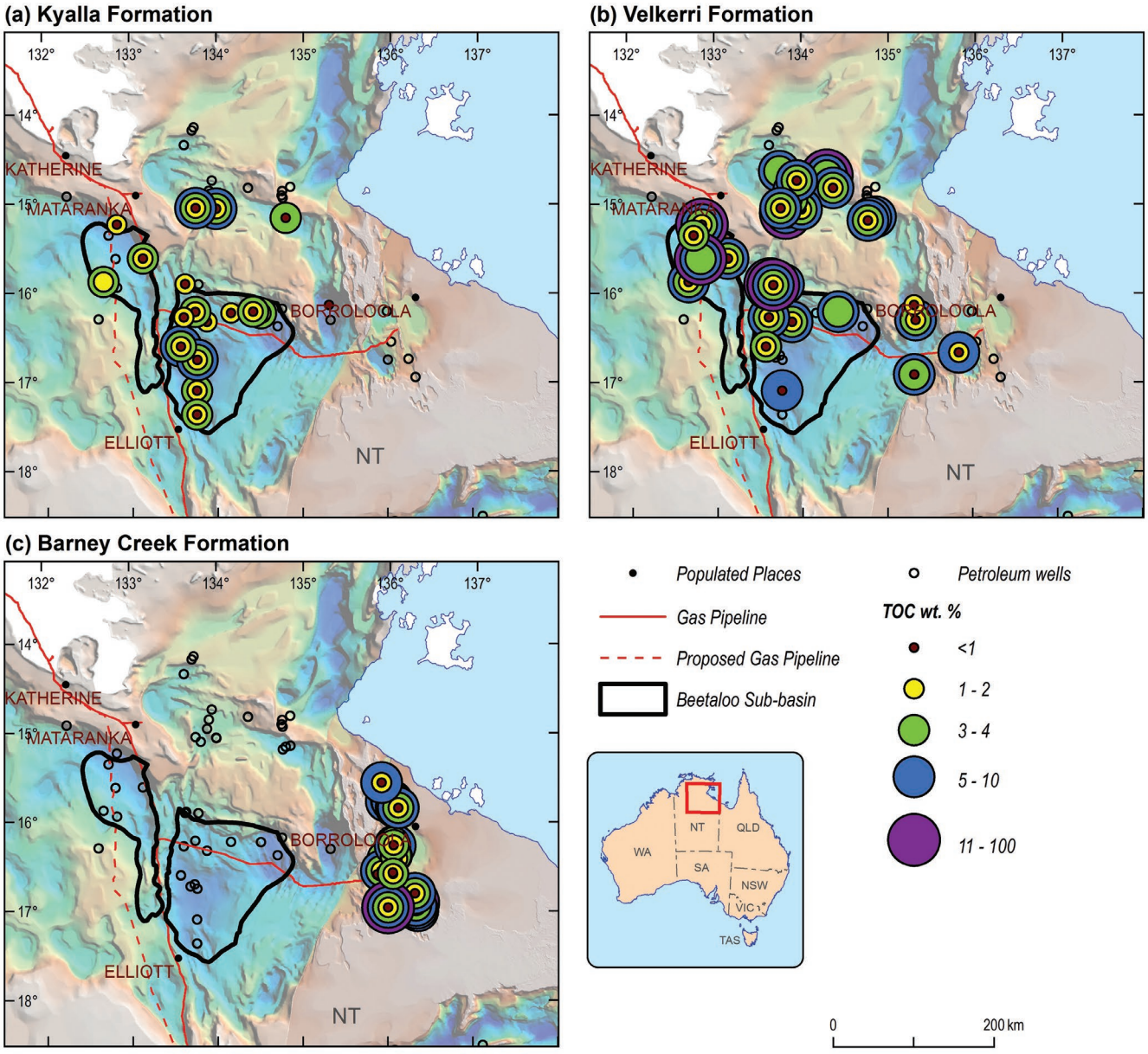

Figure 5. Spatial variations in total organic carbon (TOC wt%) of (**a**) Kyalla Formation (**b**) Velkerri Formation and (**c**) Barney Creek Formation.

chronostratigraphic and lithostratigraphic correlation between Paleoproterozoic and Mesoproterozoic basins across northern Australia has been proposed (eg Ahmad and Scrimgeour 2013, and references therein), supported with recent data for this interpretation (Hoffman 2015). We use the petroleum supersystem concept to investigate the links between families of potential source rocks in roughly time equivalent and structurally similar settings of the McArthur Basin, Birrindudu Basin, South Nicholson Basin, and Isa Superbasin (**Figure 1**).

Source rock geochemistry

A compilation of existing source rock geochemistry was used to define areas with the potential to host an active petroleum system and to target future areas for study as part of the *EFTF* program. The source rock geochemistry and maturity of all known source rock units and associated data has been reviewed from the greater McArthur Basin (Revie 2017b, Revie and Normington 2018) and compiled for the South Nicholson Basin and Isa Superbasin (Jarrett *et al* 2018a). These results, plotted in **Figures 1–4**, determined that although the Roper Group contains a significant amount of datapoints and has been thoroughly reviewed and interpreted (Revie, 2017b), higher-resolution pre-competitive source rock geochemical studies are required over multiple wells that intersect the greater McArthur and South Nicholson basins, and the Isa Superbasin. Such data density is required to better understand source rock properties used in the evaluation of resource potential in northern Australia. The large standard deviations in source rock quality (wt% TOC) within formations and supersequences plus the limited amount of Rock-Eval pyrolysis data highlight the importance of capturing uncertainty surrounding source rock properties in petroleum systems analysis and resource assessment studies (eg Jarrett *et al* 2018a).

Previously collected pyrolysis results from the greater McArthur Basin (Revie and Normington 2018, Revie 2017b) and preliminary results from this study are presented together in **Figures 2** and **3**. **Figure 2** shows the Mesoproterozoic Urapungan Petroleum Supersystem and **Figure 3** combines the data for the Paleoproterozoic McArthur Petroleum Supersystem and the Wollogorang Formation. **Figure 4** is a comparison of T_{max} (°C) versus hydrogen index (HI; mg HC/g TOC) for Proterozoic units in northern Australia based on petroleum supersystem (**Figure 4a–b**) and by region (greater McArthur Basin versus South Nicholson Basin and Isa Superbasin); the results demonstrate that although both the Urapungan and McArthur petroleum supersystems contain excellent source potential, the sampling density is highest in the greater McArthur Basin, emphasising the need for more data elsewhere in the region.

Using the classification of Peters and Casa (1994), 10 source rock units in northern Australia exhibit excellent organic richness (TOC >4 wt%). These include the Kyalla and Velkerri formations (**Figure 2; Table 1**) of the Mesoproterozoic Urapungan Petroleum Supersystem, as reported by Revie (2017b); and the Barney Creek Formation, Riversleigh Siltstone, Mount Les Siltstone, Lawn Hill Formation, Termite Range Formation, and Wollogorang Formation of the Paleoproterozoic McArthur Petroleum Supersystem (**Figure 4**). In addition, the Mesoproterozoic Mullera Formation has good organic richness reaching a maximum TOC of 2.45 wt%, and the Constance Sandstone, Battle Creek and Timber Creek formations have fair source rock potential (TOC between 0.5 and 2 wt%; **Figures 2–4; Table 1**).

Spatial variations in source rock potential in the McArthur Basin are evident in **Figure 5**. The Velkerri Formation shows a comparatively widespread distribution of very good to excellent source rock potential where data exists. There is a slight decline in organic richness towards the south of the Beetaloo Sub-basin (**Figure 5**). Although this trend is only controlled by one data point, it is likely to be related to observations of sandier facies towards the south of the basin (Munson 2016 and references therein). Revie (2017b) mapped thermal maturity within the Beetaloo Sub-basin demonstrating that the deepest and thickest intersections of the Velkerri Formation in the central region are mature to overmature, and that the Kyalla Formation is early to late mature across the entire region. Mapping the spatial variations is a significant component in play fairway analysis and risk mapping, and future work is needed to produce similar maps over the greater McArthur Basin and other Proterozoic basins in northern Australia.

The hydrogen index (HI) can determine the expelled petroleum product at the time of peak maturity (eg Peters and Casa 1994). Present day HIs demonstrate that the range of oil-prone, oil-and gas-prone, and gas-prone kerogens in the greater McArthur Basin are potential sources for the large range of petroleum shows present in the Proterozoic sections (Munson 2014, Revie 2017b, Cox *et al* 2019). Based on present-day hydrogen indices, the Urapungan Petroleum Supersystem contains oil-prone kerogen (HI >600 mg HC/g TOC) in the Kyalla and Velkerri formations and gas-prone kerogen (HI 50 to 200 mg HC/g TOC) within the Mullera Formation, Constance Sandstone, and Wondoan Hill Formation. The McArthur Petroleum Supersystem contains oil-prone kerogen in the Barney Creek, Battle Creek and Timber Creek formations and in the Riversleigh Siltstone. The Doomadgee Formation and Walford Dolostone (termed Walford Dolomite in Queensland) contain oil- and gas-prone kerogen (HI 200 to 300 mg HI/g TOC). Gas-prone kerogen characterises the Lawn Hill and Termite Range formations and the Mount Les Siltstone. Additionally, the Wollogorang Formation contains gas-prone kerogen.

The present day HI is affected by thermal maturity, which needs to be taken into account for extrapolation to initial/original HI (HI_o). Hence HI_o for mature to overmature potential source rocks in the greater McArthur Basin and Isa Superbasin (Jarrett *et al* 2018a, b) requires an understanding of depositional environments and organic facies. However, additional data are required from immature samples of all units to have a better understanding of expelled petroleum products.

The generative hydrocarbon potential of potential source rocks can be further quantified using kerogen kinetics. Both the newly acquired and previously published kinetic results (Revie and Normington 2018) are combined in **Figures 6** and **7** to show the bulk petroleum potential of the greater

McArthur Basin. Hydrocarbon generation of all the greater McArthur Basin samples are characterised by a typically narrow activation energy distribution (Ea), although a slightly broader Ea distribution exists in one sample from the Velkerri Formation (**Figure 6d**). The main activation energies are 51–54 kcal/mol in the Kyalla Formation, 53 kcal/mol in the Velkerri Formation, and 52–55 kcal/mol in the Barney Creek Formation (**Figure 6**). Application of the kinetic models was performed on samples using the ZetaWare–Kinex software. This involved a discrete Ea distribution and a single frequency factor (A sec^{-1}) to a geologic heating rate of 3°C/Ma (close to midway between the range of 1°C/Ma to 10°C/Ma in most sedimentary basins). **Figure 6** shows the comparison of predicted transformation ratio (TR) against Pepper and Corvi's (1995) five standard kerogen types. The Pepper and Corvi kerogen types are preferred in this study over the traditional Tissot and Welte (1984) 'Type I – IV' kerogen classifications that. classified kerogen into groups using a combination of geochemistry and petrology. Proterozoic source rocks predate Vitrinite, and there are issues with our understanding of petrology and reflectance in pre-Vitrinite source rocks (eg Palu *et al* 2018).

In **Figure 7**, TR = 0.1 indicates that the onset of hydrocarbon generation occurs between 120°C and 140°C and at maturities between 0.8% and 1.0% Rc; TR = 0.5 approximates peak hydrocarbon generation at relatively high temperatures between 140°C and 160°C. The bulk of primary gas generation is completed at TR = 0.9 and occurs between 150°C and 175°C from the residual refractory organic matter. The narrow range in Ea and steep generation gradient in the three McArthur Basin source rocks analysed can be effectively modelled using type C lacustrine organofacies similar to 'type I' kerogen (eg Pepper and Corvi 1995). Revie (2017b) demonstrated that Roper Group source rocks are a mixture of 'Type I' and 'Type II' source rocks and more work is likely required to model these different organic types. Additionally, there are also samples where the generation profile is more comparable with a type D/E fluvio-deltaic organofacies of terrestrial type III kerogen. These interpretations of organofacies and kerogen type are incompatible with our understanding of the Proterozoic biosphere. Revie (2017b) suggested that Roper Group 'type III' to 'type IV' kerogen are the results of maturation from type II kerogen, this may explain some of the data. However there are many immature samples with low HI values, in addition to the kinetic results described above. These results largely reflect the limited range in standard kerogen types and thus require further investigation and refinements for early

Table 1. Rock-Eval pyrolysis statistics of potential source rocks of northern Australia. Data sourced from Revie and Normington (2018) and Jarrett *et al* (2018a,b).

Petroleum Supersystem	Basin	Formation	No. of Samples		Total Organic Carbon (TOC; wt %)			S1 + S2 (mg HC / g rock)			Hydrogen Index **(HI; mg HC/ g TOC)**			T_{max} (°C)		
			TOC	**Rock-Eval**	**Av**	**Stdev**	**Range**	**Av**	**Stdev**	**Range**	**Av**	**Stdev**	**Range**	**Av**	**Stdev**	**Range**
Urapungan	McArthur	Kyalla Formation	640	549	1.40	0.90	0.50-9.00	3.20	4.60	0.10-24.70	165	174	6-777	451	21	384-530
	McArthur	Velkerri Formation	1967	960	2.90	2.50	0.50-31.0	9.20	11.30	0.10-82.40	191	142	1-946	437	29	381-618
	Birrindudu	Wondoan Hill Formation	24	4	0.14	0.11	0.01-0.4	0.21	0.07	0.11-0.29	108	48	43-148	480	21	449-490
	South Nicholson	Mullera Formation	38	36	0.81	0.48	0.19-2.45	0.50	0.28	0.16-1.21	57	21	19-86	465	24	441-545
	South Nicholson	Constance Sandstone	222	39	0.18	0.27	0.00-1.59	0.30	0.19	0.11-0.82	53	43	16-191	475	41	420-603
McArthur	McArthur	Barney Creek Formation	1162	667	1.35	1.3	0.00-13.4	4.94	9.08	0.00-71.29	212	177	3-907	445	22	419-566
	Isa	Doomadgee Formation	117	76	1.17	2.95	0.01-18.36	2.52	5.67	0.00-28.17	110	47	37-262	443	12	412-467
	Isa	Lawn Hill Formation	480	77	1.4	1.82	0.02-9.8	0.69	1.19	0.11-5.52	37	32	2-126	483	59	388-603
	Isa	Termite Range Formation	33	9	1.55	1.58	0.16-7.1	0.20	0.19	0.08-0.51	24	37	2-104	530	49	471-599
	Isa	Walford Dolomite	90	15	0.51	1	0.00-8.2	2.3	1.7	0.13-5.87	121	42	37-200	439	14	397-462
	Isa	Riversleigh Siltstone	289	18	2.25	2.11	0.03-11.3	1.1	3.2	0.11-13.41	242	931	2-3855	510	62	418-603
	Isa	Mt Les Siltstone	48	12	0.97	0.97	0.03-4.07	1.40	0.69	0.10-1.94	85	34	37-132	453	6	441-463
	Birrindudu	Battle Creek Formation	31	13	0.22	0.18	0.01-0.67	0.16	0.06	0.12-0.60	162	243	43-800	527	69	406-609
	Birrindudu	Timber Creek Formation	45	4	0.12	0.17	0.01-0.87	1.55	1.13	0.12-0.45	348	273	88-731	449	32	421-494
Unspecified	McArthur	Wollogorang Formation	94	23	1.18	1.57	0.02-6.97	2.90	2.71	0.18-10.78	92	45	6-158	438	15	412-475

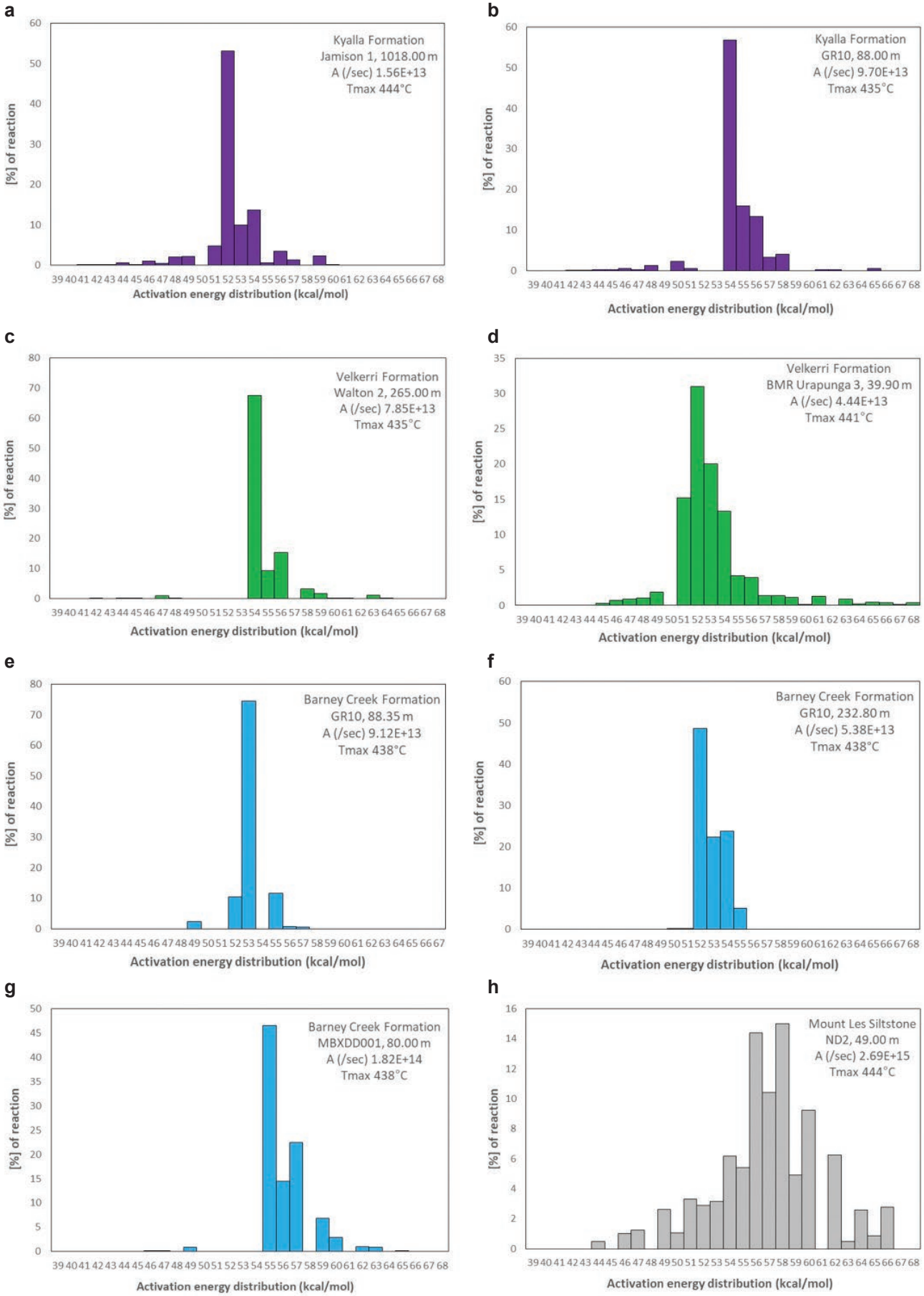

Figure 6. Bulk kinetic discrete activation energy distributions of source rocks. (**a–b**) the Kyalla Formation. (**c–d**) Velkerri Formation. (**e–g**) Barney Creek Formation in addition to the Mount Les Siltstone of the Isa Superbasin. (**h**) Activation energy distribution based on multiple heating rates (0.7; 2.0; 5.0; 15.0 K/min). Data generated in this study (**d, e** and **f**) and from Revie and Normington (2018) (**a, b, c, g** and **h**).

Palaeozoic and older (pre-land plants) organic matter (eg Shannon *et al* 2018).

Variations in the geochemistry of the preserved organic matter may be inherited from differences in the contributing biomass, degree of reworking, and the depositional environment; this results in different frequency factors (A) and HI_o (Hantschel and Kauerauf 2009). It is important to understand this variation for a petroleum systems model as different kinetics will result in the petroleum generation occurring at different times and temperatures. One sample from the Isa Superbasin, the Mount Les Siltstone from *ND2* (**Figure 1**), has a broad Ea distribution, peak conversion temperature (TR = 0.5) at 165°C and primary conversion >200°C. This suggests very high thermal stability and a kerogen type between the fluvio-deltaic organofacies D/E and F (**Figure 7**). The differences in bulk kinetics between the Mount Les Siltstone and the coeval Barney Creek Formation suggests that there are complexities in the initial petroleum supersystem framework defined by Bradshaw *et al* (1994), and that predictions from one source rock might not be transferable to other coeval units. Future work is required to obtain a larger bulk kinetic dataset for northern Australian source rocks to determine how representative these results are at a regional scale.

Bulk kinetics focus on kerogen cracking and cannot distinguish between various petroleum products. We therefore recommend further experiments to better characterise the organic matter including: compositional and phase kinetics

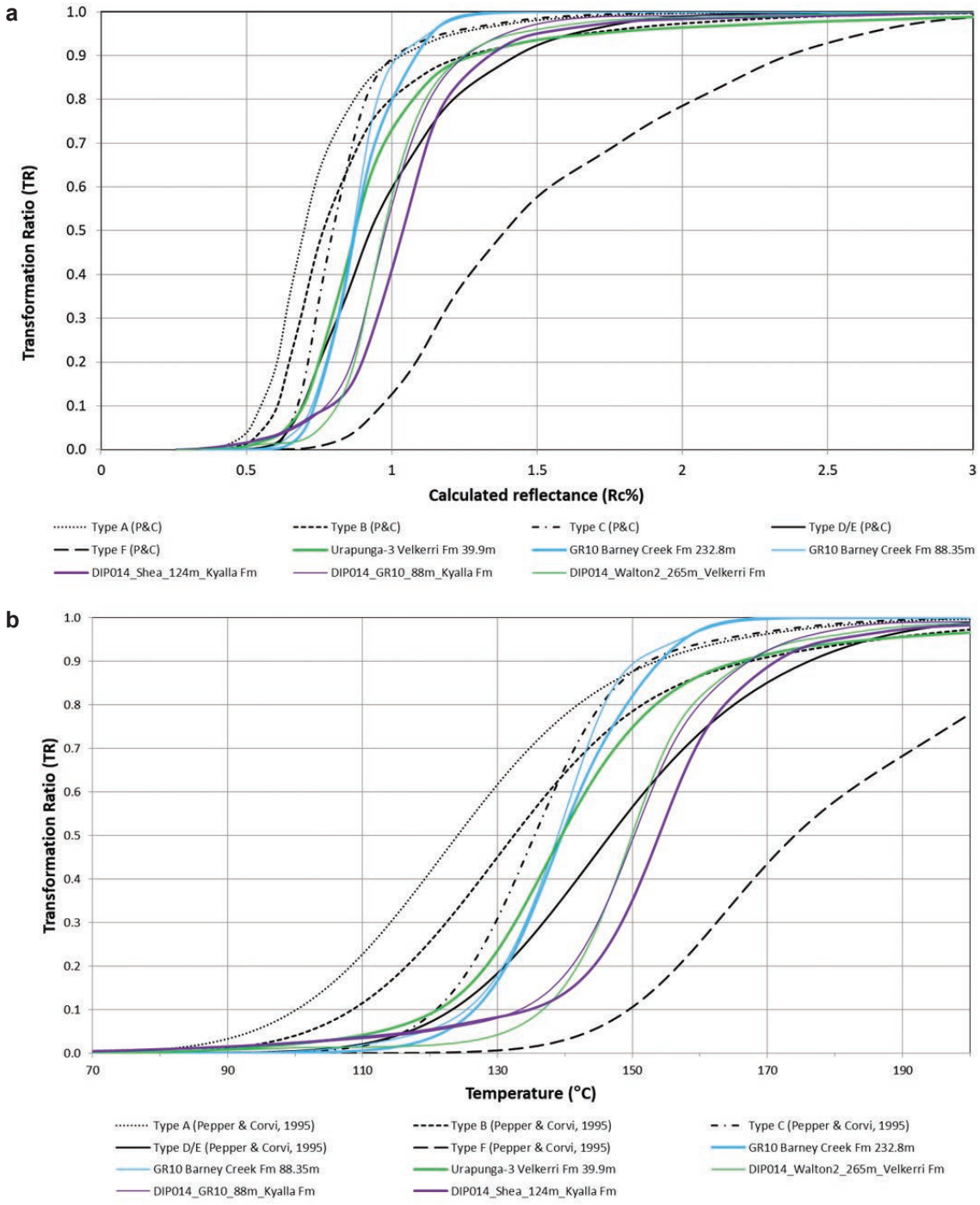

Figure 7. Transformation ratio (TR) curves calculated using bulk kinetics generated in this study in addition to data from Revie and Normington (2018). **(a)** TR plotted against maturity (calculated vitrinite reflectance equivalent; Rc%). **(b)** TR plotted against temperature (°C).

to predict evolving gas-to-oil ratios with maturation and to model fluid properties at surface conditions; Microscale sealed vessel (MSSV) pyrolysis for organofacies type distributions (eg Mahlstedt *et al* 2015); and spatial variability definition of bulk kinetics to determine heterogeneity of organic matter, which is useful in calibrating a petroleum systems model.

Fluid geochemistry

Identifying the source/s of migrated hydrocarbon fluids is important in defining the petroleum system and assisting in petroleum exploration (Magoon and Dow 1994). The source of the oil collected during a drill stem test from well *Jamison 1* (**Figure 1**) in the McArthur Basin within the Jamison sandstone, for example, has not been geochemically typed to a source rock. Geochemically differentiating between the Kyalla and Velkerri formations has remained elusive due to the similarities between the typical biomarker (triterpane) assemblage prevalent in Mesoproterozoic systems and the relative homogeneity of isotopes over the so called 'boring billion' time period (eg Cawood and Hawkesworth 2014, Pawlowska *et al* 2013, Jarrett *et al* 2019).

Hydrocarbon biomarkers show general similarities in saturated fractions, such as a large unresolved complex mixture (UCM) and a relatively high proportion of monomethyl alkanes relative to regular *n*-alkanes and regular diahopanes, but there are differences in both the saturated and aromatic isoprenoids between formations due to a shift in microbial assemblages and different water chemistries. Euxinic waters in the Barney Creek Formation contain 2,3,4- and 2,3,6-trimethyl aryl isoprenoids, which are biomarkers for the purple and green sulfur bacteria respectively (Brocks *et al* 2005, Jarrett *et al* 2018d); however, the largely ferruginous Roper Group does not contain these molecules (Jarrett *et al* 2018d, Jarrett *et al* 2019; **Figures 8** and **9**).

Stable carbon isotopic signatures ($\delta^{13}C$) of *n*-alkanes and the bulk saturated and aromatic hydrocarbon fractions were used to identify differences between source rocks, the produced oil, and oil stains in the McArthur Basin, as $\delta^{13}C$ has proved useful for determining oil–oil and oil–source rock correlations (eg Murray *et al* 1994, Boreham and Ambrose 2007, Edwards *et al* 2013). Source rocks in the Velkerri Formation have *n*-alkane $\delta^{13}C$ values ranging from -35.0‰ to -30.7‰ and those the Kyalla Formation range from -33.6‰ to -28.7‰, indicating a large overlap between the source rocks in the Roper Group (**Figure 10**). However, there is an isotopic differentiation between the Mesoproterozoic Roper Group and the Paleoproterozoic Barney Creek Formation, which has more isotopically enriched values between -24‰ and -29‰ (**Figure 10**). As the Barney Creek Formation dataset is limited to one well, further analyses are required to produce a statistically significant regional dataset.

The $\delta^{13}C$ of *n*-alkanes of oil stains in the Velkerri Formation are in the range from -33.7‰ to -31.9‰ and sit within the most isotopically depleted source rock interval within this formation (**Figure 9**). This provides strong evidence for self-sourcing of the oil stains. Oil stains from

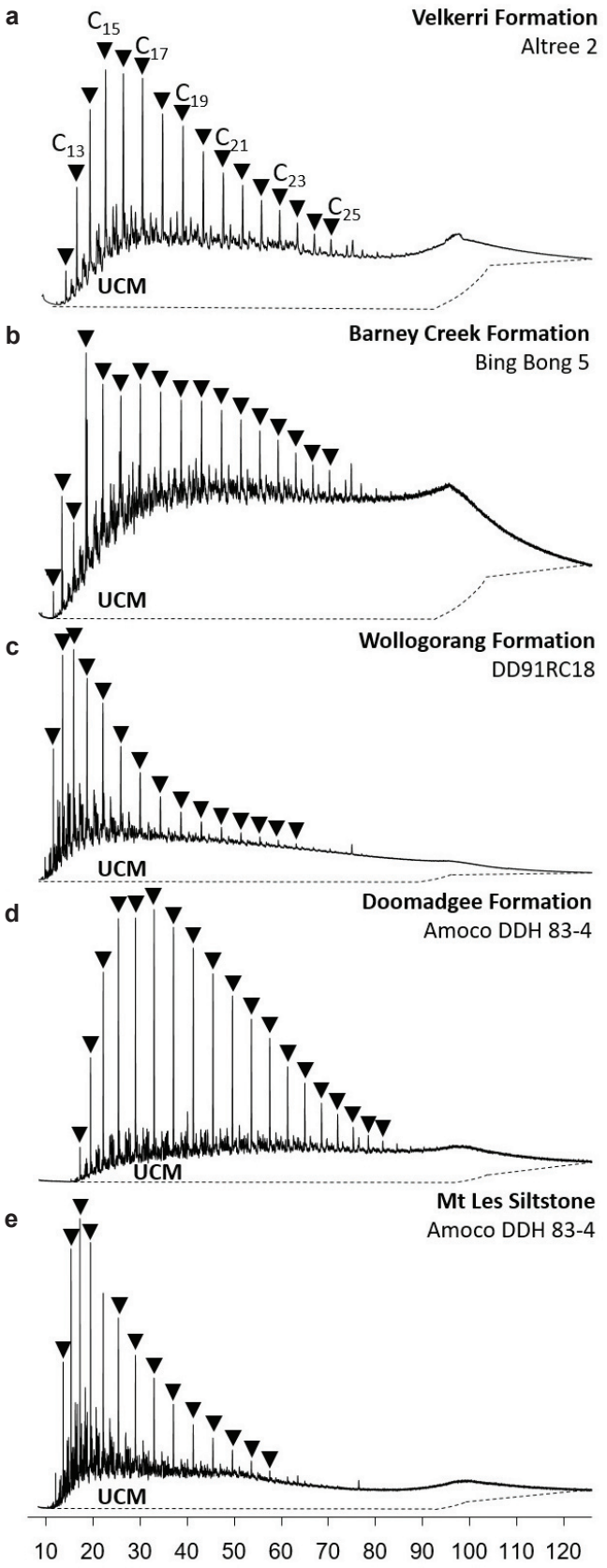

Figure 8. Gas chromatograph-mass spectrometer (GC–MS) total ion chromatograms of characteristic source rock extracts in the (**a**) Velkerri, (**b**) Barney Creek, (**c**) Wollogorang formations of the McArthur Basin, and the (**d**) Doomadgee and (**e**) Mount Les Siltstone of the Isa Superbasin. All extracts contain a large UCM, high ratios of mid-chained and terminal branching mono methyl alkanes to *n*-alkanes. Only the Barney Creek and Wollogorang formations contain high concentrations of saturated isoprenoids including pristine and phytane.

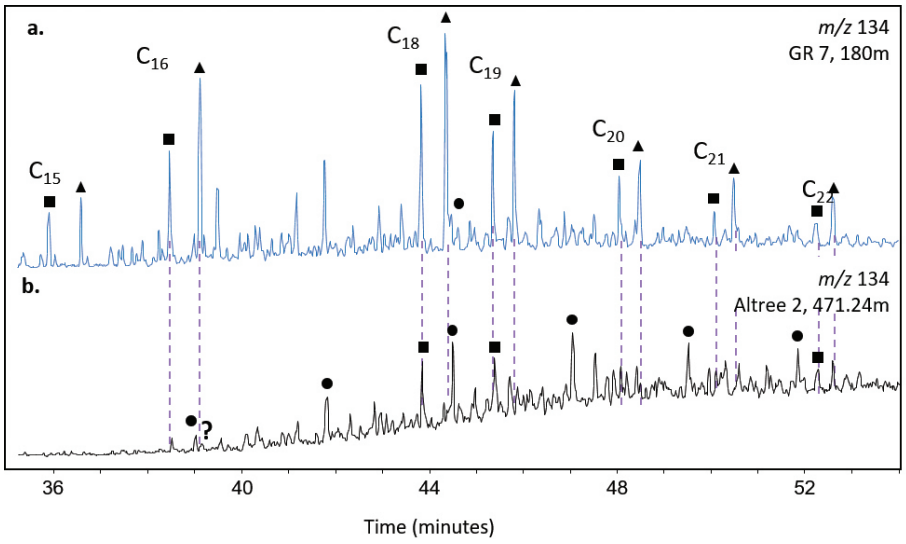

Figure 9. The Barney Creek Formation (GR7 180 m; blue lines) is dominated by 2,3,4- and 2,3,6- trimethyl aryl isoprenoids (triangles and squares), biomarkers for green and purple sulfur bacteria respectively, which inhabit the euxinic photic zone. These molecules are below detection limits in the Velkerri (Altree 2 471.24 m; black lines), Kyalla and Doomadgee formations, and Mount Les Siltstone; these sediments contain trimethyl alkylbenzenes (circles).

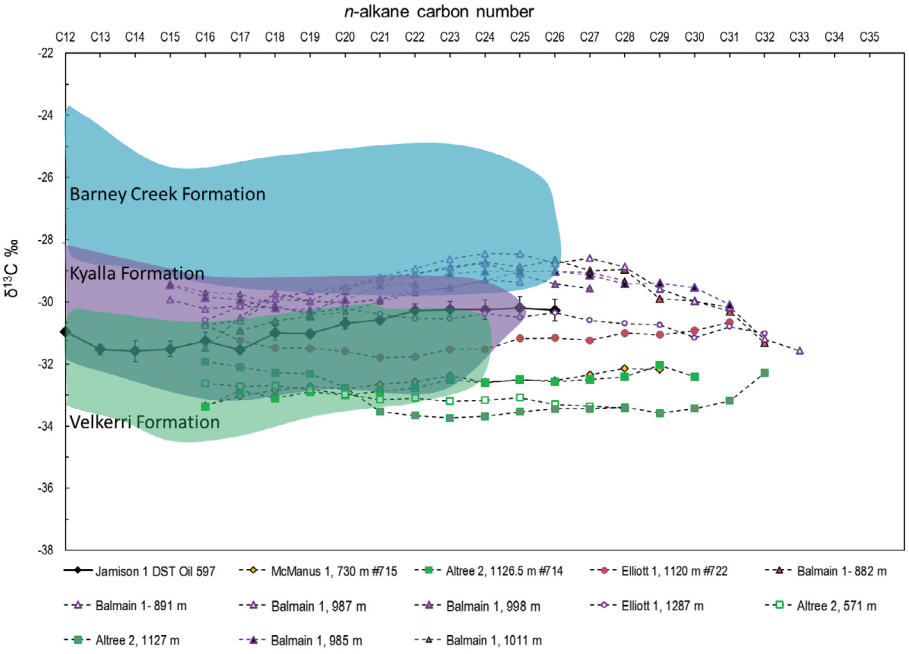

Figure 10. Carbon specific isotope analysis of *n*-alkanes for oil-source rock correlations in the Roper Group, McArthur Basin. Solid black line indicates the *Jamison 1* oil, the only fluid from a drill stem test; dashed lines indicate oil stains from the Kyalla Formation (purple), Velkerri Formation (green), Moroak Sandstone (red) and the Jamison sandstone (yellow). Shaded areas demonstrate the ranges of source rocks from the Kyalla Formation (purple), Velkerri Formation (green) and Barney Creek Formation (blue).

the Kyalla Formation are in the range -31.5‰ to -28.45‰. These values are within the envelope of Kyalla Formation source rocks; however, low- to medium-chained *n*-alkanes (<*n*-C_{20}) also overlap into values of the most enriched Velkerri Formation (**Figure 9**). Carbon specific isotopes of *n*-alkanes in the *Jamison 1* oil range from -31.5‰ to -30.2‰ and sit within the Velkerri Formation source rock envelope for values <*n*-C_{20} and within the Kyalla Formation for values >*n*-C_{20} (**Figure 7**). The *n*-alkane profile of the *Jamison 1* oil appears to have a similar trend to the Kyalla Formation self-sourced oil stains and is therefore likely to have been sourced from the Kyalla Formation. The *n*-alkane envelope for the Barney Creek Formation is significantly more enriched in $\delta^{13}C$ than those values seen for both source rocks and oils derived from the Roper Group (**Figure 9**).

A comparison of stable carbon ($\delta^{13}C$) saturate and aromatic isotopic values has been shown to define major Palaeozoic oil families in Australia (Edwards and Summons 1996, Edwards *et al* 1997, Summons *et al* 2002). These general trends in bulk $\delta^{13}C$ are depicted in **Figure 11** for oils and oil shows in the Arafura Basin, Northern Territory (Moore *et al* 1996); Canning Basin, Western Australia (Edwards *et al* 1997, 2013); and in the Georgina Basin, Northern Territory and Queensland (Boreham and Ambrose 2005). These results show that, in general, Palaeozoic marine oils become isotopically depleted with age. Roper Group oils and oil stains are isotopically even more depleted than the Palaeozoic oils, and have some of the most depleted carbon isotopic signatures of any Australian crude oil. Oil stains within the Velkerri Formation are the most isotopically depleted with $\delta^{13}C$ values between -35‰ and -31‰. Kyalla Formation oil stains are slightly more enriched, with values ranging from -32‰ to -29‰, similar to Cambrian and Ordovician oils. The *Jamison 1* oil sits within the cluster of Kyalla Formation oil stains, thus providing further evidence for a Kyalla Formation source (**Figure 11**).

Thermal and burial history

Proterozoic sedimentary basins in northern Australia have a complex thermal history due to a multitude of factors

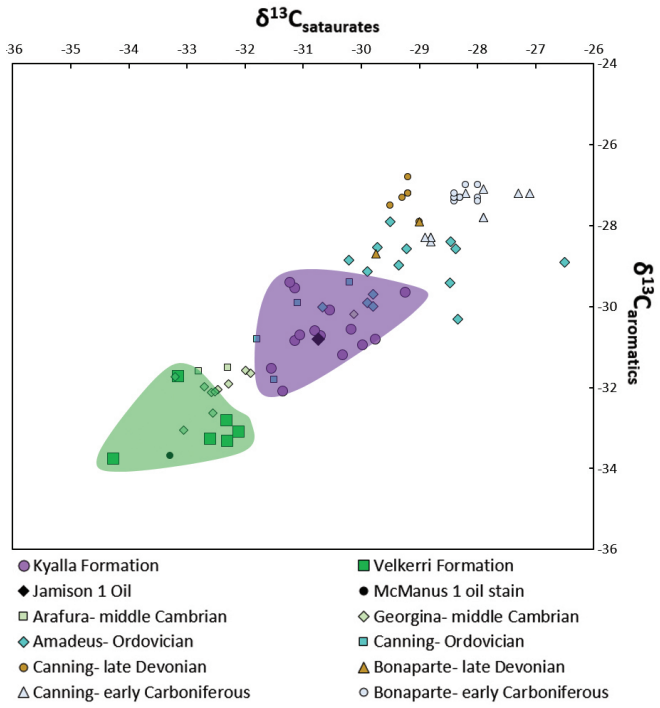

Figure 11. Cross plot of $\delta^{13}C$ saturated verses $\delta^{13}C$ aromatic hydrocarbon fractions comparing the Urapunga Supersystem oils and oil shows from the McArthur Basin with Australian Palaeozoic oils. Data sourced from Boreham and Ambrose (2007), Edwards and Summons (1996), Edwards and Zumberge (2005) and Edwards *et al* (1997, 2013).

including: faulting (Etheridge and Wall 1994), hydrothermal fluid flow (Glikson *et al* 2006, Golding *et al* 2006 and references therein), igneous intrusions (Abbott *et al* 2001), and uncertainties on the overburden desposition through time (eg Palu *et al* 2018). To date, the only published burial history models for the McArthur Basin are by Crick (1989), Silvermann *et al* (2005) and Hoffman (2016). Silvermann *et al* (2005) and Hoffman (2016) both modelled wells in the Beetaloo Sub-basin; Crick (1989) modelled two drillholes and one petroleum well in the Glyde Sub-basin. The models of Crick (1989) demonstrate oil-window maturity in both the Barney Creek Formation and the Velkerri Formation. Despite variability in the input parameters used in the Hoffman (2016) and Silvermann *et al* (2005) models, eg the heat flow applied and the amount and timing of burial, both come to a similar conclusion as that of Crick (1989). Although source rock deposition occurred during the Mesoproterozoic, primary and secondary migration may have been active much later.

The *EFTF* program is investigating the regional burial and thermal history of Proterozoic sedimentary basins in northern Australia. Recent petroleum systems modelling work on the Lawn Hill Platform indicates a major burial event during the middle Mesoproterozoic related to deposition of the South Nicholson Basin (Palu *et al* 2018). Further work will investigate the thermal and burial history of the greater McArthur Basin and the South Nicholson Basin with a focus on the newly imaged Barkly Sub-basin (see Carr *et al* 2019).

Conclusions

Geoscience Australia is undertaking a detailed geochemical and petroleum systems study of northern Australian basins to better understand the hydrocarbon prospectively of the region and thus reduce exploration risk. One technique is to use the petroleum systems approach to compare the McArthur Basin to the frontier South Nicholson Basin and Isa Superbasin. This study has focused on the source rock component of the Mesoproterozoic Urapungan and Paleoproterozoic McArthur petroleum supersystems.

Geochemical data has demonstrated that the Urapungan and McArthur petroleum supersystems host good to excellent source rocks with the potential to generate both oil and gas in the McArthur Basin, as well as in the South Nicholson Basin and Isa Superbasin. Most kerogens in greater McArthur Basin source rocks are characterised by narrow activation energy distributions with high thermal stability that require high (140–160°C) temperatures for peak generation. Inherent variabilities within the kerogen kinetics and petroleum generative potential may be due to differences in organofacies; this requires further investigation. Although there are many similarities between the biomarker signatures, the stable carbon isotopes of both bulk saturate and aromatic fractions and *n*-alkanes can differentiate between source rocks and their derived oils within the Proterozoic. Specifically, the Paleoproterozoic Barney Creek Formation is more enriched in $\delta^{13}C$ than the Mesoproterozoic Roper Group. Importantly, the only oil to have flowed to surface in the McArthur Basin is from the *Jamison 1* drill stem test, which has been geochemically typed to a source rock within the Kyalla Formation. The results of this study provide a platform to target future work in northern Australia.

Acknowledgments

We would like to thank Junhong Chen, Ziqing Hong, Neel Jinadasa, Prince Palatty and Jacob Sohn for technical assistance in the organic geochemistry and isotope laboratory at Geoscience Australia; and Tamara Buckler for managing the Oracle databases. Darryl Stacey from the Darwin Core Library of the Northern Territory Geological Survey and Jamie Langford (Geoscience Australia) facilitated access to drillcore. Dr Junhong Chen and Dr Jade Anderson are thanked for their internal peer reviews. This extended abstract is published with the permission of the CEO, Geoscience Australia.

References

Abbott ST, Sweet IP, Plumb KA, Young DN, Cutovinos A, Ferenczi PA, Brakel A and Pietsch BA, 2001. *Roper Region: Urapunga and Roper River Special, Northern Territory (Second Edition). 1:250 000 geological map series explanatory notes, SD 53-10, SD53-11.* Northern Territory Geological Survey, Darwin.

Ahmad M and Scrimgeour IR, 2013. Chapter 2: Geological Framework: in Ahmad M and Munson TJ (compilers). *'Geology and Mineral Resources of the Northern Territory'. Northern Territory Geological Survey, Special Publication* 5.

Boreham CJ and Ambrose G, 2007. Cambrian petroleum systems in the southern Georgina Basin, Northern

Territory, Australia: in '*Central Australian Basins Symposium II (CABS), Alice Springs, NT, 16–18 August, 2005'. Northern Territory Geological Survey, Special Publication* 2. 254–281.

Bradshaw MT, Bradshaw J, Murray AP, Needham JD, Spencer L, Summons RE, Wilmot J and Winn S, 1994. Petroleum systems in West Australian basins: in '*The Sedimentary Basins of Western Australia, Proceedings of Petroleum Exploration Society of Australia Symposium, 1994'*, 93–118.

Brocks JJ, Love GD, Summons RE, Knoll AH, Logan GA and Bowden SA, 2005. Biomarker evidence for green and purple sulphur bacteria in a stratified Palaeoproterozoic sea. *Nature* 437, 866–870.

Carr LK, Southby C, Henson P, Carson P, Anderson J, MacFarlane SK, Jarrett A, Fomin T and Costelloe R, 2019. Exploring for the Future: South Nicholson Basin Region project outcomes and sequence stratigraphy: in '*Annual Geoscience Exploration Seminar (AGES) Proceedings, Alice Springs, Northern Territory, 19–20 March 2019*'. Northern Territory Geological Survey, Darwin (this volume).

Cawood PA and Hawkesworth CJ, 2014. Earth's middle age. *Geology* 42(6), 503–506.

Close DF, 2014. The McArthur Basin: NTGS' approach to a frontier petroleum basin with known base metal prospectivity: in '*Annual Geoscience Exploration Seminar (AGES) 2014. Record of abstracts'. Northern Territory Geological Survey, Record* 2014-001.

Coté A, Richards B, Altmann C, Baruch E and Close D, 2018. Australia's premier shale basin: five plays, 1 000 000 000 years in the making. *The APPEA Journal* 58, 799–804.

Cox GM, Jarrett AJM, Shannon AV, Close D, Baruch ET, Blades ML, Hall PA, Yang B, Collins, AS and Farkas J, 2018. A very unconventional hydrocarbon play: the ca. 1.5 to 1.3 billion year old Roper Basin of northern Australia. *AAPG Bulletin* (Preprint).

Crick IH 1989. *Petrological and maturation characteristics of organic matter from the middle Proterozoic McArthur Basin, Australia*. PhD thesis, University of Wollongong, Australia.

Department of Primary Industry and Resources, 2017. *Concealed Geological Boundaries*. ANZLIC Identifier: 5EFEB9B61E918EA1E050CD9B2144457E. [Accessed June 2018].

Edwards DS and Summons RE, 1996. Petrel Sub-basin Study 1995–96. Organic Geochemistry of Oils and Source Rocks. *Australian Geological Survey Organisation (AGSO), Record* 1996/42, Canberra.

Edwards DS and Zumberge JE, 2005. *The oils of Western Australia II. Regional petroleum geochemistry and correlation of crude oils and condensates from Western Australia and Papua New Guinea*. Geoscience Australia and GeoMark Research Ltd unpublished report, Canberra and Houston. GEOCAT 37512.

Edwards DS, Summons RE, Kennard JM, Nicoll RS, Bradshaw J, Bradshaw M, Foster CB, O'Brien GW and Zumberge JE. 1997. Geochemical characterisation of Palaeozoic petroleum systems in north-western Australia. *APPEA Journal* 37, 351–79.

Edwards DS, Boreham CJ, Chen J, Grosjean E, Morey AJ, Sohn J and Zumberge JE, 2013. Stable carbon and hydrogen isotopic compositions of Paleozoic marine crude oils from the Canning Basin: comparison with other west Australian crude oils: in Keep M and Moss S (editors). '*The sedimentary basins of West Australia IV. Proceedings of the Petroleum Exploration Society of Australia Symposium, Perth, WA, 18–21 August 2013*'.

Etheridge MA and Wall V, 1994. Tectonic and structural evolution of the Australian Proterozoic. *Geological Society of Australia Abstracts* 37, 102–103.

Frichot L, Revie D and Munson TJ, 2017. The Vaughton Siltstone of the northern McArthur Basin: Preliminary data and issues related to assessing its potential as a petroleum source rock. *Northern Territory Geological Survey, Technical Note* 2017-002.

Frogtech Pty Ltd, 2006. *OZSEEBASE Proterozoic Basins Study*. Report to Geoscience Australia.

Frogtech Geoscience, 2018a. SEEBASE® study and GIS for greater McArthur Basin. *Northern Territory Geological Survey, Digital Information Package* DIP 017.

Frogtech Geoscience, 2018b. North West Queensland SEEBASE® Study and GIS. *Queensland Geological Record* 2018/03.

Glikson M, Golding SD and Southgate P, 2006. Thermal evolution of the ore-hosting Isa Superbasin: Central and Northern Lawn Hill Platform. *Economic Geology* 101, 1211–1229.

Golding SD, Uysal IT, Glikson M, Baublys KA and Southgate PN, 2006. Timing and chemistry of fluid-flow events in the Lawn Hill Platform, northern Australia. *Economic Geology* 101(6), 1231–1250.

Hantschel TA and Kauerauf AI, 2009. *Fundamentals of Basin and Petroleum Systems Modelling*. Springer, USA.

Hoffman TW, 2015. Recent drilling results provide new insights into the western Palaeoproterozoic to Mesoproterozoic McArthur Basin: in '*Annual Geoscience Exploration Seminar (AGES) 2015. Record of abstracts'. Northern Territory Geological Survey, Record* 2015-002.

Hoffman TW, 2016. Roper Basin burial history modelling: inferences for the timing of hydrocarbon generation: in '*Annual Geoscience Exploration Seminar (AGES) Proceeding, Alice Springs, Northern Territory 15–16 March 2016'*. Northern Territory Geological Survey, Darwin.

Jarrett AJM, Hall L, Carr L, Anderson J, Orr ML, Bradshaw BE and Henson P, 2018a. Source rock geochemistry of the Isa Superbasin and South Nicholson Basin, northern Australia: baseline regional hydrocarbon prospectivity. *Geoscience Australia, Record* 2018-038.

Jarrett, AJM, Chen J, Hong Z, Palatty P, Anderson J, McLennan S, Lewis C and Henson P, 2018b. Exploring for the Future - Source rock geochemistry data of the Isa Superbasin and South Nicholson Basin, TOC and Rock-Eval data release, northern Australia: baseline regional hydrocarbon prospectivity. *Geoscience Australia, Record* 2018/45.

Jarrett AJM, Cox GM, Brocks JJ, McLennan SM, Thorne J, Huston D, Champion D, Shannon AV, Vinnichenko G,

Johnson B and Henson P, 2018d. Geochemistry of organic rich shales in the Roper and Isa Superbasins of northern Australia. *Australian Geoscience Council Convention Abstract*. 14–18 October 2018, Adelaide, South Australia.

Jarrett AJM, Cox GM, Brocks JJ, Boreham CJ, Edwards DS and Grosjean E, in press. Microbial assemblage and paleoenvironmental reconstruction of the 1.3 Ga Velkerri Formation, McArthur Basin, northern Australia. *Geobiology*.

Magoon LB and Dow WG, 1994. The Petroleum System–From source to trap. *American Association of Petroleum Geologists Memoir* 60.

Mahlstedt N, di Primio R, Horsfield B and Boreham CJ, 2015. Multicomponent kinetics and late gas potential of selected Cooper Basin source rocks. *Geoscience Australia, Record* 2015/19.

Moore A, Bradshaw J and Edwards D, 1996. Geohistory modelling of hydrocarbon migration and trap formation in the Arafura Sea. *Petroleum Exploration Society of Australia (PESA) Journal* 24, 35–51.

Munson TJ, 2014. Petroleum geology and potential of the onshore Northern Territory, 2014. *Northern Territory Geological Survey, Report* 22.

Munson TJ, 2016. Sedimentary characterisation of the Wilton package, greater McArthur Basin, Northern Territory. *Northern Territory Geological Survey, Record* 2016-003.

Murray AP, Summons RE, Boreham CJ, Dowling LM. 1994. Biomarker and *n*-alkane isotope profiles for Tertiary oils: relationship to source rock depositional setting. *Organic Geochemistry* 22, 521–542.

Palu TJ, Jarrett AJM, Boreham C, Hall LS, Bradshaw BE and Orr M, 2018. Challenges and possible solutions for burial and thermal history modelling of the Lawn Hill Platform, Isa Superbasin: in Edwards DS, Grosjean E, Brocks JJ and van Maldegem M (compilers). '*20th Australian Organic Geochemistry Conference: Origins of Oil, Old Organics and Organisms Program and Abstracts: 3–7 December 2018, Canberra, Australia'. Geoscience Australia, Record* 2018/44, 117–118.

Pawlowska MM, Butterfield NJ and Brocks JJ, 2013. Lipid taphonomy in the Proterozoic and the effect of microbial mats on biomarker preservation. *Geology* 41, 103–106.

Pepper AS and Corvi PJ, 1995. Simple kinetic models of petroleum formation. Part I: oil and gas generation from kerogen. *Marine and Petroleum Geology* 12, 291–319.

Peters KE and Cassa MR, 1994. Applied source rock geochemistry: in Magoon, LB and Dow, WG (editors). '*The Petroleum System - From source to trap'. American Association of Petroleum Geologists Memoir* 60, 93–120.

Raymond OL, Totterdell JM, Stewart AJ and Woods MA 2018. *Australian Geological Provinces, 2018.01 edition*. Geoscience Australia, Canberra. <https://ecat.ga.gov.au/geonetwork/srv/eng/catalog.search?node=srv#/metadata/116823>.

Revie D 2017a. Volumetric resource assessment of the lower Kyalla and middle Velkerri formations of the McArthur Basin: in '*Annual Geoscience Exploration Seminar (AGES) Proceedings, Alice Springs, Northern Territory, 28 – 29 March 2017*'. Northern Territory Geological Survey, Darwin.

Revie D, 2017b. Unconventional petroleum resources of the Roper Group, McArthur Basin. *Northern Territory Geological Survey, Record* 2017-002.

Revie D and Normington VJ, 2018. Shale resource data from the greater McArthur Basin. *Northern Territory Geological Survey, Digital Information Package* DIP 014.

Shannon AV, Cox GM, Jarrett AJM, Blades M, Hall P, Cassidy E, Bishop C and Collins A, 2018. Are Precambrian type III and IV kerogens the result of heterotrophic communities? *Australian Geoscience Council Convention*, *Abstract*. 14–18 October 2018, Adelaide, South Australia.

Silvermann MR, Landon SM, Leaver JS, Mather TJ and Bery E, 2005. No fuel like an old fuel: Proterozoic oil and gas potential in the Beetaloo Basin, Northern Territory, Australia: in Munson TJ and Ambrose GT (editors). '*Proceedings of the Central Australian Basins Symposium (CABS), Alice Springs, Northern Territory, 16–18 August 2005*'. *Northern Territory Geological Survey, Special Publication* 2, 205–215.

Summons RE, Zumberge JE, Boreham CJ, Bradshaw MT, Brown SW, Edwards DS, Hope JM and Johns N, 2002. *The oils of eastern Australia: Petroleum geochemistry and correlation*. Geoscience Australia, Canberra. GeoMark Research Inc, Houston. http://www.ga.gov.au/metadata-gateway/metadata/record/68754/.

Tissot BP and Welte DH, 1984. *Petroleum formation and occurrence*. Springer-Verlag, Berlin Germany.

Weatherford Laboratories, 2017. Kyalla and middle Velkerri Resource Assessment: Gorrie, Beetaloo, OT Downs, and Broadmere Sub-basins. Study Project No. AB-74329. *Northern Territory Geological Survey, Record* 2017-003.

A multidisciplinary evaluation of the Velkerri Formation in the Beetaloo Sub-basin: Implications for geological history and reservoir quality

Claudio Delle Piane[1,2], I Tonguc Uysal[1], Zhejun Pan[3], Julien Bourdet[1], Zhongsheng Li[4], Mark D Raven[5] and David N Dewhurst[1]

Introduction

The Proterozoic (ca 1.43 Ga) Velkerri Formation of the Roper Group (McArthur Basin, Northern Territory) is believed to host one of the world's oldest petroleum systems (Jackson *et al* 1986). Due to its excellent source rock characteristics, the formation is currently the target of exploration activities in the Beetaloo Sub-basin within the greater McArthur Basin, Northern Territory. This unconventional resource hosts vast quantities of liquid and gas hydrocarbons and spans an aerial extent of nearly 80 000 km^2 with thicknesses reaching up to 800 m (Abbott and Sweet 2000, Munson 2016).

The preservation of this 'live' petroleum system is a geological wonder and implies that the Velkerri Formation has not been dramatically affected by major tectonic or metamorphic events. It has remained at relatively shallow depths since its deposition approximately 1.4 billion years ago, and has been exposed to maximum temperatures consistent with hydrocarbon generation. Moreover, the composition of the oil found in the Velkerri Formation is consistent with derivation from organic matter composed of bacteria and primitive algae deposited in a marine environment (eg Munson 2016). The Velkerri Formation has been divided into three members, the Kalala (lower), Amungee (middle) and Wyworrie (upper) members (Munson and Revie 2018). The Amungee Member, previously referred to as the middle Velkerri, shows the highest organic richness and thermal maturation of the same, which has resulted in large quantities of potentially recoverable resources estimated as 118–293 trillion cubic feet in volume (Revie 2017). Of prime importance among the sources of uncertainty associated with this wide range of estimated resources are: i) reservoir characterisation, and ii) age dating of burial and tectonic events controlling the thermal evolution, hydrocarbon generation and expulsion history of the sedimentary rocks hosting the resource. Moreover, sills of the Derim Derim Dolerite emplaced at ca 1.32 Ga intrude the Velkerri Formation, as seen in a number of wells in the Beetaloo Sub-basin, providing a thermal perturbation likely affecting the maturity of the hydrocarbon source rock, at least locally.

The scope of this work, therefore, was to complement the existing knowledge on the characteristics of the Velkerri Formation summarised in data released by the Northern Territory Geological Survey (eg Revie and Normington 2018). In particular, our study focuses on samples at various levels of thermal maturation collected from the cored sections of the Amungee Member of the Velkerri Formation intersected in six wells (Altree 2, Borrowdale 2, Walton 2, Lady Penrhyn 2, Shenandoah 1A and Tarlee S3) in order to characterise the following parameters:

- whole rock and clay mineralogy and crystallinity [via x-ray diffraction (XRD)]
- maceral types and maturity assessment (via light reflectance, pyrolysis and Raman spectroscopy)
- porosity and pores size distribution (via mercury intrusion porosimetry)
- methane adsorption capacity (via laboratory measurements at reservoir conditions)
- permeability and its anisotropy (via multidirectional laboratory measurements)
- diagenetic events affecting the shales microstructure (via optical and electron microscopy)
- geochronology of diagenetic events (via K–Ar dating of diagenetic illite and U–Pb dating of diagenetic calcite).

Thermal maturity cannot be determined by conventional vitrinite reflectance analysis because deposition of these ancient sedimentary rocks predate the evolution of land plants; therefore, we used different organic and mineral thermal maturation indices including: i) illite crystallinity, ii) other maceral reflectances, and iii) Raman spectroscopy of organic material.

Results

XRD results indicate that the mineralogy of the whole rock samples is dominated by quartz and clay minerals. Analysis of the clay fraction shows that these are mainly mixed layer smectite/illite with illite content between 70 and 90%. Detailed analysis of the 0.2–2 µm fraction show that the 10Å illite peak is best fitted by two almost overlapping peaks interpreted as two generations of diagenetic illite. For this limited dataset, illite crystallinity increases almost linearly with depth and is highest in samples located in proximity to documented doleritic intrusions (ie Tarlee S3 samples).

Organic richness of the shale samples, as quantified by the total organic carbon (TOC) content, ranges between 1.2% (Shenandoah 1A sample, 2517.28 m) to 10.7% (Walton 2 sample, 397.85 m). For all samples studied, the organic components identified by optical microscopy are mainly composed of bitumen with lesser amount of alginite, with one exception (Walton 2 sample: 397.85 m) having major alginite instead. The bitumens have mean reflectance values ranging between 0.28% (Walton 2: 397.85 m) to 4.03% (Tarlee S3: 1438.61 m).

Maximum palaeo-temperatures were estimated from the analysis of the Raman spectra obtained from organic

[1] CSIRO Energy, Australian Resources Research Centre, 26 Dick Perry Avenue, Kensington WA 6151, Australia
[2] Email: claudio.dellepiane@csiro.au
[3] CSIRO Energy, Private Bag 10, Clayton South VIC 3169, Australia
[4] CSIRO Energy, 11 Julius Ave, North Ryde NSW 2113, Australia
[5] CSIRO Land and Water, Waite Road, Urrbrae SA 5064, Australia

particles using the geothermometer proposed by Kouketsu *et al* (2014). The data set returns palaeo-temperatures ranging between 67°C (Lady Penrhyn 2: 376.66 m) and 233°C (Tarlee S3: 1438.61 m). The data recorded a positive correlation between estimated palaeo-temperatures and mean bitumen reflectance, with anomalously high values recorded in the sample from the Tarlee S3 well closest to the top of the dolerite intrusion.

Microstructural analysis reveals the presence of common features in samples, irrespective of their thermal maturity and geographical position. These are illustrated in **Figure 1** and include:

- a bedded appearance defined by the alignment of elongate detrital particles and stringers of organic matter (**Figure 1a**)
- diagenetic phases like blocky pyrite (**Figure 1a**) and apatite spherules of possible bacterial origin (**Figure 1b**)
- a microcrystalline matrix composed of interspersed clays and quartz (**Figure 1c**)
- micron to sub-micron scale pores hosted in what is interpreted to be migrated bitumen (**Figure 1d**).

Bitumen porosity is interpreted to be the dominant contribution to the total porosity of the samples as shown by a positive correlation between TOC and the volume of mesopores (10 nm < size < 50 nm), measured by mercury intrusion porosimetry. Indeed, methane adsorption curves measured on this data set at temperatures up to 80°C also show that TOC is one of the main factors controlling the amount of adsorbed gas in the Velkerri Formation. The laminated nature of the sediment imparts a significant anisotropy to the permeability experimentally measured in the laboratory on cubic samples. At an effective pressure of 6.7 MPa, permeability along the bedding can be up to 0.2 mD and around 3 orders of magnitude higher than across the bedding.

K–Ar dating of diagenetic illite extracted from samples of the Altree 2, Borrowdale 2, Shenandoah 1A and Tarlee S3 wells consistently show a well-defined thermal maximum at 1030 ± 25 Ma. Considering that hydrocarbon generation and smectite illitisation occur within the same range of temperature, these dates can help improve the understanding of the timing of hydrocarbon generation within the Velkerri Formation. Furthermore, analysis of selected samples under ultraviolet light reveal strong fluorescence from oil trapped

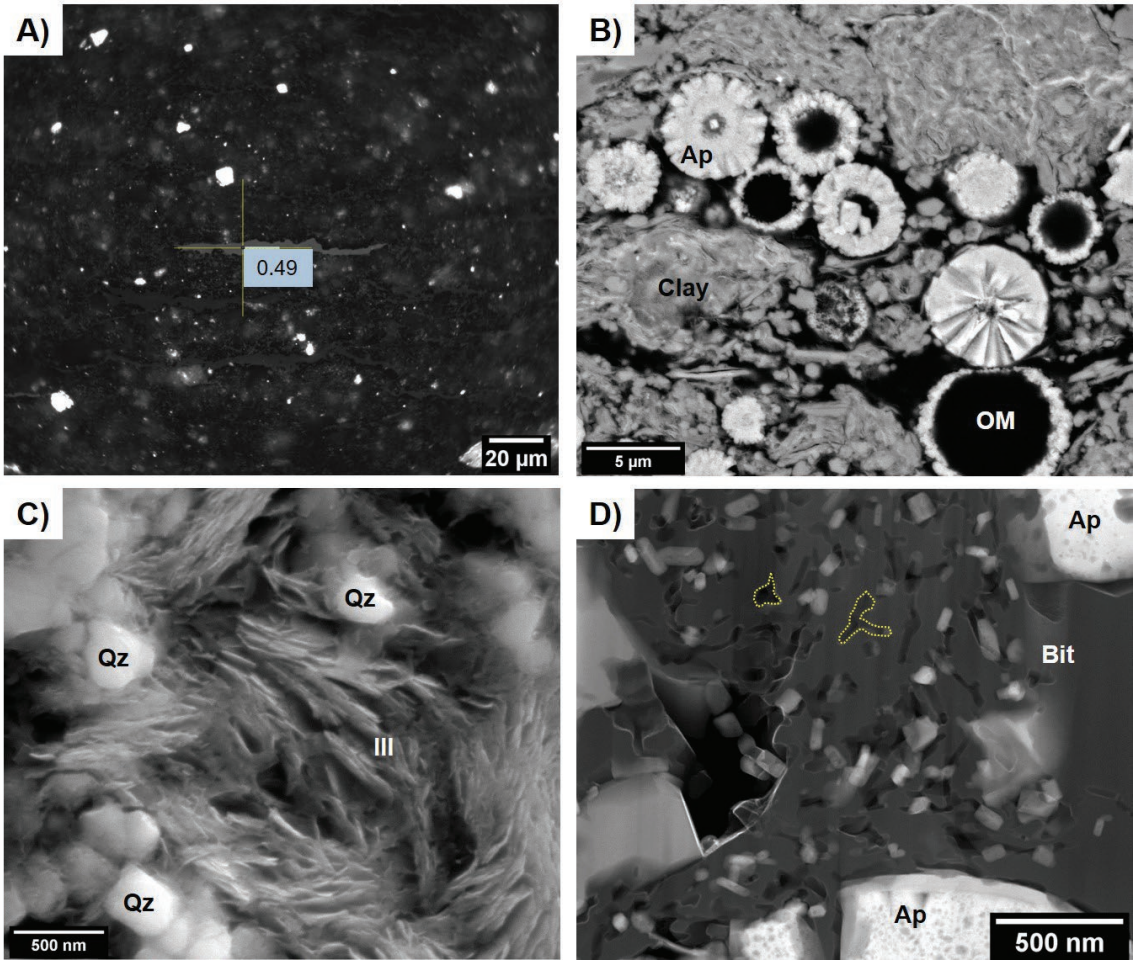

Figure 1. Microstructural characteristics of the Amungee Member of the Velkerri Formation. (**a**) Reflected light image of an elongate alginate particle with reflectance of 0.49%, sedimentary bedding is horizontal. White euhedral crystals are pyrite (Walton 2: 397.85 m). (**b**) Scanning electron microscope (SEM) image of apatite spherules (Ap), spatially associated with organic matter (OM) and surrounded by clay matrix (Clay). (Walton 2: 397.85 m) (**c**) SEM image of interspersed sub-micron sized quartz (Qz) and illite (Ill) (Lady Penhryn 2: 399.7 m). (**d**) Transmission electron microscope image of bitumen (Bit) with irregularly shaped pores (examples highlighted by dashed yellow contours). Bright particles are apatite (Ap) (Tarlee S3: 1438.61 m).

in fluid inclusions within carbonate cements in samples from wells Tarlee S3 and Lady Penrhyn 2, and in carbonate-filled fractures in well Borrowdale 2. These observations suggest that oil migration possibly occurred through fluid-assisted brittle deformation within a well-compacted and lithified mudstone. Ongoing dating of the oil inclusion-bearing calcite-filled fractures will provide further constraints on the timing of hydrocarbon migration.

References

Abbott ST and Sweet IP, 2000. Tectonic control on third-order sequences in a siliciclastic ramp-style basin: an example from the Roper Superbasin (Mesoproterozoic), northern Australia. *Australian Journal of Earth Sciences* 47(3), 637–657.

Jackson MJ, Powell TG, Summons RE and Sweet IP, 1986. Hydrocarbon shows and petroleum source rocks in sediments as old as 1.7 × 109 years. *Nature* 322(6081), 727.

Kouketsu Y, Mizukami T, Mori H, Endo S, Aoya M, Hara H, Nakamura D and Wallis S, 2014. A new approach to develop the Raman carbonaceous material geothermometer for low-grade metamorphism using peak width. *Island Arc* 23(1), 33–50.

Munson TJ, 2016. Sedimentary characterisation of the Wilton package, greater McArthur Basin, Northern Territory. *Northern Territory Geological Survey, Record* 2016-003.

Munson TJ and Revie D, 2018. Stratigraphic subdivision of the Velkerri Formation, Roper Group, McArthur Basin, Northern Territory. *Northern Territory Geological Survey, Record* 2018-006.

Revie D, 2017. Unconventional petroleum resources of the Roper Group, McArthur Basin. *Northern Territory Geological Survey, Record* 2017-002

Revie D and Normington VJ, 2018. Shale resource data from the greater McArthur Basin. *Northern Territory Geological Survey, Digital Information Package* DIP 014.

New geophysical and remote sensed data in the Northern Territory

Tania Dhu[1,2]

In 2018, the Northern Territory Geological Survey (NTGS) acquired one of the largest high-resolution airborne magnetic and radiometric surveys ever undertaken in the Northern Territory. The NTGS Tanami Region Airborne Magnetic and Radiometric Survey covers more than 42 000 km^2, extending from the WA border to ~300 km west of Tennant Creek (**Figure 1**). The survey was flown at 200 m line spacing and acquired more than 240 000 line km of data. The northern half of the survey was flown east–west and the southern half, north–south. The survey was managed by Geoscience Australia on behalf of NTGS and funded through the Northern Territory Government's *Resourcing the Territory* initiative. Industry partners also funded an additional 30 000 line km of infill data at 100 m line spacing.

Five co-funded geophysical surveys were completed under round 10 of the Geophysics and Drilling Collaborations (GDC) program (**Figure 2**). Two airborne electromagnetic (AEM) surveys were flown in the Aileron Province by Independence Group NL (IGO) at the Lake Mackay project using the SPECTREM system. More than 3000 line km were acquired over projects to the east (Winzar and Whitford 2018a) and west (Winzar and Whitford 2018b) of the Grapple and Bumblebee prospects (**Figure 2**: red and blue polygons). Gempart Pty Ltd acquired 1100 line km of AEM data in the Musgraves Province (Archer 2017) over the Docker Copper project (**Figure 2**: purple polygon). A ground gravity survey was also completed by Bowgan Minerals at their Jervois Project in the Aileron Province (Price 2017) where more than 300 ground gravity stations were acquired infilling existing 2 km spaced stations to 1 km spacing (**Figure 2**: green polygon). Lastly, 3D induced polarisation (IP) and magnetotellurics (MT) surveys were trialled by Emmerson Resources (Walters 2017) at the Rover Field west of Tennant Creek using the MIMDAS system (**Figure 2**: black polygon).

Eight HyLogger™ data packages (HDP 0067–0074) were released in 2018 and early 2019 (**Figure 3**). The HyLogger captures high-resolution imagery of drill core and measures reflectance spectra from which minerals can be identified. A component of these HDPs integrate reporting of stratigraphy and rock property measurements within the HyLogger datasets. These HyLogger datasets are included in the HDP along with a summary of major findings.

Six HDPs (HDP 0067–0072) cover results of HyLogging drill core from rounds 9 and 10 of the GDC program. HDP 0067 (Smith 2018a) summarises results from TCDD002, drilled by PNX Metals Limited at their Tractor Corner prospect (Bennett 2017) near the southern margin of the Pine Creek Orogen. HyLogging (with XRD validation) identified K-feldspar alteration, along with garnet, epidote, possible minor pyroxene and carbonates with some similarities to skarn-style alteration. Results from HMRD100001 are reported in HDP 0068 (Smith 2018b). This hole was drilled by ABM Resources (now Prodigy Gold NL) at their Homestead project in the Tanami Region in order to resolve the depth of cover and confirm the presence and depth of Antrim Plateau Volcanics (van Roij A 2017).

Three HDPs report on drill testing of different targets within the Barney Creek Formation in the McArthur Basin: YLDD001 drilled by Teck Australia (Sully 2017), NB17DD049 drilled by MMG Exploration Pty Ltd (Cohalan and Gianfriddo 2018), and BJD04 drilled by Pacifico Minerals Ltd (Pacifico Minerals Ltd 2017a). The results for each drillhole are summarised in HDP 0069 (Smith 2018c), HDP 0070 (Smith 2018d) and HDP 0071 (Smith 2018e) respectively. HDP 0072 (Smith 2019a) reports results from scanning with the HyLogger of CCD10, also drilled in the McArthur Basin. CCD10 was drilled at the Coppermine Creek project to test stratiform copper mineralisation within the Amelia Dolostone (Pacifico Minerals Ltd 2017b).

HDP 0073 (Smith 2019b) presents results from STDH03 (Chapman 2012); this drill core from the Stromberg prospect was loaned to the NTGS for scanning as part of the rare earths (REE) spectral characterisation project. Most recently, results from scanning of Pangaea Resources Pty Ltd's Manbulloo S1 drill core from the greater McArthur Basin have been released in HDP 0074 (Smith 2019c).

An update of the Rock Properties Dataset (DIP013: Hallett 2018) was released in 2018. This dataset is a compilation of rock property values comprising data compiled from industry statutory reports, academic publications, and measurements conducted by NTGS. The dataset contains 66 000 individual rock property values from more than 1000 locations around the NT, including both downhole and outcrop measurements. Since the previous release in 2017, approximately 4000 density values and 15 000 magnetic susceptibility values have been added.

References

Archer G, 2017. Round 10 Geophysics and Drilling Collaboration Final report: Docker Copper – EL31531, EL27581. *Northern Territory Geological Survey, Open File Report* CR2017-0337.

Bennett A, 2017. Final report for drilling and geophysics collaborations funding, Tractor Corner prospect. *Northern Territory Geological Survey, Open File Report* CR2017-0037.

Chapman A, 2012. Combined annual exploration report GR042-09 (CR109) EL25222, EL25223, EL25224, EL25229, EL29026, EL29242 for period ending 8th November 2012: Daly River Project NT, Report 2012-05. *Northern Territory Geological Survey, Open File Company Report* 2012-1068.

[1] Northern Territory Geological Survey, GPO Box 4550, Darwin NT 0801

[2] Email: tania.dhu@nt.gov.au

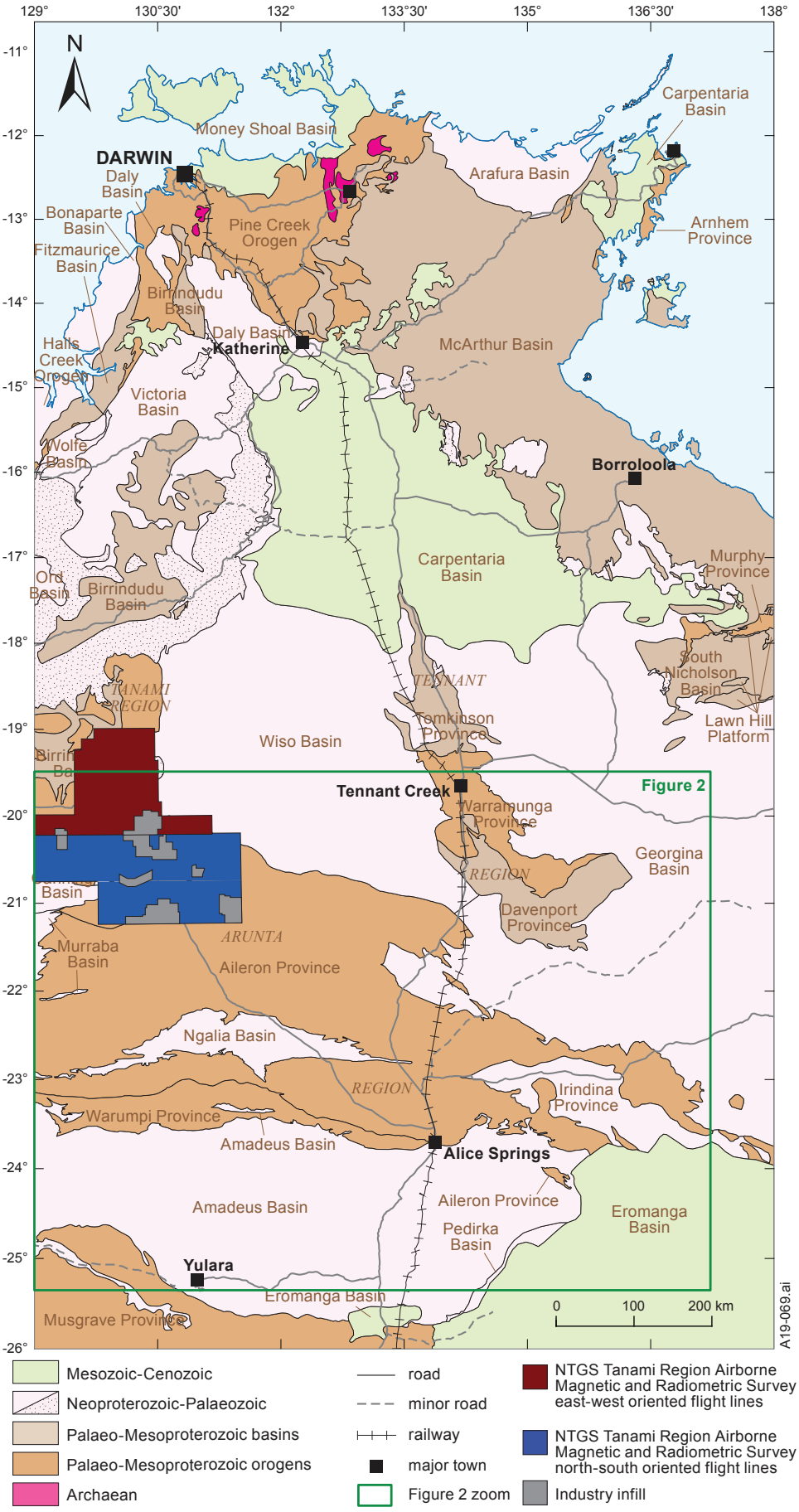

Figure 1. Location of NTGS Tanami Region Airborne Magnetic and Radiometric Survey overlain on the geological regions map of the Northern Territory. The maroon polygon was flown east–west at 200 m line spacing; the blue polygon was flown north–south at 200 m line spacing; the grey polygons are industry sponsored infill to 100 m line spacing.

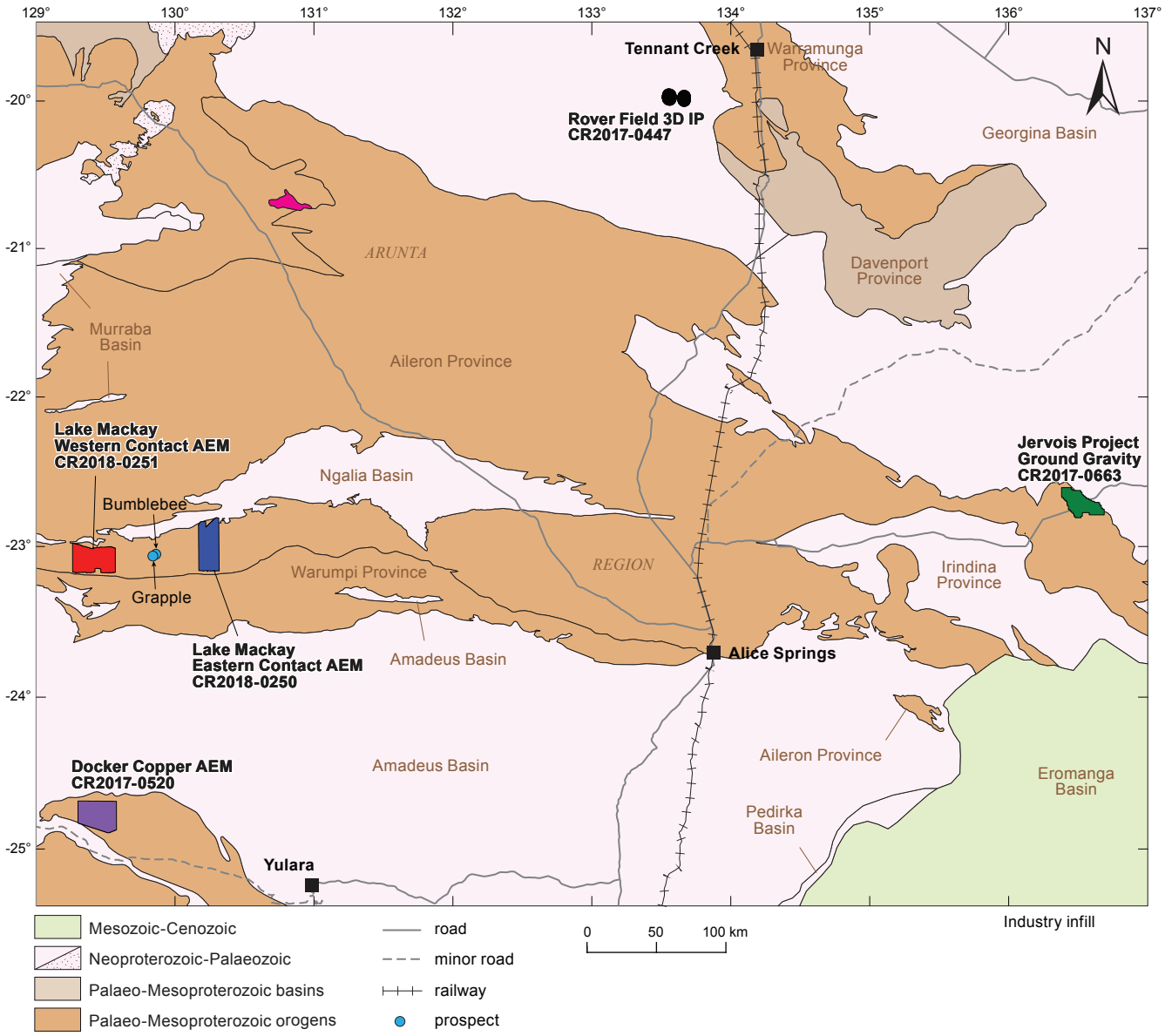

Figure 2. Location of geophysical projects from Round 10 of the GDC program overlain on the geological regions map of the Northern Territory.

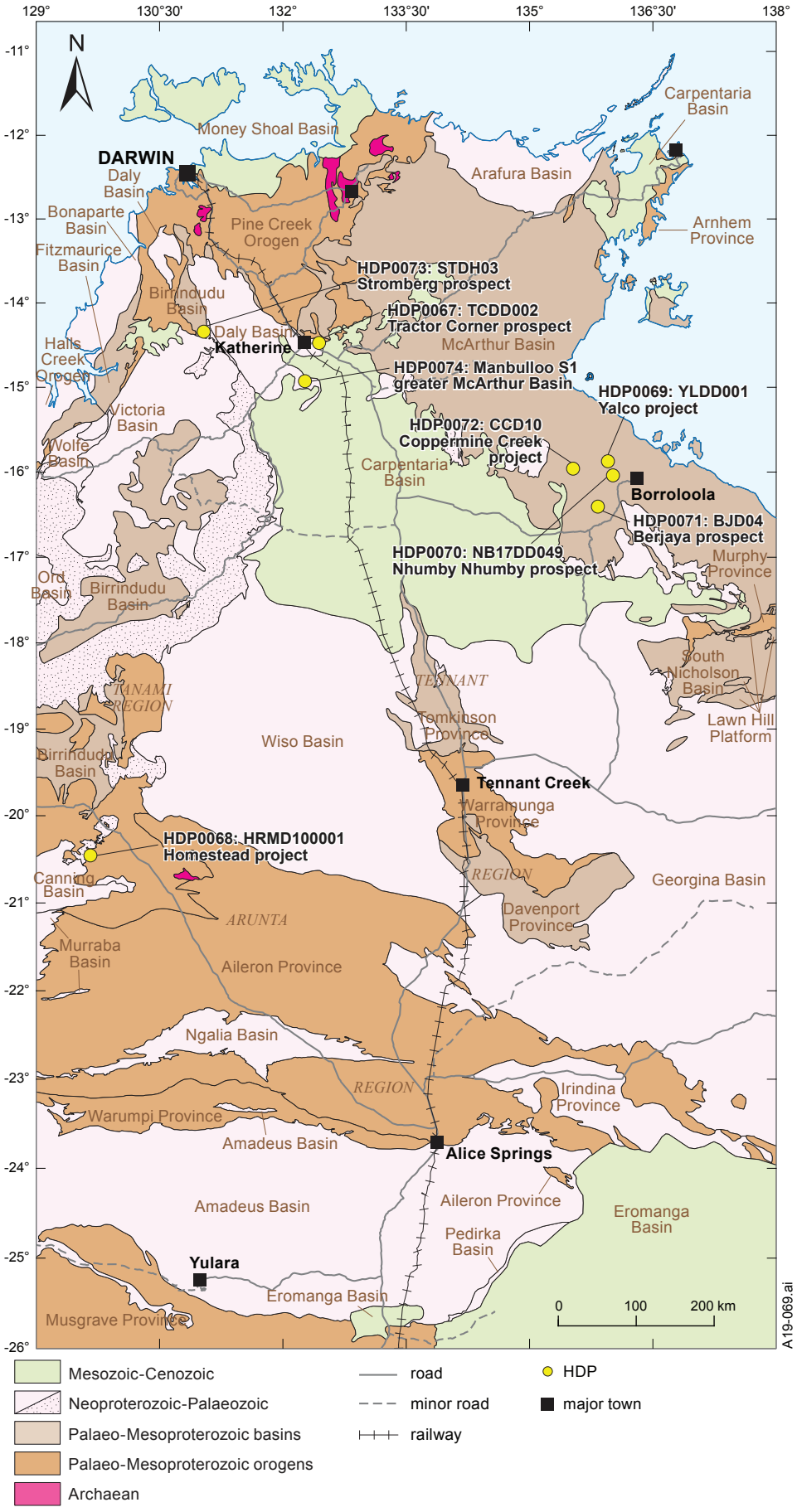

Figure 3. Location of drillholes that are the subject of recently released HyLogger Data Packages overlain on the geological regions map of the Northern Territory.

Cohalan L and Gianfriddo C, 2018. CORE Geophysics and Drilling Collaborations Round 10, 2017: Nhumby Nhumby EL30156. MMG Exploration Pty Ltd. *Northern Territory Geological, Survey Open File Company Report* CR2018-0044.

Hallett L, 2018. Rock property dataset of the Northern Territory. *Northern Territory Geological Survey, Digital Information Package* DIP 013.

Pacifico Minerals Ltd, 2017a. 2017 Geophysics and drilling collaborations completion report, EL28508 – Berjaya. *Northern Territory Geological Survey, Open File Company Report* CR2017-0469.

Pacific Minerals Ltd, 2017b. Geophysics and drilling collaborations report, EL26938 – Coppermine Creek. *Northern Territory Geological Survey, Open File Company Report* CR2017-0470.

Pangaea Pty Ltd 2015. Basic well completion report. NT EP-167 Manbulloo-S1. *Northern Territory Geological Survey, Open File Petroleum Report* PR2015-0017.

Price G, 2017. Jervois Project Summary Report for the program of gravity surveying conducted by Atlas Geophysical Pty Ltd at the Jervois Project: Core Initiative, Round 10. *Northern Territory Geological Survey, Open File Company Report* CR2017-0663.

Smith BR, 2018a. HyLogger drillhole report for TCDD002, 'Tractor Corner' prospect, Pine Creek Orogen, Northern Territory. *Northern Territory Geological Survey, HyLogger Data Package* 0067.

–––, 2018b. HyLogger drillhole report for HMRD10001, Homestead Project, Tanami Region, Northern Territory. *Northern Territory Geological Survey, HyLogger Data Package* 0068.

–––, 2018c. HyLogger drillhole report for YLDD001, Yalco Project, McArthur Basin, Northern Territory. *Northern Territory Geological Survey, HyLogger Data Package* 0069.

–––, 2018d. HyLogger drillhole report for NB17DD049, Nhumby Nhumby prospect, McArthur Basin, Northern Territory. *Northern Territory Geological Survey, HyLogger Data Package* 0070.

–––, 2018e. HyLogger drillhole report for BJD04, McArthur Basin, Northern Territory. *Northern Territory Geological Survey, HyLogger Data Package* 0071.

–––, 2019a. HyLogger drillhole report for CCD10, Coppermine Creek, McArthur Basin, Northern Territory. *Northern Territory Geological Survey, HyLogger Data Package* 0072.

–––, 2019b. HyLogger drillhole report for STDH03, Stromberg prospect, Pine Creek Orogen, *Northern Territory. Northern Territory Geological Survey, HyLogger Data Package* 0073.

–––, 2019c. HyLogger drillhole report for Manbulloo S1, greater McArthur Basin, Northern Territory. *Northern Territory Geological Survey, HyLogger Data Package* 0074.

Sully D, 2017. Geophysics and Drilling Collaborations Final Report, deep diamond drilling proposal Yalco Project: EL25467. *Northern Territory Geological Survey, Open File Company Report* CR2017-0489.

van Roji A, 2017. ABM Resources NL. Geophysics and Drilling Collaborations Final Report: Deep diamond drilling proposal for Homestead Project – EL25912. *Northern Territory Geological Survey, Open File Company Report* CR2017-0243.

Walters A, 2017. Geophysics and Drilling Collaboration Final Report for Rover Project 3D IP: EL27372. *Northern Territory Geological Survey, Open File Company Report* CR2017-0447.

Winzar D and Whitford M, 2018a. IGO Core Geophysics Collaboration Final Report: Eastern Contact Airborne Electromagnetic Survey Lake Mackay Project – EL30729, EL30730, EL30731 and EL30732. *Northern Territory Geological Survey, Open File Company Report* CR2018-0250.

Winzar D and Whitford M, 2018b. IGO Core Geophysics Collaboration Final Report: Western Contact Airborne Electromagnetic Survey Lake Mackay Project – EL30729, EL30730, EL30731 and EL30732. *Northern Territory Geological Survey, Open File Company Report* CR2018-0251.

Application of electrical geophysics to exploration at the Lake Mackay Project

Michael Whitford[1,2]

Introduction

The Lake Mackay Project is a joint venture between Independence Group NL (IGO), Prodigy Gold NL and Castile Resources Pty Ltd. It is located ~400 km northwest of Alice Springs and consists of 8058 km^2 of granted tenure and 4900 km^2 of tenement applications within the southwestern Aileron Province (**Figure 1**). Initially, IGO identified much of this area to be prospective for lode gold deposits; however, in 2016 significant drill intersections confirmed the area as also being prospective for high-grade polymetallic base and precious metal deposits (Winzar 2016). Consequently, the exploration methodology was reviewed to ensure these attractive target styles are also effectively explored.

[1] Independence Group NL, Suite 4 Level 5, 85 South Perth Esplanade, South Perth WA 6951, Australia
[2] Email: Mike.Whitford@igo.com.au

Historical exploration

The project area has had very little historical exploration. In 1999, a previous explorer had targeted the Andrew Young Igneous Complex for magmatic Ni-Cu mineralisation with a large airborne electromagnetic (AEM) survey using the GEOTEM system. This led to follow-up of generated targets using ground-based moving loop electromagnetics (MLEM); subsequently, 10 RC holes were drilled (**Figure 2**) but failed to produce any significant assay results.

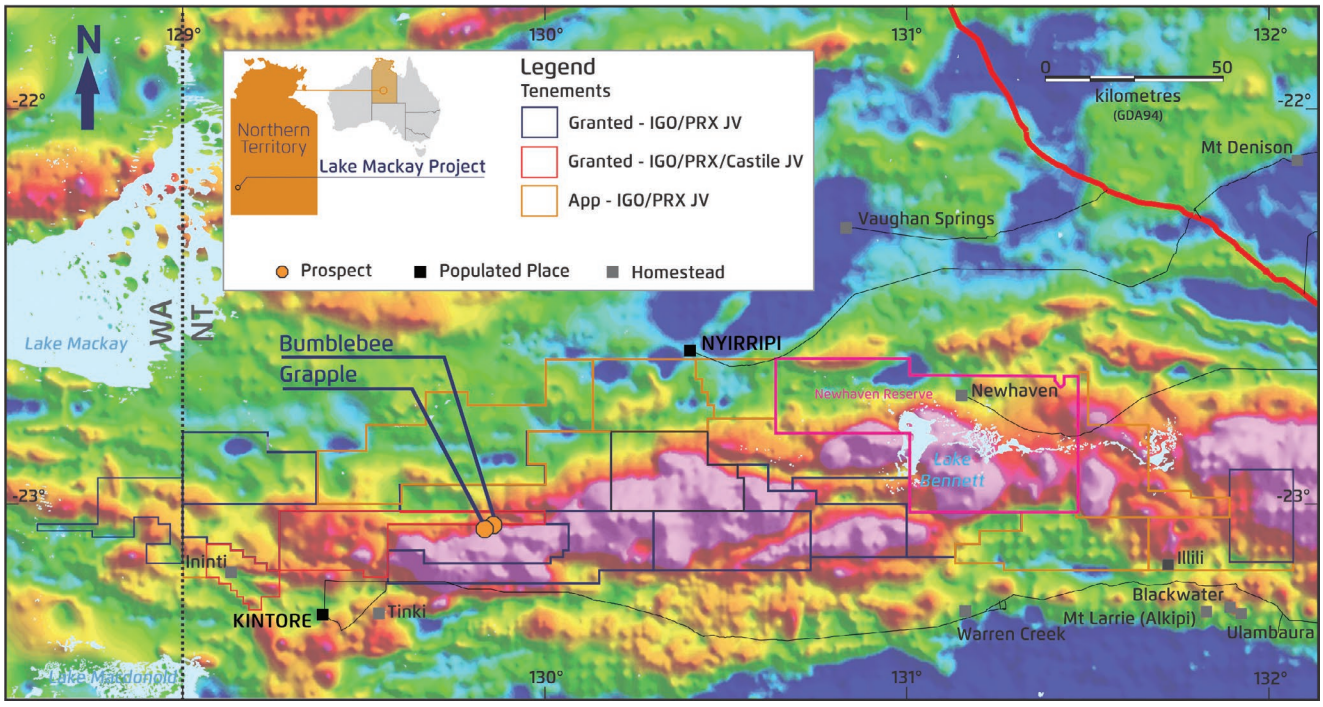

Figure 1. Location of the Lake Mackay Project over Bouguer gravity image.

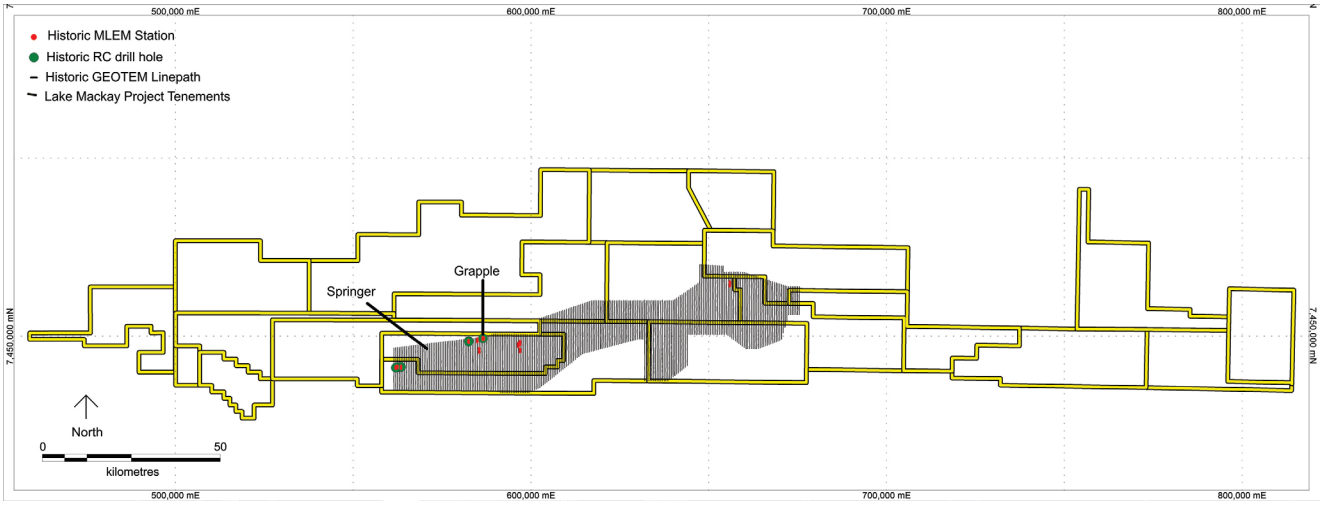

Figure 2. Location of previous exploration activities.

IGO initiated project-wide broad-spaced, reconnaissance soil sampling to locate gold mineralisation. This work culminated in the discovery of the *Bumblebee* prospect. Follow-up air core (AC) drilling returned a best result of 7 m at 3.29 g/t Au, 37.7 g/t Ag, 3.25% Cu, 0.87% Pb, 1.34% Zn, 0.09% Bi and 0.08% Co (15LMAC031).

Application of geophysics

The highest priority targets, including the Bumblebee polymetallic sulfide prospect, were outside of the existing GEOTEM coverage. With this in mind, the JV undertook an initial orientation EM survey in early 2016 over Bumblebee. A small MLEM survey was conducted using a 200 m loop, fluxgate receiver, and battery pack source in a slingram (receiver out of loop) configuration. Lines were spaced at 200 m with 100 m station spacing, providing excellent coverage over the geochemical anomaly. The eleven lines of the survey produced a significant response (**Figure 3**): a late time channel grid of the X component showing a strong single peaked anomaly. This result provided encouragement that EM could be an effective exploration tool.

Using the same configuration, the MLEM surveys were expanded later in the 2016 field season to cover lesser ranked soil anomalies, particularly those which showed anomalous copper. These surveys highlighted anomalies at both the *Springer* and *Grapple* prospects. The Grapple prospect, located only ~2 km southwest of Bumblebee, was previously identified in the historic GEOTEM survey. **Figure 4** shows a late time channel grid of the MLEM X component of the Grapple target. The target consists of two separate conductors. Initially, 11 reverse circulation (RC) drillholes were collared into the Grapple target, with the first (16GRRC001) directed into the eastern conductor.

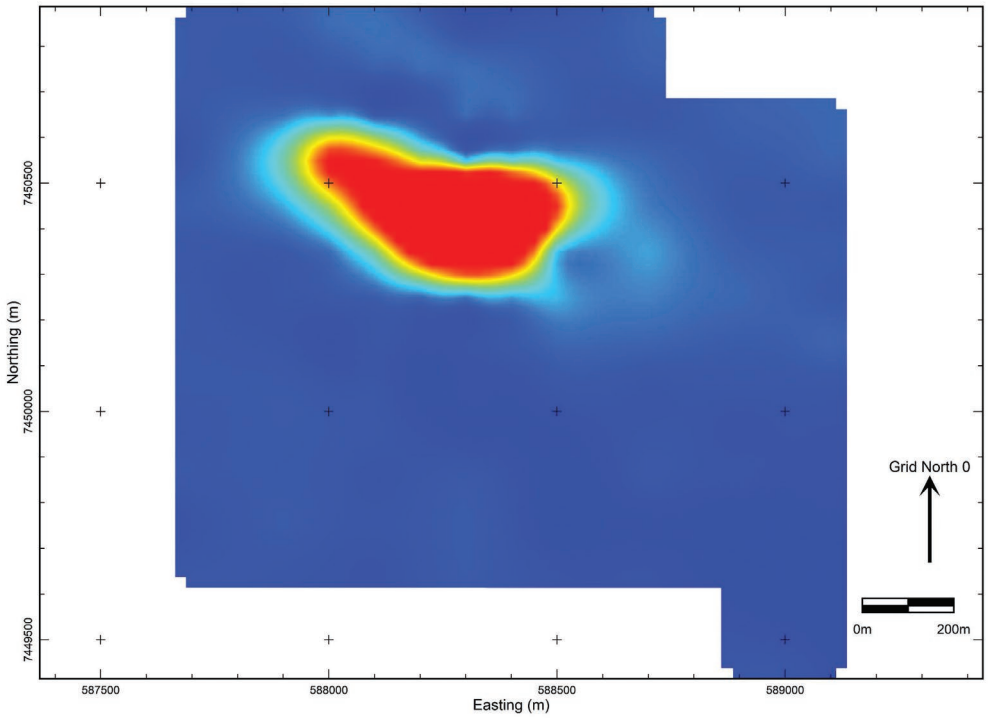

Figure 3. Bumblebee MLEM X component 15.7–20.2 ms channel.

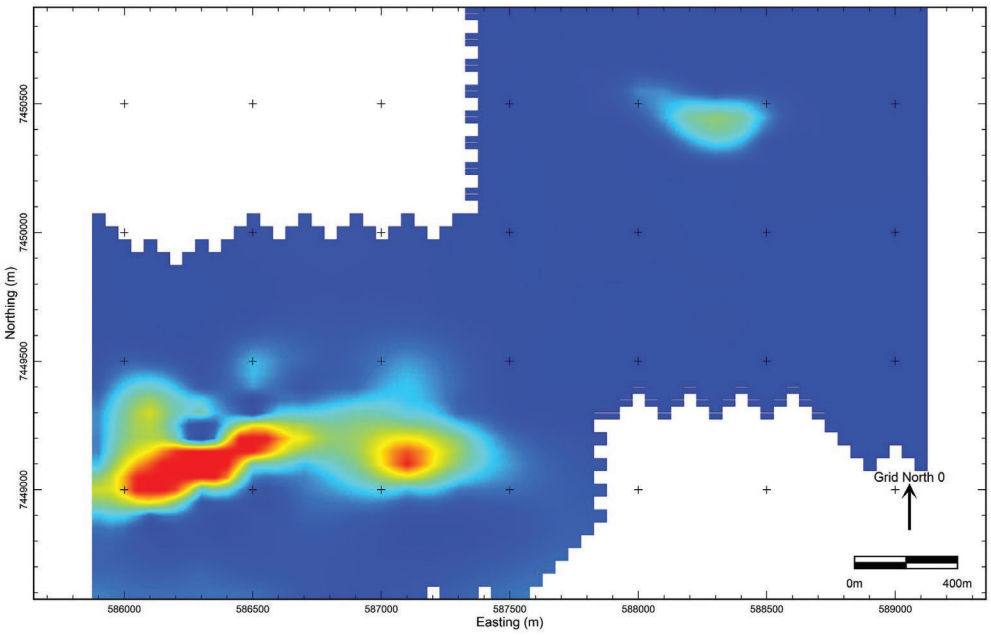

Figure 4. Grapple and Bumblebee MLEM X component 15.7–20.2 ms channel.

This drillhole intersected minor pyrrhotite mineralisation at ~160 m depth. Down-hole electromagnetic (DHEM) was completed on this drillhole using a 400 × 400 m square loop and a Digi Atlantis receiver system. Two distinct off-hole anomalies were identified (**Figure 5**) that clearly indicated the Grapple target had not been effectively tested.

The third RC drillhole (16GRRC003) in the campaign targeting the EM conductor was located further southwest and drilled under outcropping gossanous material. This drillhole intersected a zone of multiple sulfide horizons from ~80 m depth to ~160 m depth, with the most significant assayed interval being 9 m at 1.81 g/t Au, 49.1 g/t Ag, 3.26% Cu and 3.63% Zn from 85 m depth. This result confirmed the Grapple discovery.

DHEM was again completed in this drillhole using the same configuration; results indicated that multiple conductors had been intersected, and again, that off-hole conductors were present. The DHEM log not only confirmed the mineralisation was conductive and amenable to exploration through EM methods, but also confirmed that there was further scope to extend the mineralisation with EM through the identification of off-hole conductors. **Figure 6** shows the profile of the mid-time EM data from 16GRRC003 where the multiple conductors can be clearly seen.

The ground MLEM conducted in 2016 had also identified a significant conductor at the Springer prospect, which the historic GEOTEM survey had failed to identify. Recognising the large area of tenement holdings and the ineffectiveness of soil sampling in areas under cover, it was decided in 2017 to conduct orientation surveying using airborne EM to determine if modern EM systems could detect this conductor. The SPECTREM system was chosen to complete a four line orientation survey over Springer. The system clearly detected the prospect and provided very comparative results to the MLEM.

Figure 7 shows a comparison between similar time channels for the MLEM, the SPECTREM AEM and the historic GEOTEM survey. The MLEM shows a clear, well-defined conductor, while the SPECTREM shows a weaker, but clearly above noise levels conductor. The GEOTEM hints at a conductor; however, the strength is not considered significantly above noise levels. It should be noted here that there is a decrease in lateral resolution for each survey, the MLEM was conducted using 200 m spaced lines, the SPECTREM was completed using 300 m lines, and the GEOTEM was completed using 500 m lines. The completion of this orientation survey and comparison to the MLEM results has provided the confidence that a modern AEM system would be capable of effectively screening for conductive mineralisation under shallow cover.

Through a process of successive orientation surveys, the following strategy for applying EM to the Lake Mackay Project has been developed. A large SPECTREM AEM survey will identify anomalies that could represent conductive mineralisation; follow-up ground-based MLEM will then be conducted to define and rank each target prior to drilling; and finally, every drillhole will be logged with DHEM to confirm the target has been effectively tested. The example from Grapple has indicated that, although EM will be an effective tool for exploration, the method will also detect unmineralised conductors; therefore, it is important that the conductor is fully understood by considering all geological and geochemical as well as geophysical observations when ranking and testing targets.

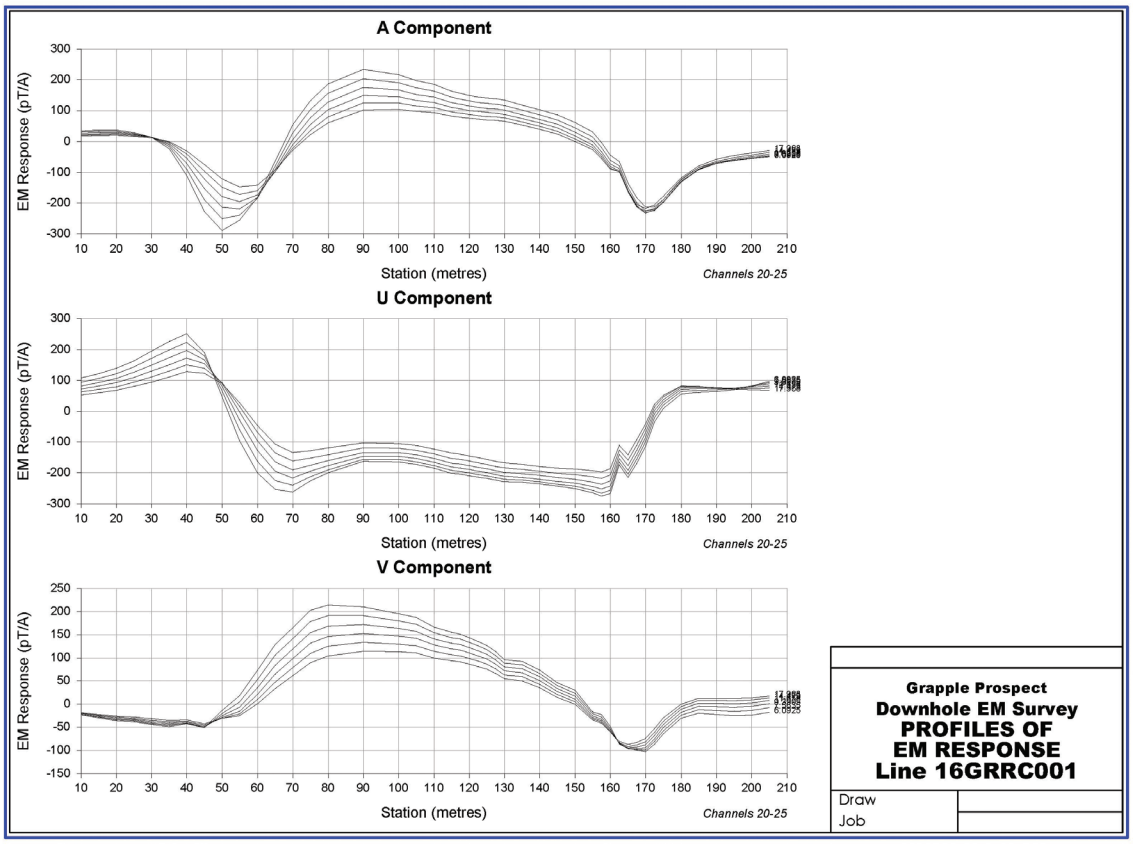

Figure 5. Drillhole 16GRRC001 DHEM profile of late time channels. Two clear off hole responses are present.

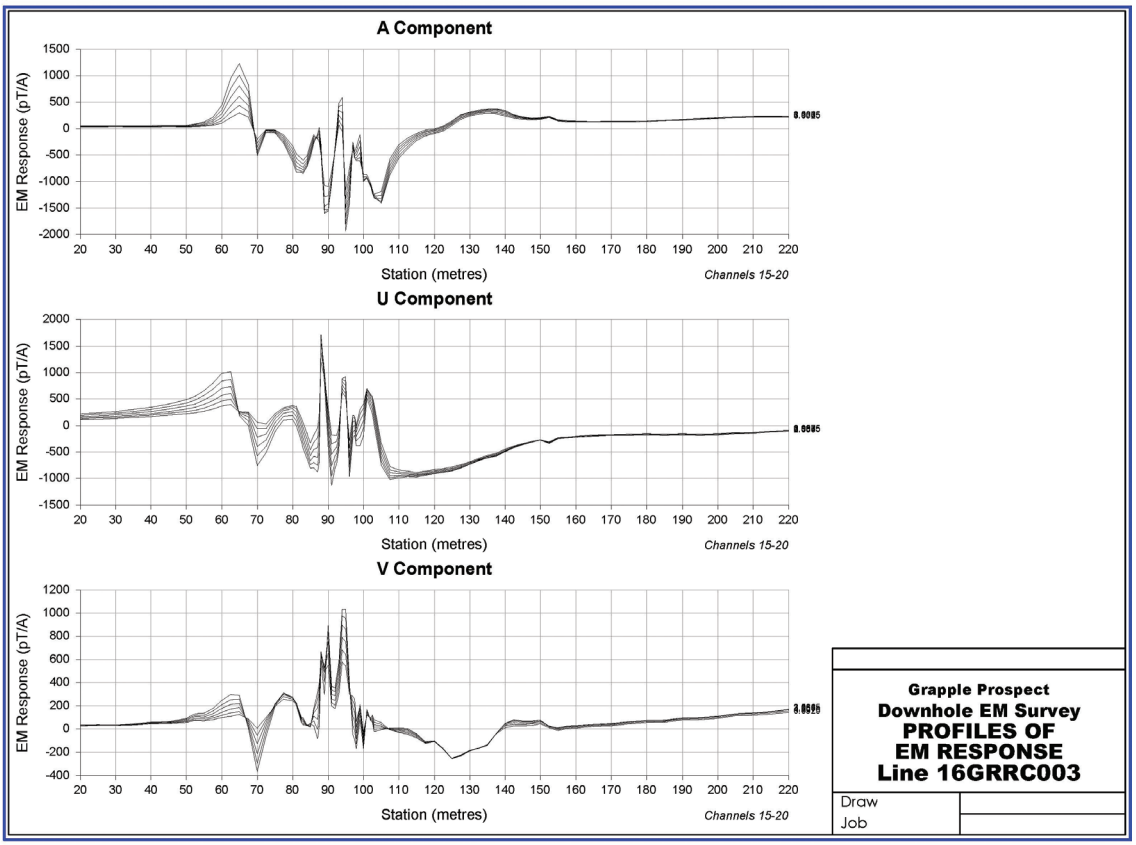

Figure 6. Drillhole 16GRRC003 DHEM profile of late time channels. Numerous significant in-hole and off-hole responses are present.

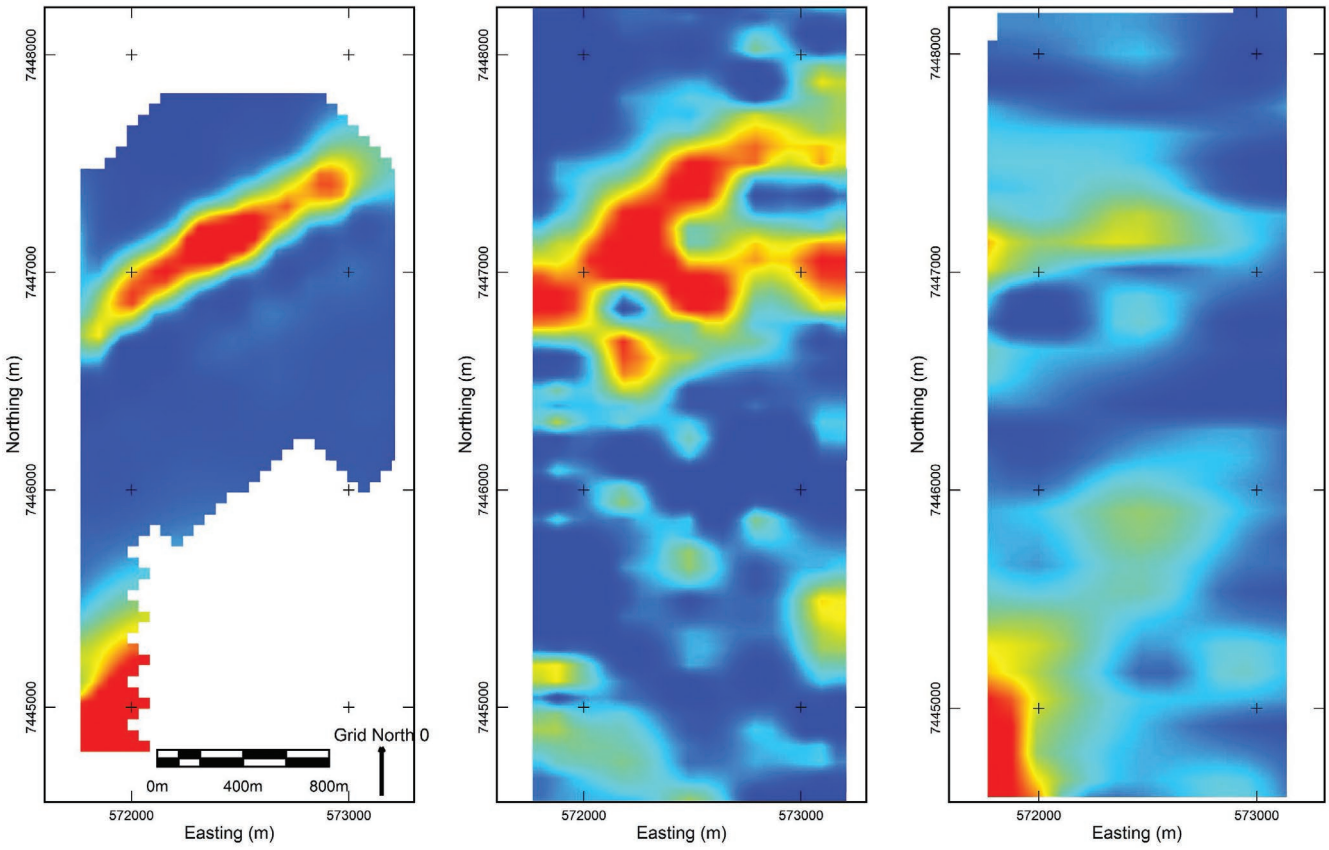

Figure 7. Left-MLEM Z component 1.8–2.3 ms channel. Centre-SPECTREM Z component 1.6–3.3 ms channel. Right-GEOTEM Z component 2.3–2.7 ms channel.

Acknowledgements

The author wishes to thank and acknowledge the Northern Territory Geological Survey for providing co-funding for a number of airborne magnetic and electromagnetic surveys within the project under the Northern Territory Government's Geophysics and Drilling Collaborations program. IGO and Prodigy Gold are thanked for allowing the publication and presentation of these results. Doug Winzar, Brett Keillor, Paull Parker and the IGO exploration team (past and present) who have been involved in this project are all thanked for their support and input.

Reference

Winzar D, 2016. Early indications of a copper-gold belt in the southwestern Aileron Province: in *'Annual Geoscience Exploration Seminar (AGES) Proceedings, Alice Springs, Northern Territory 15–16 March 2016'*. Northern Territory Geological Survey, Darwin.

The greenfield Grapple and Bumblebee discoveries of the western Aileron Province: First constraints on sulfide mineralising processes

Matt V McGloin[1], Barry L Reno[1,2], Natalie Kositcin[3], Simon Cornwell[4], Doug Winzar[4], Eloise E Beyer[1], David Huston[3], David C Champion[3] and Anthony Crawford[5]

Ore deposit discovery rates are in steady decline and forcing savvy explorers into underexplored terrains and more challenging environments. The long-term, regional-scale and systematic exploration strategies needed to buck this negative trend are emphasised by the successful greenfields discovery of polymetallic sulfide mineralisation at the Grapple and Bumblebee prospects in the western Aileron Province (**Figure 1**). The Aileron and Warumpi provinces of central Australia have not received the same attention as other apparently more mineral-rich provinces in Proterozoic Australia; these discoveries raise expectations that economic mineralisation may lie undercover (see Winzar 2016 and Whitford *et al* 2019, this volume).

Drilling and mapping of Grapple and Bumblebee provide a first opportunity to assess the nature of this mineralising system and collect valuable evidence that can be interpreted and applied directly to exploration. Using field observations integrated with petrographic, isotopic, geochemical, and chronological analyses, this abstract focuses on explaining our understanding of some of the processes and controls involved in mineralisation at these two prospects. The new data reported herein provide the first temporal constraints on sulfide mineralisation at Grapple and Bumblebee and help to constrain the nature of this mineralisation.

This study provides evidence that this hydrothermal base and precious metal mineralisation could have formed at or after ca 1.67 Ga; however, it is also possible that sulfide mineralisation was formed at ca 1.84 Ga and then reworked at ca 1.67 Ga. Analytical work is ongoing to test competing models for mineralisation. Although syngenetic or diagenetic mineralisation cannot be precluded, the breccia-hosted pyrrhotite-dominant sulfide mineralisation at these prospects may be younger than other base and precious metal mineralisation previously reported in the Aileron Province; furthermore, it may be related to voluminous magmatism at ca 1.69–1.63 Ga in MOUNT RENNIE[6].

[1] Northern Territory Geological Survey, GPO Box 4550, Darwin NT 0801, Australia
[2] Email: barry.reno@nt.gov.au
[3] Geoscience Australia, GPO Box 378, Canberra ACT 2601, Australia
[4] Independence Group NL, PO Box 496, South Perth WA 6151
[5] A&A Crawford Geological Consultants, 493 Tinderbox Rd, Hobart TAS 7054, Australia

Regional Geology

The Lake Mackay project of Independence Group NL is located at the southern margin of the Palaeoproterozoic North Australian Craton, straddling the Aileron Province to the north, and the Warumpi Province to the south (see MOUNT RENNIE 1:250 000-scale map). These provinces are separated by the Central Australian Suture (CAS), a major deep crustal-scale structure comprising a series of east–west-trending major faults and shear zones (Shaw *et al* 1992, Scrimgeour *et al* 2005a, Selway *et al* 2009, Morrissey *et al* 2011, Wong *et al* 2015).

The Warumpi Province records a ca 1.69–1.60 Ga history of voluminous, dominantly felsic magmatism, crustal thickening, and metamorphism along the southern margin of the Aileron Province (Close *et al* 2004, Scrimgeour *et al* 2005a, b). The Warumpi Province is divided into three main domains of which the most relevant to this study is the Yaya Domain. This domain comprises a sequence of metasedimentary rocks interpreted to have been deposited between ca 1.66 and 1.64 Ga (Close *et al* 2003, Scrimgeour 2005a,b) then subsequently metamorphosed and intruded by voluminous felsic and mafic magmatism during the ca 1.64–1.63 Ga Liebig Orogeny.

Felsic and mafic magmatism related to the Liebig Orogeny also occurred in the Aileron Province in MOUNT

[6] Names of 1:250 000-scale mapsheets are shown in capital letters, eg MOUNT RENNIE.

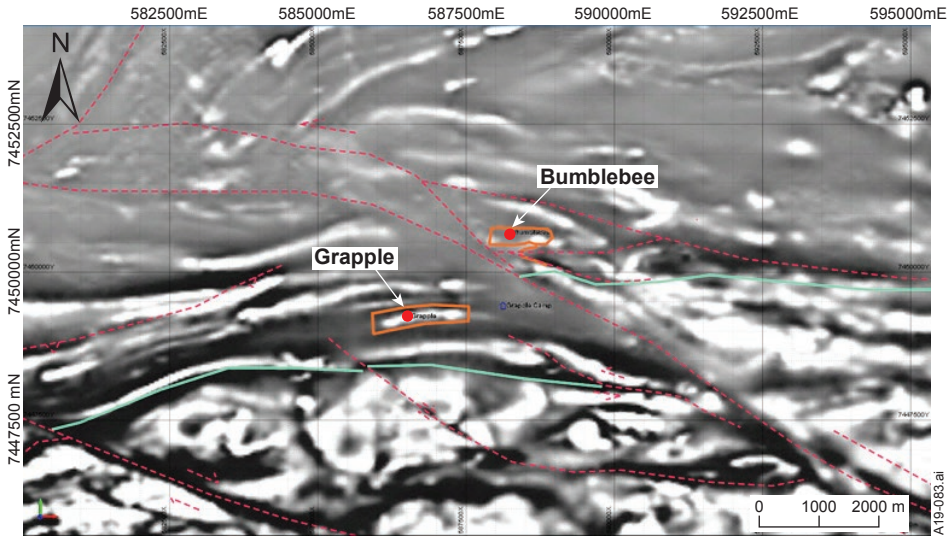

Figure 1. Reduced to pole first derivative magnetic image showing location of Grapple and Bumblebee prospects and their similar stratigraphic position compared to the Nyrripi Beds (south of the teal coloured line). The prospects have been offset by a large sinistral strike slip fault (red dashed line).

RENNIE, MOUNT DOREEN, and WEBB (eg Andrew Young Igneous Complex; Wyborn *et al* 1998, Cross *et al* 2005, Scrimgeour *et al* 2005a, Hollis *et al* 2013).

Sulfide mineralisation at Grapple and Bumblebee occurs in the western Aileron Province, hosted in low hills of poorly-exposed rocks covered by sand plains and dunes (Close *et al* 2004). The oldest rocks are ca 1.84–1.81 Ga metasedimentary rocks of the Lander Rock Formation (Close *et al* 2005, Hollis *et al* 2013, Kositcin *et al* in prep). Between ca 1.81–1.70 Ga, this metasedimentary succession was intruded and metamorphosed by several phases of magmatism (Scrimgeour 2013, Hollis *et al* 2013), including the ca 1.80 Ga mafic Du Faur Suite and the loosely defined ca 1.77 Ga felsic Carrington Suite (Close *et al* 2004, Edgoose *et al* 2008, Kirkland *et al* 2009, Hollis *et al* 2013).

Local geology

Logging and mapping suggests the Grapple and Bumblebee prospects share a stratigraphic sequence with the prospects subsequently displaced to their current positions by a large sinistral strike slip fault (**Figure 1**). The stratigraphy is dominated by metasedimentary rocks of the Lander Rock Formation (metasandstone and schists; **Figure 2a**). An early lower amphibolite facies metamorphic assemblage is recorded by andalusite and biotite porphyroblasts that contain aligned biotite inclusions. A pervasive mylonitic S_2 foliation fabric, evidenced by aligned mica and elongate quartz in schistose metasedimentary rocks, strikes east–west and dips steeply- to near-vertically to the north. The S_2 fabric deforms and rotates the andalusite and biotite porphyroblasts (**Figure 2a**), which suggests at least two periods of deformation at the prospects. Structural analysis from drill core and surface mapping indicates that the entire stratigraphic package may be tightly folded.

At Grapple, vergence patterns in outcropping metasandstone and porphyroblastic schists are consistent with a south-dipping antiform centred where mineralisation is located. The mineralised lenses have an apparent plunge of approximately 30–40° to the west. This geometry correlates well with lineation measurements from surface mapping (L_2 on S_1). The Bumblebee prospect is hosted in a similar south-dipping antiform but additionally shows evidence for a D_3 fold set. The F_3 fold structures possess axial-planar S_3 disjunctive cleavage, crenulation, and kink-banding seen at surface; in the macroscale they give the Bumblebee prospect a distinctive U-shape.

The foliated metasedimentary rocks are locally intruded by mafic sills and dykes that vary from 1 m to 50 m thickness (**Figure 2b**). A majority of mafic sills and dykes predate S_2; however, one observed mafic intrusion at Bumblebee has an unusual porphyritic augite–actinolite–plagioclase mineralogy and overprints the mylonitic S_2 fabric of the host rock (**Figure 2c**). Minor felsic and syenite sills and dykes also occur at the prospects (Crawford 2017).

The vast majority of sulfide mineralisation at Grapple and Bumblebee generally occurs as two massive to semi-massive lenses of mineralised breccia ≤ 9 m thick, hosted by the Lander Rock Formation; they occur between and bounded by mafic sills (**Figure 2b, 3a, 3b**). Stringer and quartz vein-hosted sulfides also overprint adjacent metamafic and metasedimentary rocks around the breccia zones (**Figure 4a**).

The visible sulfides are dominated by pyrrhotite with lesser chalcopyrite, stringer sphalerite, and coarse-grained arsenopyrite, with minor galena and pyrite occurring as inclusions within pyrrhotite. All main sulfide minerals also occur as inclusions within other sulfides, or on their grain boundaries (**Figure 4c, d**). The breccia also contains sub-angular, lithic clasts of altered country rock including metadolerite and metasedimentary rocks (**Figure 3a, b**). These clasts are sometimes poikiloblastic and/or contain smaller inclusions of sulfides (eg pyrrhotite, sphalerite, minor chalcopyrite, and galena) or other silicates. The breccia also includes monomineralic amphibole, clinopyroxene, and carbonate.

Stringers and quartz-vein related sulfides have similar mineralogy to the pyrrhotite breccias but typically contain higher concentrations of chalcopyrite, sphalerite, and galena (**Figure 3a, 4a**). In one drill core interval at Bumblebee, a different style of mineralisation occurs whereby minor S_2-foliated and re-crystallised, net-textured pyrrhotite (lacking enrichment in economic metals) is found in mm- to cm-scale discrete layers within siliceous bands hosted in metasandstone (**Figure 4b**). This pyrrhotite probably represents minor diagenetic pyrite that was subsequently metamorphosed, as typical of metamorphosed sedimentary sequences.

Metasedimentary rocks on the margins of sulfide mineralisation are commonly bleached, silicified, and weakly micaceous. The metasedimentary host rocks to the main sulfide mineralisation, particularly where they are adjacent to mafic rocks, are typically altered to a series of amphibole–quartz–chlorite and calcic-skarn assemblages (**Figure 4f**). Typical alteration minerals identified include hornblende, fibrous actinolite, clinopyroxenes (cummingtonite, grunerite and augite), garnet, carbonate (calcite?), chlorite, clinozoisite, biotite, and quartz. Some intervals also contain significant tourmaline and fluorite.

The base of mineralisation at the Grapple prospect is associated with a tremolite schist of the Lander Rock Formation. This schist is of particular economic interest because it also contains the highest gold enrichment at the prospects; the gold occurs as non-visible electrum, distinct from mineralisation in the massive sulfide zones. Importantly, the highest-grade gold is not directly associated with massive, base metal-rich sulfide.

Both prospects appear to have similar element enrichments, sulfide assemblages, grade, and distribution of metals. Assay data from the main mineralised zones at Grapple indicate significant enrichment in ore-forming elements Fe, S, Cu, and Zn. There are also significant enrichments in Pb, As, Co, and Bi; and the precious metals Ag, Te, and Au. Compared to average upper crustal abundances, the highest enrichments are in Te, Bi, and S; with significant enrichments in Cu, Ag, Pb, As, Zn, Au, Co, and Sn. The net-textured S_2-foliated pyrrhotite, which is found only at the Bumblebee prospect, lacks enrichment in economic metals compared to the breccia, stringer and vein sulfides (Crawford 2017).

Indirect constraints on timing of mineralisation

New chronologic data provide the first analytical constraints on the timing of mineralisation at the Grapple and Bumblebee prospects. Maximum age constraints are provided by a metasandstone sample that yielded a maximum depositional age of ca 1.86 Ga (Kositcin *et al* in prep). This age is within uncertainty of a maximum depositional zircon age of 1858 ± 5 Ma yielded from turbiditic Lander Rock Formation from the Dufaur Hills in MOUNT RENNIE (Cross *et al* 2005). The zircon inheritance spectra and interpreted maximum depositional age are consistent with numerous samples of the Lander Rock Formation across the Aileron Province that yielded zircon maximum depositional ages of ca 1.86–1.84 Ga (Scrimgeour 2013 and references thererin).

Monazite aligned in and overprinting the main mylonitic fabric in schist at Grapple yielded a $^{207}Pb/^{206}Pb$ age of 1668 ± 7 Ma (Reno *et al* 2018). The internal morphology of most monazite grains is consistent with dissolution–reprecipitation during fluid interaction; the age is most likely related to fluid-flow during, or shortly after, mylonite formation. The timing of fabric formation also provides a maximum timing constraint on sulfide breccia formation because the sulfide breccia cross-cuts the main foliation of the host rock (**Figure 3a–b**). The timing of sulfide breccia formation may reflect the timing of

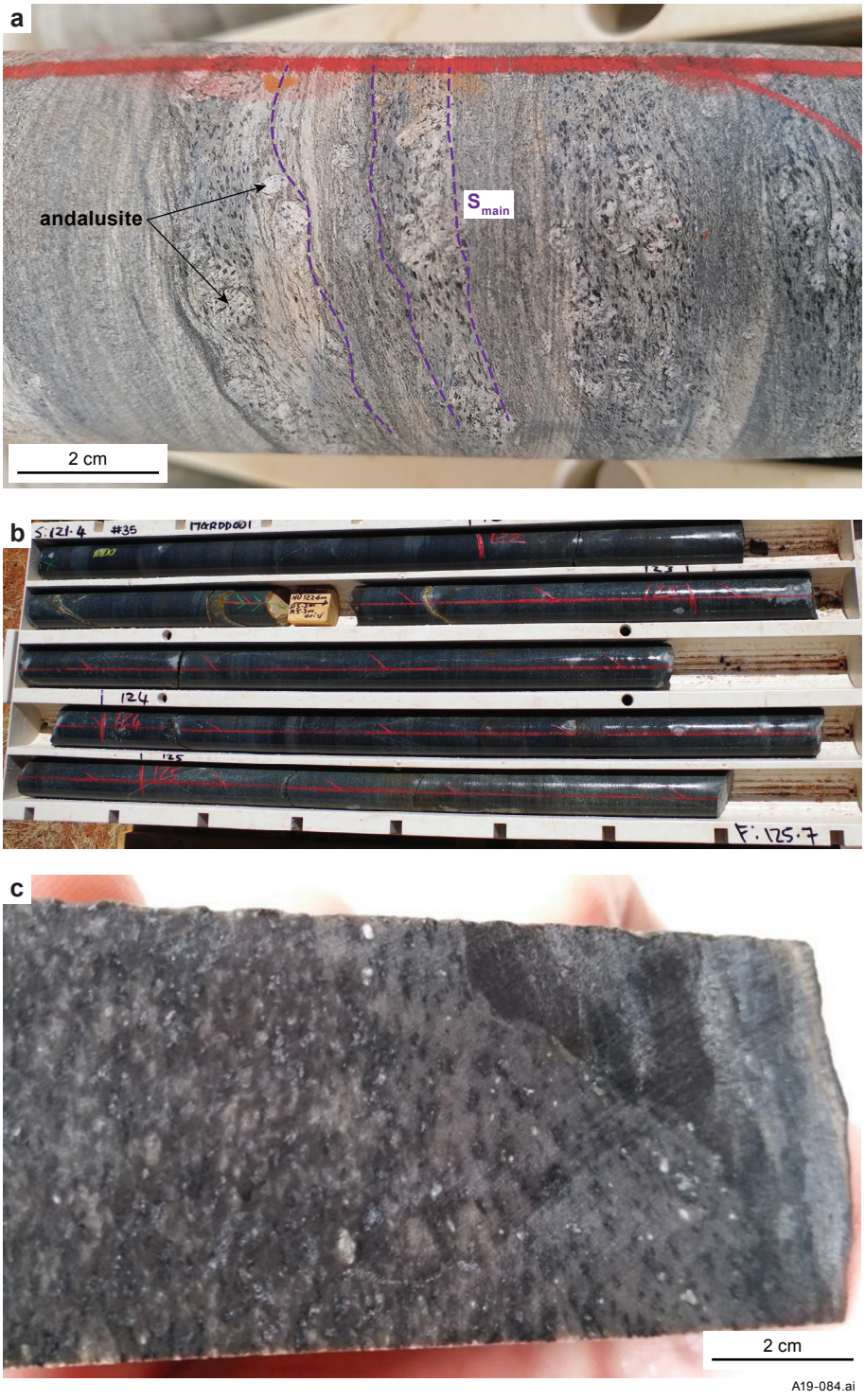

Figure 2. Photographs of country rocks and associated intrusive rocks at the prospects: (**a**) S_2-foliated andalusite–biotite–muscovite schist of the Lander Rock Formation. (**b**) Mafic sill inferred to be part of the mafic Du Faur Suite. (**c**) Mafic of intermediate composition that overprints the S_2-foliation fabric of the host metasedimentary schist of the Lander Rock Formation.

mineralisation (eg formation of a breccia) or, alternatively the timing of remobilisation or deformation of pre-existing massive sulfide (eg formation of 'durchbewegung' textures). In the former case, the ca 1.67 Ga age represents the maximum age of mineralisation; in the latter case, this age is a minimum age of mineralisation.

An unnamed porphyritic dacite intrusion from the Warumpi Province, ~80 km southwest of the prospects and containing trace chalcopyrite and pyrite, yielded a $^{207}Pb/^{206}Pb$ zircon magmatic crystallisation age of ca 1.63 Ga (Kositcin *et al* in prep). Four mafic intrusions at the prospects (including one cross-cutting foliated schist) all yielded lower minimum zircon intercept ages ca 1.63 Ga (Kositcin *et al* in prep, Beyer *et al* in prep). These ages are consistent with isotope disturbance associated with magmatism and magmatic-hydrothermal activity during the Liebig Orogeny.

Direct dating of mineralisation

Direct dating of mineralisation was attempted through Re–Os isotope analyses of arsenopyrite and Pb isotope analyses of Pb-rich galena-bearing samples. However, neither method produced clearly definitive results. Petrographic and structural relationships suggest that all dated sulfides have a post-metamorphic origin based on their overprinting relationship with the main S_2 fabric; this suggests ages should match or post-date the ca 1.67 Ga age for S_2 development recorded by Reno *et al* (2018).

An average Re–Os age of ca 1.96 Ga for three arsenopyrite samples from the main mineralised breccia at Grapple is older than the host rocks and must therefore be considered geologically meaningless. The exact reason for old Re–Os model ages remains unknown and is the current subject of further NTGS work. It is possible that microscale intergrowths of löllingite and pyrrhotite (**Figure 4d**) within the arsenopyrite crystals analysed may have contributed to the artificial model age produced.

Pb model ages of ca 1.84–1.83 Ga for three Pb-rich breccia samples at Grapple using the model of Hussey *et al* (2006) resemble plausible actual depositional ages for the host metasedimentary rocks (ca 1.86–1.81 Ga, Kositcin *et al* in prep). This may suggest a syn-depositional (syngenetic or diagenetic) timing for mineralisation, which was then remobilised or deformed at ca 1.67 Ga. However, caution should be exercised in assessing these results as, in some situations, model ages can be significantly different to the ages of mineralisation. For example, long term depletion of U relative to Pb in the source rocks could produce anomalously old model ages; it is possible that pre-metamorphic Pb isotope signatures were inherited in post-metamorphic sulfide assemblages, thus resulting in older apparent ages. The apparent conflict between the petrographic and structural observations that suggest a syn- to post-1.67 Ga age for mineralisation, and the calculated Pb model ages that suggest a ca 1.84 Ga age for mineralisation, is a topic of ongoing research.

Mineralising processes

The results of this study provide new constraints on the mineralising process at Grapple and Bumblebee. The

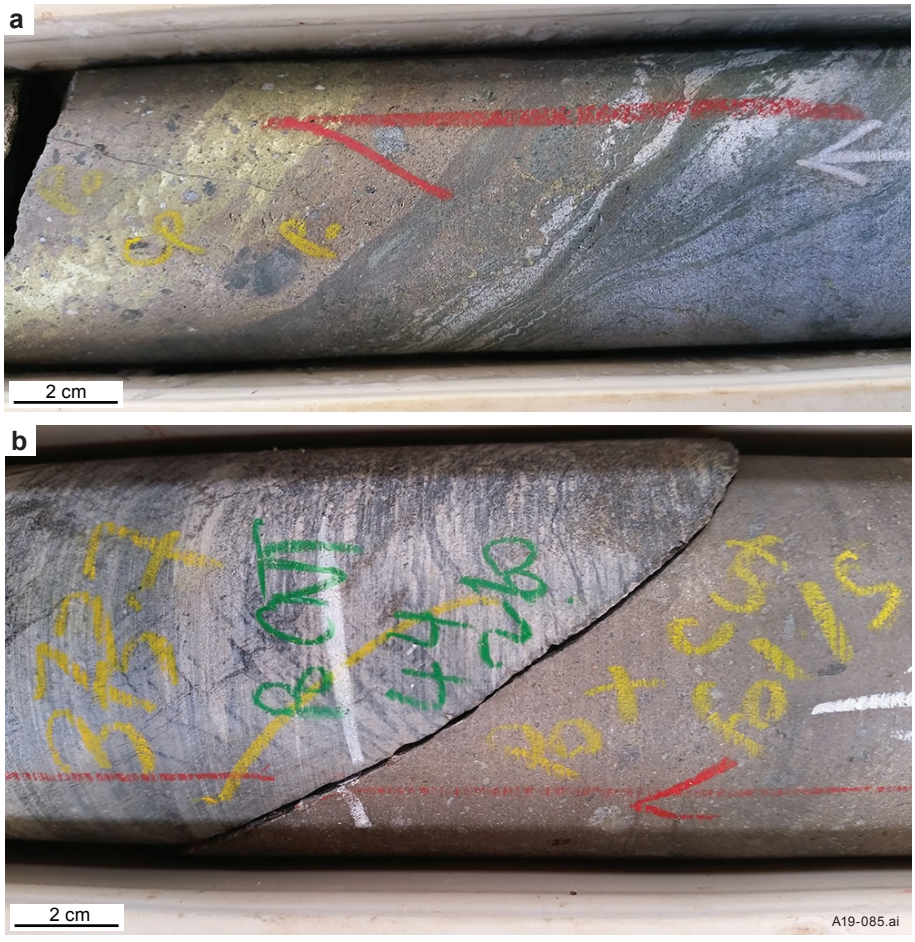

Figure 3. Images of mineralised and altered diamond drill core from the Grapple prospect. (**a**) Brecciated and stringer pyrrhotite (metallic bronze colour) and chalcopyrite (brass colour) that overprints a pervasive mylonite fabric in schist of the Lander Rock Formation. (**b**) Massive pyrrhotite breccia (metallic bronze colour) that overprints foliated andalusite schist of the Lander Rock Formation.

sulfide-bearing breccias, stringers, and veins cross-cut the ca 1.67 Ga mylonitic fabric; this is interpreted to constrain breccia formation, as observed, to a syn- to post-deformation timing at or after ca 1.67 Ga. However, the available data do not preclude the possibility that mineralisation was syn-depositional and then was subsequently deformed or remobilised. Hence, genetic models and exploration targets must consider two different models.

If the prospects formed at ca 1.84 Ga, ie during formation of the host succession, the two options would be volcanic-hosted or sediment-hosted massive sulfide mineralisation; in both cases the prospects would form syn-genetically on the seafloor, or diagenetically or epigenetically just below the seafloor. The location of the prospects would be controlled by stratigraphy and/or syn-depositional faults. Such mineralisation might be associated with meta-exhalites and/or metavolcanics. Based on present data, there are no rocks at Grapple or Bumblebee that could be interpreted as metaexhalites or metavolcanic rocks. However, many districts that contain metamorphosed volcanic-hosted or

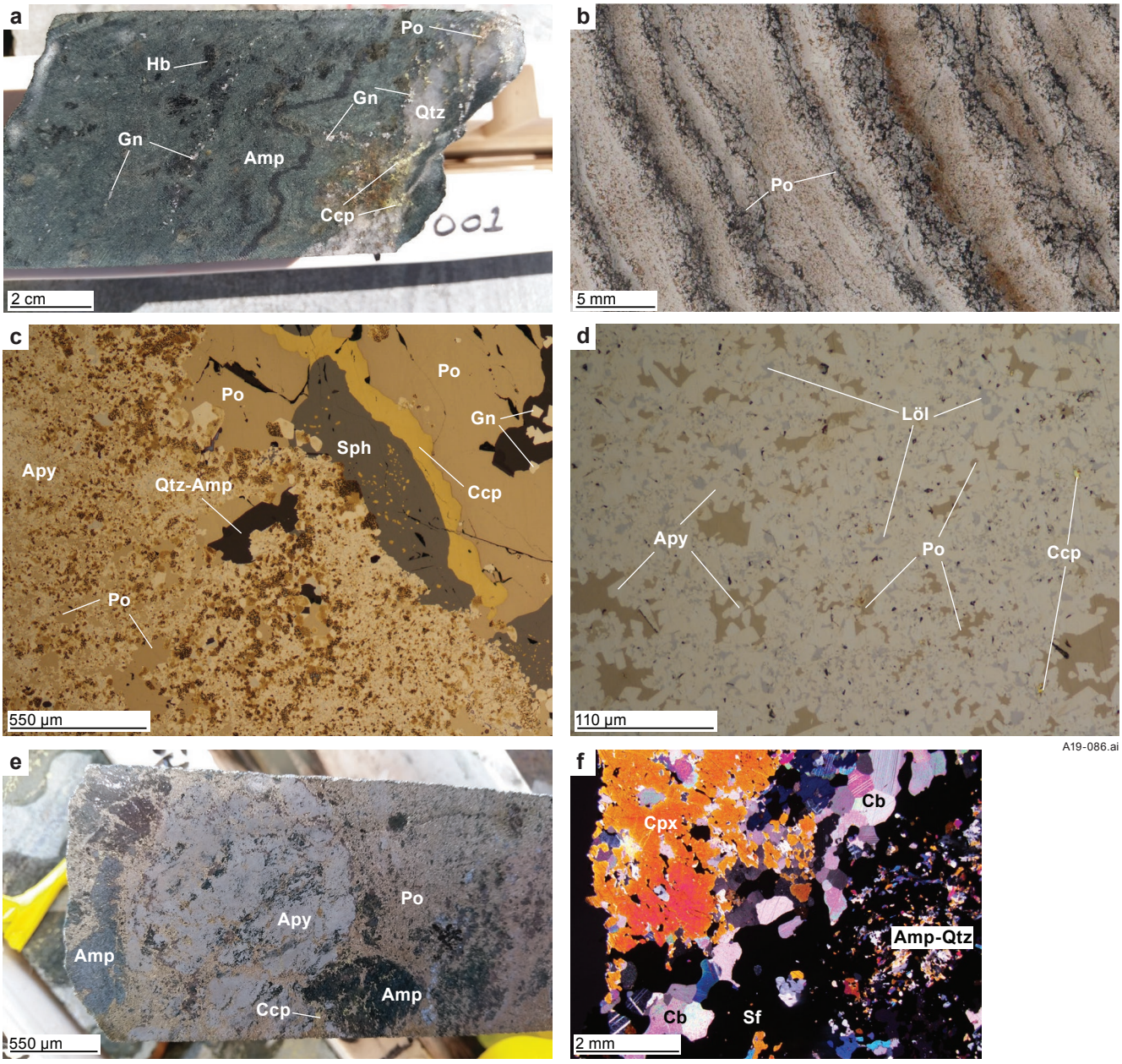

Figure 4. Images of mineralised and altered diamond drill core and associated photomicrographs from the Grapple and Bumblebee prospects. (**a**) Photograph of a chalcopyrite–pyrite-bearing quartz vein that cross cuts the S_2 foliated amphibole–quartz rock of the Lander Rock Formation. The quartz vein is also associated with minor galena mineralisation. (**b**) Thin section image in plane polarised light of net-textured pyrrhotite (opaque) foliated within S_2 fabric in metasandstone of the Lander Rock Formation. (**c**) Photomicrograph in reflected light showing coarse arsenopyrite crystals within a pyrrhotite breccia. The amphibole has an unusual mottled texture. The pyrrhotite–arsenopyrite breccia engulfs clasts of amphibole–quartz. Pyrrhotite, sphalerite, chalcopyrite, and galena occur on grain boundaries of the breccia. Note the chalcopyrite disease within sphalerite grains. (**d**) Photomicrograph in reflected light showing complex intergrowths within the arsenopyrite grains. Arsenopyrite is intergrown with löllingite, pyrrhotite and occasional chalcopyrite. (**e**) Photograph of coarse-grained arsenopyrite within a pyrrhotite breccia. Blebby chalcopyrite is also evident in macroscale. The breccia engulfs clasts of amphibole–quartz rock. (**f**) Photomicrograph of sulfide stringers overprinting an amphibole–quartz–clinopyroxene–carbonate assemblage. Ccp = chalcopyrite; Qtz = quartz; Amp = amphibole; Gn = galena; Po = pyrrhotite; Apy = arsenopyrite; Sph = sphalerite; Löl = löllingite; Sf = sulfide; Cpx = clinopyroxene; Cb = carbonate.

sediment-hosted massive sulfide deposits do not contain metaexhalites or metavolcanic rocks. Hence, although there is no compelling evidence for an 'early' origin, such an origin cannot be excluded.

If the prospects formed at or after ca 1.69 Ga, they could have formed in association with ca 1.69–1.63 Ga magmatism that affected both the Aileron and Warumpi provinces. At the prospect- to regional-scale, both prospects are spatially associated with ultramafic, mafic and lesser felsic intrusions with ages of ca 1.67–1.63 Ga (eg local mafic, intermediate and felsic intrusions and the Andrew Young Igneous Complex), which indicates the possibility of a magmatic-hydrothermal origin to the mineralisation. In this case, an exploration target would be spatially-associated 1.69–1.63 Ga magmatic bodies, an obviously different criteria to the 'early' origin for mineralisation. Intrusion-related deposits associated with mafic rocks are commonly magnetite-rich and base-metal-poor (Einaudi *et al* 1981; Ĉerný *et al* 2005; Goldfarb *et al* 2005; Meinert *et al* 2005), although relatively reduced base metal and gold mineralisation does occur in some settings (eg Meinert 1995). However, intrusion-related base-metal- and gold-bearing deposits are predominantly associated with felsic to intermediate magmatic rocks. There are no abundant ca 1.69–1.63 Ga felsic to intermediate igneous rocks occurring locally at Grapple or Bumblebee. Only minor granite and aplite is associated with the ca 1.64 Ga Andrew Young Igneous Complex (Young *et al* 1995), and extensive felsic- to intermediate-magmatism is present in the Yaya Domain of the Warumpi Province to the south (Waluwiya Suite, Illili Suite and Papunya Igneous Complex: Scrimgeour *et al* 2005a,b). For this 'late' model of mineralisation, potential exploration targets would extend southward into the Warumpi Province.

Because current geochronological and textural characteristics do not definitively determine the origin of the Grapple and Bumblebee prospects, additional samples were submitted for sulfur and oxygen isotope analysis. The sulfur isotope analyses have a very limited $\delta^{34}S$ range near 0‰, which is consistent with derivation of the sulfur from igneous rocks, either directly from magmatic-hydrothermal fluids or indirectly from the leaching of volcanic or other magmatic rocks. The sulfur isotope data are consistent with a 'late' magmatic-hydrothermal model, but they are also consistent with an 'early' syn-depositional model as > 1.8 Ga volcanic-hosted and sediment-hosted deposits generally have $\delta^{34}S$ values near 0‰ (Huston *et al* 2015).

Samples of both unaltered and altered host rocks have been submitted for whole rock oxygen isotope analysis as a critical test of the origin of the ore fluids. In either of the 'early' options, the ore fluid, in most cases, would be evolved seawater; whereas in the 'late' option, the ore fluid would be magmatic-hydrothermal. These fluids have quite different oxygen isotope characteristics that will be imparted into the altered rocks. Hence, the data should provide a reasonably robust test of the presence of magmatic-hydrothermal fluids in the mineral system that formed the Grapple and Bumblebee prospects. These results will be the subject of a future NTGS–GA record.

Acknowledgements

Rob Creaser (University of Alberta, Canada) is thanked for conducting Re–Os arsenopyrite analyses. Roland Maas (University of Melbourne) is thanked for lead isotope analyses and Iso-Analytical (UK) are thanked for sulfur isotope analyses. The authors also wish to thank Jay Carter and Max Heckenberg for help and assistance in the field and at the Alice Springs Core Facility.

References

Beyer EE, McGloin MV, Thompson JL and Meffre S, in prep. Constraints On timing of mafic magmatism at the Grapple Cu–Au–Ag–Zn Prospect, Central Australia: *In-situ* LA–ICP–MS zircon geochronology of a new Proterozoic greenfields discovery. *Northern Territory Geological Survey, Record*.

Ĉerný P, Blevin PL, Cuney M and London D, 2005. Granite-related ore deposits. *Economic Geology 100th Anniversary Volume*, 337–370.

Close DF, Scrimgeour I, Edgoose C, Cross A, Clauoé-Long J, Kinny P and Meixner T, 2003. Redefining the Warumpi Province. in: *'Annual Geoscience Exploration Seminar (AGES) 2003. Record of Abstracts'. Northern Territory Geological Survey, Record* 2003–2011.

Close DF, Scrimgeour IR and Edgoose CJ, 2004. *Mount Rennie, Northern Territory (Second Edition). 1: 250 000 geological map series, SF 52-15*. Northern Territory Geological Survey.

Close DF, Scrimgeour IR, Edgoose CJ, Wingate MTD and Selway K, 2005. Late Palaeoproterozoic oblique accretion of a 1690–1660 Ma magmatic arc onto the North Australian Craton: *Geological Society of Australia*, *Abstracts* 81, 36.

Crawford T, 2017. *Petrography, lithogeochemistry, alteration and mineralisation, towards a genetic model for mineralisation at the Bumblebee and Grapple prospects, Lake MacKay Project*. Independence Group NL.

Cross A, Claoué-Long JC, Scrimgeour IR, Close DF and Edgoose CJ, 2005. Summary of results. Joint NTGS–GA geochronology project: southern Arunta Region. *Northern Territory Geological Survey, Record* 2004-003.

Edgoose CJ, Close DF and Scrimgeour, IR 2008. *Lake Mackay, Northern Territory (2nd Edition), 1:250 000 geological map series, SF 52–11*. Northern Territory Geological Survey, Darwin.

Einaudi MT, Meinert LD and Newberry RJ, 1981. Skarn deposits. *Economic Geology 75th Anniversary Volume*, 317–391.

Goldfarb RJ, Baker T, Dubé B, Groves DI, Hart CJR and Gosselin P, 2005. Distribution, character, and genesis of gold deposits in metamorphic terranes. *Economic Geology 100th Anniversary Volume*, 407–450.

Hollis JA, Kirkland CL, Spaggiari CV, Tyler IM, Haines PW, Wingate MTD, Phillips C, Sheppard S, Belousova E and Murphy RC, 2013. Zircon U–Pb–Hf isotope evidence for links between the Warumpi and Aileron Provinces,

West Arunta Region. *Geological Survey of Western Australia, Record* 2013/9.

Hussey KJ, Huston DL and Claoué-Long JC, 2006. Geology and origin of some Cu-Pb-Zn (-Au-Ag) deposits in the Strangways Metamorphic Complex, Arunta Region, Northern Territory. *Northern Territory Geological Survey, Report* 17.

Huston DL, Eglington BM, Pehrsson S and Piercey SJ, 2015. The metallogeny of zinc through time: links to secular changes in the atmosphere, hydrosphere, and the supercontinent cycle, in Archibald SM and Piercey SJ (editors). *'Current perspectives on zinc deposits'. Irish Association for Economic Geology* 1–16.

Kirkland CL, Wingate MTD, Tyler IM and Spaggiari CV 2009. 184367: metagranodiorite, Dwarf Well; *Geological Survey of Western Australia, Geochronology Record* 846.

Kositcin N, McGloin MV and Reno BL, in prep. Summary of results. Joint NTGS–GA geochronology project: Cu-Au-Ag-Zn mineralisation on MOUNT RENNIE, Aileron Province, March–September 2018, *Northern Territory Geological Survey, Record*.

Meinert LD, 1995. Compositional variation of igneous rocks associated with skarn deposits - Chemical evidence for a genetic connection between petrogenesis and mineralization: in Thompson JFH, (editor). '*Magmas, fluids, and ore deposits'. Mineralogical Association of Canada. Short Course Series* 23, 401–418.

Meinert LD, Dipple GM and Nicolescu RJ, 2005. World skarn deposits. *Economic Geology 100th Anniversary Volume*, 299–336.

Morrissey L, Payne JL, Kelsey, DE and Hand M, 2011. Grenvillian-aged reworking in the North Australian Craton, central Australia: Constraints from geochronology and modelled phase equilibria. *Precambrian Research* 191, 141–165.

Reno BL, McGloin MV and Meffre S, 2018. Constraints On The Timing Of Sulfide Breccia Formation At The Grapple Cu–Au–Ag–Zn Prospect, Central Australia: *In-situ* LA–ICP–MS monazite geochronology of a new Proterozoic greenfields discovery. *Northern Territory Geological Survey, Record* 2018-013.

Scrimgeour IR, 2013. Chapter 12. The Aileron Province: in Ahmad M and Munson TJ (compliers). 'Geology and mineral resources of the Northern Territory'. *Northern Territory Geological Survey, Special Publication* 5.

Scrimgeour IR, Close DF and Edgoose CJ, 2005a. *Mount Liebig, Northern Territory. 1:250 000 geological map series explanatory notes, SF 52-16*. Northern Territory Geological Survey.

Scrimgeour IR, Kinny PD, Close DF And Edgoose CJ, 2005b, High-T granulites and polymetamorphism in the southern Arunta Region, central Australia: Evidence for a 1.64 Ga accretional event. *Precambrian Research*, 142, 1–27.

Selway K, Hand M, Heinson G and Payne JL, 2009. Magnetotelluric constraints on subduction polarity: reversing reconstruction models for Proterozoic Australia. . *Geology* 37, 799–802.

Shaw RD, Zeitler PK, McDougall I and Tingate PR 1992. The Palaeozoic history of an unusual intracratonic thrust belt in central Australia based on ^{40}Ar–^{39}Ar, K–Ar and fission track dating. *Journal of the Geological Society of London* 149, 937–954.

Whitford M, 2019. Application of electrical geophysics to exploration at the Lake Mackay Project: in *'Annual Geoscience Exploration Seminar (AGES) Proceedings, Alice Springs, Northern Territory, 19–20 March 2019'*. Northern Territory Geological Survey, Darwin (this volume).

Winzar D, 2016. Early indications of a copper-gold belt in the southwestern Aileron Province, Northern Territory: in *'Annual Geoscience Exploration Seminar (AGES) Proceedings, Alice Springs, Northern Territory 15–16 March 2016'*. Northern Territory Geological Survey, Darwin.

Wong BL, Morrissey LJ, Hand M, Fields CE and Kelsey DE, 2015. Grenvillian-aged reworking of late Paleoproterozoic crust of the southern North Australian Craton, central Australia: Implications for the assembly of Mesoproterozoic Australia. *Precambrian Research* 270, 100–123.

Wyborn L, Hazell M, Page R, Idnurm M and Sun S, 1998. A newly discovered major Proterozoic granite-alteration system in the Mount Webb region, central Australia, and implications for Cu–Au mineralisation. *AGSO Research Newsletter* 1–6.

Young DN, Fanning CM, Shaw RD, Edgoose CJ, Blake DH, Page RW and Camacho A, 1995. U–Pb zircon dating of tectonothermal events in the northern Arunta Inlier, central Australia. *Precambrian Research* 71, 45–68.

Mapping under cover with geochemistry

Matt Briggs[1,2], James Davis[2], Neil Jones[2] and Lara Bowlt[2]

The Tanami Region on the border between the Northern Territory and Western Australia is an orogenic gold province with several operating and past producing gold mines. The Capstan Prospect within the Bluebush Project is located 700 km northwest of Alice Springs.

Although the general tectono-stratigraphic evolution of the Tanami Region is reasonably well established through the efforts of recent multi-disciplinary studies (Lambeck *et al* 2008, Joly *et al* 2012, Bagas *et al* 2008, Bagas *et al* 2014), there is still considerable debate as the accuracy of stratigraphic correlations across the Tanami Region. The contacts between adjacent formations in field exposures are few and far between, making the correlation of stratigraphy across the Tanami Region difficult. This has resulted in several complete reversals of the stratigraphic successions, the most recent in 2014 (Bagas *et al* 2014).

Understanding of the geology, and specifically the stratigraphic succession, is key to unlocking the Tanami Region due to the strong stratigraphic control on mineralisation. Of the significant deposits known in the Tanami Region, 13 out of 15 are exposed at surface. Mapping (and understanding stratigraphy and alteration footprints related to mineralisation) is critical for effective exploration under the cover sequences for the next generation of discoveries.

Regional targeting by Prodigy Gold NL utilises magnetic and gravity survey data in combination with the mapping of the limited outcrop. Just 2% of the interpreted favourable stratigraphy is exposed within the project area. An extensive veneer of Quaternary cover, along with very minor outcrop, limits the ability to reliably correlate geology across the Tanami Region. Historic bedrock lithology mapped from drilling in the regolith has commonly been misclassified due to partial or complete weathering, or due to silcrete intervals being misidentified.

Prodigy Gold has been updating regional- and prospect-scale geology maps using end of hole geochemistry, and building on previous stratigraphic correlations (Lambeck 2010) in collaboration with the CSIRO (Schmid 2018, Schmid in prep). A large magnetic anomaly at the Capstan Prospect has long been flagged as possibly analogous to the 'Dead Bullock' stratigraphic succession of the Callie deposit. The magnetic anomaly at Capstan has a potentially analogous geological and structural setting to the Callie deposit. There is very limited, if any, outcrop. The target area is for the most part covered by a veneer of sandy, alluvial cover and a hard silica cap that has limited previous exploration attempts in the area.

Up until 2018, there was no previous diamond drilling in the Capstan area. Little information on the Dead Bullock Formation exists in the public domain, with virtually no other core drilling into the Dead Bullock Formation outside of Dead Bullock Soak and The Granites Mine. The lack of drill core intersecting the Dead Bullock Formation outside of these mines makes the ability to correlate stratigraphy with the recognised mine sequence uncertain.

Prodigy Gold has completed three reconnaissance aircore/RAB programs and two stratigraphic core holes over the Capstan Prospect. Drilling successfully intersected the Dead Bullock Formation as indicated by chlorite-altered sedimentary rocks, calcite nodules, mafic sills/flows and tuffaceous units (**Figures 1**,**2**). Litho-geochemistry

[1] Prodigy Gold NL, 141 Broadway, Nedlands WA 6009, Australia
[2] Email: MBriggs@prodigygold.com.au

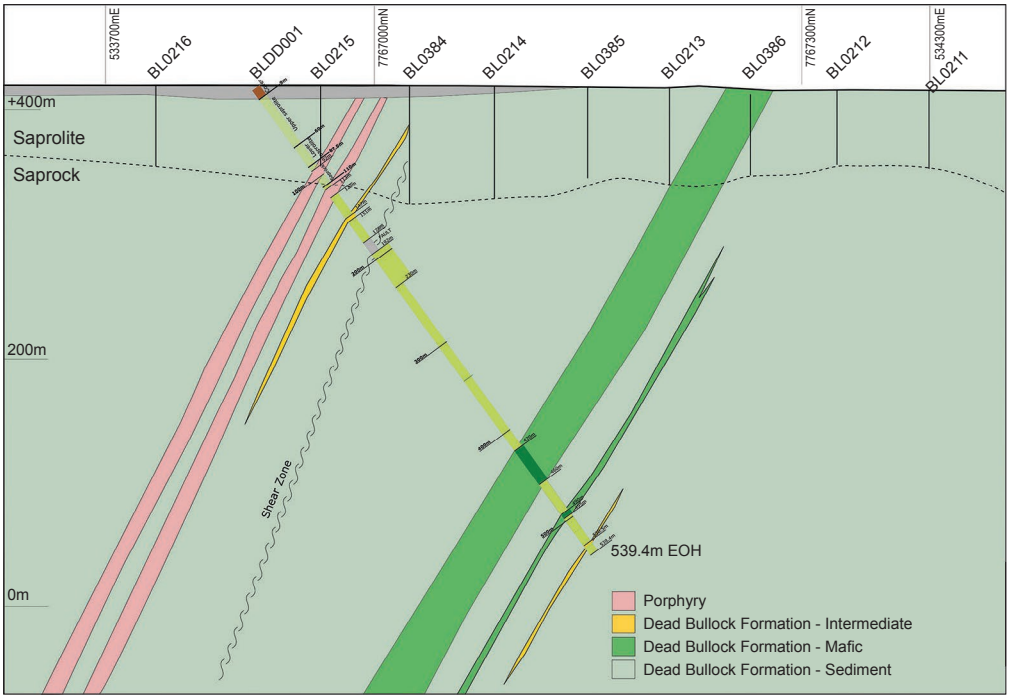

Figure 1. Cross section through Capstan Prospect drillhole BLDD001.

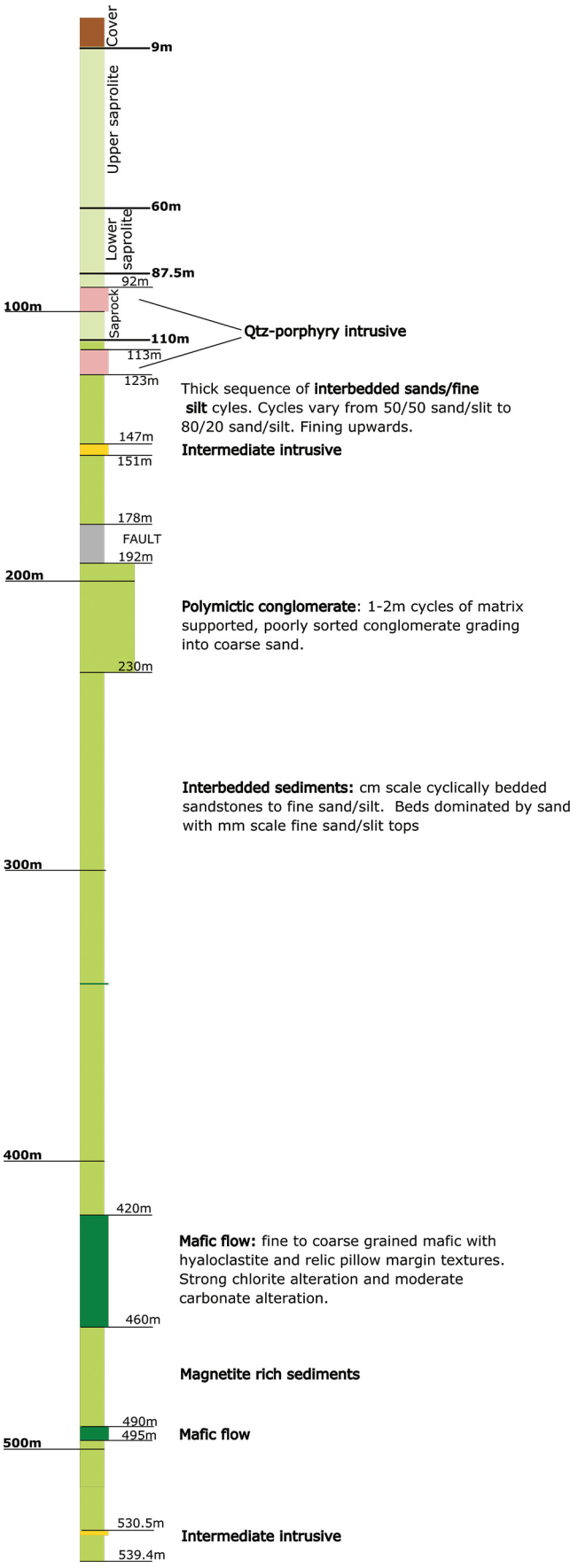

Figure 2. Downhole log for Capstan Prospect drillhole BLDD001.

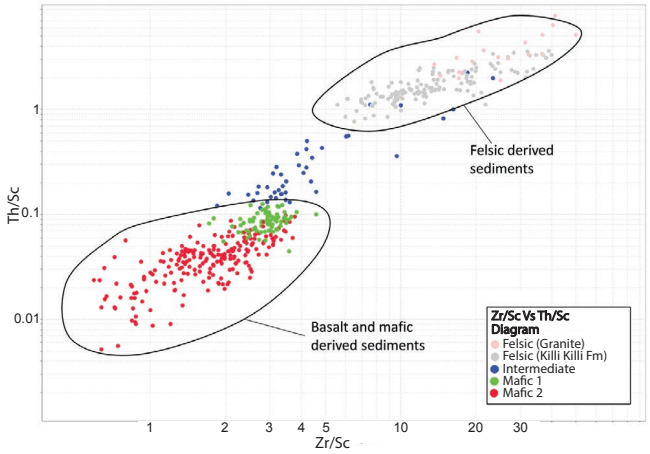

Figure 3. Geochemical classification after Lambeck *et al* (2008) from 'end of hole' samples from Capstan aircore drilling.

samples/data collected indicates the hole intersected 'Lower Dead Bullock' as first described by Lambeck (2004); the results correlate with the data collected by Radzik (1998) and Lambeck *et al* (2004, 2008; **Figure 3**). Further sampling of core from the stratigraphic diamond holes suggests the drilling at Capstan has intersected the lateral equivalent of the Lower Blake beds. The prospect-scale bedrock geology has been interpreted and seven new multi-km scale gold targets have been defined.

Acknowledgements

Acknowledgements to Prodigy Gold's current and former geologists and Susanne Schmid at the CSIRO. The Company received funding for diamond drilling from the Northern Territory Government as part of the *Resourcing the Territory* initiative.

References

Bagas L, Bierlein FP, English N, Anderson JAC, Maidment D and Huston DL, 2008. An example of a Paleoproterozoic back arc basin: Petrology and geochemistry of the ca 1864 Ma Stubbins Formation as an aid towards an improved understanding of the Granites–Tanami Orogen, Western Australia. *Precambrian Research* 166(1), 168–194.

Bagas L, Boucher R, Li B, Miller J, Hill P, Depauw G, Pascoe J and Eggers B, 2014. Paleoproterozoic stratigraphy and gold mineralisation in the Granites–Tanami Orogen, Northern Australian Craton. *Australian Journal of Earth Sciences* 61, 89–111.

Joly A, Porwal A and McCuaig C, 2012. Exploration targeting for orogenic gold deposits in the Granites–Tanami Orogen: Mineral system analysis, targeting model and prospectivity analysis. *Ore Geology Reviews* 48, 349–383.

Lambeck A, 2004. Sequence stratigraphy framework for mineralised units in the Tanami region: in '*Annual Geoscience Exploration Seminar (AGES) 2004. Record of Abstracts.*' *Northern Territory Geological Survey, Record* 2004-001.

Lambeck A, Huston D, Maidment D and Southgate P, 2008. Sedimentary geochemistry, geochronology and sequence stratigraphy as tools to typecast stratigraphic units and constrain basin evolution in the gold mineralised Palaeoproterozoic Tanami Region, Northern Australia. *Precambrian Research* 166, 185–203.

Radzik N, 1998. *The relationship between magnetite occurrence and gold mineralization in the Callie gold deposit, Tanami Region, Northern Territory, Australia*. BSc (Hons) thesis, School of Physical Sciences, University of Adelaide, Adelaide.

Schmid S, Davis J, Jones N, Schaubs P and Miller J, 2018. Geochemical classification of the Tanami Group - a tool for gold exploration: in '*Annual Geoscience Exploration Seminar (AGES) Proceedings. Alice Springs, Northern Territory, 20–21 March 2018*. Northern Territory Geological Survey, Darwin.

New insights into the Neoproterozoic to early Palaeozoic stratigraphy, structure and palaeogeography of the Amadeus Basin, Northern Territory

Verity J Normington [1,2], Chris J Edgoose [1], Nigel Donnellan[1], Anett Weisheit[1] and Charles Verdel[1]

Introduction

The Neoproterozoic to Palaeozoic Amadeus Basin is a large (~170 000 km^2), elongate, intracratonic basin in central Australia, located predominantly in the Northern Territory (NT) and extending into Western Australia (**Figure 1**). The basin has a protracted depositional history extending from sedimentation of the Heavitree Formation and Dean Quartzite possibly in the early Tonian (>820 Ma) to molasse deposition of the Pertnjara and Finke groups in response to the ca 450–300 Ma Alice Springs Orogeny. Up to 14 km of marine and minor terrestrial sedimentary successions are preserved locally (Edgoose 2013). The depositional history is punctuated by a number of significant epeirogenic, orogenic and erosional episodes and includes a number of unconformities and time breaks of greater or lesser regional significance.

Since 2014, the Northern Territory Geological Survey (NTGS) has conducted studies in the Amadeus Basin from 1:100 000–1:250 000 map scale to regional- and basin-wide scales. The map- and regional-scale projects have largely focused on the Neoproterozoic successions where the biggest issues in intra-basin correlation occur. These studies began with characterising the Neoproterozoic stratigraphy in the northeast of the basin (Normington and Donnellan in review) where the stratigraphy is best exposed. This work was undertaken as a 'base-line' study on which subsequent projects on the lesser known Neoproterozoic successions in the central and southern parts of the basin could be founded. The knowledge gained from this study has been applied to delineating the Neoproterozoic succession in the north-central part of the basin in detail through geological mapping (HENBURY[3] and Henbury Special; Donnellan *et al* in prep, and Donnellan and Normington in prep, respectively; **Figure 1**). The field-based studies have also improved the understanding of the basin-wide distribution and thickness variations of many Neoproterozoic units through stratigraphic revisions of a number of key drillholes (Normington and Edgoose 2015 and 2018, Normington 2018, and Normington *et al* in prep). Combined, the stratigraphic characterisation, geological and structural mapping, and drillhole revisions are being integrated with geophysical datasets to produce two interpretative 1:500 000-scale maps and accompanying explanatory notes on the pre-Mesozoic geology and structure of the Amadeus Basin in the NT (Weisheit in prep).

[1] Northern Territory Geological Survey, GPO Box 4550, Darwin NT 0801, Australia
[2] Email: verity.normington@nt.gov.au
[3] Names of 1:250 000 and 1:100 000 mapsheets are shown in large and small capital letters respectively, eg HENBURY, Henbury Special

Neoproterozoic to early Palaeozoic stratigraphy

Northeast study

The stratigraphic characterisation of the Neoproterozoic succession along the structurally-controlled northeast margin of the basin (**Figure 1**) has significantly improved understanding of this period of basin history. The study took a field-based approach to systematically describe, characterise and correlate the lithostratigraphic units, updating nomenclature where required (**Figure 2**). This work has been reported previously at AGES (Normington *et al* 2015, Donnellan and Normington 2017, Normington and Edgoose 2018), and is described in detail in Normington and Donnellan (in review). The work has:

- identified Johnnys Creek Formation as a widespread unit
- provided detailed descriptions of sub-facies within the Gillen Formation
- recognised the Wallara Formation in outcrop for the first time (previously only known from 2 drillholes in the central basin)
- created new and refined existing type sections for many lithostratigraphic units
- upgraded the Bitter Springs formation to Bitter Springs Group
- re-defined the Gillen and Loves Creek members as formations of the Bitter Springs Group
- formalised Johnnys Creek 'beds' as Johnnys Creek Formation of the Bitter Springs Group
- formalised the 'Finke beds' as the Wallara Formation
- renamed the Heavitree Quartzite as Heavitree Formation in recognition of the variation in siliclastic component lithologies.

Mapping - central Basin

The Neoproterozoic Inindia beds (Ranford *et al* 1965) is an informal unit that has been recorded and mapped across much of the central and southern basin (**Figure 1**). It comprises a sequence of siltstone, sandstone, conglomerate, chert, chert breccia, and dolostone (Ranford *et al* 1965); it is equivalent to almost the entire post-Bitter Springs Group Neoproterozoic succession. (**Figure 2**). NTGS mapping in the central basin (HENBURY in 2015–2017) has successfully subdivided areas previously mapped as Inindia beds into the formal units of the northeast margin, including recognising previously unmapped Johnnys Creek and Wallara formations; the Aralka Formation including its constituent Limbla Member; and the Pioneer Sandstone and Pertatataka Formation.

The overlying latest Neoproterozoic to early Cambrian Winnall beds has been divided into the newly-defined

Breaden, Gloaming, Froud, Liddle and Puna Kura Kura formations, and the Chookla Member in Henbury Special and HENBURY, which are now collectively assigned to the Winnall Group (**Figure 2**). These definitions and unit descriptions are published in Donnellan and Normington (2017), Donnellan and Normington (in prep) and Donnellan *et al* (in prep).

In addition to targeting the Neoproterozoic, the new mapping also covered the much better known and defined Palaeozoic succession in the central-northern basin. In northern HENBURY, early to mid-Palaeozoic successions are relatively thick by comparison with the same units exposed in southern HENBURY. This contrast in thickness can be better understood when viewed in the context of the current model of the basin architecture (**Figure 1b**), which formed in response to the ca 580–530 Ma Petermann Orogeny (see Edgoose 2013). The southern part of the mapping area coincides with the 'southern platform' element (**Figure 1b**) whilst the northern area largely coincides with the 'Missionary Plains Trough' (Lindsay and Korsch 1991, and references therein). These features are interpreted to have been separated by a high of basement rock and lower basin successions – the 'central ridge' (Lindsay and Krosch 1991, Shaw *et al* 1991). The southern platform lacks the major Palaeozoic depocentres present in the north; however, shallow marine depositional environments predominate in

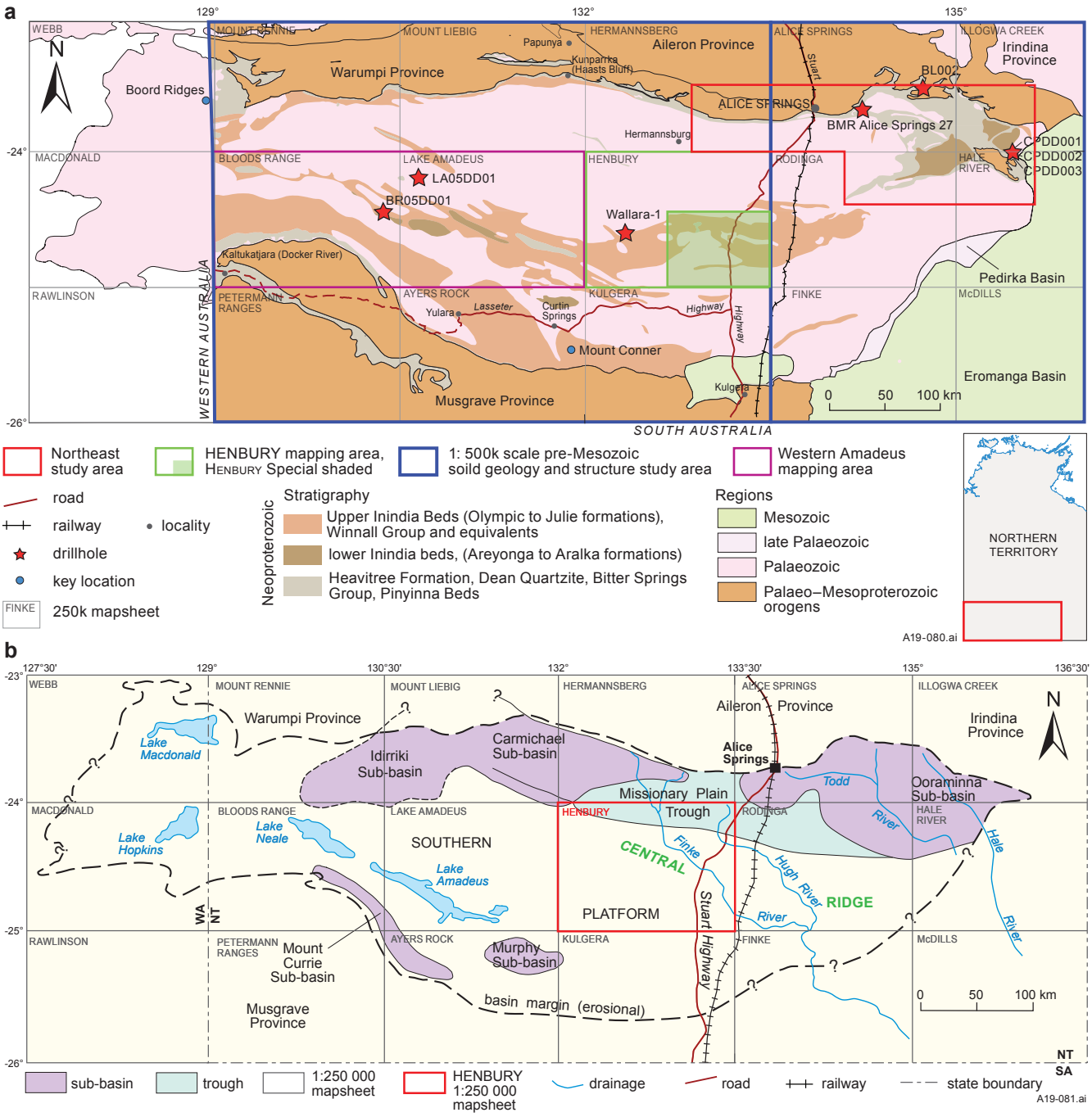

Figure 1. (**a**) Regional geological setting of the Amadeus Basin in the Northern Territory. The surface distribution of the Neoproterozoic units across the basin is shown (Edgoose 2013), as well as the drillholes studied. Outcrop geology is derived from NTGS 1:2.5M-scale geological regions GIS dataset. (**b**) Architecture of the Amadeus Basin, showing drainage and locations of sub-basins, Missionary Plain Trough, Central Ridge and Southern Platform elements (slightly modified after Marshall *et al* 2007 and references therein).

both elements. Not only is the succession thinner in the south, the lithofacies for some units also vary across the architectural components. One example is the Ordovician Stairway Sandstone (Larapinta Group) where a newly recognised interval with distinctive inchnofauna is mapped (and being defined as a member) across a wide area in the north of HENBURY (Missionary Plain Trough) but not in the south. The observed variation in thickness and facies within the one unit provides lithostratigraphic evidence to support the basin architectural model shown in **Figure 1b**.

Additionally, brittle fault structures, previously unrecognised in the central part of the Amadeus Basin, have been identified from both mapping and the interpretation of geophysical data. Structural analyses of outcrop data

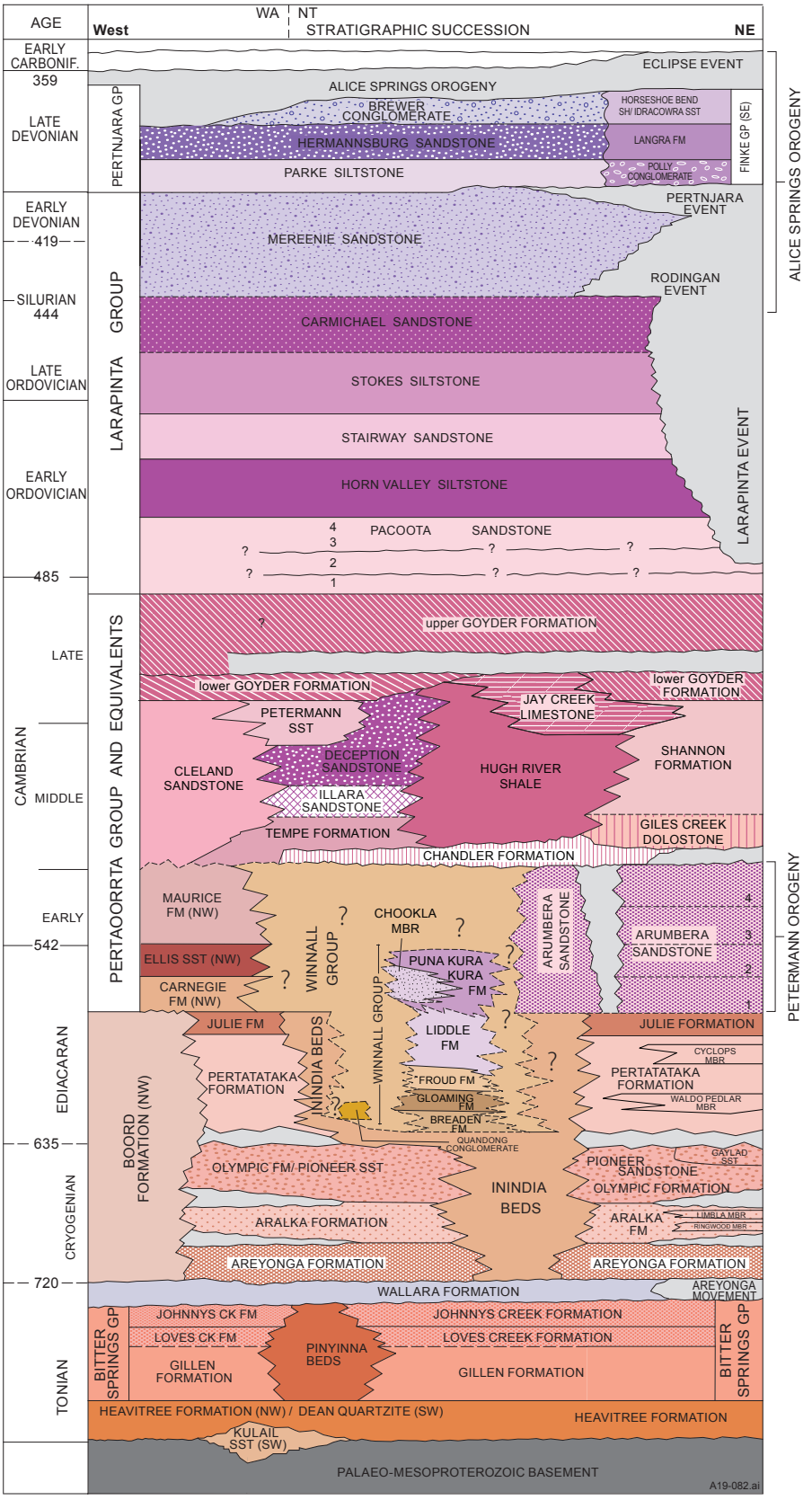

Figure 2. Revised stratigraphy of the Amadeus Basin succession (modified after Edgoose 2013, Haines and Allen 2014, Haines *et al* 2015, Donnellan and Normington 2017, and Normington 2018). The Neoproterozoic to early Cambrian succession is preliminary and will be revised based on 2019 field observations by NTGS.

have shown that the characteristic km-scale folding in the central part of the Amadeus Basin is fault-related (Weisheit and Donnellan 2018; Weisheit *et al* 2018; Normington and Donnellan in prep). The age-relationships of folded and faulted stratigraphy indicates that deformation was initiated during the ca 580–530 Ma Petermann Orogeny and continued during the ca 450–300 Ma Alice Springs Orogeny.

Mapping - western Amadeus Basin

The western part is the most remote, inaccessible and therefore least known and understood region of the Amadeus Basin. However, significant exposures of the post-Bitter Springs Group Neoproterozoic successions (Inindia and Winnall beds) are scattered in low ranges and isolated outcrops across this region (LAKE AMADEUS, BLOODS RANGE; **Figure 1**). Commencing in 2019, NTGS will undertake systematic 1:250 000-scale mapping across this area aimed at continuing the revision of the Neoproterozoic succession and interpretation of the structural architecture that has been achieved in the central area of the basin (see above). It is anticipated that the Inindia beds will be divided into the formalised units of the northeast and central basin, and that the subdivision of the Winnall Group into separate formations will continue. In addition, this work aims to correlate NT stratigraphic units and nomenclature with the revised Neoproterozoic succession in WA published by GSWA (Haines *et al* 2012, Haines and Allen 2014, Allen *et al* 2018). An additional objective is to further improve the understanding of the basin's tectonic history as expressed through surface observations of faults and folds, in conjunction with the subsurface interpretation at 1:500 000-scale (see below).

Basin-wide program

1:500 000-scale pre-Mesozoic interpreted geology and structure

NTGS is continuing to re-interpret the pre-Mesozoic geology and structure of the entire Amadeus Basin in the NT by integrating the results of mapping in the central basin with interpretation of basin-wide geophysical datasets. Preliminary outcomes of this project have been presented in Weisheit and Donnellan (2018) and Weisheit *et al* (2018). They include the recognition that much of the km-scale folding in the Amadeus Basin is fault-related. Structures that formed during the Petermann Orogeny are recognised in the southern and central Amadeus Basin as thick-skinned, north- to northeast-directed fault-propagation folds, possibly re-activating pre-existing basement structures. During the Alice Springs Orogeny, these structures were partly reactivated and overprinted by several sets of 100 km long, south-directed fault-bend folds and fault-propagation folds, which are widely recognised across the basin. Later, sets of thick-skinned, oblique-slip to strike-slip faults developed, causing the disruption of pre-existing structures. This protracted, syn-depositional tectonic development of the Amadeus Basin resulted in variable stratigraphic relationships and varying degrees of preservation of the succession throughout the basin (eg stratigraphic thinning/thickening; allochthonous versus autochthonous; lateral changes). The recognition that much of the development of the Amadeus Basin is fault-related has implications for both mineral and petroleum systems via the possible existence of multiple fluid pathways in both space and time, potential tapping of basement source rocks, and the formation of traps and seals.

Drillhole correlations

Given the increased understanding of the Neoproterozoic succession of the Amadeus Basin through field-based studies, a need for applying this work to update the stratigraphy of key drillholes was recognised. To date, seven key drillholes have been reassessed: mineral exploration holes CPDD001, CPDD002 and CPDD003 from the Pipeline Prospect, BL002 from Blueys Prospect, and stratigraphic drillhole BMR Alice Springs 27, all located in the northeast of the Amadeus Basin; and NTGS drillholes LA05DD01 and BR05DD01 in the western-central Amadeus Basin (**Figure 1**). The revised drill logs were compiled from a combination of relogging (where necessary), correlation with hyperspectral data sets (HyLogger®), review of published logs and existing lithological descriptions, and incorporation of recent biostratigraphic studies.

Stratigraphic units not previously identified or well-described in these drillholes include the Gillen, Loves Creek and Johnnys Creek formations of the Bitter Springs Group, and the Wallara, Areyonga and Aralka formations. These stratigraphic revisions, along with field observations in HENBURY and in the western basin in WA (Haines *et al* 2012, Haines and Allen 2014, Allen *et al* 2018), have considerably expanded the known distribution and thickness variations of these units across the basin. The results have been released through a number of NTGS publications comprising Normington and Edgoose (2015), Normington (2018) and Normington and Edgoose (2018), plus soon to be released Normington *et al* (in prep).

Geochronology and isotope geochemistry

Given the limitations of biostratigraphic control in Neoproterozoic successions, U–Pb detrital zircon geochronology can be a useful tool in determining intra-basin stratigraphic relationships where field evidence of rock relationships is missing or ambiguous. All units studied in the northeast and central basin have now been dated, with maximum deposition ages and provenance spectra compiled. There is now sufficient data to enable some trends in zircon population ages to be observed across the Neoproterozoic and Palaeozoic successions. For example, the spectra of early Palaeozoic units in the central basin can be distinguished from the spectra of Neoproterozoic units by the greater proportion of zircon in the age range ca 700–500 Ma, as well as by generally younger maximum deposition ages. Although the Neoproterozoic-early Palaeozoic succession includes sedimentation prior to the Petermann Orogeny (which comprised deformation and uplift of the Musgrave Province and basal formations of the basin) as well as post-orogenic deposition, the Musgrave Province is the dominant

sediment source for all units. In some instances where field relationships are difficult to decipher (eg missing intervening stratigraphy), the detrital zircon spectra has been able to provide another line of evidence for interpreting the most likely age of poorly constrained units.

New isotopic data for the Neoproterozoic and Cambrian has been obtained from several University of Adelaide honours projects supported by SANTOS and NTGS. Detrital zircon provenance spectra for the Heavitree Formation indicates that there is a consistent maximum deposition age of ca 1030 Ma and no zircon grains with U–Pb ages <1000 Ma (Al-Kiyumi 2018). This result is in line with previous data collected from samples of this unit and equivalents from both northern and southern basin margins. Al-Ghafri (2018) further constrained the maximum depositional ages of the Areyonga and Pertatataka formations to ca 685 Ma and ca 650 Ma respectively. Wong (2018) suggested the prominent zircon source for the Neoproterozoic–Cambrian succession may have been the Musgrave Province with lesser input from the Aileron and Warumpi provinces, and the Paterson and Rudall provinces in WA. New Ce anomaly data from some Cambrian carbonate units are interpreted to suggest a progressive change from oxygenated to more anoxic waters up stratigraphy (Albusaidi 2018). New $\delta^{13}C$ and $^{87}Sr/^{86}Sr$ data for the Aralka Formation (Al-Khanjari 2018) correlates well with both local and global Neoproterozoic isotope records.

References

Al-Ghafri M, 2018. *The age and sediment sources of the Amadeus Basin Cryogenian-Ediacaran stratigraphy.* BSc (Hons) thesis, School of Physical Sciences, University of Adelaide, Adelaide.

Al-Kiyumi M, 2018. *Constraining the age and provenance of the basal quartzites of the Centralian Superbasin – revisiting the Heavitree Formation*. BSc (Hons) thesis, School of Physical Sciences, University of Adelaide, Adelaide.

Albusaidi QH, 2018. *Chemostratigraphy of Cambrian carbonates of the Amadeus Basin: Implications for Palaeo-depositional environments and marine redox*. BSc (Hons) thesis, School of Physical Sciences, University of Adelaide, Adelaide.

Allen HJ, Grey K, Haines PW, Edgoose CJ and Normington VJ, 2018. The Cryogenian Aralka Formation, Amadeus Basin: a basinwide biostratigraphic correlation. *Geological Survey of Western Australia, Record* 2018-11.

Al-Khanjari HA, 2018. *Carbon and strontium isotope chemostratigraphy of the Neoproterozoic carbonates from the Amadeus Basin, NT.* BSc (Hons) thesis, School of Physical Sciences, University of Adelaide, Adelaide.

Donnellan N and Normington VJ, 2017. Towards a revised stratigraphy for the Neoproterozoic and probable early Cambrian in the central Amadeus Basin, Northern Territory: in '*Annual Geoscience Exploration Seminar (AGES) Proceedings, Alice Springs, Northern Territory, 28–29 March 2017*'. Northern Territory Geological Survey, Darwin.

Donnellan N and Normington VJ, in prep. *Geology of Henbury Special, Northern Territory (First Edition). 1:100 000 geological map series, 5548 and parts of5448, 5449 and 5549*. Northern Territory Geological Survey, Darwin.

Donnellan N, Edgoose CJ, Normington VJ and Weisheit A, in prep. *Henbury, Northern Territory (Second Edition). 1:250 000 geological map series explanatory notes, SG 5301*. Northern Territory Geological Survey, Darwin.

Edgoose CJ, 2013. Chapter 23 - Amadeus Basin: in Ahmad M and Munson TJ (compilers). '*Geology and mineral resources of the Northern Territory*.' *Northern Territory Geological Survey, Special Publication* 5.

Haines PW and Allen HJ, 2014. Geology of the Boord ridges and Gordon Hills: key stratigraphic section in the western Amadeus Basin, Western Australia, *Geological Survey of Western Australia, Record* 2014-11.

Haines PW, Allen HJ, Grey K and Edgoose CJ, 2012. The western Amadeus Basin: revised stratigraphy and correlations: in Ambrose GJ and Scott K (editors). '*Central Australia Basins Symposium (CABS) III'. Petroleum Exploration Society of Australia, Special Publication.*

Kositcin N, Normington VJ and Edgoose CJ, 2018. Summary of results. Joint NTGS – GA geochronology project: Amadeus Basin, July 2017–June 2018. *Northern Territory Geological Survey, Record* 2018-010.

Lindsay JF and Korsch RJ, 1991. The evolution of the Amadeus Basin, central Australia: in Korsch RJ and Kennard JM (editors). *'Geological and geophysical studies in the Amadeus Basin, central Australia'. Bureau of Mineral Resources, Australia, Bulletin* 236, 7–32.

Normington VJ, 2018. Revised stratigraphy of drillholes CPDD001, CPDD002 and CPDD003, Pipeline Prospect, northeast Amadeus Basin, Northern Territory. *Northern Territory Geological Survey, Record* 2017-015.

Normington VJ and Donnellan N, in review. Characterisation of the Neoproterozoic stratigraphy of the northeast Amadeus Basin, Northern Territory. *Northern Territory Geological Survey, Record*.

Normington VJ and Donnellan N, in prep. *Henbury Special, Northern Territory 1:100 000 geological map series explanatory notes*. Northern Territory Geological Survey, Darwin.

Normington VJ and Edgoose CJ, 2015. Revised stratigraphy of drillhole BMR Alice Springs 27, northeast Amadeus Basin, Northern Territory. *Northern Territory Geological Survey, Technical Note* 2015-003.

Normington VJ and Edgoose CJ, 2018. Neoproterozoic stratigraphic revisions to key drillholes in the Amadeus Basin – implications for basin paleogeography and petroleum and minerals potential: in '*Annual Geoscience Exploration Seminar (AGES) Proceedings, Alice Springs, Northern Territory, 20–21 March 2018'*. Northern Territory Geological Survey, Darwin.

Normington VJ, Allen HJ, Edgoose CJ, Haines PW and Grey K, in prep. Revised stratigraphy and biostratigraphy for NTGS stratigraphic drillholes LA05DD01 and BR05DD01, southwestern Amadeus Basin. *Northern Territory Geological Survey, Record*.

Randford LC, Cook PJ and Wells AT, 1965. The Geology of the central part of the Amadeus Basin, Northern Territory. *Bureau of Mineral Resources, Report* 86.

Shaw RD, Korsch RJ, Wright C and Goleby BR, 1991. Seismic interpretation and thrust tectonics of the Amadeus Basin, along the BMR regional seismic line: in Korsch RJ and Kennard JM (editors). *'Geological and geophysical studies in the Amadeus Basin, central Australia. Bureau of Mineral Resources, Australia, Bulletin* 236, 385–408,

Weisheit A, in prep. *West Amadeus Basin, Northern Territory. 1:500 000 geological map series explanatory notes*. Northern Territory Geological Survey, Darwin,

Weisheit A and Donnellan N, 2018. Developing new 1:500 000 interpreted geology maps for the Amadeus Basin, Northern Territory: insights into the structural evolution of the fold-and-thrust belt: in *'Annual Geoscience Exploration Seminar (AGES) Proceedings, Alice Springs, Northern Territory, 20-21 March 2018'*. Northern Territory Geological Survey, Darwin.

Weisheit A, Donnellan N, Normington V and Edgoose C, 2018. The Amadeus Basin fold-and-thrust belt, central Australia: stages of intraplate deformation: in *'Australian Geoscience Council Convention (AGCC), Adelaide, South Australia, 14–18 October 2018'*. Australian Geoscience Council.

Wong YH, 2018. *Detrital constraints of zircon and apatite analysis in the southern Amadeus Basin*. BSc (Hons) thesis, School of Physical Sciences, University of Adelaide, Adelaide.

Integration of reprocessing, depth imaging and interpretation in legacy data to provide new insights into salt tectonics and sub salt imaging in the Amadeus Basin, NT

Julie Daws[1,2], Jason Nycz[3] and Greg Staples[4]

The Neoproterozoic geology of the Amadeus Basin is highly complex with many salt-induced tectonic features resulting from multiple phases of deformation. Structural and stratigraphic features within the study area, below the Petermann Unconformity, were poorly imaged on the existing vintage 2D seismic data resulting in low confidence in any structural and stratigraphic interpretation. Reprocessing of the vintage seismic data across the Walker Anticline in the northern Amadeus basin has significantly improved data quality in the Neoproterozoic section. Salt structures and basement horizons became apparent with the improved imaging such that a viable interpretation has been possible.

The reprocessed 2D data has been tied to key deep wells in the basin using the AMSAN regional lines; this has further improved confidence in identification of key stratigraphic horizons and potential leads. Significant extensional structuring below the salt indicates a strong likelihood of traps similar to that drilled by Magee-1 in the southern part of the basin. Interpretation of the new data also supports the likelihood of multiple salt emplacement episodes as observed elsewhere in the basin.

This study has shown that the application of new technology to vintage 2D seismic can significantly aid geological interpretation at depth. Reprocessing legacy 2D data should be one of the first steps in any exploration program when chasing deeper, relatively unexplored targets prior to the acquisition of new seismic data.

[1] Mosman Oil and Gas Limited, Suite 305, Level 3, 35 Lime Street, Sydney NSW 2000
[2] Email: jdaws@mosmanoilandgas.com
[3] Earth Signal Processing Ltd, Suite 1600, 715-5th Avenue SW, Calgary, Alberta, Canada T2P 2X6
[4] Synterra Technologies Ltd, 221-10th Avenue SE, Calgary, Alberta, Canada T2G 0V9

The discovery and mining of the ultra-high-grade Edna Beryl Gold Mine – the trials and tribulations

Robert Bills[1,2], Ana Liza Cuison[1] and Steve Russell[1]

Summary

The discovery of the greater Edna Beryl mineralisation marks a successful journey of systematic, science-based exploration over a nine-year period. It is as much about the tenacity of the Emmerson exploration team and the quest for unlocking the geological code, as about the capability of the Board to secure funding to support this aggressive exploration during the usual peaks and troughs of the capital markets. Like most successful endeavours, the journey has always been with a clear business focus around effective and efficient exploration, taking into account the probabilities of discovery whilst using the failures as the fertiliser for improvement.

The Tennant Creek Mineral Field is famous for hosting some of the highest grade gold and copper deposits in Australia, the majority of which were discovered either by surface prospecting or by innovative modelling of the various magnetic geophysics – the obvious 'tool of choice' considering that the host to the gold and copper mineralisation is predominantly hydrothermal magnetite (locally termed ironstone).

In 2008 when Emmerson commenced exploration in Tennant Creek, it was recognised that most, if not all, of the obvious magnetic anomalies had been tested, thus leading Emmerson on a very different journey that was predicated on refining the exploration models with a more holistic view of the entire mineral system across all geological scales. Emanating from this was the hypothesis that oxidised fluid sources played a far more important role in the genesis of these deposit types, and that these fluids were in fact instrumental in the deposition of ultra-high grades of gold and copper. Therefore, much of the research and data collection was specifically aimed at trying to better understand the role of these fluids, their possible connection to the Tennant Event and their pathways via refining the 3D structural framework.

Ultimately this approach has been successful in discovery of the Goanna and Monitor copper-gold systems, the Mauretania gold, and the more recent, ultra-high-grade Edna Beryl gold mineralisation (**Figure 1**). All of these discoveries display the common theme of an association with highly oxidised, hematite-rich fluids and an association typically with little or at best, very weak magnetic signatures (**Figure 2**).

Mining at Edna Beryl is now underway with the first parcel of ~3000 t of ore averaging between 25 to 70 g/t Au – making it one of the highest grade gold mines in Australia, but also presenting some challenges in reconciling of these high ore grades against the surrounding drillholes and projecting them forward into a Life of Mine plan.

[1] Emmerson Resources, 3 Kimberley Street, West Leederville WA 6007, Australia

[2] Email: rbills@emmersonresources.com.au

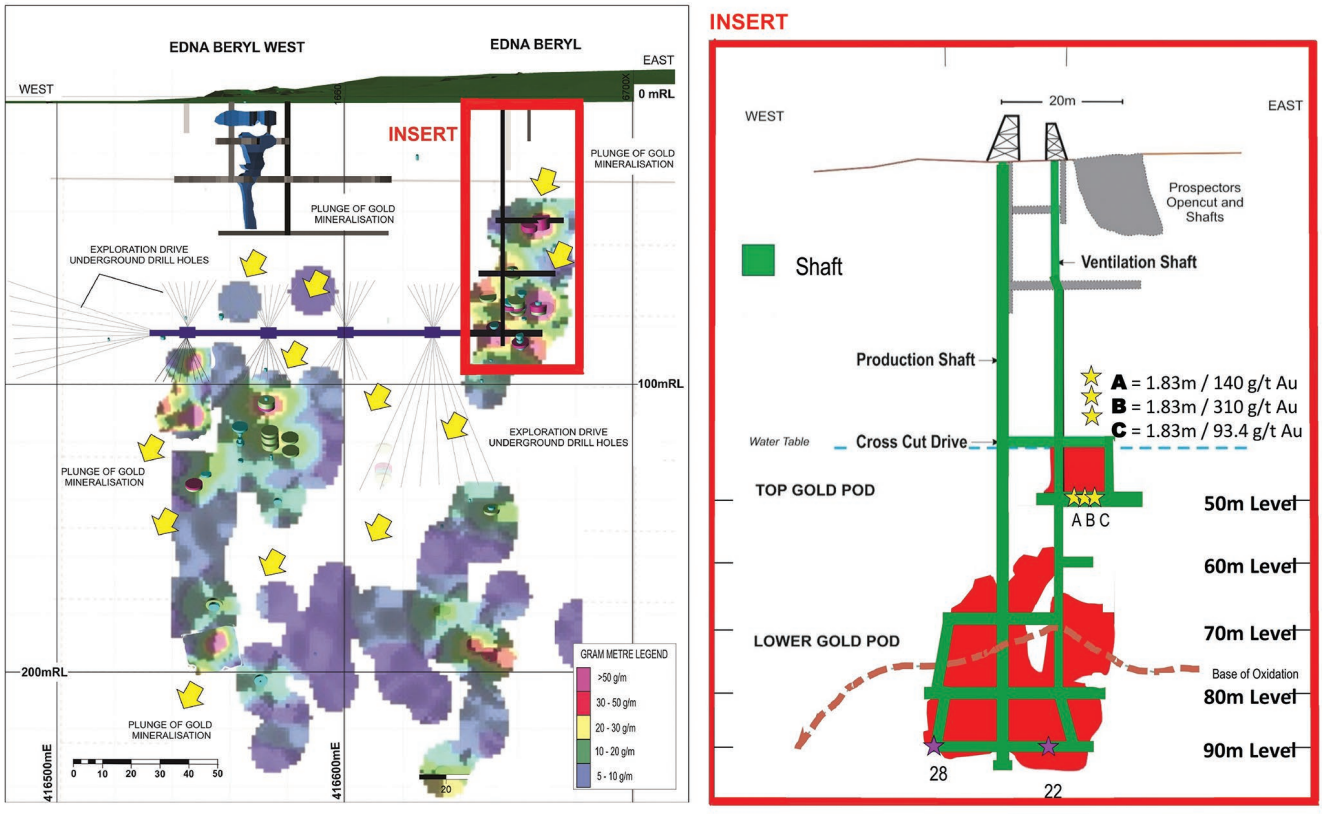

Figure 1. Edna Beryl Gold Mine. Note the existing Tribute Area (red outlined insert), plus exploration drive with proposed fan drilling (background colours = gold gram/metre from surface drilling).

Figure 2. Visible gold from the 80 m level at Emmerson's Edna Beryl Gold Mine. Note the association with hematite (steely grey).

Acknowledgements

We acknowledge the Emmerson exploration team and numerous joint venture partners, the contribution to the geophysics by Jeremy Cook, geochemistry by Ned Howard, and structural geology by Roric Smith.

Refreshing the Alligator River Uranium Field exploration toolkit – Angularli and Such Wow

Penny Sinclair[1,2]

The Wellington Range and King River Joint Venture (JV) comprises a group of five contiguous exploration tenements located on the eastern side of the Cobourg Peninsular ~250 km to the east–northeast of Darwin (**Figure 1**) in the Alligator Rivers Uranium Field (ARUF). The focus of current exploration by the JV partners, Vimy Resources (75%, project operator) and Rio Tinto Exploration (25%), is the discovery of a high-grade uranium resource amenable to underground mining.

The JV tenements all overlie the Nimbuwah Domain in the northeastern part of the Pine Creek Orogen. The oldest stratigraphy recognised in the Nimbuwah Domain are the Archaean felsic gneiss of the Njibinjibinj Gneiss, the Arrarra Gneiss and the Kukalak Gneiss (**Figure 2**; Hollis and Glass 2012, Whelan *et al* 2016). These suites of Archean gneisses are unconformably overlain by metamorphosed Palaeoproterozoic sedimentary and volcanic rocks of the Cahill Formation and Nourlangie Schist, part of the Pine Creek Orogen. The rocks of the Archaean basement and the sedimentary stratigraphy of the Pine Creek Orogen underwent moderate- to high-grade metamorphism and deformation during the Nimbuwah Event. The suites of variably eroded Archaean and Palaeoproterozoic rocks are unconformably overlain by the Mamadawerre Sandstone, the basal member of the Mesoproterozoic Kombolgie Subgroup. The entire stratigraphic succession has been intruded by mafic dykes and sills of the Oenpelli Dolerite between 1734–1688 Ma (Whelan *et al* 2016). Variable thicknesses of the Cretaceous Bathurst Island Formation (Money Shoal Basin) unconformably overlie the crystalline Proterozoic basement.

The local geology in the vicinity of the Angularli deposit comprises Cahill Formation unconformably overlain by Mamadawerre Sandstone and poorly consolidated sediments of the Bathurst Island Formation (**Figure 3**). The Angularli uranium mineralisation is hosted by a multiply reactivated and altered deformation corridor, the Angularli Fault Zone (AFZ). The fault zone has a width of up to 100 m, strikes north–northwest (345°) and dips at approximately 60° towards 075˚. The deposit straddles the angular unconformity between the Cahill Formation and the overlying Mamadawerre Sandstone at a depth of

[1] Vimy Resources Limited, PO Box 23, West Perth WA 6872, Australia
[2] Email: psinclair@vimyresources.com.au

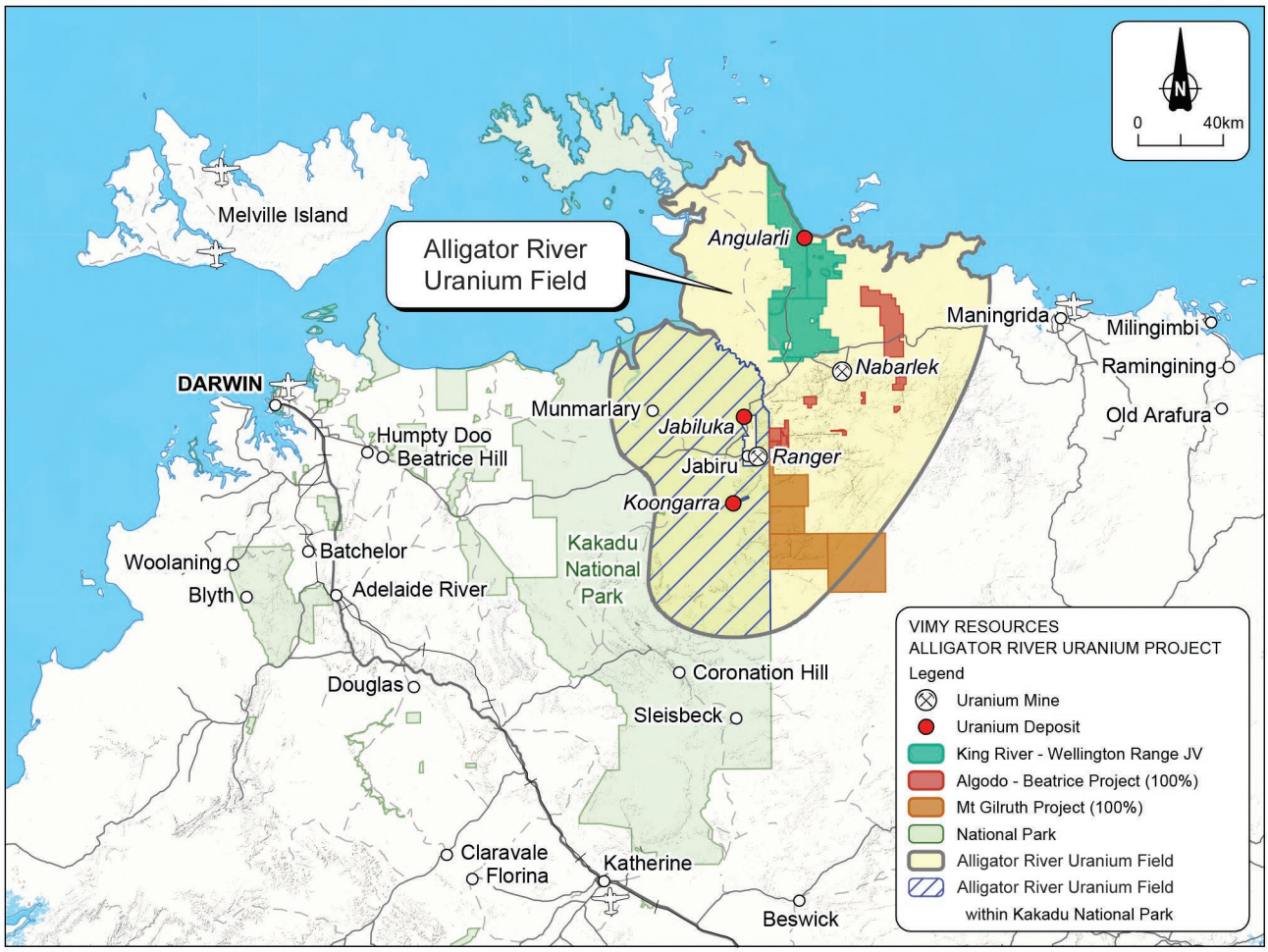

Figure 1. Vimy Resources projects in the Alligator Rivers Uranium Field.

approximately 250 m below the surface. The Angularli deposit has a south–southeast-plunging, ellipsoidal-shaped geometry and is approximately 315 m × 125 m × 25 m in size. In March 2018, Vimy announced a maiden, inferred-category Mineral Resource of 0.91 Mt at 1.3% U_3O_8 at a cut-off grade of 0.15% U_3O_8 containing 25.9 Mlbs U_3O_8 (Vimy Resources 2018).

Unlike other documented uranium resources in the ARUP, primary uranium mineralisation at Angularli occurs above, at and below the unconformity. The primary uranium resource below the unconformity is hosted within a brittle fracture network overprinting the multiply deformed silica-flooded breccia. The mineralised veins have classic open space fill textures with void spaces lined by botryoidal, amorphous pitchblende and in-filled by fine-grained (<10 µm) euhedral, zoned uraninite crystals, intergrown with intermediate chlorite, white mica, and silica. Several brittle fault strands observed within the silica-flooded breccia extend up into the unconformably overlying Mamadawerre Sandstone. Brecciated sandstone within and marginal to these fault strands host massive pitchblende, chlorite, and silica veins. Evidence of post-mineralisation alteration and re-mobilisation is present in some parts of the lodes with uraninite and pitchblende altered to coffinite and other secondary silicate and oxide species.

The mineralisation hosted below the unconformity is associated with two mineralogically and spatially distinct styles of alteration: a proximal white mica (now sericite),

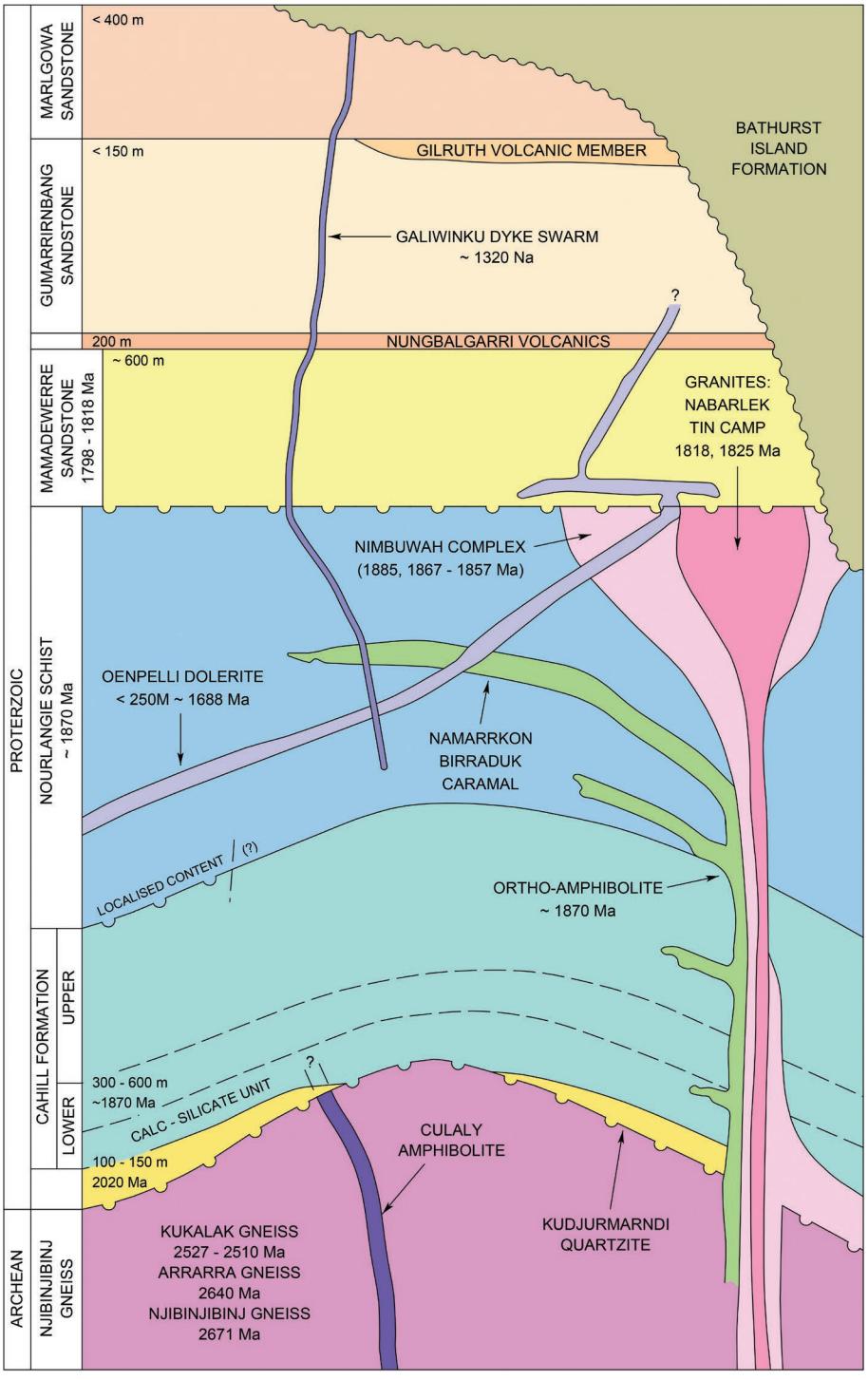

Figure 2. Stratigraphic column for the Nimbuwah Domain of the Pine Creek Orogen.

pyrite and silica alteration; and a distal intermediate chlorite alteration zone. The proximal alteration halo is mapped cross-cutting and in the hanging wall to the silicified breccia zone. This proximal alteration zone is broadly parallel to the upper contact of the silicified breccia, extending 15 to 50 m into the basement. The white mica, pyrite and silica alteration occurs as pervasive replacement of the protolith; in zones, it is sufficiently intense to destroy the primary metamorphic mineral assemblage. The distal intermediate chlorite alteration zone is observed from the outer limit of the white mica halo. The chlorite alteration can extend as far as 200 m into the hanging wall. No obvious hydrothermal alteration was noted in the footwall to the AFZ.

The proximal alteration halo mapped in the overlying Mamadawerre Sandstone is mineralogically very similar to that observed in the basement, comprising an assemblage of white mica–silica–pyrite infilling the sandstone matrix. A distal halo of fracture/fault controlled dravite (Mg-bearing tourmaline) and diaspore extends at least 250 m up into the overlying sandstone above the mineralised pod over a strike length of up to 500 m. A 150 m wide zone of pyrophyllite clay alteration parallel to the unconformity has also been mapped overlying the mineralisation (Smith 2018).

ICP–MS U–Pb dating of uraninite from the basement-hosted veins returned a mineralisation age of 1736 ± 17 Ma for Angularli. Oenpelli Dolerite dykes that are observed within the Angularli alteration zone lack obvious signs of post-intrusion alteration or mineralisation. This implies that the uranium mineralisation predates the Oenpelli Dolerite intrusion.

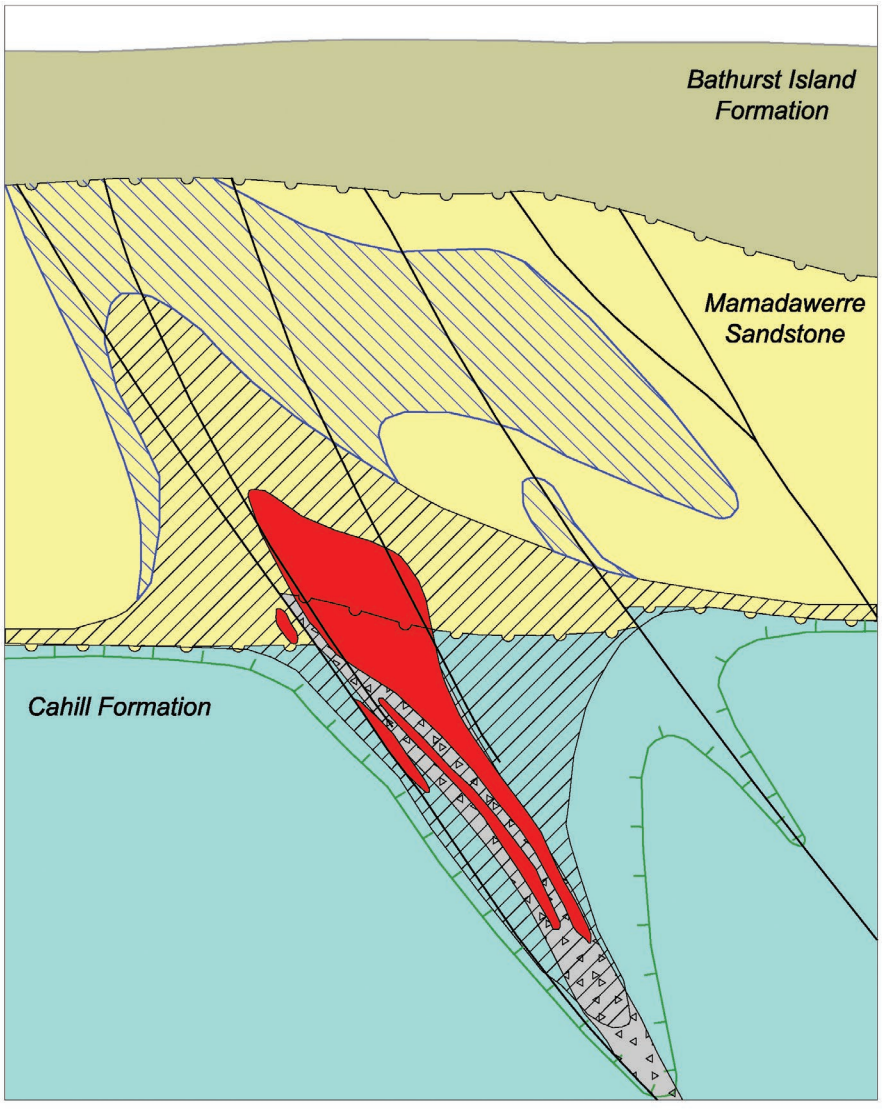

VIMY RESOURCES
ALLIGATOR RIVER PROJECT

Legend

- Bathurst Island Formation
- Mamadawerre Sandstone
- Cahill Formation
- uranium mineralisation
- silica flooded breccia
- intermediate chlorite alteration
- unconformity
- fault
- dravite (boron) alteration
- silica-sericite-pyrite alteration

Figure 3. Schematic cross-section for the Angularli Deposit.

An improvement in the understanding of the controls on the distribution of mineralisation, the composition and distribution of associated hydrothermal alteration, and geochemical pathfinders at Angularli has resulted in a reassessment of the targeting criteria applied to regional exploration. Higher grade resources (ie Nabarlek and Angularli), which are the primary target of the JV, are hosted by regional scale, steeply dipping, northwest–north-northwest-striking fault zones. These deposits have alteration systems that can extend several hundred metres into the overlying sandstone. Pathfinder geochemical halos (ie boron, gold, copper, lead isotopes etc) in the sandstone above Angularli extend up to and over a kilometre along the strike of the AFZ. Both the alteration and associated geochemical anomalism can be used as exploration vectors for exploring through extensive sandstone cover, effectively reducing the cost of first pass exploration programs in covered terrain.

Exploration efforts between 2016 and 2018 have largely focused on a broad north-northwest-striking, northeast-dipping fault zone (Telstra fault) located near the western margin of the JVs tenement package. As a result of ground reconnaissance, mapping, and rock-chip sampling, the exploration focus was directed in an area where the Telstra fault was mapped cross-cutting interpreted Cahill Formation, unconformably overlain by Mamadawerre Sandstone – an area known as Such Wow (**Figure 4**). Rock chip samples in this area returned elevated uranium, boron (after tourmaline) and pathfinder anomalism co-incident with outcropping dravite and diaspore veins. A surface sampling program was conducted directly to the north of Such Wow in an area where the Mamadawerre Sandstone had been eroded off the basement. As a result, a significant linear uranium anomaly was detected along strike of one of the Telstra Fault strands.

In 2018, the JV completed a first pass, six hole reverse circulation (RC) drilling program at Such Wow to test for the presence of Cahill Formation rock types (amphibolite, metapelite, semi-metapelite and metapsammite) below the Mamadawerre Sandstone, and to demonstrate that the surficial geochemical anomalism translated to structural fertility at depth.

The drilling results confirmed that in the Such Wow area, Mamadawerre Sandstone unconformably overlies metasedimentary rocks consistent with the Cahill Formation. Significant zones of Mg-rich chlorite and phengitic–illite alteration were intersected in faulted semi-metapelite in several holes (**Figure 5**). Elsewhere in the ARUP, Mg-rich chlorite and phengitic alteration are observed in the proximal and distal alteration halos at Ranger, Koongarra and Nabarlek. These zones of basement-hosted alteration are co-incident with significant uranium (**Table 1**), lead, lead isotope and copper anomalism. The JV's best drilling result from Such Wow was 1 m at 1332 ppm U_3O_8 from drillhole ARRC0016.

Additional mapping within the Such Wow Prospect in 2018 identified a 400 m × 200 m, northwesterly-striking zone of intense clay alteration, ~100 m to the east of the RC holes completed in the south of the prospect. This mappable surficial alteration system has been named 'Shiba'. The style and intensity of alteration, along with the tenor of pathfinder geochemical anomalism at Shiba, exceeds that observed in the sandstone escarpment directly to the south of Angularli. Exploration efforts in 2019 will focus on completing a first pass drill-test of the Shiba zone.

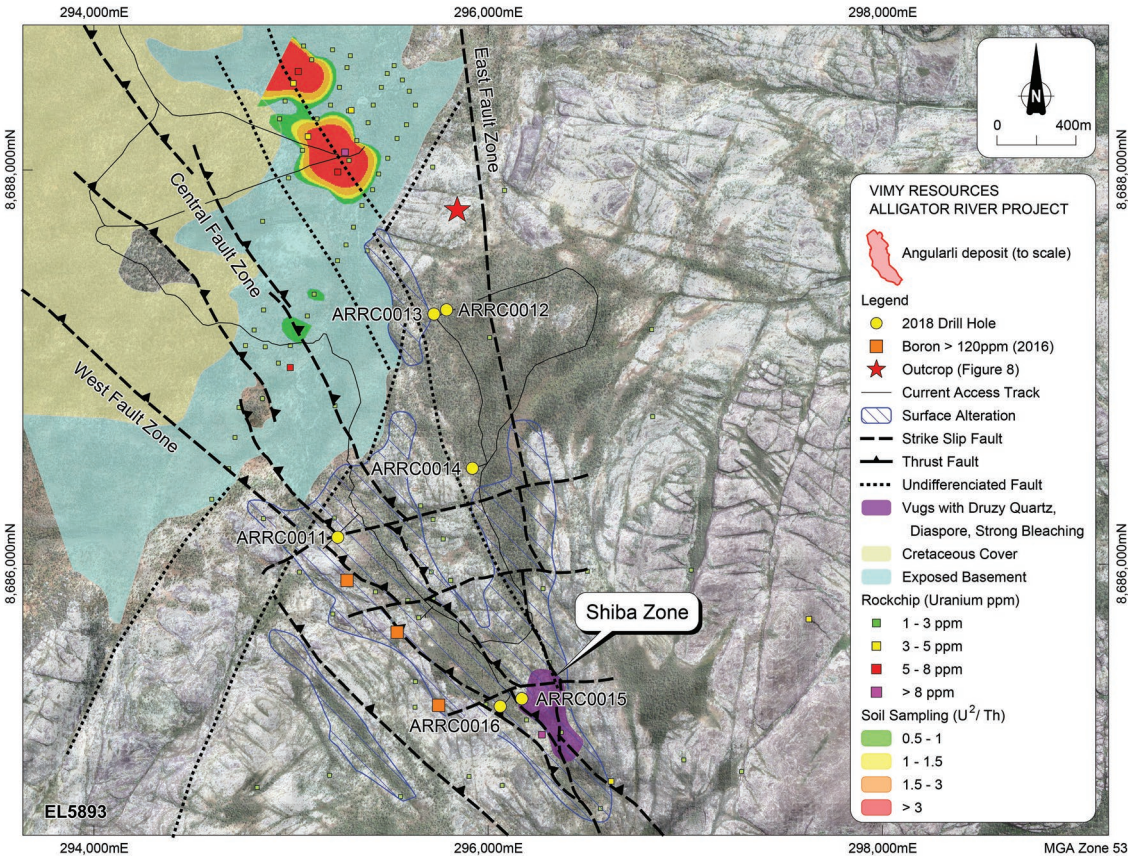

Figure 4. Satellite imagery over the Such Wow and Shiba prospect areas showing location of RC drillholes completed in 2018.

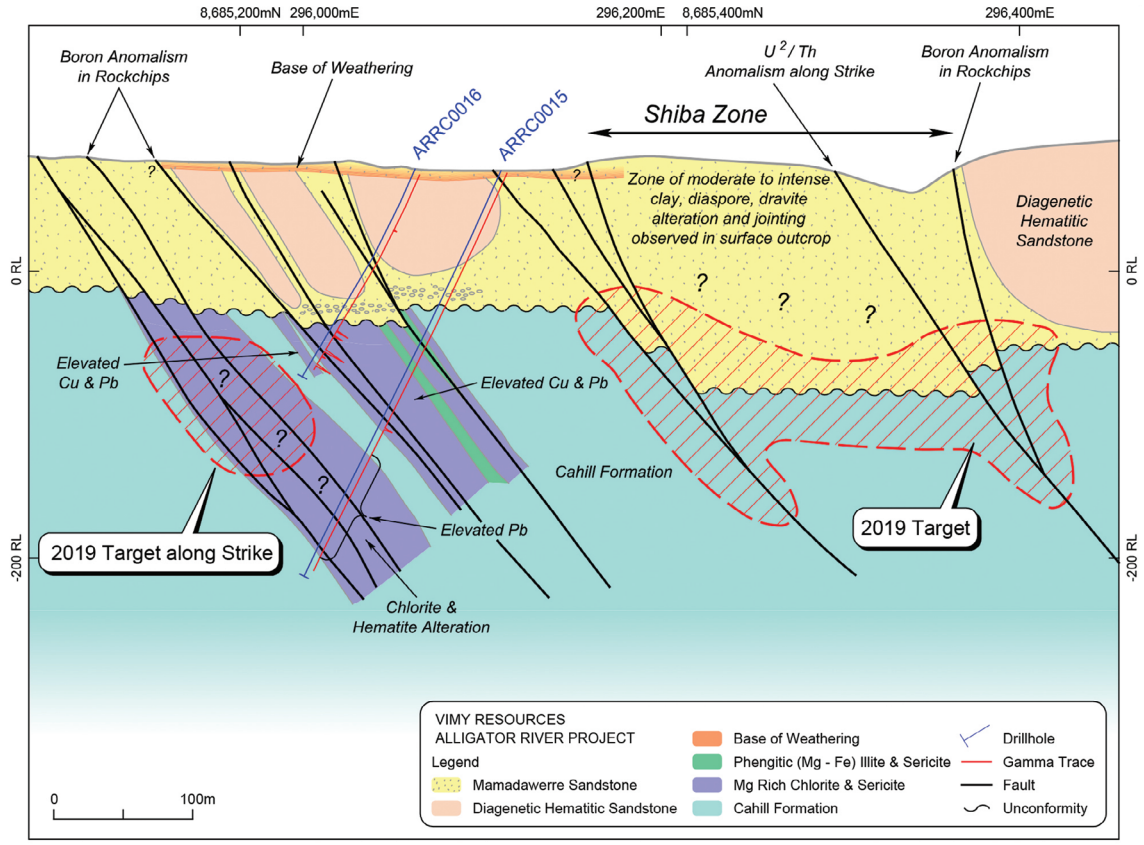

Figure 5. Interpreted cross-section from the Such Wow Prospect showing RC drillholes completed by Vimy Resources in 2018.

Table 1. Uranium intersections from RC drilling completed at the Such Wow Prospect in 2018.

Hole ID	Easting	Northing	RL	Depth	Dip	Azimuth	From (m)	To (m)	Grade[1] (% eU_3O_8)
ARRC015	8685317.6	296110.8	75.9	324	-65	225	203.3	204.1	0.01
ARRC016	8685278.7	296061.4	75.3	168	-65	225	127.0	127.7	0.02
							130.7	131.4	0.02
							142.5	143.0	0.02
							143.4	144.8	0.07
							155.8	156.6	0.03

[1] Elevated radiometric responses interpreted to be related to heavy mineral bands are not reported.

References

Hollis JA and Glass LM, 2012. *Howship and Oenpelli, Northern Territory. 1:100 000 geological map series explanatory notes, 5572, 5573*. Northern Territory, Geological Survey, Darwin.

Smith B, 2018. Mineralogy variations in the Mamadawerre Sandstone, Kombolgie Subgroup at Angularli Uranium Prospect: applications to exploration in other areas: in *'Annual Geoscience Exploration Seminar (AGES) Proceedings, Alice Springs, Northern Territory, 20–21 March 2018'*. Northern Territory Geological Survey, Darwin.

Vimy Resources Limited, 2018. *Maiden mineral resource at Angularli deposit, Alligator River Project*. Australian Stock Exchange media release, 20 March.

Whelan JA, Beyer EE, Donnellan N, Bleeker W, Chamberlin U and Ernst RE, 2016. 1.4 billion years of Northern Territory Geology: Insights from collaborative U–Pb zircon and baddeleyite dating: in *'Annual Geoscience Exploration Seminar (AGES) Proceedings, Alice Springs, Northern Territory, 15–16 March 2016'*. Northern Territory Geological Survey, Darwin.